5-24-2012

Expression and function of small RNAs in normal and psoriatic skin

Cailin Joyce
Washington University in St. Louis

WASHINGTON UNIVERSITY IN SAINT LOUIS

Division of Biology and Biomedical Sciences

Molecular Genetics and Genomics

Dissertation Examination Committee:

Anne Bowcock, Chairperson
Jeffrey Arbeit
Ted Hansen
Michael Lovett
Cristina de Guzman Strong
Weixiong Zhang

Expression and function of small noncoding RNAs in psoriatic skin

by

Cailin Elizabeth Joyce

A dissertation presented to the
Graduate School of Arts and Sciences
of Washington University
in partial fulfillment of the
requirements for the degree
of Doctor of Philosophy

May 2012

Saint Louis, Missouri

ABSTRACT OF THE DISSERTATION

Expression and function of small noncoding RNAs in psoriatic skin

by

Cailin Elizabeth Joyce

Doctor of Philosophy in Molecular Genetics and Genomics

Washington University in Saint Louis, 2012

Anne Bowcock, PhD, Chairperson

Psoriasis is a chronic, inflammatory skin disease characterized by hyperproliferation and altered differentiation of keratinocytes, and infiltration of activated immune cells in the epidermis. Array based genome-wide expression studies by our lab and others have revealed over 1,300 alterations in mRNA transcript levels in psoriatic skin. microRNAs (miRNAs) are a class of short, regulatory RNAs that play critical roles in human development and disease. I hypothesized that differential expression of miRNAs might underlie some of the gene expression changes in psoriatic skin. Thus, I sought to characterize the global landscape of miRNA expression in human skin, and to investigate the functional roles of miRNAs with respect to psoriasis pathogenesis. I profiled small RNAs in human skin with Next Generation sequencing, and detected known miRNAs, variants of known miRNAs, and novel miRNAs with unprecedented sequencing depth. Eighty known and 18 novel miRNAs were two- to 42-fold differentially expressed in psoriatic skin. Computational and experimental analysis of miRNA targets revealed that three differentially expressed miRNAs directly regulate

components of the skin barrier, and that these regulatory interactions have recent evolutionary origins. I also identified other species of small RNAs, such as endogenous small interfering RNAs (siRNAs) in skin, but determined that they are typically less abundant than miRNAs. Like miRNAs, some of these are differentially expressed in psoriasis, and may function as regulators of gene expression. Overall, this work has greatly increased our understanding of the depth and breadth of small RNA species expressed in human skin, and implicated a large number of small RNAs in psoriasis pathogenesis.

ACKNOWLEDGEMENTS

To Dr. Anne Bowcock, thank you for your excellent guidance and inspired ideas, and for allowing me room to grow under your mentorship. It has been a pleasure working with you.

To my fellow lab members, thanks for your support, and for lots of laughs along the way. Special thanks to my dear friend Li Cao, for so many enlightening conversations (both scientific and personal) over the years.

To my thesis committee, thank you for your valuable insight and encouragement. In particular, computational analyses completed by Weixiong Zhang and his graduate students, Jing Xia and Xiang Zhou, have been critical to the completion of this work. Special thanks to Dr. Michael Lovett who has provided equal and ample shares of sage advice and hearty laughs.

To Dr. Catherine Freudenreich, Dr. Michelle Gaudette and other members of the Biology Department at Tufts University, thank you for challenging me and inspiring me to pursue a career in research.

To Adam, Saint Louis will always be a special place to me because its where I fell in love with you. Thank you for all the happy memories, and for the countless ways in which you brighten my life every single day.

To my brothers, Michael and Adam, thank you for being at my side and on my side from preschool to grad school. You bring the perfect mix of honesty, understanding, and comic relief to my life.

To my mom and dad, since this is a genetics thesis, I feel compelled to first thank you for sharing many heritable traits that have helped me get this far. More importantly,

thank you for teaching me to live a full and balanced life; for investing in my strengths and interests; and for being proud of me at my best and worst. I could never have arrived here without you.

TABLE OF CONTENTS

TABLES AND FIGURES

Chapter 1.

Introduction and perspective

Clinical and molecular features of psoriasis

Human skin is a complex organ that serves many vital functions; these include preventing dehydration, forming a barrier against infection, and regenerating in response to injury (1). The epidermis is the outermost layer of the skin. It consists of the basal layer, spinous layer, granular layer, and stratum corneum. The basal layer is populated by proliferative keratinocytes and epidermal stem cells (2). As basal keratinocytes migrate outwards through the spinous and granular layers, they undergo a process called terminal differentiation (2). Many transcriptional and morphological changes occur as terminal differentiation progresses such that by the time keratinocytes reach the skin surface, they are enucleated and encased in a proteinaceous cornified envelope (2). Terminally differentiated keratinocytes, termed corneocytes, are cemented together by a lipid-rich matrix, forming an organized, impenetrable, and renewable epidermal barrier (2). In normal skin, the process of terminal differentiation occurs over approximately 40 days (3).

In addition to keratinocytes, immune cells such as T cells and dendritic cells are present at low levels in normal skin (4). Cytokine signaling between keratinocytes and immune cells is an important regulator of proliferation, differentiation, inflammation, and regeneration in the skin. Indeed, defective cross talk between these cells is thought to be a key mediator of the common skin disease psoriasis (4,5,6).

Psoriasis is a chronic, inflammatory skin disease characterized by the presence of inflamed, scaly lesions on the skin (Figure 1-1). Psoriasis affects 2-3% of Caucasians, and is less prevalent in Asians and Africans (7). There are several types of psoriasis, the most common of which is psoriasis vulgaris, or plaque psoriasis, which accounts for

~90% of cases (8). Other less common forms of psoriasis include guttate, inverse, pustular and erythrodermic (8). Psoriasis patients experience profound psychosocial effects and are at increased risk for metabolic syndrome, cardiovascular disease and stroke (9,10,11,12). Moreover, 10-30% of psoriasis patients develop a progressive, inflammatory arthritis termed psoriatic arthritis (13). There is currently no cure for psoriasis, although treatments such as phototherapy, topical medications, and systemic biologics can reduce the frequency and severity of outbreaks (14).

Cellular alterations in involved psoriatic skin include hyperproliferation and altered differentiation of keratinocytes, and infiltration and activation of immune cells (Figure 1-2; 5). Involved psoriatic keratinocytes undergo an alternative differentiation program similar to that seen during regeneration (15), and they reach the surface of the skin within 6-8 days (3,5). Involved psoriatic keratinocytes also secrete a number of factors that promote leukocyte adhesion and activation, such as beta-defensin and the S100 proteins (16). Immune cell subsets thought to be involved in psoriasis pathogenesis include Th1 and Th17 cells (17,18). Th1 cells secrete inflammatory cytokines such as interleukin-1 (IL1), tumor necrosis factor alpha (TNFA), and interferon gamma (IFNG), while Th17 cells secrete interleukin-17 (IL17) and interleukin-22 (IL22). All of these cytokines are upregulated in involved skin compared to uninvolved and normal skin (17,18,19). These cytokines likely act on resident keratinocytes to promote hyperproliferation and serve to recruit additional immune cell populations which perpetuates inflammation.

The onset and severity of psoriasis depends on genetic and environmental factors. While many cases are sporadic, siblings of psoriasis patients have a 4-6 fold increased

risk of developing the disease compared to the general population (7). Environmental triggers include skin trauma, HIV infection, and certain drugs (20,21,22). Genetic studies have identified risk alleles related to the immune system and skin barrier.

Genomic approaches to understanding psoriasis

Family based linkage studies have implicated up to 20 loci as contributing to psoriasis susceptibility (6). However, most of these loci failed to replicate in multiple families or populations. This may be due to weak effects; contribution of population specific, familial, or private risk alleles; or confounding environmental factors. The major histocompatibility complex (MHC) is the one locus that has been replicated in all of these linkage studies, and has also been robustly linked to other autoimmune diseases such as systemic lupus erythematosus, type 1 diabetes, and rheumatoid arthritis (6). Another locus that was replicated in two large families is PSORS2 on 17q.25 (23,24). Recent exome sequencing of the region of linkage has revealed independent gain of function mutations in the *CARD14* gene in two independent multiplex psoriasis families (25). *CARD14* is expressed in keratinocytes and encodes an activator of NF-kB. The familial mutations augment NF-kB activation (25,26). This finding adds to the increasing body of evidence that keratinocyte-derived factors can drive psoriasis pathogenesis.

Genome wide association studies (GWAS) have unveiled additional psoriasis risk loci, many of which are related to immunity and inflammation. Consistent with linkage analyses, the strongest of these associations is the HLA-Cw6 allele within the MHC, which is present in ~46% of psoriasis patients, but only ~7% of controls (27). Components of the Th17 pathway (IL12B, IL23A, IL23R) are also associated with

psoriasis, as are regulators of NF-kB (TNFAIP3, TNIP1) (28,29,30). Additionally, GWAS has uncovered epidermal genes that contribute to psoriasis susceptibility. One example is the cluster of genes on chromosome 8 encoding B-defensin (DEFB), which is secreted by keratinocytes in psoriatic skin. DEFB copy number is highly polymorphic in the population, and increased copy number is associated with psoriasis (31). A deletion polymorphism within the epidermal differentiation complex (EDC) on chromosome 1 is associated with psoriasis in European and Chinese populations (30,32). This deletion results in the loss of the late cornified envelope genes LCE3B and LCE3C, and an enhancer element related to keratinocyte differentiation.

Our lab and others have performed genome-wide expression studies with array based technologies, and identified over 1,300 alterations in mRNA transcript levels in involved and uninvolved psoriatic skin (Table 1-1; 18,19). Keratinocyte derived transcripts such as defensin-B4 (DEFB4), S100 calcium binding proteins, keratin 16 (KRT16), and late cornified envelope-3D (LCE3D; are among the most highly upregulated. Macrophage-derived interleukin-8 (IL8) is the most highly upregulated cytokine (19). Strongly downregulated genes include the Wnt inhibitory factor-1 (WIF1), interleukin-1 family member 7 (IL1F7), chemokine (C-C motif) ligand-27 (CCL27), keratin-1B (KRT1B), and fatty acid binding protein 7 (FABP7; 19). Overall, upregulated genes are enriched for immune/defense/wounding response, mitotic cell cycle, ectoderm development, and keratinocyte differentiation functions; downregulated genes are enriched for organismal/system/organ development, fatty acid and lipid metabolic processes, and blood circulation functions (19).

Systems biology of psoriasis

Linkage analysis, GWAS, and microarray studies undertaken over the last 20 years have revealed many psoriasis susceptibility factors and led to a greater understanding of the pathways involved in disease pathogenesis. Despite this, a recent study combining ten of the most significant psoriasis risk loci could only account for ~12% of the genetic susceptibility to psoriasis (33). Moreover, the identification of true causative variants and assessment of their contribution to psoriasis susceptibility and pathogenesis will require innovative new approaches.

Along these lines, the Bowcock laboratory is taking an integrative approach towards a systems biological understanding of psoriasis. That is to say, we are interested in the in the cumulative and sometimes combinatorial effects of coding and noncoding DNA sequence variation, quantitative and qualitative changes in gene expression, and perturbation of regulatory networks mediated by protein and RNA on psoriasis susceptibility and pathogenesis. One important piece of this puzzle is the expression and function of small noncoding regulatory RNAs (sncRNAs). sncRNAs play critical roles in gene regulation for nearly all biological processes in eukaryotic organisms including mRNA cleavage, RNA degradation, translation inhibition, and DNA methylation (34). microRNAs (miRNAs) in particular have been heavily studied in recent years and shown to be essential gene regulators that broadly contribute to disease pathogenesis.

miRNAs: Discovery, biogenesis and function

The founding member of the miRNA family, *lin-4*, was discovered as part of a screen for developmental phenotypes in *C. elegans* (35,36). Mutations in *lin-4* lead to

reiteration of the earliest larval (L1) cell division patterns during a later developmental stage (L2; 36). Conversely, mutations in another gene, *lin-14*, lead to the opposite developmental phenotype, premature exit from L1 (37). Twelve years later, it was found that the *lin-4* gene encodes a 22 nucleotide (nt) noncoding RNA, which is partially complementary to seven sites within the 3'UTR of the *lin-14* mRNA transcript (38). Thus, it was hypothesized that direct interactions between *lin-4* and the *lin-14* 3'UTR resulted in repression of *lin-14* expression. Indeed, biochemical experiments confirmed the physical interaction between the *lin-4* small RNA and *lin-14* 3'UTR and suggested that translational inhibition was the mechanism underlying *lin-14* repression (39,40,41). A second developmentally regulated gene in *C. elegans*, *lin-28*, also harbors *lin-4* sites within its 3'UTR and is negatively regulated by the miRNA (42). This finding highlights one key feature of the miRNA family, which is the ability to regulate multiple target genes.

To date, nearly 2000 distinct human miRNAs have been cataloged in the miRNA database miRBase (v18; 43,44,45). miRNA genes can be intergenic or intronic, and some are found within genomic clusters that are transcribed as polycistronic primary transcripts (pri-miRNAs; 46,47). Most miRNA genes are transcribed by RNA polymerase II, and pri-miRNAs are polyadenylated RNAs that can be up to several kilobases long and contain one or more hairpin sequences (48,49). These hairpins are typically comprised of a ~33nt double stranded region connected by a terminal loop and flanked by single stranded RNA(50). Such structures are recognized and cleaved by the RNase type III enzyme Drosha and its binding partner DGCR8 in the nucleus, resulting in the release of a ~60nt precursor miRNA (pre-miRNA) hairpin (50). The pre-miRNA is exported to the

cytoplasm via the nuclear transport receptor exportin-5 (XPO5; 51,52,53). In the cytoplasm, the pre-miRNA is recognized and cleaved by another RNase type III enzyme, Dicer, resulting in the release of a ~22nt double stranded RNA (54,55,56,57,58). Following Dicer cleavage, the RNA duplex is unwound by an as yet unknown helicase and a single strand of the RNA duplex (miRNA strand) is incorporated into the RNA-induced silencing complex (RISC). The unincorporated strand (miRNA* strand) was thought to be rapidly degraded, although subsequently a number of retained miRNA* species have been identified (59,60). Strand selection depends partially on thermodynamic properties of the miRNA/miRNA* duplex, but tissue specific variability in strand selection supports either some amount of stochasticity or the existence of additional regulatory mechanisms (61).

Mature miRNAs function as guide sequences which direct the RISC complex to particular target mRNAs. The components of RISC have been somewhat difficult to pin down, and RNA silencing activity has been associated with a variety of complexes ranging from 160-550kDa (62). However, it is known that an Argonaute family protein and a GW182 protein are essential to the complex (63). In humans, there are four Ago family members, referred to as Ago1-4. Ago family proteins contain three domains: a Piwi/Argonaute/Zwille (PAZ) domain, a middle (MID) domain, and a P-element induced wimpy testes in Drosophila (PIWI) domain. The PAZ and MIDI domains recognize the 3’ and 5’ ends of the miRNA, respectively, while PIWI is an RNase H domain that can mediate single stranded RNA cleavage and also binds GW182 (64,65,66). In humans, Ago1-4 associate with largely overlapping sets of miRNAs and proteins, although Ago2

is the only human Ago protein for which the PIWI RNase H domain is catalytically active (67,68).

GW182 is another essential RISC component. In fact, it is likely to be an important functional subunit, as tethering of the C-terminal fragment of GW182 to an mRNA is sufficient to induce translational repression and mRNA destabilization (69,70,71). There are three GW182 proteins in humans, which are encoded by the genes TNRC-A, -B, and –C. The GW182 proteins contain four known domains: a N-terminal glycine-tryptophan (GW) repeat domain, a ubiquitin-associated domain (UBA), a glutamine-rich domain (Q-rich), and an RNA recognition motif (RRM). The N-terminal GW repeat domain interacts with Ago proteins while a domain of unknown function and the C-terminal RRM comprise the RNA silencing region (70,71).

miRNA target recognition is largely dependent on reverse complementarity between the 5' end of the miRNA and a short segment of the target 3'UTR (72). The key bases for target recognition appear to be nucleotides 2-8 of the miRNA, which are collectively referred to as the "seed" sequence (72). The rest of the miRNA typically exhibits degenerate complementarity, with a characteristic bulge at positions ~9-11 (73,74,75). This bulge interrupts base pairing at the potential Ago2 cleavage site (76), such that direct mRNA cleavage is not a common mechanism for miRNA-mediated repression in humans. In addition to seeded binding sites, there exist "3' compensatory" binding sites, where degeneracy in the seed region can be overcome by complementarity in the remaining sequence (77). Target recognition may also be influenced by local sequence context; for example, sequence flanking miRNA target sites tends to be AU-rich (72). Overall, the principles governing target recognition are still not well

understood. Nevertheless, various target prediction algorithms exist, such as TargetScanS, miRanda, and PicTar. Each of these algorithms applies some combination of weighted parameters accounting for seed match, free energy of binding, and conservation (78). Recent estimates indicate that ~60% of human mRNAs contain conserved miRNA binding sites in the 3'UTR and that a particular miRNA family (comprised of miRNAs with identical seed regions) targets ~500 conserved 3'UTR sites, on average (79).

Early miRNA studies in *C. elegans*, among others, found that miRNA binding resulted in decreased protein levels, independent of mRNA levels (40,63). Thus, it was thought that translational repression was the primary mechanism of miRNA-mediated RNA silencing in metazoans. Despite this, more recent work has pointed towards mRNA destabilization via deadenylation and decapping. In 2005, it was shown that decreases in *lin-14* and *lin-28* mRNA levels in L2 stage worms are *lin-4* dependent (80). More recently, ribosome profiling experiments on exogenous and endogenous miRNA-targeted transcripts have indicated that mRNA destabilization accounts for a large proportion of miRNA-mediated repression (81). Based on the number of conflicting studies, it remains unclear which mechanism is dominant in metazoans. However, it seems likely that both mechanisms may contribute to some extent, depending on the exact nature of the miRNA:mRNA interaction, transcript abundance, or expression of cofactors in particular cells and organisms. Key features of miRNA biogenesis and function are summarized in Figure 1-3.

Role of miRNAs in human development and disease

miRNAs have important roles in development and disease. Indeed, deletion of the miRNA processing enzyme Dicer is lethal in mice and zebrafish (82,83). This is perhaps not surprising in light of the myriad biological processes mediated by miRNAs, including cell differentiation, apoptosis, metabolism, developmental timing and patterning, and organogenesis, among others (84). In the case of skin, epidermal specific knockouts of Dicer1 or its binding partner Dgcr8 in the mouse embryo perturb the development of the epidermal barrier and epidermal appendages (Figure 1-3; 85,86). Knockout animals are born in expected Mendelian ratios and appear normal at birth, despite increased apoptosis in the prenatal epidermis and hair germ. However, by postnatal day 1.5 (P1.5), epidermal cysts begin to form due to evagination of hair germs. By P2, knockout mice begin to lose body mass due to dehydration, and perish by P6.

Individual miRNAs have been implicated in skin homeostasis by expression profiling during the course of keratinocyte differentiation. Calcium-induced differentiation of normal human epidermal keratinocytes resulted in differential expression of many miRNAs after three or seven days (87). Moreover, populations of epidermal stem cells, transient amplifying keratinocytes, and terminally differentiated keratinocytes derived from human skin biopsies exhibited differential miRNA expression (87). A few miRNAs are also upregulated during the formation of cultured epidermal equivalents, in which primary keratinocytes are exposed to an air/liquid interface that stimulates epidermal stratification (88).

In addition to keratinocytes, human skin contains small populations of immune and immune-regulatory cells, which modulate the cutaneous response to injury and infection. These include skin homing T cells, resident dendritic cells, neutrophils,

Langerhan's cells, and regulatory T cells. miRNAs have been shown to influence the development, survival, and activation of these cells (89), and immune cell-derived miRNAs have been shown to modulate cytokine expression in the skin (90). Thus, immune-derived miRNAs also influence proliferation, differentiation, inflammation, and regeneration in the skin.

Recently, genomic miRNA profiling techniques and identification of miRNA targets in human tissues and cell lines have provided insights into many human diseases, particularly cancer (91,92,93,94). For example, in the case of melanoma, microarray-based miRNA profiling led to the observation that miR-211 was downregulated in an invasive melanoma derivative cell line compared to a non-invasive derivative (91). Interestingly, miR-211 lies within an intron of the melastatin-1 (MLSN1) gene, long thought to be a melanoma tumor suppressor. In fact, expression of miR-211, but not the melastatin protein, suppress cell migration and invasiveness in melanoma cell lines, indicating that the miRNA is the true tumor suppressor (95). miR-211 likely exerts its tumor suppressor function by targeting at least two central node genes in the melanoma metastasis gene expression network: TGFBR2 and NFAT5 (95).

Current understanding of miRNAs in psoriasis

In the case of psoriasis, two independent miRNA microarray studies interrogating ~561 known miRNAs have implicated 82 miRNAs (Table 1-2). The first study reported ±1.4-fold differential expression of 29 miRNAs in involved psoriatic versus normal skin, and noted that 20 of these are not differentially expressed in another inflammatory skin disease, atopic dermatitis (96). The second study reported ±1.2-fold differential

expression of 53 miRNAs, including 10 miRNAs that are differentially expressed in uninvolved psoriatic versus normal skin (97). Discordance between these studies was fairly high, with only 9 overlapping differentially expressed miRNAs overall. A lower rate of discordance is observed for more highly differentially expressed genes: nine of 23 miRNAs (39%) with two- to eight-fold changes were concordant between the two studies. Overall, high rates of discordance between the two studies are likely a reflection of natural variation (genotype, disease severity, etc.), low sensitivity of microarrays, and hybridization nuances that are particularly relevant to short sequences. Moreover, the small number of consistent miRNA expression changes and the low magnitude of differential expression are inconsistent with the dramatic shift in cellular composition, differentiation, and gene expression characteristic of involved psoriatic skin.

Likewise, little progress has been made on the identification of biologically relevant miRNA targets in psoriatic skin. This is likely due to technical obstacles and to the complex cellular architecture of the skin, particularly in the case of inflamed psoriatic skin. It was initially reported that upregulation of miR-203 in involved skin led to repression of the suppressor of cytokine signaling-3 (SOCS-3) mRNA (96), but subsequent studies have failed to replicate this finding (98,99). These studies point towards miR-203 repression of a particular p63 isoform (ΔNp63) in the suprabasal layers as a mechanism for decreasing the proliferative potential of terminally differentiating keratinocytes (98,99). Other studies have reported miRNA mediated repression of tissue inhibitor of metalloproteinase-3 (TIMP3), insulin-like growth factor-1 receptor (IGF1R), and fibroblast growth factor receptor-2 (FGFR2) by miR-221/222, miR-99a, and miR-125b, respectively, in involved skin (97,100).

The paucity of consistent results from microarrays indicated that more sophisticated techniques were needed to advance our understanding of the role of miRNAs in psoriasis. Successful applications of Next Generation sequencing (NGS) to small RNA expression profiling highlight the utility of this platform (92,93,94). Thus, I have used NGS to comprehensively profile small RNA expression in normal and psoriatic skin. This approach confers distinct advantages over microarray platforms such as the ability to detect low abundance small RNAs; novel small RNAs; and small RNA sequence variants due to underlying DNA sequence variation, RNA editing, or variability in small RNA processing. In the following chapters, I describe the global landscape of sncRNAs in human skin, the misexpression of a subset of sncRNAs in psoriatic skin, and potentially pathogenic functions of differentially expressed sncRNAs. This work has greatly improved our understanding of sncRNA expression in normal and diseased human skin and provided a valuable resource for the psoriasis and small RNA communities.

TABLES AND FIGURES

Table 1-1. Top differentially expressed genes in involved psoriatic versus normal skin, from Gudjonsson *et al.* 2010 (19).

Gene symbol	Gene title	Fold change	FDR *P*-value	Mean in control (log2)	Mean in uninvolved (log2)	Mean in lesional (log2)
(A) Upregulated PP versus NN						
SERPINB4	Serpin peptidase inhibitor, clade-B, member-4	377	0	4.9	5.5	13.5
DEFB4	Defensin, β4	197	0	6.2	6.8	13.9
S100A7L1	S100 calcium-binding protein-A7-like-1	150	0	5.0	5.2	12.2
PI3	Peptidase inhibitor-3, skin-derived (SKALP)	131	0	6.5	7	13.5
SERPINB3	Serpin peptidase inhibitor, clade-B, member-3	64	0	7.0	7.4	13.0
SPRR2C	Small proline-rich protein-2C	58	2.2E-264	4.4	4.6	10.3
AKR1B10	Aldo-keto reductase family-1, member-B10	58	0	5.9	6.4	11.8
S100A12	S100 calcium-binding protein-A12 (calgranulin-C)	57	0	4.7	4.9	10.6
S100A9	S100 calcium-binding protein-A9 (calgranulin-B)	57	0	8.7	9.3	14.5
C10orf99	Chromosome-10 open reading frame-99	32	0	6.0	6.9	11.4
KYNU	Kynureninase (L-kynurenine hydrolase)	25	0	6.1	6.1	10.8
LCE3D	Cornified envelope-3D	24	0	8.9	9.7	13.5
S100A7	S100 calcium-binding protein-A7 (psoriasin-1)	18	3.3E-114	9.9	10.7	14.1
IL-8	Interleukin-8	17	1.3E-53	4.3	4.4	8.4
KRT16	Keratin-16	17	5.7E-272	9.4	9.4	13.5
(B) Downregulated PP versus NN						
WIF1	Wnt-inhibitory factor-1	−14.0	4.5E-91	9.6	9.4	5.8
BTC	β-Cellulin	−13.9	5.6E-167	8.4	8.6	4.6
THRSP	Thyroid hormone responsive spot-14	−9.4	1.6E-24	11.1	10.5	7.9
IL1F7	Interleukin-1 family, member-7 (zeta)	−8.4	3.5E-79	9.4	9.7	6.3
CCL27	Chemokine (C–C motif) ligand-27	−7.7	7.5E-76	9.9	10.1	7.0
KRT1B	Keratin-1B	−7.6	4.9E-112	11.6	11.7	8.7
MSMB	Microseminoprotein, β	−6.5	2.4E-55	7.3	7.1	4.6
ELOVL3	Elongation of very long chain fatty acids-like-3	−6.5	1.4E-18	8.9	8.0	6.2
GAL	Galanin	−6.4	1.1E-16	9.4	8.5	6.7
FABP7	Fatty acid binding protein 7, brain	−6.0	1.7E-19	9.5	9.1	6.9
ACSBG1	Acyl-CoA synthetase bubblegum family member-1	−5.7	3.8E-19	9.2	8.5	6.6
MLSTD1	Male sterility domain containing-1	−5.2	9.8E-20	8.8	7.8	6.3
HS3ST6	Heparan sulfate (glucosamine) 3-*O*-sulfotransferase-6	−4.2	2.9E-79	8.6	8.6	6.5
WDR72	WD repeat domain-72	−4.2	5.3E-46	8.3	8.1	6.2
SERPINA12	Serpin peptidase inhibitor, member-12	−4.1	1.5E-38	11.2	11.5	9.2

Abbreviations: FDR, false discovery rate; NN, non-psoriatic normal; PP, psoriatic plaque.

Table 1-2. Summary of previously described differentially expressed miRNAs in psoriatic skin, adapted from Sonkoly *et al.*, 2007 (96) and Zibert *et al.*, 2010 (97).

Upregulated miRNAs

Sonkoly *et al.* 2007			Zibert *et al.* 2010		
miRNA	**Fold change**	**Comparison[a]**	**miRNA**	**Fold change**	**Comparison**
miR-146b[b]	**3.31**	PP vs. NN	let-7g	1.5	PP vs. NN
miR-20a	**2.9**	PP vs. NN, AD vs. NN	let-7i	1.79	PP vs. NN
miR-146a	**3.3**	PP vs. NN, AD vs. NN	**miR-141**	**1.56**	**PP vs. NN**
miR-31	**4.69**	PP vs. NN	miR-200a	2.01	PP vs. NN
miR-200a	2.75	PP vs. NN	miR-16	2.33	PP vs. NN
miR-17-5p	**3.77**	PP vs. NN, AD vs. NN	**miR-17**	**1.73**	**PP vs. NN**
miR-30e-5p	3.61	PP vs. NN	**miR-20a**	**2.4**	**PP vs. NN**
miR-141	**3.45**	PP vs. NN	miR-106b	1.68	PP vs. NN
miR-203	**5.86**	PP vs. NN	**miR-21**	**7.65**	**PP vs. NN**
miR-142-3p	**2.55**	PP vs. NN	miR-27a	2.36	PP vs. NN
miR-21	**2.51**	PP vs. NN, AD vs. NN	miR-27b	1.71	PP vs. NN
miR-106a	2.37	PP vs. NN, AD vs. NN	miR-29a	1.65	PP vs. NN
			miR-29c	1.73	PP vs. NN
			miR-30b	1.53	PP vs. NN
			miR-30c[b]	*1.4*	*PP vs. NN*
			miR-31	**4.14**	**PP vs. NN**
			miR-107	1.47	PP vs. NN
			miR-125a-3p	1.53	PP vs. NN
			miR-126	2.13	PP vs. NN
			miR-136	1.34	PP vs. NN
			miR-142-3p	**4.69**	**PP vs. NN**
			miR-142-5p	2.32	PP vs. NN
			miR-146a	**3.1**	**PP vs. NN**
			miR-146b-5p	**2.73**	**PP vs. NN**
			miR-148b	1.48	PP vs. NN
			miR-155	1.24	PP vs. NN
			miR-183	1.24	PP vs. NN
			miR-193a-3p	2.34	PP vs. NN
			miR-199a-3p	1.89	PP vs. NN
			miR-203	**2.02**	**PP vs. NN**
			miR-205	1.8	PP vs. NN
			miR-221	1.54	PP vs. NN
			miR-222	1.47	PP vs. NN
			miR-223	4.82	PP vs. NN
			miR-324-3p	1.31	PP vs. NN
			miR-342-3p	1.68	PP vs. NN
			miR-378	2.15	PP vs. NN
			miR-518a-5p	1.87	PP vs. NN
			miR-22	*2.3, 1.41*	*PP vs. NN, PN vs. NN*
			miR-24-1	1.51, 1.41	PP vs. NN, PN vs. NN
			miR-498	1.54, 1.71	PP vs. NN, PN vs. NN
			miR-551a	1.36, 1.98	PP vs. NN, PN vs. NN
			miR-10b	1.32	PN vs. NN
			miR-501-3p	1.58	PN vs. NN
			miR-612	1.62	PN vs. NN
			miR-654	1.51	PN vs. NN
			miR-760	1.47	PN vs. NN

Downregulated miRNAs

Sonkoly *et al.* 2007			Zibert *et al.* 2010		
miRNA	**Fold change**	**Comparison**	**miRNA**	**Fold change**	**Comparison**
miR-125b	-1.82	PP vs. NN	miR-138	-1.48	PP vs. NN
miR-99b	-1.72	PP vs. NN	miR-183*	-1.44	PP vs. NN
miR-122a	-5.56	PP vs. NN, AD vs. NN	miR-338-5p	-1.31	PP vs. NN
miR-197	-1.56	PP vs. NN	miR-627	-1.24	PP vs. NN
miR-100	-1.69	PP vs. NN	miR-659	-1.25	PP vs. NN
miR-381	-1.41	PP vs. NN	miR-518c*	-1.35	PN vs. NN
miR-518b	-1.79	PP vs. NN			
miR-524*	-2.00	PP vs. NN			
let-7e	-1.67	PP vs. NN			
miR-30c	*-1.59*	*PP vs. NN*			
miR-365	-1.61	PP vs. NN			
miR-133b	-4.55	PP vs. NN, AD vs. NN			
miR-10a	-1.49	PP vs. NN			
miR-133	-2.50	PP vs. NN			
miR-22	*-1.64*	*PP vs. NN*			
miR-326	-1.79	PP vs. NN, AD vs. NN			
miR-215	-1.79	PP vs. NN, AD vs. NN			

Normal skin, NN; Uninvolved psoriatic skin, PN; Involved psoriatic skin, PP; Atopic dermatitis skin, AD
miRNAs in bold were concordant between the two studies; miRNAs in italics were discordant

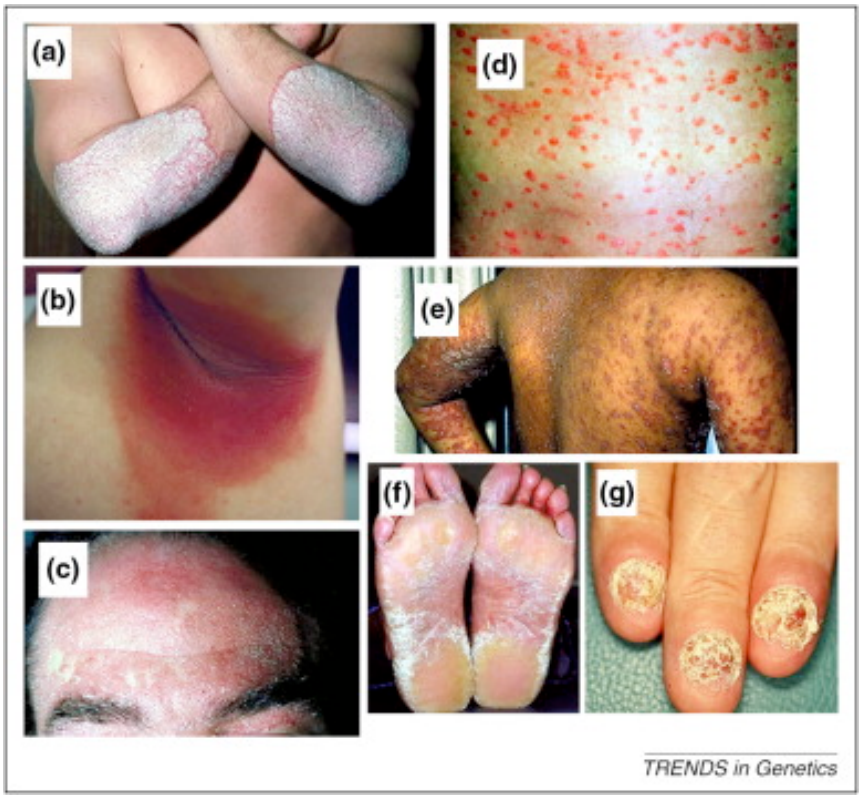

Figure 1-1. Clinical manifestations of psoriasis, from Roberson & Bowcock, 2010 (5). a) plaque psoriasis, b) inverse psoriasis, c) seborrheic psoriasis, d) guttate psoriasis, e) pustular psoriasis, f) palmoplantar psoriasis, and g) nail pitting associated with psoriasis.

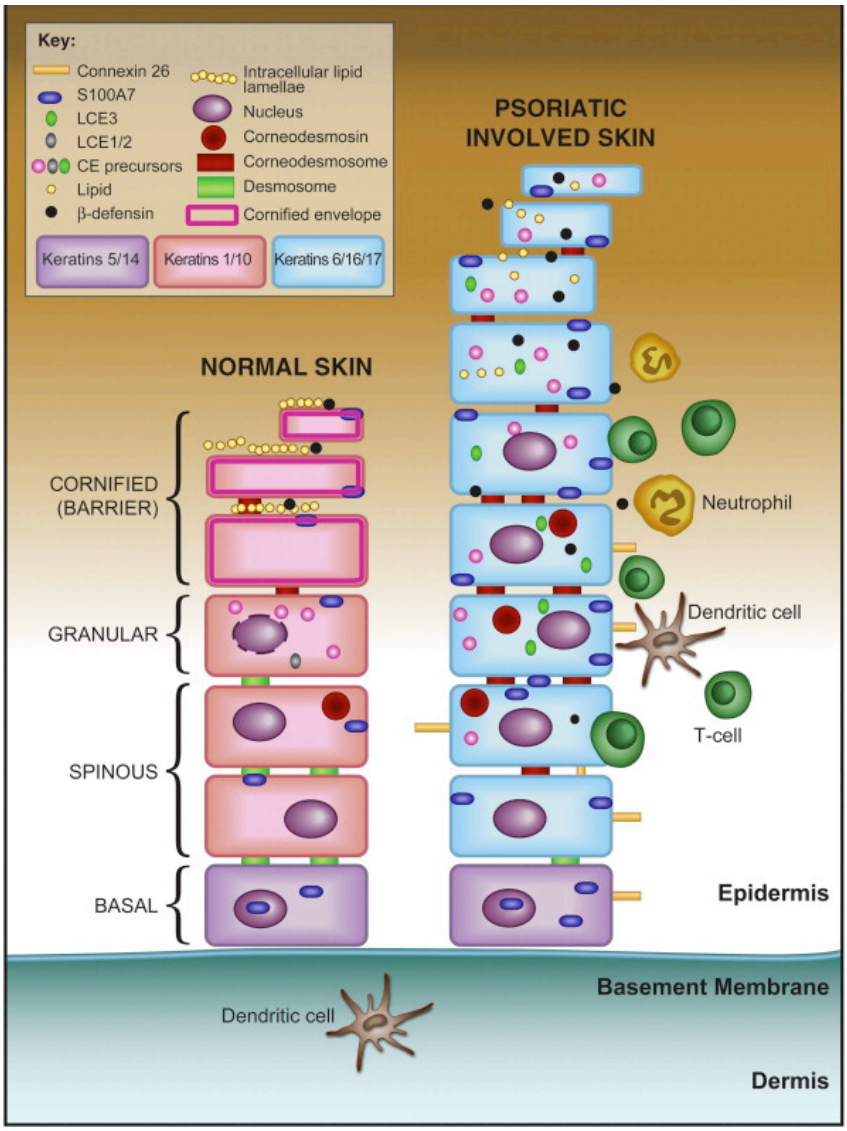

Figure 1-2. Molecular and cellular alterations in involved psoriatic skin, from Roberson & Bowcock, 2010 (5).

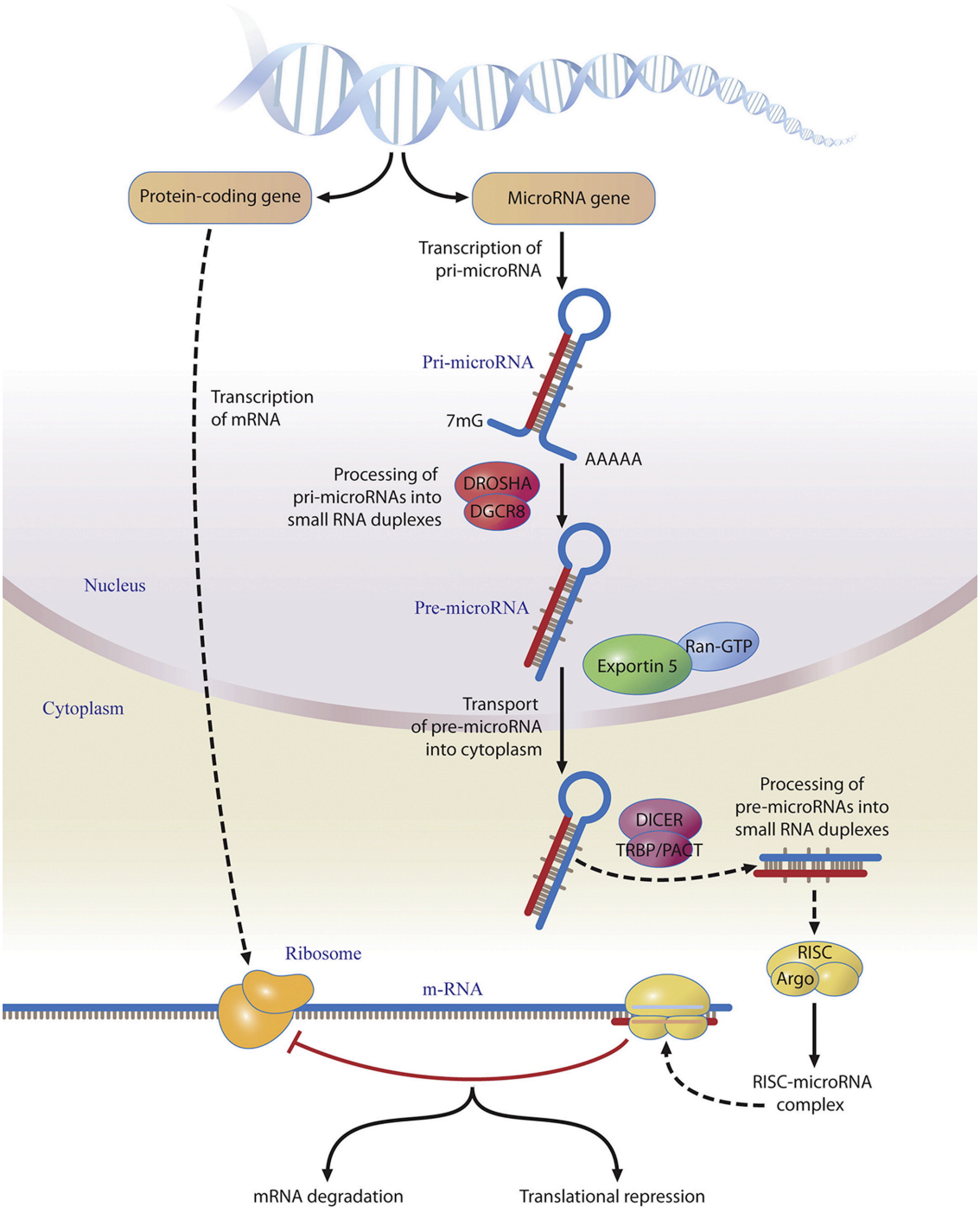

Figure 1-3. microRNA biogenesis and function, adapted from Chen *et al.* 2005 (101).

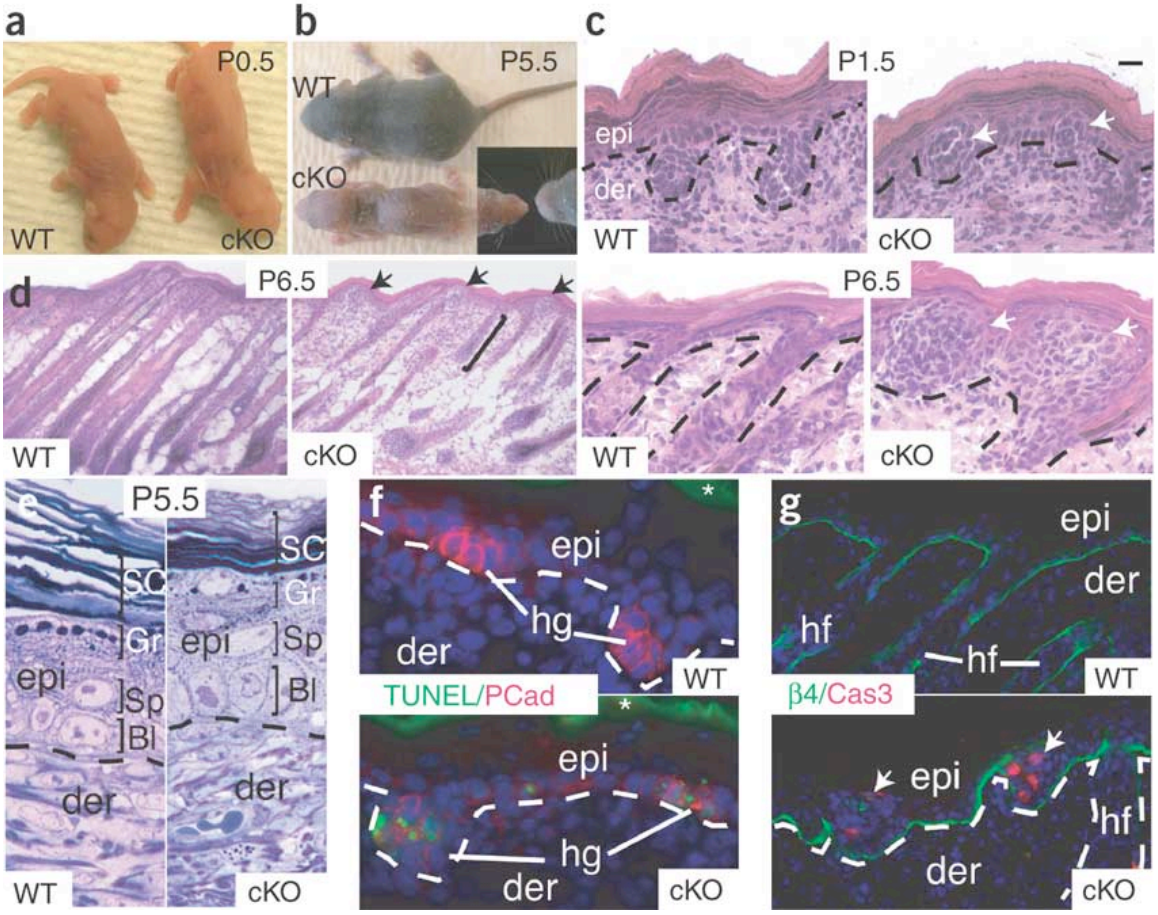

Figure 1-4. Conditional knockout of Dicer in the developing epidermis, from Yi *et al.* 2006 (85). Gross morphological features of wild-type and epidermal Dicer1 knockout litter mates at a) P0.5 and b) P5.5. Development of follicular cysts in knockouts at c) P1.5 and d) P6.5. e) Normal epidermal stratification in WT and knockout littermates. f) Apoptosis in the epidermis and hair follicles labeled by f) TUNEL at E17.5 and g) caspase-3 at P6.5. P-cadherin labels hair germs and integrin-β4 labels basement membrane.

Chapter 2.

The global miRNA landscape in human skin

ABSTRACT

microRNAs (miRNAs) are a class of short, regulatory RNAs that play critical roles in human development and disease. In the skin, conditional knockout of the miRNA processing enzyme, Dicer, leads to epidermal abnormalities. I profiled global miRNA expression in human skin with Next Generation sequencing. I generated $6.7x10^8$ qualified small RNA reads, representing the largest small RNA sequencing dataset derived from any human tissue to date. The global landscape of miRNAs in normal and psoriatic skin included 717 known miRNAs and 176 cognate miRNA*s; a number of previously undescribed miRNA*s from known miRNA loci; known miRNA variants such as isomiRs and edited miRNAs; and 284 expressed novel miRNA loci. I validated the endogenous expression and processing of three novel miRNAs in skin and other human cell lines or tissues. Of particular note was the discovery and validation of a novel antisense miRNA derived from the miR-203 locus, which has a role in epidermal differentiation. The global profiling of miRNAs in human skin is a critical first step towards understanding how miRNAs contribute to the skin's ability to regenerate and respond to the environment.

INTRODUCTION

microRNAs (miRNAs) are a class of short, regulatory RNAs that play critical roles in human development and disease (38,47,84,102). They are transcribed as long stem-loop precursors, which undergo a number of processing steps resulting in the generation of a functional ~22 nucleotide (nt) single-stranded miRNA. Most miRNA precursors are cleaved through a canonical pathway involving the RNase type III enzymes Drosha and Dicer (103). One key exception is some intronic miRNAs, termed miRtrons, for which spliceosome processing replaces the Drosha cleavage step (104,105). Following cleavage, one or both strands of the RNA duplex (RISC; 59,60). Because double stranded miRNA precursors encode two potential mature miRNAs (the miRNA and miRNA*, also referred to as -3p and -5p arms) with distinct seed sequences and target profiles, strand selection is an important regulatory step in miRNA biogenesis. Mature miRNAs function by directing the RNA silencing machinery to partially complementary target mRNA transcripts. A single miRNA has the potential to regulate many different targets within a given cell (106,107), and thus the spatial and temporal regulation of miRNAs is likely to be of critical importance for the proper development and maintenance of many human cells and tissues.

The first evidence for a role for miRNAs in skin differentiation came from the observation that epidermal specific knockouts of *Dicer1* (and later *Dgcr8*) in the mouse embryo perturb development of the epidermis and epidermal appendages (85,86). Subsequently, the roles of a few specific miRNAs have been examined. For example, the

expression of miR-203 is induced in the skin at the onset of epidermal stratification, where it is restricted to the suprabasal epidermis (99). Precocious expression of miR-203 in the basal epidermis leads to a decrease in proliferative potential whereas inhibition of miR-203 in the suprabasal epidermis enhances proliferation (99). A key evolutionarily conserved target of miR-203 is the transcription factor, p63 (98,99). p63 is expressed in the highly proliferative keratinocytes of the basal epidermis, and p63-/- mice have no epidermis (108). The current model is that miR-203 expression in the suprabasal layers of the epidermis inhibits expression of p63, thereby suppressing the proliferative potential of terminally differentiating keratinocytes. Induction of miR-203 in proliferating keratinocytes is not sufficient to induce differentiation (98) and p63 is indeed regulated by other regulatory interactions, such as ubiquitination (109). However, it is likely that miR-203 regulation is one of many factors contributing to the establishment and maintenance of the stratified epidermis.

A deeper understanding of miRNA expression in normal and diseased human skin would provide insights into the gene regulatory networks that are critical to the skin's ability to regenerate and respond to the environment. Here, I describe miRNA expression profiling of 67 normal and psoriatic human skin biopsies with Next Generation sequencing (NGS) of small RNAs. The global landscape of miRNAs in normal and psoriatic skin included 717 known miRNAs and 176 cognate miRNA*s; a number of previously undescribed miRNA*s from known miRNA loci; known miRNA variants such as isomiRs and edited miRNAs; and 284 expressed novel miRNA loci. This work has greatly increased our understanding of miRNA expression in human skin and

provides a critical foundation for functional characterization of miRNAs in normal and diseased human skin.

RESULTS

Next Generation deep sequencing of small RNAs

I obtained punch biopsies from the involved (PP) and uninvolved (PN) skin of psoriasis patients and normal skin (NN) from healthy donors (Table 2-1). Such biopsies are predominantly composed of keratinocytes, but also contain cells derived from epidermal appendages, vasculature, dermal fibroblasts, and skin homing immune cell populations. I extracted total RNA with a method that preserved small RNAs and constructed small RNA libraries from 20 NN, 23 PN, and 24 PP biopsies. I independently sequenced each of the 67 libraries on the Illumina GAIIx platform, generating 1.1 billion raw and 670 million (M) qualified reads. Three technical replicates produced from a single PP skin biopsy were highly correlated in pairwise comparisons (r^2=0.994, 0.990, and 0.989; Figure 2-1A). The lengths of the adapter-trimmed, qualified reads were normally distributed around an average length of 22 nt (Figure 2-1B). I aligned qualified reads to miRNA precursors, functional noncoding RNAs (ncRNAs), and build 37 (hg19) of the human genome. The number of reads and mapping proportions were roughly equivalent in the NN, PN, and PP skin categories (Table 2-2).

The distribution of read alignments in the cumulative dataset (NN, PN, and PP combined) is summarized in Figure 2-2. Briefly, 305M (46%) reads aligned to known miRNA precursors, with 99.9% of these overlapping the annotated, mature miRNA or

miRNA* sequence ±3nt. Another 187M reads aligned to a variety of other functional ncRNAs such as small nucleolar RNAs, small cajal body associated RNAs, and transfer RNAs (data not shown). An additional 41M reads aligned to other regions of the human reference sequence, including intergenic, intronic, and less frequently, exonic regions. Novel miRNA predictions were derived from this pool of reads. The remaining 136M reads that did not align perfectly to any of these databases were re-mapped to known mature miRNAs with relaxed stringency for the analysis of global miRNA editing patterns, leaving only 6.6% of reads unaligned.

Known miRNAs expressed in human skin

We first characterized the expression of known miRNAs in skin by examining reads that aligned perfectly to mature miRNA sequences with a 3nt extension at either end. This flexibility was introduced to allow the detection of various miRNA isoforms that differ at the 3' or 5' end because of imperfect enzymatic processing, termed isomiRs (Figure 2-3; 110,111). While 3' heterogeneity between isomiRs is thought to be largely inconsequential for target recognition, heterogeneity at the 5' end is predicted to change the function of the miRNA by shifting the seed sequence. Consistent with this, 5' heterogeneity was much less prevalent than 3' heterogeneity, indicating that the vast majority of mature miRNAs derived from a given precursor strand have identical target profiles (Figure 2-3 and data not shown).

A total of 717 mature miRNAs and 176 mature miRNA*s were represented by at least one read in the cumulative dataset (222). I also detected miRNA* production from several known miRNA loci that are currently lacking miRNA* annotations, including the

well-characterized keratinocyte miRNA, miR-1-1 and miR-203 (Figure 2-3 and data not shown). The ten miRNAs represented by the most reads in each skin category (NN, PN and PP) were largely overlapping and accounted for 70% of miRNA reads overall (Table 2-3). Notably, eight of the ten most highly represented miRNAs in NN skin (let-7a/b/c/f, miR-143, miR-203, miR-21, and miR-24) overlapped with a set of 47 highly abundant miRNAs previously cloned and sequenced from murine skin (85). The two highly represented miRNAs in human skin that were not detected by cloning and sequencing in murine skin, miR-26a and miR-451, have murine homologs. Thus, their absence may reflect species-specific differences in skin architecture (112). Alternatively, their high read counts in this dataset may be due to intrinsic bias introduced by miRNA library preparation (113,114), resulting in an overestimation of abundance. All other highly expressed miRNAs in murine skin were also detected by NGS in human skin. Differential expression for these and other known miRNAs in psoriasis will be discussed in Chapter 3, following a description of the global miRNA landscape in skin.

MiRNA strand selection in skin and other human tissues

To gain insight into miRNA strand selection in the skin, I queried the relative relationships of miRNA/miRNA* pairs in the dataset. By definition, miRNA* strands are incorporated into RISC at a lower frequency than their miRNA counterparts, and are thought to be rapidly degraded in the cytoplasm. However, for 12/139 pairs (9%) in the dataset, the miRNA* strand was more abundant than the miRNA strand in NN skin (Table 2-4). I validated the relative expression levels of four miRNA/miRNA* pairs with stem-loop quantitative real time PCR (qRT-PCR). In agreement with the digital read

counts, miR-431, miR-624, and miR-675 were all less abundant than their respective miRNA*s while miR-205 was more abundant than miR-205* (Figure 2-4A).

I hypothesized that the high relative abundance of the miRNA* strand for miR-431, miR-624, and miR-675 may be skin specific, and assessed the relative abundance of these miRNA/miRNA* pairs in a panel of 20 human tissues. Each miRNA/miRNA* pair displayed a unique tissue specific expression pattern. The only pair that was ubiquitously expressed in all tissues was miR-675/675*. MiR-624 was undetectable by qRT-PCR in all tissues, so we excluded the miR-624/624* pair from subsequent analyses. miR-675* was more abundant than miR-675 in all tissues, although the miRNA:miRNA* ratio varied substantially. Thus, it appears that this miRNA has been improperly annotated (Figure 2-4C). In contrast, miR-431* was more abundant than miR-431 in skin, but not in the two other tissues where the pair was expressed (Figure 2-4B). Overall, these results suggest that there are mechanisms beyond thermodynamic stability that modulate tissue specific miRNA strand selection.

Global patterns of miRNA editing in skin

In order to analyze global editing patterns for known miRNAs in the skin, I examined reads that aligned to mature miRNAs with one mismatch. I first filtered out spurious editing events by removing mismatches with a low quality score or mismatches that were consistent with non-templated nucleotide additions at the 3' terminus. The remaining single mismatch reads represented 1% of total miRNA reads, indicating that miRNA editing occurs at a low frequency. I next analyzed the frequencies of all possible single base substitutions, with particular focus on the two forms of substitutional RNA

editing that have been previously described in mammals: cytosine deamination (C→U conversions), and adenosine deamination (A→I conversions; 115,116). A→I and C→U conversions would appear as A→G and C→T mismatches in the sequencing dataset, respectively. If there were an unbiased distribution of all possible substitutions, each would represent ~8.3% of mismatched reads. However, I observed a clear over-representation of A→G and C→T substitutions, which accounted for 16.3% and 12.3% of single mismatch reads in the cumulative dataset, respectively ($p<0.0001$; Figure 2-5A). A high relative frequency of T→C substitutions (14.7%) was also observed, although the underlying mechanism is unknown (Figure 2-5A).

I next examined the frequency of single base substitutions specifically in the miRNA seed region, which is the primary determinant of target recognition. I found that the frequency of A→G substitutions in the seed region was 8.7% higher than in the full-length miRNA ($p<0.0001$; Figure 2-5B). In contrast, the frequency of C→T substitutions in the seed region was 4.3% lower than in the full-length miRNA, restoring the frequency of C→T substitutions to background levels within the seed (Figure 2-5B). Taken together, these results suggest that mature miRNAs are subject to cytosine and adenosine deamination, and that adenosine, but not cytosine, deamination in the miRNA seed region might be an important mechanism for modulating miRNA target interactions.

Features and genomic distribution of novel miRNAs

Over 1200 mature human miRNAs are registered in miRBase v16. However, as NGS methods improve the depth and quality of miRNA profiling, much debate remains about the true number of human miRNAs. I computationally predicted and prioritized

novel miRNAs from small RNA reads that mapped to the human reference sequence on the basis of four criteria: 1) predicted RNA hairpin structure, 2) presence of miRNA and miRNA* reads aligning to the hairpin stems, 3) characteristic 3' overhangs of the Dicer-cleaved miRNA/miRNA* duplex, and 4) evidence of spliceosome processing for some predicted intronic novel miRNAs.

I identified 284 putative novel miRNA loci which produced 284 mature miRNAs and 227 cognate miRNA*s that were represented by at least one read in the cumulative dataset (222). However, pending additional validation of loci associated with very few reads, the bulk of subsequent analyses focused on the 57 novel miRNA loci that were represented by at least four reads per library (268 total reads).

Compared to the known miRNAs expressed in skin, novel miRNAs were typically represented by fewer reads. For example, the most highly represented novel miRNA overall, novel #117, would have ranked in the 72nd percentile for known miRNA read count. Collectively, the top ten most highly represented mature novel miRNAs accounted for less than 0.01% of miRNA reads overall (Table 2-5). In addition to these novel miRNAs, I validated 21 newly reported miRNA loci from other recent high-throughput sequencing studies as well as a previously described but unannotated noncanonical miRNA processed from the ACA45 snoRNA (92,117,118,119,222).

Table 2-6 provides the genomic distribution of novel miRNAs with respect to intergenic regions, introns, 3'UTRs, 5'UTRs, exons, and ncRNAs compared to the distribution of the known miRNAs detected in skin. Novel miRNAs showed a higher frequency of intronic localization and a lower frequency of intergenic localization

compared to known miRNAs. Of the 183 novel miRNAs that aligned to introns, 68 (37%) aligned to the 3' end such that the 3' end of the mature miRNA sequence was within 2nt of the intron-exon boundary. Ten intronic novel miRNAs aligned to putative miRtrons that were less than 100nt in length. Six novel miRNAs aligned uniquely to the antisense strand of known miRNA loci: novel #195/miR-33b, #117/miR-203, #220/miR-371, #273-1/miR-219-1, #273-2/miR-219-2, and #233/miR-1245.

Comparative genomic analysis reveals a recent origin for novel miRNAs

I used comparative genomics to assess conservation of the 57 most highly represented novel and recently described miRNA loci in skin (data not shown). miRNAs were classified as conserved if both the seed sequence and local hairpin structure were maintained. Interestingly, 24/47 (51%) novel and 5/10 (50%) recently described miRNAs were human-specific. An additional 21/47 (45%) novel and 4/10 (40%) recently described miRNAs were conserved in *M. mulatta* but not *M. musculus*, suggesting that they may be primate specific. Only three novel or recently described miRNAs were conserved further down the mammalian lineage: novel #116 (*L. africana*), novel #117 (*C.l. familiaris*), and ACA45 small RNA/novel #2456 (*L. africana*). However, these loci overlapped with other conserved genomic elements: miR-203 (antisense strand), *TRAF3* 3'UTR, and *ACA45*. Thus, conservation of these three miRNAs is likely to be an indirect consequence of the conservation of overlapping genomic features. The overall lack of conservation of novel and recently described miRNAs suggests they may have human or primate specific functions. However, the possibility remains that some of these newly evolved miRNAs are transient evolutionary intermediates that have yet to develop important regulatory functions.

Experimental validation of computationally predicted novel miRNAs

Experimental validation of novel miRNAs is important, particularly in the face of low abundance and poor conservation. I used quantitative RT-PCR (qRT-PCR) to validate the expression and processing of two novel and one recently described miRNAs: novel #107, novel #117, and miR-3613/novel #115. I found that all three miRNAs yielded a PCR product of the same length as an abundant known miRNA, miR-203, in NN skin, indicating that these novel miRNAs are endogenously expressed in skin (Figure 2-6A). To further confirm that the predicted novel miRNA precursors were recognized by the human miRNA processing machinery, I ectopically expressed the novel #107, novel #117, and miR-3613/novel #115 precursors in HEK293 cells. Each over-expressed precursor yielded a mature miRNA product that was at a substantially higher level than that seen in wild-type cells indicating that these novel miRNA precursors were indeed processed into mature miRNAs in human cells (Figure 2-6B). Variability in the degree of over-expression from each novel miRNA construct probably reflects differences in precursor processing efficiency.

I next assessed whether these three novel miRNAs were skin-specific by performing qRT-PCR on RNA from 20 different human tissues. Each miRNA was expressed in other human tissues at highly variable levels, indicating that these miRNAs are not skin-specific and are subject to tissue-specific transcriptional or post-transcriptional regulation (Figure 2-6C).

Novel #117 was of particular significance because it appeared to be an antisense miRNA derived from the miR-203 locus (Figure 2-7A). The existence of #117 as a *bona*

fide miRNA was confirmed by several lines of evidence. First, it displayed all of the features of miRNA biogenesis including hairpin formation, the presence of miRNA and miRNA* reads, and 3' overhangs on the highest likelihood miRNA/miRNA* duplex (Figure 2-7B,C). Second, ectopic expression of the #117 locus in HEK293 cells (which do not endogenously express this miRNA) resulted in two distinct northern blot bands of ~65nt and ~22nt, a pattern that is consistent with the expected sizes of the precursor and mature miRNA species, respectively (Figure 2-7D). Third, ectopically expressed #117 co-immunoprecipitated with Argonaute 2 (Ago2), a core component of the RISC complex, in HEK293 cells, suggesting that the mature miRNA is functionally competent (Figure 2-7E). Fourth, there was no correlation between the expression patterns of miR-203 and novel #117 in a panel of human tissues (Figure 2-7F). Taken together, these results support the transcription and processing of two distinct miRNAs derived from the sense and antisense strands at this locus. Henceforth, I will refer to novel #117 as miR-203-AS. Notably, miR-203 and miR-203-AS do share sequence similarity, but the imperfect palindromic nature of the locus leads to the production of distinct sense and antisense products. Of particular importance is a single base difference in their seed regions, which would indicate that the two miRNAs have distinct target profiles. Predicted targets of miR-203-AS are listed in Table 2-7. Because miR-203 is more abundant than novel #117 in all human tissues, and has long been recognized as a miRNA, we conclude that miR-203-AS is the minor product derived from this locus.

DISCUSSION

Deep sequencing of small RNAs has made it possible to comprehensively define the miRNAome of human tissues. I have leveraged this technology in skin to produce the largest small RNA dataset from any human tissue to date. The depth of sequencing allowed detection of low abundance, novel, and edited miRNAs with unparalleled sensitivity.

New variation in known miRNAs

Known miRNAs detected in this study exhibited a striking amount of subtle variation. Most notably, the high prevalence of isomiRs may be indicative of stochastic or regulated heterogeneity in miRNA processing. While 3' isomiRs, which were widely detected in this study, would be inconsequential for target recognition, the possibility remains that such isomiRs would be differentially incorporated into the RISC complex and/or targeted for specific modifications. Indeed, the adenylation and uridylation of miRNAs (not analyzed in this study) appear to modulate their stability in mammalian cells (120). Secondly, the analysis of miRNA* sequences in this dataset indicates that some miRNA* sequences do accumulate in cells, and thus may not always be subject to rapid degradation. Moreover, the variability in miRNA* abundance that I observed point to thermodynamic features and sequence content of individual miRNAs as well as tissue-specific regulatory mechanisms as determinants of miRNA strand selection.

Significance of miRNA editing

Analysis of single mismatch miRNA reads led to the observation that miRNAs are subject to adenosine and cytidine deamination. There are various examples of functionally important A→I editing of miRNAs catalyzed by adenosine deaminases acting on RNA (ADARs; 121,122). For example, targeted A→I editing within the seed region of miR-376 in some human tissues alters the recognition of mRNA targets (122). The role of cytidine deaminases, such as APOBECs, in miRNA editing is not well understood. However, a recent meta-analysis of small RNA sequences derived from *O. sativa* and *A. thaliana* revealed a similar over-representation of C→T substitutions, suggesting that cytidine deamination may be a predominant mechanism for miRNA editing in eukaryotes (123). Further experiments will be required to determine whether the majority of cytidine deamination events are spontaneous or enzymatically catalyzed.

Novel miRNA identification

I have reported 284 putative novel miRNA genes, and 22 recently described miRNA genes that were expressed in skin, three of which were subjected to extensive experimental validation. Recently described miRNAs were initially characterized as novel, but were independently annotated by other groups while I was analyzing and validating my findings. These annotations were largely due to the recent publication of miRNA profiles from melanoma cell lines and tissues of the female reproductive tract, which each applied similar prediction criteria as the present study (92,117,119). The partial overlap between this study and others provides reassuring validation of my NGS-based *in silico* method, and suggests that the unprecedented size of our dataset was responsible for the identification of such a large number of completely novel miRNAs.

The majority of novel miRNA loci were poorly conserved, which is perhaps not surprising, based on the fact that some miRNA discovery studies have relied on conservation as a prediction criterion. However, in more recent NGS-based studies as well as the present study, conservation was excluded as a prediction criterion in order to obtain a comprehensive profile of all miRNAs that are expressed in human skin, including those that may be newly evolved or evolutionarily transient (92,117,119).

One small class of novel miRNAs was comprised of miRNAs derived from the antisense strand at known miRNA loci. To date, only a few known miRNA loci in humans, such as miR-103-1 and miR-103-2, have antisense miRNAs registered in miRBase. However, this phenomenon has been described in detail at the *miR-iab-4* locus in *D. melanogaster*. Both *miR-iab-4* and its antisense counterpart *miR-iab-8* regulate Hox genes during larval development, but they are functionally distinct based on their discordant expression patterns and unique target profiles (124). While there were many antisense reads present in my dataset, most were consistent with RNA degradation, potential siRNA production, or artifacts of palindromic sequence. However, six antisense miRNAs reported in this study showed strongly convincing features of miRNA biogenesis. These sense and antisense miRNAs could functionally interact to create complex regulatory networks or feedback loops.

The largest class of novel miRNAs aligned to introns, which has important implications for biogenesis and function. MiRtrons were first described in Drosophila as ~60nt introns that resembled pre-miRNAs, and thus do not require Drosha for biogenesis (105). While such small introns are rare in humans, I identified ten putative novel

miRtrons ranging from 55-94nt in length. The remaining intronic miRNAs aligned to longer introns, but were biased towards 3'-5' intron-exon boundaries. This non-random distribution of intronic novel miRNAs strongly supports spliceosome involvement in the processing of some human miRNAs. The processing of intronic miRNAs may also vary with the expression of alternatively spliced transcripts.

Conclusions and future directions

Further characterization of the miRNA landscape in skin should include editing analysis for individual miRNAs at the single nucleotide level. Additionally, it would be interesting to investigate whether the novel miRNAs described in this chapter were produced by the canonical Drosha/Dicer pathway, or whether some of them may rely on noncanonical biogenesis pathways, such as the Ago2 pathway which generates the abundant miR-451 in skin (125). The functionality of novel miRNAs should be confirmed by RISC loading assays. Overall, the global patterns of miRNA expression described in this chapter provide an unprecedented glimpse into the breadth and diversity of miRNA expression in an adult human tissue. This work also laid the foundation for the characterization of miRNA expression and function in psoriatic skin, described in Chapters 3 and 4.

MATERIALS AND METHODS

Samples. 4-6mm punch skin biopsies were collected from healthy controls and the uninvolved and involved skin of PS patients. PS patients enrolled in this study received no systemic, photo, or topical therapy in the four weeks prior to sample collection. Biopsies were stored in RNAlater (Qiagen) at -80°C prior to RNA extraction.

Small RNA library preparation and sequencing. RNA was extracted with the miRNeasy Mini Kit (Qiagen), with on-column DNase I digestion. RNA was prepared for sequencing on the Illumina GAIIx platform with the Small RNA Sample Prep Kit (Illumina) according to manufacturer's instructions (protocol v1.5). This protocol required the use of a proprietary 3' adapter that has a high affinity for Dicer cleavage products. Briefly, 3' and 5' adapters were ligated to 1ug total RNA. cDNA was synthesized with SuperScript II Reverse Transcriptase (Invitrogen) and subjected to 12 cycles of PCR amplification with high fidelity Phusion Polymerase (Finnzymes Oy). Each library was loaded on a single Illumina lane at 20pM and subjected to 36 cycles of sequencing.

Read processing and mapping. Each deep sequencing library was processed independently. Reads with a 3' adapter substring less than 6nt or trimmed sequence length less than 17nt were removed from the dataset. Trimmed reads were mapped to multiple human sequencing databases with Bowtie: miRNA precursors (miRBase v.16, http://www.mirbase.org/ftp.shtml), ncRNAs (fRNAdb,

http://www.ncrna.org/frnadb/download), and the hg19 build of the human genome (UCSC Genome Browser, http://genome.ucsc.edu/cgi-bin/hgTables?command=start) (43,44,45,126,127,128,129). Reads that mapped to miRNA precursors were attributed to mature miRNAs if they aligned to the annotated mature sequences with 3nt up- and downstream extensions.

Novel miRNA prediction. Qualified reads that aligned to the hg19 build of the human genome were subjected to our novel miRNA prediction pipeline. Any reads that mapped to previously described miRNA loci were removed, and loci that shared adjacent reads within a gap ≤30nt were merged. For each locus, a series of overlapping DNA sequence segments was extracted for secondary structure analysis with RNAfold (http://www.tbi.univie.ac.at/~ivo/RNA/; 130,131,132). The starting sequence segment extended 220nt upstream of the locus, and subsequent segments were extracted by a sliding window of 250nt, with an increment of 100nt, until the window reached 220nt downstream of the sequence reads. Segments lacking stems of at least 18nt and segments lacking reads that mapped to any of their stems were excluded. Candidate miRNAs were prioritized based on 1) occurrence of sequencing reads on the stem of a predicted hairpin structure (minimum free energy less than -18kcal/mol); 2) presence of miRNA* reads on the opposite stem of the hairpin; 3) presence of 3' overhangs on the highest likelihood miRNA/miRNA* duplex; and 4) evidence of spliceosome-mediated precursor processing based on alignment to intron-exon boundaries.

Novel miRNA conservation. Homology searches were performed in eight species: *M. mulatta, M. musculus, C.l. familiaris, L. africana, M. domestica, G. gallus, X.*

tropicalis, and *D. rerio*. The novel miRNA precursor sequences, defined as the maximal extension of sequences bearing the stem-loop structure, were mapped to each species' genome using blastn (http://blast.ncbi.nlm.nih.gov/Blast.cgi/) with a minimal word-size of seven. Blastn hits that were reported in any given species shared greater than 90% sequence similarity and had a ratio of alignment length to the precursor length greater than 0.9. Secondary structure of aligned sequences was determined with RNAfold. Aligned sequences were classified as conserved novel miRNAs if the following criteria were met: 1) the highest likelihood secondary structure was a hairpin with a minimum free energy less than -18kcal/mol, 2) the mature miRNA sequence was derived from the hairpin stem, and 3) the miRNA seed region (nt 2-7) was perfectly conserved.

miRNA qRT-PCR. qRT-PCR of mature miRNAs was performed with TaqMan miRNA assays according to manufacturer's instructions (Life Technologies). Briefly, 5ng of total RNA was reverse transcribed in a 7.5ul reaction with the TaqMan MicroRNA Reverse Transcription Kit (Life Technologies). 0.67ul of cDNA was added to triplicate 10ul PCR reactions. PCR was performed on a 7900HT thermocycler (Life Technologies). MiRNA expression was normalized to the endogenous snoRNA, Z30. Relative expression levels were calculated according to the $2^{-\Delta\Delta Ct}$ method as follows: $100*2^{((Ct\ Z30)-(Ct\ miRNA))}$ (133). Significance was determined with one way ANOVA and post-hoc two tailed t-tests.

MiRNA expression constructs. MiRNA over-expression constructs were generated from the pEP-miR cloning and expression vector (Cell Bio Labs). Briefly, miRNA precursors ±100nt were amplified from genomic DNA. PCR products were

cloned into the BamHI and NheI sites of the vector. Transformants were selected on 1ug/ml ampicillin and selected transformants were validated by Sanger sequencing.

Transfections. HEK293 cells were cultured in DMEM supplemented with 2mM L-glutamine, 10mg/ml penicillin-streptomycin, and 10% fetal bovine serum at 37°C and 5% CO_2. Transfections were performed in triplicate. 24 hours prior to transfections, $1x10^5$ cells were plated in each well of a 24-well plate. Transfections were performed with TransIT-LT1 transfection reagent according to manufacturer's instructions (Mirus). Briefly, 750ng pEP-miR and 3.75ul LT-1 were incubated in 46.25ul RPMI for 30 min at 22°C before treatment. Cells were collected 48 hours post-treatment.

miRNA northern blots. 30ug of total RNA was mixed with formamide loading dye and incubated at 65˚C for 20 min. Samples were loaded on a pre-warmed 12% denaturing polyacrylamide gel (Sequagel), and run at 100V until bromphenol blue reached the bottom of the gel. RNA was transferred onto a Genescreen Plus membrane (Perkin Elmer) with a Trans-Blot SD semi-dry transfer cell (Bio-Rad) at 250mA for 15 min. The membrane was baked for one hour at 80˚C, pre-hybridized for two hours in PerfectHyb Plus (Sigma) at hybridization temperature, and hybridized overnight with a P-32 labeled DNA probe. miR-203-AS probe sequence: 5'-CCAGTGGTTCTTAACAGTTCAA-3'. The membrane was washed three times in 0.1X SSC, 0.1% SDS at hybridization temperature, and exposed for three days. For input control, the membrane was stripped with two 20 min applications of boiled 0.1% SDS with gentle agitation at 22˚C, and re-hybridized with a P-32 labeled U6 snRNA LNA probe (Exiqon).

RNA binding protein immunoprecipitation-PCR (RIP-PCR). HEK293 cells were transfected with pEP-miR-null or pEP-miR-novel #117 constructs as described above, except that transfections were scaled up to generate one 10cm plate per immunoprecipitation. Cells were washed three times in 1X PBS and UV crosslinked once for 400mJ/cm^2 and again for 200mJ/cm^2, with gentle agitation in between. Cells were pelleted by centrifugation at 4000 rpm for 5 min at 4°C. Cell pellets were washed once in 1X PBS and resuspended in 200ul 1X PBS, 0.1% SDS, 0.5% deoxycholate, 0.5% nonidet P-40, supplemented with 1U/ul RNasin (Promega) and 1X Complete Protease Inhibitor Cocktail (Roche). Lysates were incubated on ice for 10 min, and cleared by centrifugation at 10000 rpm for 10 min at 4°C. Each cleared lysate was added to 50ul protein G-coated Dynabeads (Invitrogen) which had been previously bound to 5ug anti-mouse Ago2/eIF2C2 monoclonal antibody (Abcam) or normal rabbit IgG (Cell Signaling Technology), according to the manufacturer's protocol, and incubated for 4 hours at 4°C with rotation. Beads were washed three times with 1X PBS, 0.1% SDS, 0.5% deoxycholate, 0.5% nonidet P-40 and three times with 5X PBS, 0.1% SDS, 0.5% deoxycholate, 0.5% nonidet P-40. RNA extraction and qRT-PCR were performed as described above, except that relative abundance of novel #117 in the Ago2 IP sample was calculated relative to the IgG IP sample, in lieu of an endogenous control.

Western blots. 10ul of 2X SDS reducing buffer was added directly to washed beads following immunoprecipitation, and incubated at 95°C for 5 min. Samples were loaded on a pre-warmed 4-20% polyacrylamide gel, run at 200V for 30 min, and wet transferred for 1 hour at 100V onto a 0.45um nitrocellulose membrane. The membrane was blocked in 1X TBST, 5% milk at 22°C for 1 hour. A 1:500 dilution of Ago2/eIF2C

monoclonal antibody (Abcam) in 1X TBST, 5% milk was applied to the membrane, and incubated at 22°C for 3 hours. The membrane was washed three times for 10 min in 1X TBST, 5% milk. A 1:5000 dilution of HRP-conjugated secondary antibody in 1X TBST, 5% milk was applied to the membrane, and incubated at 22°C for 1 hour. The membrane was washed three times for 10 min in 1X TBST, 5% milk. The blot was developed with 1ml of Supersignal West Femto Chemiluminescent substrate (Thermo Scientific).

MiRNA editing analysis. Reads that aligned to mature miRNAs with one mismatch were subjected to filters prior to editing analysis. Reads containing a low quality mismatch (p[sequencing error]>0.05) based on the single base Illumina quality score were removed. 3' terminal N→A or N→T mismatches were also removed. From the remaining pool of one mismatch reads, the relative frequencies of all possible substitutions at positions 1-20 of the miRNA relative to the 5' end were calculated. Significance was determined with Pearson's chi-squared test.

Data deposition. All 76 small RNA sequencing libraries from psoriatic lesion and normal human skin biopsy samples have been deposited into NCBI/GEO databases under GEO31037.

Table 2-1. Summary of clinical data associated with skin biopsies.

Patient ID[a]	sRNA-seq ID	sRNA-seq	qRT-PCR	Age	Sex	Race	Ethnicity	Fitzpatrick Skin Type	Weight	BMI	Obesity	Smoking	Alcohol Consumption
07502 NN[b]	NN #1	Y	N	Unknown	Unknown	White/Caucasian	Not Hispanic/Latino	Unknown	Unknown	Unknown	Unknown	Unknown	Unknown
091402 NN[b]	NN #2	Y	N	Unknown	Unknown	White/Caucasian	Not Hispanic/Latino	Unknown	Unknown	Unknown	Unknown	Unknown	Unknown
091702 NN[b]	NA	N	Y	Unknown	Unknown	White/Caucasian	Not Hispanic/Latino	Unknown	Unknown	Unknown	Unknown	Unknown	Unknown
112602 NN[b]	NN #3	Y	N	Unknown	Unknown	White/Caucasian	Not Hispanic/Latino	Unknown	Unknown	Unknown	Unknown	Unknown	Unknown
11502 NN[b]	NA	N	Y	Unknown	Unknown	White/Caucasian	Not Hispanic/Latino	Unknown	Unknown	Unknown	Unknown	Unknown	Unknown
2008008 NN[b]	NN #4	Y	Y	Unknown	Unknown	White/Caucasian	Not Hispanic/Latino	Unknown	Unknown	Unknown	Unknown	Unknown	Unknown
2008009 NN[b]	NA	N	Y	Unknown	Unknown	White/Caucasian	Not Hispanic/Latino	Unknown	Unknown	Unknown	Unknown	Unknown	Unknown
2008010 NN[b]	NN #5	Y	N	Unknown	Unknown	White/Caucasian	Not Hispanic/Latino	Unknown	Unknown	Unknown	Unknown	Unknown	Unknown
20080011 NN[b]	NA	N	Y	Unknown	Unknown	White/Caucasian	Not Hispanic/Latino	Unknown	Unknown	Unknown	Unknown	Unknown	Unknown
2008012 NN[b]	NN #6	Y	N	Unknown	Unknown	White/Caucasian	Not Hispanic/Latino	Unknown	Unknown	Unknown	Unknown	Unknown	Unknown
2008013 NN[b]	NN #7	Y	N	Unknown	Unknown	White/Caucasian	Not Hispanic/Latino	Unknown	Unknown	Unknown	Unknown	Unknown	Unknown
WU-HD-001 NN	NN #8	Y	N	29	F	White/Caucasian	Not Hispanic/Latino	2	60.8	21.6	N	N	Y
WU-HD-002 NN	NN #9	Y	N	27	F	White/Caucasian	Not Hispanic/Latino	1	49.9	21.5	N	Y	Y
WU-HD-003 NN	NN #10	Y	N	48	F	White/Caucasian	Not Hispanic/Latino	1	45.8	17.9	N	N	Y
WU-HD-004 NN	NN #11	Y	N	48	M	White/Caucasian	Not Hispanic/Latino	3	108.9	32.5	Y	N	Y
WU-HD-005 NN	NN #12	Y	N	23	M	White/Caucasian	Hispanic/Latino	4	95.3	27.0	N	N	N
WU-HD-006 NN	NN #13	Y	Y	34	M	White/Caucasian	Not Hispanic/Latino	1	83.9	26.5	N	Y	Y
WU-HD-007 NN	NN #14	Y	N	23	F	White/Caucasian	Not Hispanic/Latino	2	52.2	19.7	N	N	Y
WU-HD-008 NN	NN #15	Y	N	39	F	White/Caucasian	Not Hispanic/Latino	3	86.2	32.6	Y	N	N
WU-HD-009 NN	NN #16	Y	Y	38	F	White/Caucasian	Not Hispanic/Latino	2	65.8	23.4	N	N	Y
WU-HD-010 NN	NN #17	Y	N	40	F	White/Caucasian	Not Hispanic/Latino	2	102.1	41.1	Y	N	N
WU-HD-011 NN	NN #18	Y	Y	18	M	White/Caucasian	Not Hispanic/Latino	2	61.2	20.5	N	Y	Y
WU-HD-012 NN	NN #19	Y	N	20	M	White/Caucasian	Not Hispanic/Latino	2	59.0	19.8	N	Y	N
WU-HD-013 NN	NN #20	Y	Y	36	M	Black/African American	Not Hispanic/Latino	6	115.7	31.0	Y	Y	Y
WU-HD-022 NN	NA	N	Y	35	F	White/Caucasian	Hispanic/Latino	3	83.5	30.8	Y	N	Y
120202 PP	Inv #1	Y	N	Unknown	Unknown	White/Caucasian	Not Hispanic/Latino	Unknown	Unknown	Unknown	Unknown	Unknown	Unknown
2007005 PN/PP[b]	PN/PP #2	Y	Y	Unknown	Unknown	White/Caucasian	Not Hispanic/Latino	Unknown	Unknown	Unknown	Unknown	Unknown	Unknown
2007007 PN/PP[b]	PN/PP #3	Y	Y	Unknown	Unknown	White/Caucasian	Not Hispanic/Latino	Unknown	Unknown	Unknown	Unknown	Unknown	Unknown
2007009 PN/PP[b]	PN/PP #4	Y	N	Unknown	Unknown	White/Caucasian	Not Hispanic/Latino	Unknown	Unknown	Unknown	Unknown	Unknown	Unknown
2008003 PN/PP[b]	NA	N	Y	Unknown	Unknown	White/Caucasian	Not Hispanic/Latino	Unknown	Unknown	Unknown	Unknown	Unknown	Unknown
2008004 PN/PP[b]	NA	N	Y	Unknown	Unknown	White/Caucasian	Not Hispanic/Latino	Unknown	Unknown	Unknown	Unknown	Unknown	Unknown
2008005 PN/PP[b]	PN/PP #5	Y	N	Unknown	Unknown	White/Caucasian	Not Hispanic/Latino	Unknown	Unknown	Unknown	Unknown	Unknown	Unknown
2008007 PN/PP[b]	PN/PP #6	Y	N	Unknown	Unknown	White/Caucasian	Not Hispanic/Latino	Unknown	Unknown	Unknown	Unknown	Unknown	Unknown
M08 PN/PP[b]	PN/PP #7	Y	Y	Unknown	Unknown	White/Caucasian	Not Hispanic/Latino	Unknown	Unknown	Unknown	Unknown	Unknown	Unknown
WU-PSO-001 PN/F	PN/PP #8	Y	N	38	M	White/Caucasian	Not Hispanic/Latino	3	77.1	25.1	N	N	Y
WU-PSO-002 PN/F	PN/PP #9	Y	Y	42	F	White/Caucasian	Not Hispanic/Latino	2	90.3	32.1	Y	N	N
WU-PSO-003 PN/F	PN/PP #10	Y	N	49	F	White/Caucasian	Not Hispanic/Latino	3	89.8	34.0	Y	Y	Y
WU-PSO-004 PN/F	PN/PP #11	Y	Y	48	M	White/Caucasian	Not Hispanic/Latino	2	65.8	21.4	N	Y	Y
WU-PSO-005 PN/F	PN/PP #12	Y	N	50	M	White/Caucasian	Hispanic/Latino	5	113.4	36.9	Y	N	Q
WU-PSO-006 PN/F	PN/PP #13	Y	N	61	F	Black/African American	Not Hispanic/Latino	6	108.4	37.4	Y	Y	N
WU-PSO-007 PN/F	PN/PP #14	Y	N	37	F	White/Caucasian	Not Hispanic/Latino	2	63.5	21.9	N	Q	N
WU-PSO-008 PN/F	PN/PP #15	Y	N	47	M	White/Caucasian	Not Hispanic/Latino	1	99.8	34.5	Y	N	Y
WU-PSO-009 PN/F	PN/PP #16	Y	N	52	M	White/Caucasian	Not Hispanic/Latino	2	144.0	52.9	Y	N	N
WU-PSO-010 PN/F	PN/PP #17	Y	Y	37	M	White/Caucasian	Not Hispanic/Latino	2	93.0	29.4	Y	Y	N
WU-PSO-011 PN/F	PN/PP #18	Y	N	49	M	White/Caucasian	Not Hispanic/Latino	2	127.0	39.0	Y	Y	Y
WU-PSO-012 PN/F	PN/PP #19	Y	N	69	M	White/Caucasian	Not Hispanic/Latino	2	145.2	48.7	Y	Q	Y
WU-PSO-013 PN/F	PN/PP #20	Y	N	62	M	Black/African American	Not Hispanic/Latino	6	140.2	37.6	Y	Y	N
WU-PSO-014 PN/F	PN/PP #21	Y	Y	72	M	White/Caucasian	Not Hispanic/Latino	1	73.5	22.6	N	Q	Y
WU-PSO-016 PN/F	PN/PP #22	Y	N	36	F	White/Caucasian	Not Hispanic/Latino	2	49.9	19.1	N	N	N
WU-PSO-018 PN/F	PN/PP #23	Y	N	69	M	White/Caucasian	Not Hispanic/Latino	1	81.6	23.7	N	Q	Y
WU-PSO-019 PN/F	PN/PP #24	Y	Y	51	M	White/Caucasian	Not Hispanic/Latino	3	122.5	39.0	Y	Q	Y

[a] Normal skin, NN; Uninvolved psoriatic skin, PN; Involved psoriatic skin, PP.

[b] Samples lacking detailed information were obtained prior to IRB approval for ascertainment of patient history.

[c] Type 1 and type 2 correspond to age of onset greater than or less than 40, respectively.

Hypertension	Hyperlipidemia	Diabetes	Biopsy Site-PP	Biopsy site-PN	Biopsy site-NN	PASI	BSA	PGA	DLQI	Psoriatic Arthritis	Age Onset	Type[c]	Family Hx psoriasis
Unknown	Unknown	Unknown	NA	NA	Unknown	NA	NA	NA	NA	NA	NA	NA	NA
Unknown	Unknown	Unknown	NA	NA	Unknown	NA	NA	NA	NA	NA	NA	NA	NA
Unknown	Unknown	Unknown	NA	NA	Unknown	NA	NA	NA	NA	NA	NA	NA	NA
Unknown	Unknown	Unknown	NA	NA	Unknown	NA	NA	NA	NA	NA	NA	NA	NA
Unknown	Unknown	Unknown	NA	NA	Unknown	NA	NA	NA	NA	NA	NA	NA	NA
Unknown	Unknown	Unknown	NA	NA	Unknown	NA	NA	NA	NA	NA	NA	NA	NA
Unknown	Unknown	Unknown	NA	NA	Unknown	NA	NA	NA	NA	NA	NA	NA	NA
Unknown	Unknown	Unknown	NA	NA	Unknown	NA	NA	NA	NA	NA	NA	NA	NA
Unknown	Unknown	Unknown	NA	NA	Unknown	NA	NA	NA	NA	NA	NA	NA	NA
Unknown	Unknown	Unknown	NA	NA	Unknown	NA	NA	NA	NA	NA	NA	NA	NA
Unknown	Unknown	Unknown	NA	NA	Unknown	NA	NA	NA	NA	NA	NA	NA	NA
N	N	N	NA	NA	R lower back	NA	NA	NA	NA	NA	NA	NA	NA
N	N	N	NA	NA	R lower back	NA	NA	NA	NA	NA	NA	NA	NA
N	Y	N	NA	NA	L lower back	NA	NA	NA	NA	NA	NA	NA	NA
Y	N	N	NA	NA	R lower back	NA	NA	NA	NA	NA	NA	NA	NA
N	N	N	NA	NA	R lower back	NA	NA	NA	NA	NA	NA	NA	NA
N	N	N	NA	NA	L mid back	NA	NA	NA	NA	NA	NA	NA	NA
N	N	N	NA	NA	R lower back	NA	NA	NA	NA	NA	NA	NA	NA
N	N	N	NA	NA	L mid back	NA	NA	NA	NA	NA	NA	NA	NA
N	N	N	NA	NA	L mid back	NA	NA	NA	NA	NA	NA	NA	NA
N	N	N	NA	NA		NA	NA	NA	NA	NA	NA	NA	NA
N	N	N	NA	NA	R mid back	NA	NA	NA	NA	NA	NA	NA	NA
N	N	N	NA	NA	L mid back	NA	NA	NA	NA	NA	NA	NA	NA
N	N	N	NA	NA	L mid back	NA	NA	NA	NA	NA	NA	NA	NA
N	N	N	NA	NA	R lower back	NA	NA	NA	NA	NA	NA	NA	NA
Unknown	Unknown	Unknown	Unknown	Unknown	NA	Unknown	Unknown	Unknown	Unknown	Unknown	Unknown	Unknown	Unknown
Unknown	Unknown	Unknown	Unknown	Unknown	NA	Unknown	Unknown	Unknown	Unknown	Unknown	Unknown	Unknown	Unknown
Unknown	Unknown	Unknown	Unknown	Unknown	NA	Unknown	Unknown	Unknown	Unknown	Unknown	Unknown	Unknown	Unknown
Unknown	Unknown	Unknown	Unknown	Unknown	NA	Unknown	Unknown	Unknown	Unknown	Unknown	Unknown	Unknown	Unknown
Unknown	Unknown	Unknown	Unknown	Unknown	NA	Unknown	Unknown	Unknown	Unknown	Unknown	Unknown	Unknown	Unknown
Unknown	Unknown	Unknown	Unknown	Unknown	NA	Unknown	Unknown	Unknown	Unknown	Unknown	Unknown	Unknown	Unknown
Unknown	Unknown	Unknown	Unknown	Unknown	NA	Unknown	Unknown	Unknown	Unknown	Unknown	Unknown	Unknown	Unknown
Unknown	Unknown	Unknown	Unknown	Unknown	NA	Unknown	Unknown	Unknown	Unknown	Unknown	Unknown	Unknown	Unknown
N	N	N	mid back	mid back	NA	6.5	4.5	2	5	18	18	1	N
N	N	N	Below right knee	R lower back	NA	10.2	8	3	19	Y	18	1	N
N	N	Y			NA	15.6	22	3	17	N	7	1	N
N	N	N	R arm	R arm	NA	13.2	7	4		N	42	2	Y
Y	Y	N	Upper back	Upper back	NA	17.8	11	3	18	N	47	2	N
Y	Y	Y	L upper arm	L upper arm	NA	12.0	14	4	24	N	58	2	N
N	N	N	R elbow	R forearm	NA	7.2	6	4	8	N	24	1	Y
N	N	N	R lower back	Lower back	NA	13.8	12	3	6	N	32	1	Y
Y	N	N	L mid back	mid back	NA	16.2	13	3		Y	10	1	Y
N	N	N	R lower back	R lower back	NA	13.4	10	4		Y	17	1	N
N	N	N	R lower back	R lower back	NA	15.7	12	4	18	N	38	1	N
Y	N	Y	R upper arm	R upper arm	NA	26.9	33	4	24	N	68	2	N
Y	N	N	R buttock	R lower back	NA	9.2	8	4	11	N	60	2	N
Y	N	N	R lower back	R lower back	NA	14.3	14.5	3	17	N	68	2	N
N	N	N	L lower back	L lower back	NA	28.3	53	4	12	N	18	1	Y
Y	Y	Y	L forearm	L forearm	NA	16.6	24	3		N	69	2	N
Y	Y	Y	L lower back	L lower back	NA	14.7	11	3	2	N	49	2	N

Nail involvement	Scalp involvement	Palmo-plantar involvement	Flexural involvement	Guttate Lesions	No. of previous systemic/biologic agents
NA	NA	NA	NA	NA	NA
NA	NA	NA	NA	NA	NA
NA	NA	NA	NA	NA	NA
NA	NA	NA	NA	NA	NA
NA	NA	NA	NA	NA	NA
NA	NA	NA	NA	NA	NA
NA	NA	NA	NA	NA	NA
NA	NA	NA	NA	NA	NA
NA	NA	NA	NA	NA	NA
NA	NA	NA	NA	NA	NA
NA	NA	NA	NA	NA	NA
NA	NA	NA	NA	NA	NA
NA	NA	NA	NA	NA	NA
NA	NA	NA	NA	NA	NA
NA	NA	NA	NA	NA	NA
NA	NA	NA	NA	NA	NA
NA	NA	NA	NA	NA	NA
NA	NA	NA	NA	NA	NA
NA	NA	NA	NA	NA	NA
NA	NA	NA	NA	NA	NA
NA	NA	NA	NA	NA	NA
NA	NA	NA	NA	NA	NA
NA	NA	NA	NA	NA	NA
NA	NA	NA	NA	NA	NA
NA	NA	NA	NA	NA	NA
Unknown	Unknown	Unknown	Unknown	Unknown	Unknown
Unknown	Unknown	Unknown	Unknown	Unknown	Unknown
Unknown	Unknown	Unknown	Unknown	Unknown	Unknown
Unknown	Unknown	Unknown	Unknown	Unknown	Unknown
Unknown	Unknown	Unknown	Unknown	Unknown	Unknown
Unknown	Unknown	Unknown	Unknown	Unknown	Unknown
Unknown	Unknown	Unknown	Unknown	Unknown	Unknown
Unknown	Unknown	Unknown	Unknown	Unknown	Unknown
Unknown	Unknown	Unknown	Unknown	Unknown	Unknown
N	Y	N	N	N	0
N	Y	Y	N	N	1
N	Y	N	Y	N	0
N	N	N	N	N	0
N	Y	N	N	N	2
N	N	N	N	N	0
Y	N	N	N	N	0
N	Y	N	N	N	0
N	Y	N	N	N	0
Y	Y	N	N	N	0
Y	Y	N	N	N	0
N	N	N	Y	N	0
Y	Y	Y	N	N	0
Y	Y	N	N	N	0
Y	Y	N	N	N	0
Y	Y	N	Y	N	0
N	Y	N	Y	N	0

Table 2-2. Distribution of read alignments from normal, uninvolved psoriatic, and involved psoriatic skin.

	NN[a]		PN[a]		PP[a]		Cumulative	
	No. reads	**% reads**	**No. reads**	**% reads**	**No. reads**	**% reads**	**No. reads**	**% reads**
Raw reads	314739262	NA	354772543	NA	412146550	NA	1081658355	NA
Qualified reads	204087993	NA	212569115	NA	253203829	NA	669860937	NA
Known miRNAs- intergenic	67533928	33.09	62741705	29.52	92702133	36.61	222977766	33.29
Known miRNAs- intronic	23139671	11.34	21260890	10.00	26760788	10.57	71161349	10.62
Known miRNAs- exonic	3811532	1.87	3530537	1.66	3576828	1.41	10918897	1.63
ncRNA database	54021696	26.47	64088314	30.15	67802945	26.78	185912955	27.75
coding exon	594284	0.29	693970	0.33	766307	0.30	2054561	0.31
non-coding exon	61160	0.03	60773	0.03	77053	0.03	198986	0.03
3'UTR	413359	0.20	500624	0.24	567188	0.22	1481171	0.22
5'UTR	161708	0.08	198182	0.09	194866	0.08	554756	0.08
Intronic	8029544	3.93	13006192	6.12	11033750	4.36	32069486	4.79
Intergenic	1070385	0.52	1657448	0.78	1629715	0.64	4357548	0.65
Known miRNAs- 1 mismatch	28171531	13.80	25889172	12.18	29875651	11.80	83936354	12.53
Unaligned qualified reads	17079195	8.37	18941308	8.91	18216605	7.19	54237108	8.10
Total	204087993	100.00	212569115	100.00	253203829	100.00	669860937	100

[a]Normal skin, NN; Uninvolved psoriatic skin, PN; Involved psoriatic skin, PP.

Table 2-3. Most abundant known miRNAs expressed in normal, uninvolved psoriatic, and involved psoriatic skin.

	NN[a]			PN[a]			PP[a]			Cumulative		
Mature miRNA	No. reads[b]	% miRNA reads[c]	Rank	No. reads[b]	% miRNA reads[c]	Rank	No. reads[b]	% miRNA reads[c]	Rank	No. reads[b]	% miRNA reads[c]	Rank
hsa-let-7a	48065414	33.34	1	39606288	30.60	1	44266619	25.67	1	131938321	29.87	1
hsa-let-7f	15566363	10.80	2	13566250	10.48	2	19113977	11.08	2	48246590	10.79	2
hsa-miR-143	11265038	7.81	3	11234955	8.68	3	12681332	7.35	4	35181325	7.95	3
hsa-miR-203	4821268	3.34	4	5378508	4.16	4	9866015	5.72	5	20065791	4.41	5
hsa-miR-451	3743389	2.60	5	3464570	2.68	6	4089856	2.37	7	11297815	2.55	7
hsa-miR-21	3739479	2.59	6	3975815	3.07	5	18345268	10.64	3	26060562	5.43	4
hsa-let-7b	3625405	2.51	7	3360180	2.60	7	3345155	1.94	9	10330740	2.35	8
hsa-miR-26a	3526144	2.45	8	3133159	2.42	9	3160312	1.83	10	9819615	2.23	9
hsa-miR-24	3375273	2.34	9	3179154	2.46	8	5118190	2.97	6	11672617	2.59	6
hsa-let-7c	2370013	1.64	10	1873647	1.45	10	1678735	0.97	21	5922395	1.35	11
miR-378	1195818	0.83	24	1579574	1.22	12	3974309	2.30	8	6749701	1.45	10
Total	101293604	70.25	--	90352100	69.80	--	125639768	72.86	--	317285472	70.97	

[a]Normal skin, NN; Uninvolved psoriatic skin, PN; Involved psoriatic skin, PP.

[b]Reads that mapped to the annotated mature miRNA +/- 3 nt in NN, PN, or PP skin.

[c]Abundance expressed as the percentage of all reads that mapped to annotated mature miRNAs +/- 3nt in NN, PN, or PP skin.

Table 2-4. miRNA loci for which the miRNA* read counts exceeded miRNA read counts in the cumulative dataset.

	NN[a]			PN[a]			PP[a]			Cumulative		
RNA	miRNA reads	miRNA* reads	miRNA/miRNA*	miRNA reads	miRNA* reads	miRNA/miRNA*	miRNA reads	miRNA* reads	miRNA/miRNA*	miRNA reads	miRNA* reads	miRNA/miRNA*
R-144	9282	348535	0.03	9474	294013	0.03	9181	353453	0.025975165	27937	996001	0.03
R-675	9	354	0.03	7	165	0.04	2	98	0.020408163	18	617	0.03
R-202	61	1295	0.05	57	841	0.07	33	1141	0.028921998	151	3277	0.05
R-624	19	191	0.10	25	228	0.11	50	322	0.155279503	94	741	0.13
R-380	80	392	0.20	63	330	0.19	143	749	0.190921228	286	1471	0.19
R-500	1646	5452	0.30	1481	5923	0.25	2849	9192	0.309943429	5976	20567	0.29
R-374a	11379	29213	0.39	9801	27360	0.36	17933	61313	0.292482834	39113	117886	0.33
R-431	41	160	0.26	52	190	0.27	202	230	0.87826087	295	580	0.51
R-550	410	740	0.55	452	802	0.56	424	954	0.444444444	1286	2496	0.52
R-625	309	561	0.55	330	572	0.58	347	744	0.466397849	986	1877	0.53
R-376a	1226	1459	0.84	1160	1603	0.72	2304	4251	0.54199012	4690	7313	0.64
R-545	63	48	1.31	63	58	1.09	76	172	0.441860465	202	278	0.73

rmal skin, NN; Uninvolved psoriatic skin, PN; Involved psoriatic skin, PP.

le 2-5. Most abundant novel miRNAs expressed in normal, uninvolved psoriatic, and involved psoriatic skin.

		NN[a]		PN[a]		PP[a]		Cumulative	
Identifier/location	sequence[b]	No. reads[c]	Rank	No. reads[c]	Rank	No. reads[c]	Rank	No. reads[b]	Rank
/chr14:104583678-104583927(-)	TTGAACTGTTAAGAACCACTGG	1515	1	2036	2	5214	1	8765	1
/chr17:39673318-39673567 (-)	CACCGACTCTGTCTCCTGCAG	2816	2	2065	1	1199	4	6080	2
:hr17:6558659-6558908(-)	TTGGACAGAAAACACGCAGGA	1174	3	1480	3	847	6	3501	4
:hr6:33665829-33666078(+)	TCAGGTGTGGAAACTGAGGCAG	999	4	1191	4	2323	2	4513	3
:hr6:6169476-6169725(+)	TACAGATGCAGATTCTCTGACTTC	869	5	676	7	697	8	2242	6
/chr9:135820997-135821246(+)	GTCGGTGCAAAAGTCATCACGGT	683	6	817	6	554	9	2054	7
/chr3:32547709-32547958(-)	GCAAAAGTAATTGTGGTTTTTG	659	7	613	8	762	7	2034	9
:hr5:150901536-150901785(-)	TCGGGCGCAAGAGCACTGCAGT	648	8	927	5	1011	5	2586	5
:hr8:125834132-125834381(+)	TTAGCCAATTGTCCATCTTTAG	403	9	542	9	429	11	1374	10
:hr1:243509367-243509616(+)	TCTGTGAGACCAAAGAACTACT	332	10	302	14	469	10	1103	11
ır1:82174775-82175024(+)	TAAAAGTAATTGTGGTATTTGC	277	13	353	10	1414	3	2044	8
	--	10375	--	11002	--	14919	--	36296	--

nal skin, NN; Uninvolved psoriatic skin, PN; Involved psoriatic skin, PP.

: abundant sequence derived from the novel miRNA precursor.

ds that mapped to the most abundant mature miRNA +/- 3 nt in NN, PN, or PP skin.

Table 2-6. Distribution of novel and known miRNA loci with respect to overlapping genomic elements.

Genomic element	No. of novel loci	% Novel loci	% Known loci
Intergenic	53	18.66	34.56
Intronic- center	105		
Intronic- 3' boundary	68		
Intronic- 5' boundary	0		
MiRtron (<100bp intron)	10	64.44	50.53
3' UTR	14		
5' UTR	2	5.63	4.04
Coding exon	7	2.46	1.93
Non-coding RNA	2	0.70	0.00
Intronic (antisense)	14		
3' UTR (antisense)	2		
5' UTR (antisense)	0		
Coding exon (antisense)	1		
miRNA (antisense)	6	8.10	8.95

Table 2-7. TargetScan Custom predicted targets of miR-203-AS.

Predicted target	Description	PP/NN[a,b]
MECP2	methyl CpG binding protein 2 (Rett syndrome)	--
SYNGR1	synaptogyrin 1	--
B4GALNT1	beta-1,4-N-acetyl-galactosaminyl transferase 1	--
C1orf52	chromosome 1 open reading frame 52	--
DACH1	dachshund homolog 1 (Drosophila)	-2.01
DNAJB12	DnaJ (Hsp40) homolog, subfamily B, member 12	--
ETF1	eukaryotic translation termination factor 1	--
FBXO11	F-box protein 11	--
FBXO21	F-box protein 21	--
GRM3	glutamate receptor, metabotropic 3	--
HIPK1	homeodomain interacting protein kinase 1	--
HOXA7	homeobox A7	--
IL13	interleukin 13	--
KLHL14	kelch-like 14 (Drosophila)	--
LRRTM2	leucine rich repeat transmembrane neuronal 2	--
MTF1	metal-regulatory transcription factor 1	--
PLAG1	pleiomorphic adenoma gene 1	--
PRKCB1	protein kinase C, beta 1	--
RARA	retinoic acid receptor, alpha	--
SFRS1	splicing factor, arginine/serine-rich 1 (splicing factor 2, alternate splicing factor)	--
THRAP2	thyroid hormone receptor associated protein 2	--
TIMP3	TIMP metallopeptidase inhibitor 3 (Sorsby fundus dystrophy, pseudoinflammatory)	-2.11
TOX3	TOX high mobility group box family member 3	--
UHMK1	U2AF homology motif (UHM) kinase 1	--
UNQ1887	signal peptide peptidase 3	--
ZC3H11A	zinc finger CCCH-type containing 11A	--
AGPAT3	1-acylglycerol-3-phosphate O-acyltransferase 3	--
ARID1A	AT rich interactive domain 1A (SWI-like)	--
ARID2	AT rich interactive domain 2 (ARID, RFX-like)	--
BCL7A	B-cell CLL/lymphoma 7A	--
CALM1	calmodulin 1 (phosphorylase kinase, delta)	--
CAST	calpastatin	--
CDON	Cdon homolog (mouse)	-2.06
CNTNAP2	contactin associated protein-like 2	--
COX8A	cytochrome c oxidase subunit 8A (ubiquitous)	--
CREBBP	CREB binding protein (Rubinstein-Taybi syndrome)	--
CREBZF	CREB/ATF bZIP transcription factor	--
CRTAP	cartilage associated protein	--
CTSC	cathepsin C	2.04
DACT3	dapper, antagonist of beta-catenin, homolog 3 (Xenopus laevis)	--
DAG1	dystroglycan 1 (dystrophin-associated glycoprotein 1)	--
FOSB	FBJ murine osteosarcoma viral oncogene homolog B	--
GADD45G	growth arrest and DNA-damage-inducible, gamma	--
GGA2	golgi associated, gamma adaptin ear containing, ARF binding protein 2	--
GLS	glutaminase	--
GNAI1	guanine nucleotide binding protein (G protein), alpha inhibiting activity polypeptide 1	--
GPR56	G protein-coupled receptor 56	--
HIP2	huntingtin interacting protein 2	--
HMGN2	high-mobility group nucleosomal binding domain 2	--
HRBL	HIV-1 Rev binding protein-like	--
LASS1	LAG1 homolog, ceramide synthase 1 (S. cerevisiae)	--
LFNG	LFNG O-fucosylpeptide 3-beta-N-acetylglucosaminyltransferase	--
MAFG	v-maf musculoaponeurotic fibrosarcoma oncogene homolog G (avian)	--
MAPKAPK3	mitogen-activated protein kinase-activated protein kinase 3	2.01
MBNL1	muscleblind-like (Drosophila)	--
MIPOL1	mirror-image polydactyly 1	--
MTMR14	myotubularin related protein 14	--
MTMR4	myotubularin related protein 4	--
NLRP3	NLR family, pyrin domain containing 3	--
NUP153	nucleoporin 153kDa	--
PHF17	PHD finger protein 17	--
PICALM	phosphatidylinositol binding clathrin assembly protein	--
PTER	phosphotriesterase related	--
ProSAPiP1	ProSAPiP1 protein	--
RIMS1	regulating synaptic membrane exocytosis 1	--
RNF139	ring finger protein 139	--
SCAMP1	secretory carrier membrane protein 1	--
SEPT3	septin 3	--
SEPT5	septin 5	--

SERPINE1	serpin peptidase inhibitor, clade E (nexin, plasminogen activator inhibitor type 1), member 1	--
SHANK3	SH3 and multiple ankyrin repeat domains 3	--
SLC4A1AP	solute carrier family 4 (anion exchanger), member 1, adaptor protein	--
SNIP	SNAP25-interacting protein	--
SPTLC3	serine palmitoyltransferase, long chain base subunit 3	--
STX5	syntaxin 5	--
TMEM91	transmembrane protein 91	--
TNF	tumor necrosis factor (TNF superfamily, member 2)	--
TRIM3	tripartite motif-containing 3	--
TRIM9	tripartite motif-containing 9	--
TRMT5	TRM5 tRNA methyltransferase 5 homolog (S. cerevisiae)	--
ULK2	unc-51-like kinase 2 (C. elegans)	--
XAB1	XPA binding protein 1, GTPase	--
YPEL2	yippee-like 2 (Drosophila)	--
ZNF512B	zinc finger protein 512B	--
ABCA1	ATP-binding cassette, sub-family A (ABC1), member 1	--
ABHD2	abhydrolase domain containing 2	--
AKAP13	A kinase (PRKA) anchor protein 13	--
ANKRD15	ankyrin repeat domain 15	--
CIT	citron (rho-interacting, serine/threonine kinase 21)	--
FZD4	frizzled homolog 4 (Drosophila)	--
GSC	goosecoid	--
HNRPA2B1	heterogeneous nuclear ribonucleoprotein A2/B1	--
INHBB	inhibin, beta B (activin AB beta polypeptide)	--
KPNA5	karyopherin alpha 5 (importin alpha 6)	--
MAP3K4	mitogen-activated protein kinase kinase kinase 4	--
MNT	MAX binding protein	--
NHS	Nance-Horan syndrome (congenital cataracts and dental anomalies)	--
PAX3	paired box gene 3 (Waardenburg syndrome 1)	--
PHF15	PHD finger protein 15	--
PTBP1	polypyrimidine tract binding protein 1	--
PTK2B	PTK2B protein tyrosine kinase 2 beta	--
RAI16	retinoic acid induced 16	--
RND2	Rho family GTPase 2	--
SCN1A	sodium channel, voltage-gated, type I, alpha subunit	--
SIX3	sine oculis homeobox homolog 3 (Drosophila)	--
SLC24A3	solute carrier family 24 (sodium/potassium/calcium exchanger), member 3	--
SLC9A1	solute carrier family 9 (sodium/hydrogen exchanger), member 1 (antiporter, Na+/H+, amiloride sensitive)	--
SMC1A	structural maintenance of chromosomes 1A	--
TFAP2A	transcription factor AP-2 alpha (activating enhancer binding protein 2 alpha)	--
THAP11	THAP domain containing 11	--
TMEM183A	transmembrane protein 183A	--
TMEM183B	transmembrane protein 183B	--
TSC22D1	TSC22 domain family, member 1	--
VEGFA	vascular endothelial growth factor A	--
YTHDF3	YTH domain family, member 3	--

[a]Normal skin, NN; Involved psoriatic skin, PP.
[b]From Gudjonsson *et al*., 2010. "--" indicates that the transcript is not reported as differentially expressed in this study

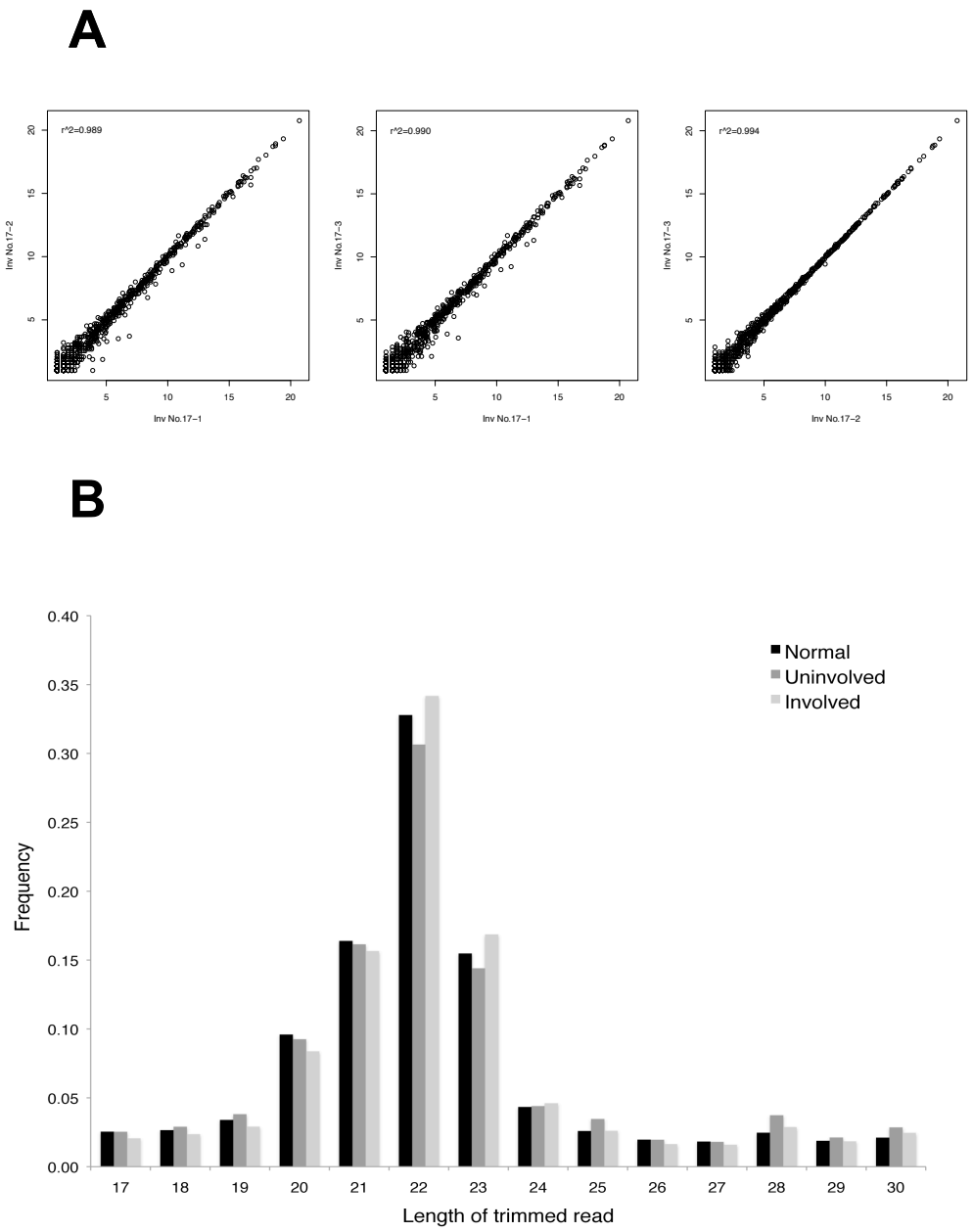

Figure 2-1. Quality control for small RNA sequencing. A) Pairwise comparisons of normalized digital read counts in three technical replicates. RNA derived from a psoriatic skin biopsy "Inv #17" was prepared and sequenced independently three times. Each pairwise comparison is plotted separately. Numerical axes represent normalized digital read counts for indicated sample. B) Length distribution of trimmed small RNA reads in normal, uninvolved psoriatic, and involved psoriatic skin.

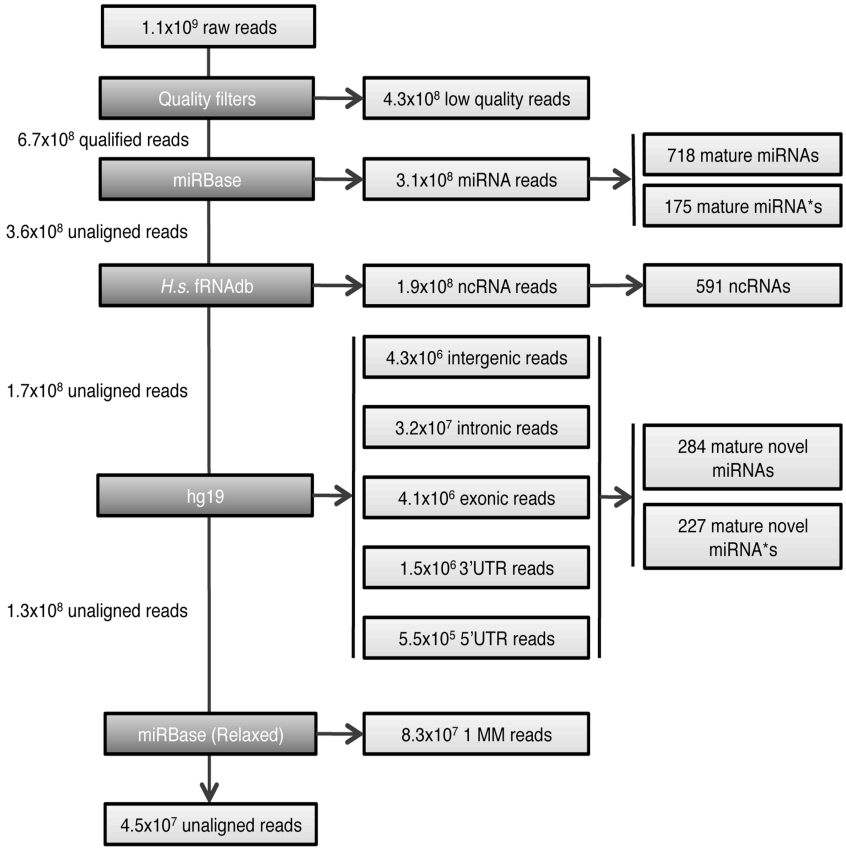

Figure 2-2. Flowchart describing alignment of small RNA reads to human sequence databases. All reads aligned with zero mismatches, unless relaxed parameters are indicated (i.e. 1MM=one mismatch). MiRNA* refers to mature miRNAs generated from the minor strand of the double stranded miRNA precursor. ncRNA refers to non-coding RNAs, such as tRNAs, piwi-interacting RNAs, snoRNAs, etc. in the *H. sapien* functional RNA database (see Materials and Methods).

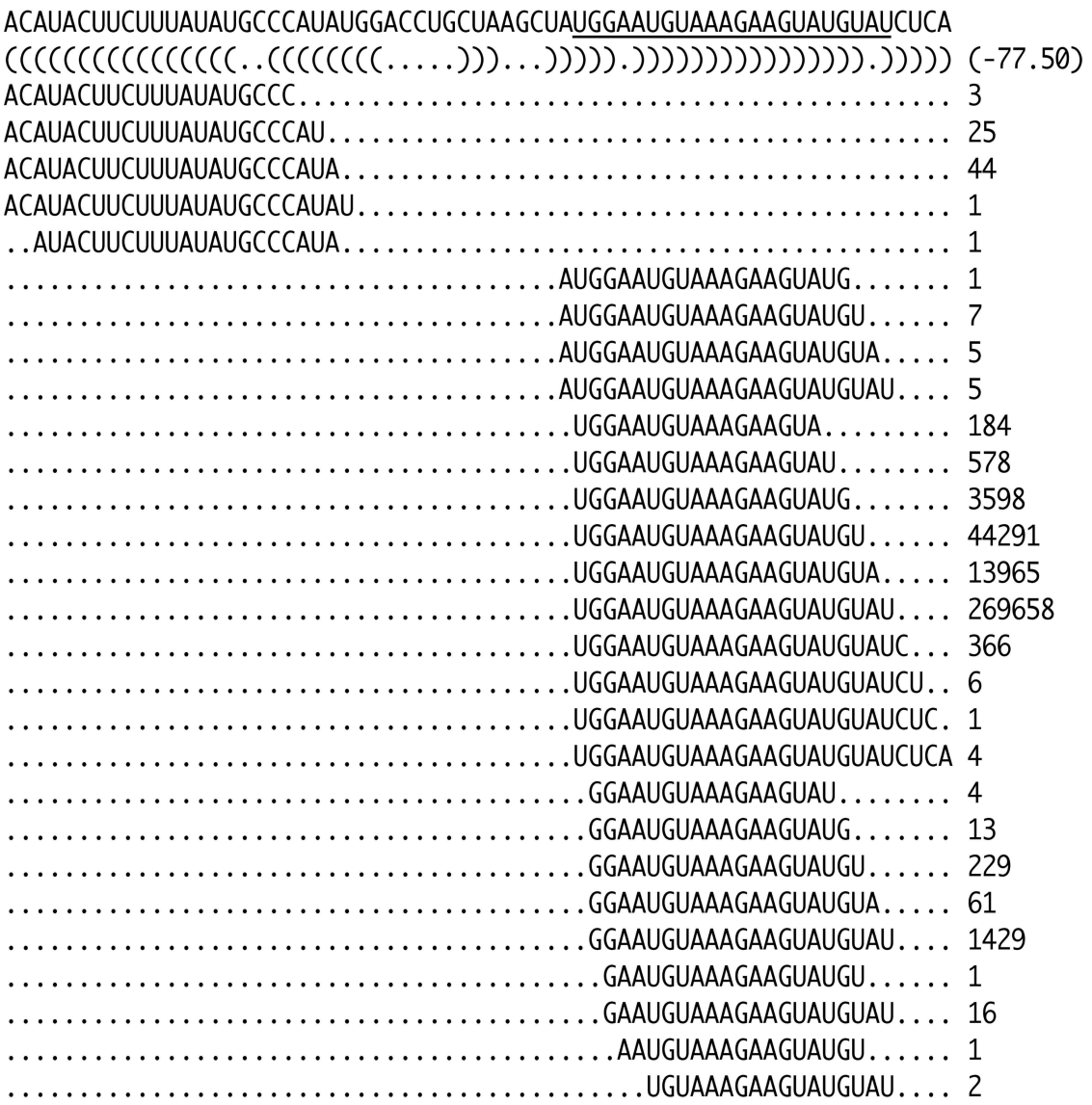

Figure 2-3. Example of small RNA reads aligning to a known miRNA precursor (miR-1-1). The mature miR-1-1 sequence, as annotated in miRBase, is underlined. The minimum free energy secondary structure is denoted by dot-bracket notation, where "(" and ")" represent complementary bases and "." represent non-complementary bases. Numbers in the right column represent the abundance of digital read counts corresponding to each sequence.

A

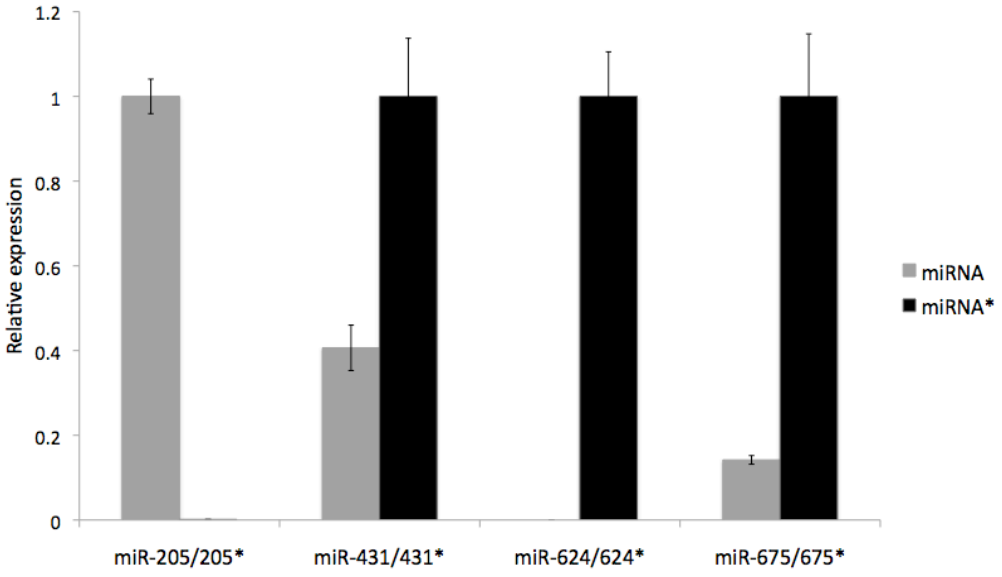
1.2
1
0.8
0.6
0.4
0.2
0
Relative expression
miRNA
miRNA*
miR-205/205*
miR-431/431*
miR-624/624*
miR-675/675*

B

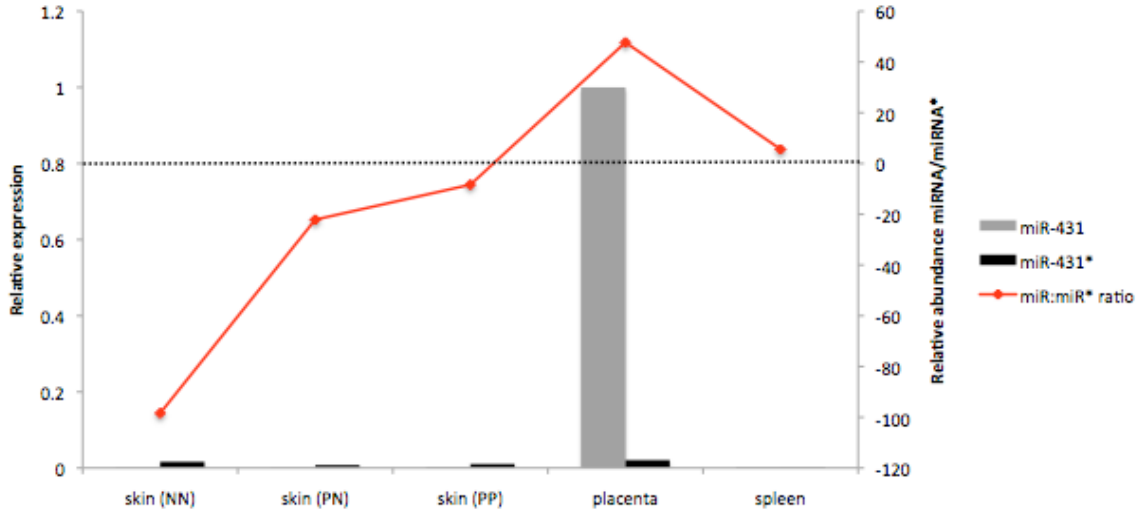
1.2
1
0.8
0.6
0.4
0.2
0
Relative expression
60
40
20
0
-20
-40
-60
-80
-100
-120
Relative abundance miRNA/miRNA*
miR-431
miR-431*
miR:miR* ratio
skin (NN)
skin (PN)
skin (PP)
placenta
spleen

C

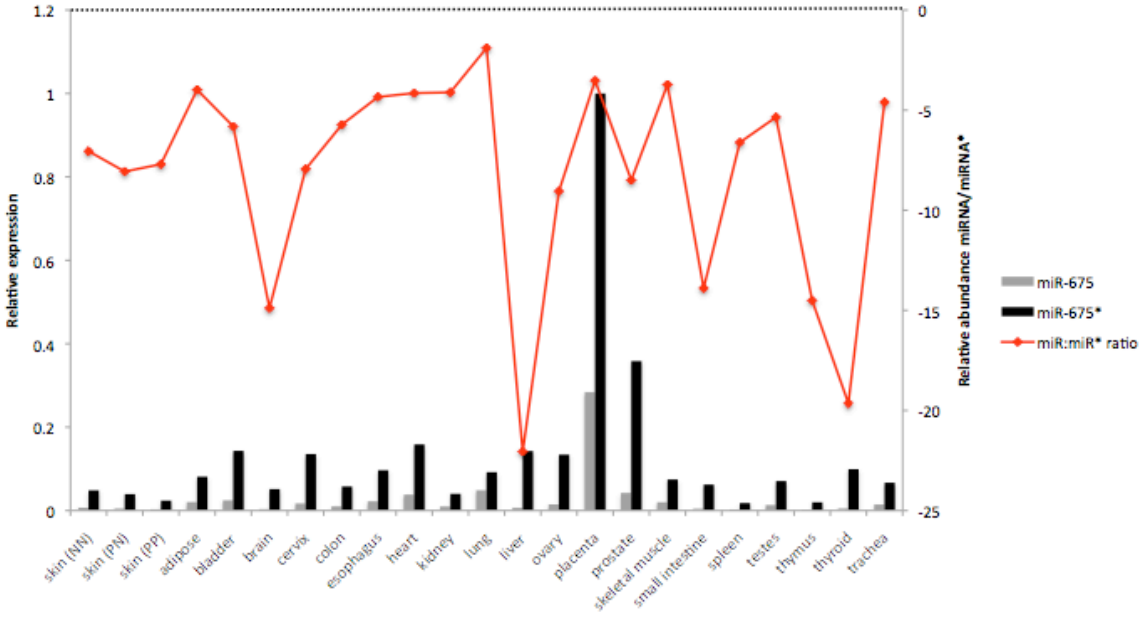

Figure 2-4. miRNA strand selection in skin and other human tissues. A) Relative expression of selected miRNAs and their cognate miRNA*s in normal human skin. Relative expression of B) miR-431 and miR-431* and C) miR-675 and miR-675* in skin and other human tissues in which it was detected. Red lines indicate relative level miRNA strand/relative level miRNA* strand in each tissue type. Dotted lines indicate threshold at which the abundance of the miRNA* strand exceeds that of the miRNA strand. Normal skin, NN; Uninvolved psoriatic skin, PN; Involved psoriatic skin, PP.

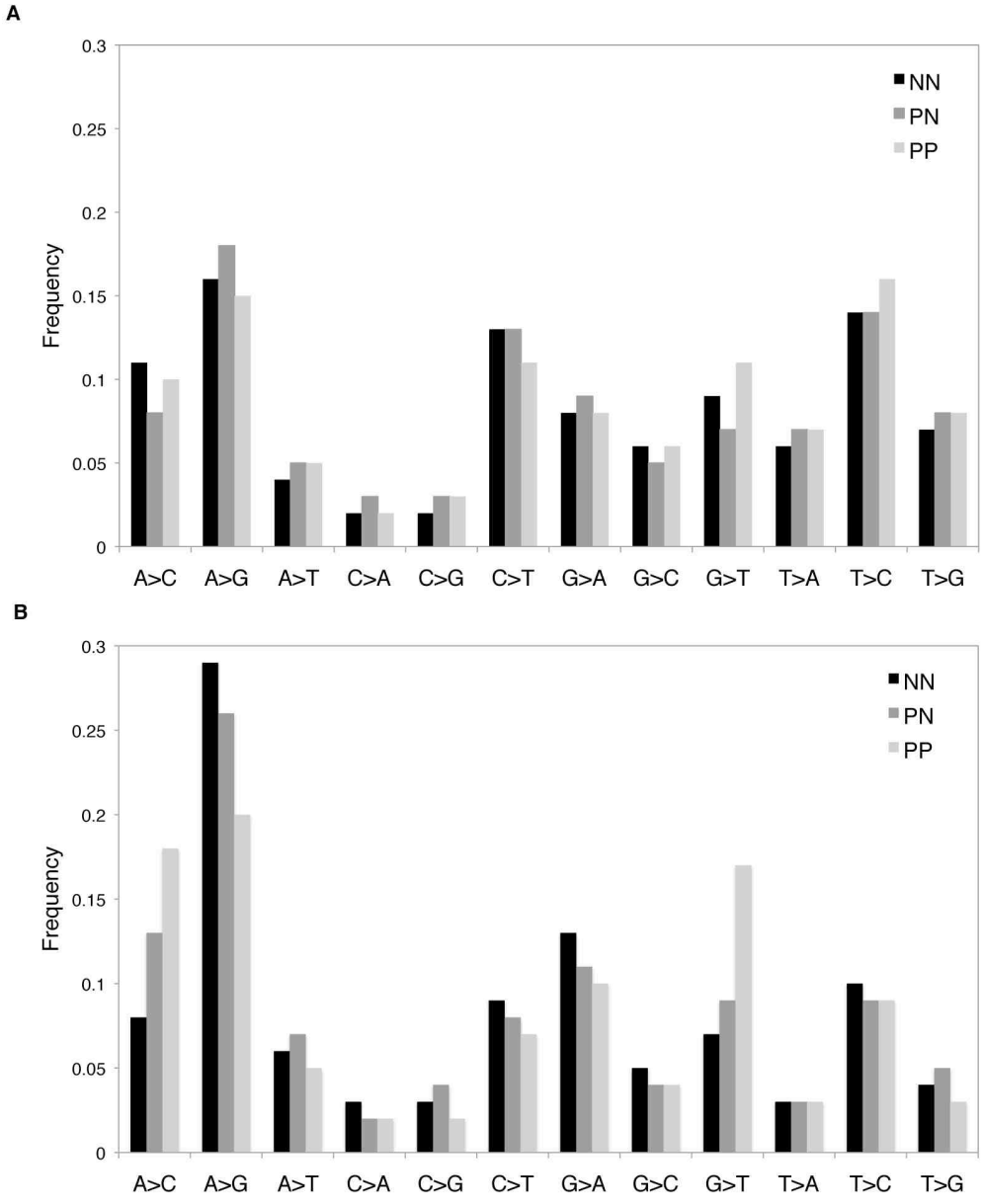

Figure 2-5. Patterns of miRNA editing in normal, uninvolved psoriatic, and involved psoriatic skin. Global frequencies of single base pair substitutions detected in (A) full length miRNAs and (B) miRNA seed regions in NN, PN, and PP skin. Normal skin, NN; Uninvolved psoriatic skin, PN; Involved psoriatic skin, PP.

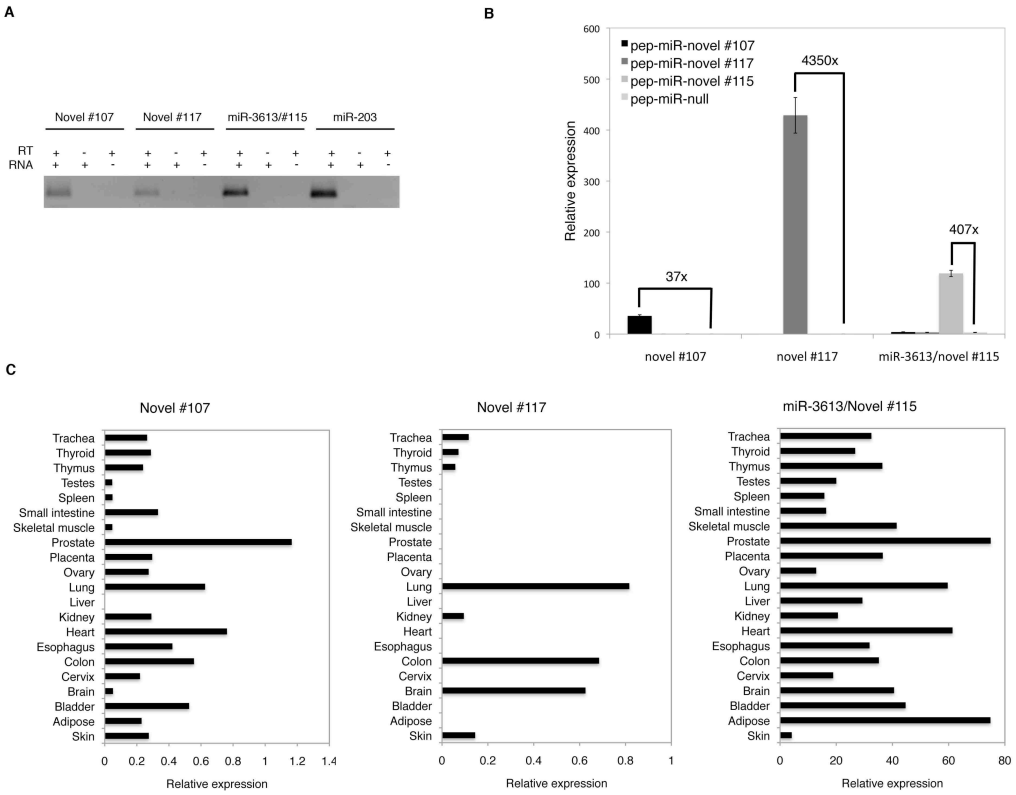

Figure 2-6. Experimental validation of novel miRNAs with qRT-PCR. (A) Endogenous expression of mature novel miRNAs in skin in the presence of RNA and reverse transcriptase, RNA only, or reverse transcriptase only. (B) Levels of mature novel miRNAs following ectopic expression of novel miRNA loci with "pep-miR" vectors in HEK293 cells (see Materials and Methods). Relative expression was calculated with respect to the endogenous snoRNA Z30 (see Materials and Methods). "X" refers to the fold change in mature miRNA expression following ectopic expression of the precursor. (C) Endogenous expression levels of novel miRNAs in 21 human tissues. Relative expression was calculated with respect to the endogenous snoRNA Z30 (see Materials and Methods).

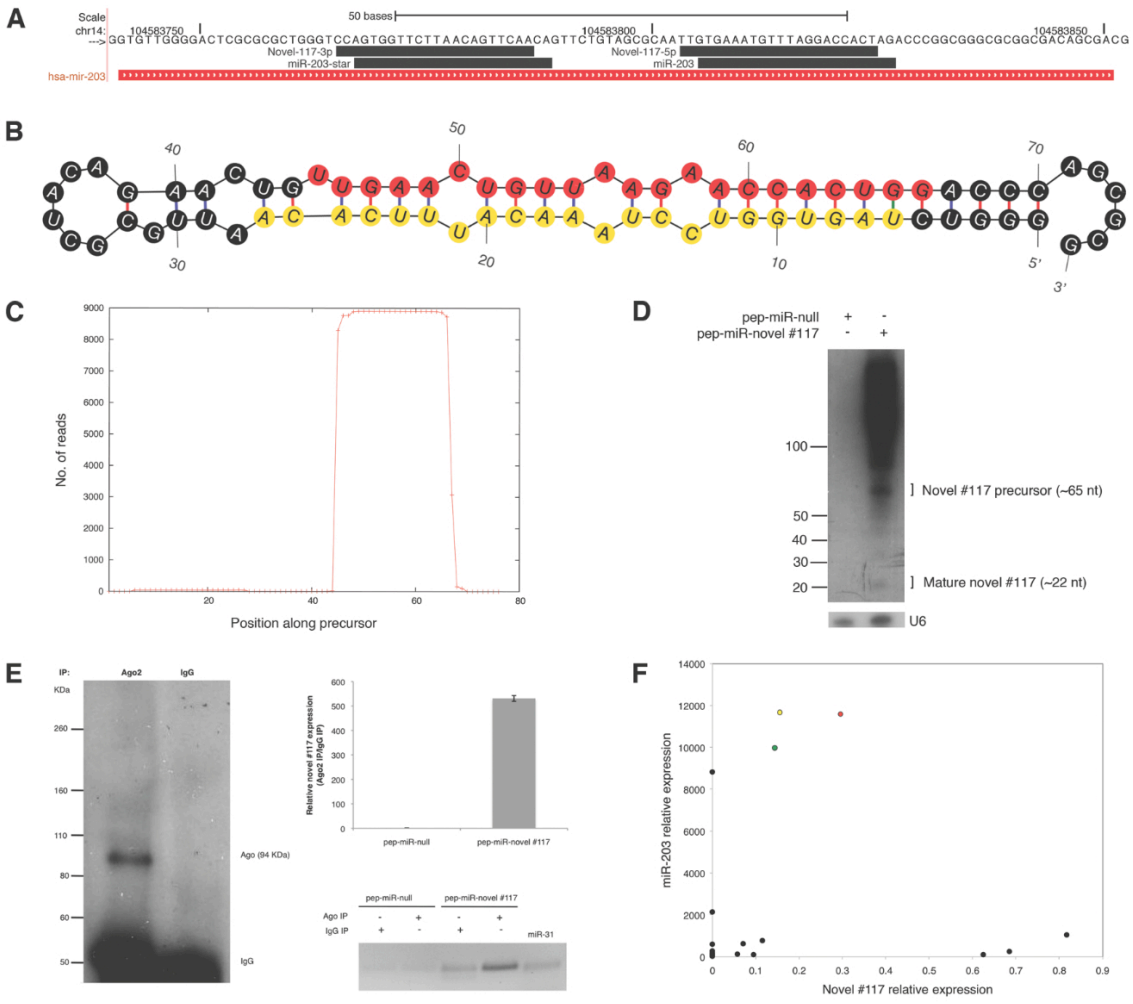

Figure 2-7. Features of a validated antisense miRNA locus (miR-203/novel #117). (A) Alignment of the dominant known and novel small RNA reads derived from the miR-203 locus. Forward strand sequence encoding miR-203 is indicated. The 3p and 5p arms of novel #117 correspond to the miRNA and miRNA* strands, respectively. (B) Predicted minimum free energy secondary structure of novel #117. Red circles represent the dominant mature miRNA sequence. Yellow circles represent the dominant mature miRNA* sequence. (C) Distribution of small RNA reads along the length of the novel #117 precursor. (D) Northern blot showing the accumulation of precursor and mature forms of novel #117 following ectopic expression of the #117 locus with a "pep-miR"

vector in HEK293 cells (see Materials and Methods). The endogenous U6 snRNA served as an input control. (E) Co-immunoprecipitation (IP) of ectopically expressed novel #117 with Argonaute 2 (Ago2). Left, western blot showing specificity of the Ago2 antibody. Top right, relative abundance of novel #117 in Ago2 IP compared to IgG control as indicated by qRT-PCR. Bottom right, RT-PCR bands corresponding to Ago2 and IgG IPs quantified in top right panel. (F) Correlation of miR-203 and novel #117 expression in NN (green circle), PN (yellow circle), and PP skin (red circle), and other human tissues (black circles). Relative expression was calculated with respect to the endogenous snoRNA Z30.

Chapter 3.

Differential expression of known and novel miRNAs in psoriatic skin

ABSTRACT

Psoriasis is a chronic, inflammatory skin disease for which there is currently no cure. Transcriptome analyses have revealed ~1300 mRNA expression changes in psoriatic skin, but much less is known about the role of microRNAs (miRNAs). I generated small RNA libraries from human skin biopsies with Next Generation sequencing (as described in Chapter 2), and performed digital gene expression analysis on 253, 212 and 204 million qualified reads from normal, uninvolved psoriatic and involved psoriatic skin, respectively. Eighty known and 18 novel miRNAs were two- to 42-fold differentially expressed in psoriatic skin, a subset of which were validated and further analyzed by qRT-PCR. Of particular significance was 1) the 2.7-fold upregulation of a validated novel miRNA derived from the antisense strand of the miR-203 locus (miR-203-AS), which plays a role in epithelial differentiation; 2) the differential expression of several intragenic miRNAs encoded within host genes that have been implicated in psoriasis; and 3) the response of some differentially expressed miRNAs to treatment with the TNF-alpha antagonist adalimumab. Overall, these analyses revealed dramatic changes in global miRNA expression, reflecting defects in keratinocytes, immune cells, and vasculature.

INTRODUCTION

Psoriasis is a chronic, inflammatory skin disease that affects 2-3% of Caucasians, and is less common in other populations (7). In involved psoriatic skin, hyperproliferation and defective terminal differentiation of keratinocytes impair barrier formation, infiltration of activated immune cells leads to inflammation, and interactions between the two cell types perpetuate disease (5,134). There is currently no cure for psoriasis, although some patients respond well to treatment with systemic biologics, such as the TNF-alpha antagonist adalimumab (135,136,137). There are over 1,000 differentially expressed transcripts in involved psoriatic (PP) skin compared to normal (NN) skin; a small subset of these are also differentially expressed in uninvolved psoriatic (PN) versus NN skin(18,19). However, much less is known about the expression of miRNAs in psoriatic skin, which may serve important regulatory functions.

Early microarray-based microRNA (miRNA) profiling studies have implicated a small number of miRNAs in psoriasis pathogenesis based on their differential expression in psoriatic skin (96,97). However, such array-based approaches are insensitive to low abundance small RNA species and limited to miRNAs that were previously known in humans or other species. In chapter 2, I described the global landscape of known and novel miRNAs expressed in human skin as determined by Next Generation sequencing (NGS). Here, I describe the differential expression of miRNAs in PP, PN, and NN skin as assessed by digital gene expression (DGE) analysis of Next Generation sequencing (NGS) reads and quantitative real-time PCR (qRT-PCR). These analyses revealed

dramatic changes in global miRNA expression, reflecting defects in keratinocytes, immune cells, and vasculature.

RESULTS

Altered expression of known and novel miRNAs in psoriatic skin

I generated small RNA libraries from 20 normal (NN), 23 uninvolved (PN), and 24 involved (PP) skin biopsies, as described in chapter 2. I detected expression of 893 known mature miRNAs, and 306 novel or recently described miRNA loci in the skin. I performed DGE analysis on these miRNAs to compare their expression in NN, PN, and PP skin. First, I normalized the number of miRNA reads to the total number of reads that mapped to the reference sequence in each skin category. Next, I implemented a detection threshold of 268 raw reads in the cumulative dataset (an average of four reads per individual library), which was empirically adjusted to allow the lowest detection threshold while minimizing noise. This resulted in a set of 512 known, 13 recently described, and 47 novel, mature miRNAs and miRNA*s (222).

Ninety-eight miRNAs, including 18 novel miRNAs, were significantly differentially expressed with a ±2-fold change in at least one comparison: PP/NN, PP/PN, or PN/NN (Bonferroni adjusted $p<0.05$; Table 3-1). Seventy-one miRNAs were upregulated while 27 were downregulated. This is substantially greater than the number of miRNAs previously shown to be ±2-fold differentially expressed in psoriatic skin from two previous microarray analyses (96,97). The majority of miRNA expression changes occurred in PP skin compared to both PN and NN (Figure 3-1). Thus, clustering of samples based on the expression of the top 98 differentially expressed miRNAs completely distinguished PP from PN and NN skin (Figure 3-1). Only five miRNAs were ±2-fold differentially expressed between PN and NN skin: miR-31, miR-206, miR-509-

5p, miR-675*, and novel #122. These findings are consistent with mRNA expression changes that have been described in psoriatic skin, in that there are more upregulated than downregulated transcripts and relatively few changes between PN and NN skin (18,19). Many additional miRNAs exhibited more modest fold changes in psoriatic skin. The fold changes for all of the known and novel miRNAs detected in skin are included in Appendices A and B. I observed only minor differences in the frequencies of A→G and C→T substitutions, (which would represent putative RNA editing events) between NN, PN, and PP skin (Figure 2-5). Still, the possibility remains that a small set of individual miRNAs are subject to differential editing in psoriatic skin.

MiRNAs that were derived from the same precursor were frequently co-regulated. There were 66 differentially expressed miRNAs/miRNA*s for which a cognate miRNA*/miRNA also passed the detection threshold for DGE. Eighty percent of these cognate strands exhibited a similar expression trend in the DGE dataset (±1.4-fold cut-off). One exception was miR-431/431*. miR-431 was upregulated in PN and PP skin compared to NN (3.2 and 3.9 fold, respectively) while miR-431* remained unchanged (1.2- and 1.0-fold). I subsequently validated this finding with stem-loop qRT-PCR (Figure 3-2). Thus, a subset of differentially expressed miRNAs may exhibit altered strand selection in psoriatic skin.

qRT-PCR validation of a subset of differentially expressed miRNAs

I selected 12 additional differentially expressed miRNAs for independent validation with stem-loop qRT-PCR, and confirmed that 7/9 known and 3/3 novel miRNAs were significantly differentially expressed in PP skin compared to PN or NN

(Figure 3-2). The two miRNAs that did not validate (miR-206 and miR-205*) showed similar trends as the DGE analysis, but the differences were not significant (p=0.10 and 0.09, respectively). Changes between NN and PN skin also validated poorly, presumably because the fold changes were typically smaller. Overall, qRT-PCR levels and normalized digital read counts for the differentially expressed miRNAs were highly correlated (R^2=0.979).

Functional annotation of miRNAs that are differentially expressed in psoriatic skin

Some of the most dramatically upregulated miRNAs in psoriatic skin included the abundant miRNAs miR-21, miR-31, and miR-378, which belong to a class of pro-angiogenic miRNAs termed "angiomiRs"; miR-155, miR-142-3p, and miR-146a, which regulate various hematopoietic cell fate decisions (89); miR-211, which inhibits melanoma metastasis (91,95); and the novel miR-203-AS, which was described in Chapter 2 (Figure 2-7). Downregulated miRNAs included miR-675* and miR-483-3p, which lie in the imprinted H19-IGF2 locus for which our lab has observed small but reproducible methylation increases in psoriatic skin (138,139); and miR-124, which is frequently epigenetically silenced in cancer (140,141). The downregulation of miR-483-3p is particularly significant because of its known role in the termination of wound healing in the skin (142). None of the differentially expressed miRNA genes overlapped with previously described psoriasis susceptibility loci (29,143), suggesting that miRNAs are more likely to function as downstream factors in disease pathogenesis.

Host gene expression for differentially expressed intronic miRNAs

Many differentially expressed miRNAs were intragenic, and these miRNAs may be under partial or full control of their host gene promoters. Several of these miRNAs are derived from genes that are likely to be involved in psoriasis pathogenesis (Table 3-2). Most notably, there were six differentially expressed intragenic miRNAs that were encoded within host genes that are differentially expressed in psoriasis (19). The upregulated miRNA, miR-147b, is located within the 3'UTR of *NMES1*, which is upregulated in PP versus NN skin. The downregulated miRNAs, miR-10a, miR-100 (and miR-125b, which just narrowly missed our two-fold cut-off), and novel #342 lie within introns of *HOXB3*, *LOC399959*, and *KRT15*, respectively, which are downregulated in PP versus NN skin. *LOC399959* encodes an uncharacterized ncRNA, and my findings suggest that this ncRNA likely functions as a polycistronic miRNA precursor. Novel #23 lies within intron 2 of *IFI27*, which is upregulated in PP versus NN skin; this miRNA was omitted from global DGE analysis because of low abundance, but showed strong evidence for upregulation in PP versus NN skin. While some intragenic miRNAs have autonomous promoters, the co-regulation of these miRNAs and their host transcripts in psoriasis suggests that these miRNAs are largely dependent on their host gene promoters for transcription. Thus, these differentially expressed intronic miRNAs may be functioning cooperatively with their misregulated host transcripts to influence psoriasis pathogenesis.

Other differentially expressed intragenic miRNAs lie within host genes whose known functions are related to psoriasis pathogenesis (Table 3-2). For example, the upregulated miRNA, miR-944, is located within an intron of the p63 gene, which is a transcription factor that regulates keratinocyte proliferation and differentiation (108,144);

the differential expression of p63 in psoriatic skin is complex in that it is isoform-specific and partially dependent on post-transcriptional mechanisms, such as miR-203 regulation (98,145,146). Two additional miRNAs that were omitted from global DGE analysis because of low abundance, but showed strong evidence for upregulation in PP versus NN skin, also fell into this category: miR-937 lies within a short intron of SCRIB, an adherens junction component and regulator of epithelial cell polarity (147); and miR-1908 lies within an intron of FADS1, a fatty acid desaturase (148).

In order to understand the relationships between miR-944, miR-937, and miR-1908 and their respective host genes, I analyzed expression patterns of the mature miRNA (mat-miRNA), the primary miRNA transcript (pri-miRNA), and the host mRNA transcript with qRT-PCR in a panel of human tissues. In the case of miR-944, expression of pri-miR-944 was strongly correlated with expression of the p63 mRNA (R^2=0.85), while expression of mat-miR-944 did not correlate well with either the pri-miR-944 or p63 (Figure 3-3A). For miR-937 and miR-1908, none of the species were highly correlated. Thus, there are complex and locus specific relationships between intragenic miRNAs and their host genes (Figure 3-3B,C). Specifically for miR-944, it appears that such tissue specific regulation occurs at the level of miRNA processing, as mat-miRNA levels correlated poorly with pri-miR-944 and p63 levels.

I next assessed whether the correlation between pri-miR-944 and p63 mRNA levels was evident in five NN, five PN, and five PP skin biopsies. Surprisingly, in NN and PN skin, mat-miR-944, but not pri-miR-944, levels were strongly correlated with p63 mRNA levels (R^2= 0.66 and 0.72, respectively, for NN and PN skin; Figure 3-3D). In contrast, neither miRNA species was strongly correlated with p63 in PP skin, but levels

of the pri-miRNA and mat-miRNA were correlated with each other (R^2=0.55). These findings suggest that in NN and PN skin, mat-miR-944 is coordinately regulated with p63. Moreover, this coordinate regulation breaks down in PP skin, perhaps due to disease-related alterations in transcription of specific p63 isoforms, alternative splicing, or miRNA processing.

miRNA responsiveness to adalimumab treatment

I obtained skin biopsy samples from a group of patients treated with the TNF-alpha antagonist adalimumab. Biopsies were taken from an involved site at zero and one month following treatment, and response to treatment was assessed by percent improvement in the Psoriasis Severity and Area Index (PASI) score at one and six months (Table 3-3). In order to determine whether miRNA expression is restored to normal following partial or complete resolution of psoriatic lesions, I assessed the levels of a subset of differentially expressed miRNAs by qRT-PCR in these samples. Differentially expressed miRNAs analyzed in these samples included some miRNAs with reported links to TNF-alpha pathways: miR-21, miR-31, miR-155, and miR-146a are all induced in cells treated with TNF-alpha (149,150,151), and miR-124 is predicted to target the 3'UTR of TNF-alpha.

For all of the miRNAs tested, their expression following one month of treatment either leveled off or worsened slightly in the majority of samples, which is consistent with the fact that lesions were only partially resolved after one month (21-65% improvement). Despite this, there were miRNAs for which the fold change at one month was correlated with treatment response at one or six months. Surprisingly, only one of the

TNF-alpha associated miRNAs, miR-31 (which was the most highly upregulated miRNA in PP and PN versus NN skin), exhibited a strong correlation with treatment response. The change in miR-31 levels at one month versus zero months was poorly correlated with treatment response at one month (R^2=0.03), but was predictive of treatment response at six months (R^2=0.61; Figure 3-4A). Changes in levels of other differentially expressed miRNAs- miR-7, miR-135b, miR-142-3p, and miR-203- at one month versus zero months were correlated with treatment response at one month, but not six months (R^2= 0.81, 0.60, 0.54, 0.65, and 0.57, respectively; Figure 3-4B). Changes in levels of miR-486-5p, miR-378, miR-483-3p, miR-944, miR-203-AS, miR-21, miR-146a, miR-155, and miR-124 were not correlated with response to treatment at one or six months (R^2<0.5). Overall, correlations between the relative values, log2 fold change and percent improvement in PASI score, were stronger than those assessed for absolute miRNA levels or PASI score at any single time point.

DISCUSSION

I have performed DGE analysis on NGS reads from NN, PN, and PP skin, and shown extensive alterations to the psoriatic miRNAome, many of which have not been previously reported. Some differentially expressed miRNAs have known functions that reflect pathogenic features of psoriasis, such as hyperproliferation of keratinocytes, immune cell activation, and increased angiogenesis, while others are of unknown function. Of particular note is the differential expression of a novel antisense miRNA derived from the miR-203 locus.

Reliability of miRNA profiling with NGS

Small RNA sequencing may be subject to intrinsic bias introduced by mechanisms such as non-random adapter ligation or sequence-based differences in PCR efficiency (113,114). Such bias could result in skewing of absolute quantification of miRNAs, but should not affect the relative quantitation of singular miRNAs across samples. Consistent with this, I observed a close correlation between normalized digital read counts and qRT-PCR levels. Thus, I conclude that NGS of small RNAs is a reliable method for miRNA profiling and that digital read count is an adequate proxy for miRNA abundance.

Significance of low abundance miRNAs

A major advantage of deep sequencing of large cohorts is enhanced sensitivity and dynamic range. The known, recently described, and novel miRNAs I detected in skin produced between one and 130M reads, with the ten most abundant miRNAs accounting

for nearly 70% of all miRNA reads. This finding is consistent with other recently published NGS studies (119,152) and prompts the question of how important the myriad low abundance miRNAs are. Normal and psoriatic skin biopsies are largely composed of keratinocytes, but contain many other cell types as well, such as fibroblasts and specialized immune cells (153). Some of these are critical for the disease process, but are low in abundance. Consequently, important miRNAs expressed in rare cell types can be drowned out by signal from keratinocyte-derived miRNAs, even if they serve important regulatory functions that influence disease pathogenesis.

Indeed, only two of the 98 differentially expressed miRNAs represented greater than 1% of miRNA reads in the cumulative dataset, indicating that miRNAs of moderate to low abundance account for most of the variation in the psoriatic miRNAome. Alternatively, bias introduced during library preparation may have led to an underestimate of miRNA abundance in some cases. It is unlikely that differential expression of these low abundance miRNAs was due to random fluctuations in digital read count because all of these miRNAs exhibited expression changes that were highly reproducible across individuals and statistically significant. Furthermore, several miRNAs that showed evidence for differential expression but did not meet my abundance threshold in the cumulative dataset were independently validated with qRT-PCR (data not shown), suggesting that accurate DGE data can be obtained for very low abundance miRNAs.

According to a recent comparative genomics study, 269 known human miRNAs are primate-specific, and these miRNAs are generally expressed at low levels in adult tissues (154). Their computationally predicted targets show functional enrichment for

early developmental processes, cell cycle, and proliferation (154). Thus, the differential expression of poorly conserved novel miRNAs in psoriatic skin could reflect an innate developmental defect in skin barrier formation. I have reported the differential expression of 18 non-conserved novel miRNAs in psoriatic skin, presenting the intriguing possibility that some newly evolved novel miRNAs may serve human- or primate-specific functions with relevance to psoriasis pathogenesis.

Comparison with previous studies

I have shown extensive alterations to the psoriatic miRNAome, many of which have not been previously reported, including the differential expression of a novel antisense miRNA derived from the miR-203 locus. I also replicated several miRNA expression changes from two previous miRNA microarray studies which identified 23 miRNAs as ±2-fold differentially expressed in psoriasis (96,97). Of these 23, I conclusively confirmed six: miR-21, miR-31, miR-142-3p, miR-146a, miR-223, and miR-378 (±2-fold change in our study). I tentatively confirmed an additional seven: miR-17-5p, miR-30e-5p, miR-122a, miR-141, miR-142-5p, miR-146b, and miR-203 (±1.4 fold change in our study). These 13 confirmed miRNAs included six out of eight miRNAs that were ±2-fold differentially expressed according to both microarray studies: miR-17, miR-21, miR-31, miR-142-3p, miR-146a/b, miR-200a, and miR-203. The remaining ten miRNAs that were previously reported as ±2-fold differentially expressed in psoriasis were detected by NGS in skin, but showed no evidence for differential expression. I also identified 67 known and 18 novel differentially expressed miRNAs that have not been previously implicated in psoriasis and have validated several of these by

stem-loop qRT-PCR. Many of the differentially expressed miRNAs reported in this study were likely to have been missed by previous studies because of their low abundance or because microarray platforms lacked probes that interrogated them.

One tentatively validated miRNA was miR-203, which was reported to be 5.86- and 2.02-fold upregulated in PP versus NN skin, according to the two previous miRNA microarray studies in psoriasis (96,97). With the DGE analysis described here, miR-203 exhibited a 1.6- and 1.4-fold upregulation in PP skin compared to NN and PN, respectively, which was lower than microarray-based fold changes. I confirmed these modest fold changes with qRT-PCR in my patient cohort (data not shown). The current model for miR-203 function is that its targeting of p63 in the suprabasal layers of the epidermis limits the proliferative potential of keratinocytes, which establishes a well-defined boundary between proliferating and terminally differentiating keratinocytes (99). Given the hyperproliferative phenotype of psoriatic keratinocytes, the upregulation of the anti-proliferative miR-203 in psoriatic skin is puzzling. However, NGS revealed upregulation of a novel antisense miRNA derived from the miR-203 locus, which I have designated miR-203-AS. While miR-203-AS was much less abundant than miR-203 in skin, it was the most abundant novel miRNA in the cumulative dataset. Furthermore, it was 2.7- and 2.2-fold upregulated in PP and PN skin, respectively, compared to NN. Taken together, these findings more strongly support a role for miR-203-AS in psoriasis, but do not exclude the involvement of miR-203. Functional characterization of miR-203-AS will likely help to reconcile apparent inconsistencies in the biological and pathogenic functions of miR-203.

Significance of intronic/intragenic miRNAs

Mounting evidence suggests that intragenic miRNAs, such as intronic miRNAs, functionally interact with their host genes. For example, miR-33, which lies in an intron of the sterol response element binding protein gene (*SREBP*), regulates cholesterol homeostasis (155). In other cases, a function that has been ascribed to a protein-coding gene may actually be mediated by an intragenic miRNA. For example, the *MLSN1* gene encodes a protein that was long thought to suppress motility and invasion of melanoma cells, but it has recently been recognized that the intronic miRNA miR-211 is actually responsible for this phenotype (95). In the case of psoriasis, several differentially expressed intragenic miRNAs lie within host genes that have been previously implicated into psoriasis. The upregulation of miR-944, which is encoded within an intron of p63, in PP skin is particularly intriguing, given the differential expression of miR-203, which directly targets p63, and the potentially related miR-203-AS in PP skin. Thus, taking into account host gene function of intragenic miRNAs could help to elucidate the pathways and specific targets they regulate.

Altered expression of angiomiRs in involved psoriatic skin

miR-21, miR-31 and miR-378 are three of the most abundant and differentially expressed miRNAs in PP skin and are members of a growing class of miRNAs termed "angiomiRs" (156). Pro-angiomiRs promote angiogenesis by targeting negative regulators in angiogenic signaling pathways, while anti-angiomiRs inhibit angiogenesis by targeting positive regulators of angiogenesis. The role of these and other differentially expressed angiomiRs in psoriatic skin is of interest, given its proclivity for

neovascularization.

Activated keratinocytes mediate angiogenesis through increased synthesis of VEGF, PDGF, and other endothelial cell mitogens, and inflammatory skin disease with some features of PS is induced by over-expression of VEGF in murine skin (157,158,159,160). miR-378 is proposed to promote VEGF expression by competing with miR-125 (which was modestly downregulated in PP skin) for the same binding site in the VEGF 3′ UTR (161). VEGF is upregulated in PP skin (162), and has been shown to induce expression of the upregulated miRNAs miR-18a, miR-31, and miR-155 (163).

Interestingly, although a number of pro-angiomiRs were upregulated in PP skin, many miRNAs that would be predicted to inhibit angiogenesis by repressing VEGF were not differentially expressed. This includes miR-15b, miR-16, and miR-20a/b (156). One anti-angiomiR, miR-100, was downregulated in PP skin. miR-100 has been shown to inhibit angiogenesis by repressing the mammalian target of rapamycin (mTOR) in endothelial cells (164). Interestingly, the mTOR binding partner, regulatory associated protein of mTOR (RAPTOR), is encoded at 17q25, directly under a psoriasis association peak, pointing to mTOR upregulation in lesions through loss of RAPTOR activity or decreased levels of miR-100. These findings suggest that therapeutic application of anti-angiomiR mimics might improve symptoms of psoriasis.

Altered expression of oncogenic and tumor suppressive miRNAs

Several miRNAs that were differentially expressed in psoriasis have been implicated in tumorogenesis, such as miR-21, miR-31 and the miR-17-92 cluster miRNAs miR-18a/19a/19b-1/92a-1 (165). These miRNAs have also been implicated in

other diseases such as cardiovascular disease (miR-21), Duchenne muscular dystrophy (miR-31), and systemic lupus erythematosus (miR-17-92) (166,167,168). Taken together, these findings suggest that these miRNAs do not function as classical oncogenes and tumor suppressors. Instead, their roles in cancer, psoriasis, and other diseases may be related to non-transformative pathways such as cell growth and survival, angiogenesis and inflammation. Alternatively, these miRNAs may be functioning pleiotropically by targeting distinct mRNAs in different tissues, developmental stages, or disease states. In one case, differential expression of a tumor suppressive miRNA may provide insight into psoriasis as a benign hyperplasia. miR-211 is a tumor suppressor in cutaneous melanoma, and its downregulation is correlated with increased metastasis (91,95). I found that miR-211 was upregulated in PP versus PN and NN skin. Thus, upregulation of miR-211 may be one feature that distinguishes psoriatic skin from metastatic cutaneous tumors.

miR-31 predicts response to treatment

The angiomiR miR-31, which is induced by TNF-alpha in endothelial cells, was the most highly differentially expressed miRNA in PP and PN skin versus NN (42-fold and 14-fold upregulation, respectively). This miRNA was associated with 55,893 reads in the cumulative sequencing dataset, and ranks as the 136th most abundant miRNA in skin. The change in miR-31 level following one month of adalimumab treatment predicted response to treatment at six months. This finding is significant because patients who have a low likelihood of response could be identified early on during the course of treatment based on miR-31 levels. Since 20-47% of patients receiving high or low doses of adalimumab, respectively, in a randomized, double-blind, placebo controlled study did

not achieve 75% improvement in PASI score after 12 weeks, a substantial number of patients could be helped by early screening (137). One drawback is that miR-31 levels in the blood are uninformative (data not shown), so skin biopsies would need to be collected at zero and one month to complete this assessment. The lack of response of other TNF-alpha-induced miRNAs to adalimumab treatment is curious, and suggests that positive feedback loops may be contributing to their sustained expression even in the absence of TNF-alpha signaling.

Conclusions and future directions

I have shown that at least 98 miRNAs are differentially expressed in psoriatic skin. These miRNAs are likely to influence many processes that are involved in psoriasis pathogenesis such as angiogenesis, epidermal differentiation, and inflammation. In terms of understanding the normal and pathogenic functions of these and other differentially expressed miRNAs, target identification is crucial. The identification of targets for the upregulated miRNAs, miR-203-AS and miR-944, would be of particular interest because of their connections to the p63 pathway. Overall, cutaneous diseases such as psoriasis are likely to be on the front line of miRNA-based diagnostics and therapeutics. The comprehensive profiling of the miRNAome in normal and psoriatic skin represents a critical first step towards such translational applications.

MATERIALS AND METHODS

Digital gene expression analysis. Reads that aligned perfectly to mature known and novel miRNAs with 3nt extension were subjected to digital gene expression analysis. Reads that mapped to multiple mature miRNAs were attributed to all potential derivative miRNAs. Read counts in each skin category (NN, PN, and NN) were normalized to adjust for slight variation in total read count between categories. Let *N* be the number of qualified reads that aligned to hg19, *C* the number of categories, and *M* the number of qualified miRNA reads. Thus, the normalized number of reads for each miRNA in a given category is $(N^{total}*M^{category})/(C*N^{category})$. A detection filter was applied such that miRNAs that were represented by fewer than 268 raw reads in the cumulative dataset were removed. Fold changes were calculated from normalized read counts, and Pearson's chi-squared test with Bonferroni correction was applied to determine significance.

miRNA qRT-PCR. qRT-PCR of mature miRNAs was performed as described in Chapter 2.

mRNA qRT-PCR. Total RNA was reverse transcribed with the Superscript First Strand Synthesis System (Invitrogen). Briefly, 100ng-1ug of total RNA was primed with 50ng random hexamer and reverse transcribed in a 20ul reaction with 50U SuperScript II reverse transcriptase. cDNA synthesis conditions were as follows: 25°C for 10 min, 42°C for 50 min, 70°C for 15 min, 4°C hold. PCR reactions were performed with Power SYBR Green master mix (Life Technologies). Briefly, 0.2ng of input cDNA was amplified in 10ul PCR reactions. Final primer concentration was 0.25uM and primer sequences were as follows: p63 F 5'- and R 5'; SCRIB F 5'- and R 5'; and FADS1 F 5'- and R 5'. PCR

was performed on a 7900HT thermocycler (Life Technologies) under the following conditions: 50°C for 2 min; 95°C for 10 min; 40 cycles [95°C for 10 sec; 60°C for 1 min]; 4°C hold. Raw expression values were normalized to 18S rRNA. Relative expression levels were calculated according to the 2-ΔΔCt method as follows: $2^{((Ct\ 18S)-(Ct\ mRNA))}$.

Table 3-1. miRNAs that are ± 2 fold differentially expressed in psoriatic skin.

Mature miRNA	Sequence	Normalized no. reads			Fold change			Bonferroni adjusted p value	Total reads (raw)	% miRNA reads
		NN[b]	PN[b]	PP[b]	PP/NN	PP/PN	PN/NN			
hsa-miR-31	AGGCAAGATGCTGGCATAGCT	1063.44	3255.25	45690.24	42.93	14.03	3.06	0	55883	0.012528
hsa-miR-31*	TGCTATGCCAACATATTGCCAT	250.54	358.19	8679.14	34.51	24.17	1.43	0	10412	0.002334
hsa-miR-206	TGGAATGTAAGGAAGTGTGTGG	119.25	317.23	1538.82	12.80	4.84	2.65	0	2156	0.000483
hsa-miR-21*	CAACACCAGTCGATGGGCTGT	712.24	1032.56	6278.75	8.80	6.08	1.45	0	8754	0.001963
hsa-miR-135b*	ATGTAGGGCTAAAAGCCATGGG	62.36	66.18	506.18	8.00	7.55	1.06	5.732E-131	694	0.000156
hsa-miR-33b*	CAGTGCCTCGGCAGTGCAGCCC	61.27	67.23	353.62	5.70	5.20	1.10	5.8762E-73	521	0.000117
hsa-miR-135b	TATGGCTTTTCATTCCTATGTGA	643.31	682.77	3636.74	5.65	5.32	1.06	0	5362	0.001202
hsa-miR-222*	CTCAGTAGCCAGTGTAGATCCT	440.91	736.34	2467.41	5.59	3.35	1.67	0	3902	0.000875
hsa-miR-1268	CGGGCGTGGTGGTGGGGG	1514.20	2227.94	6745.25	4.45	3.03	1.47	0	11154	0.002501
Novel #6	TAAAAGTAATTGTGGTATTTGC	303.06	370.80	1246.93	4.10	3.36	1.22	1.086E-185	2044	0.000458
hsa-miR-21	TAGCTTATCAGACTGATGTTGA	4091259.64	4176278.01	16177715.35	3.95	3.87	1.02	0	26060562	5.842373
hsa-miR-431	TGTCTTGCAGGCCGTCATGCA	44.86	54.62	178.13	3.91	3.22	1.21	1.3599E-23	295	0.000066
Novel #47	TCTGATCAGGCAAAATTGCAG	77.68	68.28	296.30	3.78	4.29	-1.14	1.1163E-46	472	0.000106
hsa-miR-7	TGGAAGACTAGTGATTTTGTTGT	9314.93	12290.97	28373.42	3.05	2.31	1.32	0	52390	0.011745
hsa-miR-496	TGAGTATTACATGGCCAATCTC	148.79	190.13	451.51	3.02	2.37	1.28	3.2601E-42	829	0.000186
hsa-miR-3065-5p	TCAACAAAATCACTGATGCTGGA	537.19	474.79	1622.60	3.02	3.41	-1.13	9.559E-204	2783	0.000624
Novel #35	CCACTTGGATCTGAAGGCTGCC	61.27	65.13	183.42	2.96	2.79	1.06	4.7232E-18	326	0.000073
hsa-miR-592	TTGTGTCAATATGCGATGATGT	54.70	77.73	161.38	2.92	2.06	1.41	8.4232E-12	307	0.000069
hsa-miR-545*	TCAGTAAATGTTTATTAGATGA	52.52	60.92	151.68	2.85	2.47	1.16	1.1638E-12	278	0.000062
hsa-miR-944	AAATTATTGTACATCGGATGAG	8181.47	7959.04	23300.16	2.85	2.93	-1.03	0	41477	0.009298
hsa-miR-200c*	CGTCTTACCCAGCAGTGTTTGG	530.62	584.03	1485.03	2.80	2.54	1.10	6.205E-142	2725	0.000611
hsa-miR-940	AAGGCAGGGCCCCCGCTCCCC	66.74	66.18	187.83	2.79	2.81	-1.01	9.8759E-18	337	0.000076
hsa-miR-147b	GTGTGCGGAAATGCTTCTGCTA	64.55	81.93	181.66	2.79	2.20	1.27	1.1065E-13	343	0.000077
Novel #117	TTGAACTGTTAAGAACCACTGG	1657.52	2138.66	4597.95	2.77	2.15	1.29	0	8765	0.001965
hsa-miR-155	TTAATGCTAATCGTGATAGGGGT	18527.02	19220.60	50098.60	2.70	2.61	1.04	0	92043	0.020635
hsa-miR-378	ACTGGACTTGGAGTCAGAAGG	1308311.11	1659217.08	3504731.56	2.68	2.11	1.27	0	6749701	1.513178
hsa-miR-1303	TTTAGAGACGGGGTCTTGCTCT	100.65	153.36	269.85	2.66	1.75	1.52	1.6677E-16	544	0.000122
hsa-miR-3176	ACTGGCCTGGGACTACCGG	87.53	82.98	234.57	2.66	2.80	-1.05	1.0309E-21	425	0.000095
hsa-miR-3613/Novel #115	TGTTGTACTTTTTTTTTTGTTC	5674.95	5138.66	14804.44	2.61	2.88	-1.10	0	26867	0.006023
hsa-miR-211	TTCCCTTTGTCATCCTTCGCCT	3135.61	6034.67	8157.96	2.60	1.35	1.92	0	17862	0.004004
Novel #69	TACATGGATGGAAACCTTCAAGC	80.96	81.93	207.23	2.54	2.51	1.01	2.1902E-16	387	0.000087
hsa-miR-142-3p	TGTAGTGTTTCCTACTTTATGGA	91176.69	77835.12	229401.86	2.52	2.95	-1.17	0	417574	0.093614
hsa-miR-455-3p	GCAGTCCATGGGCATATACAC	12226.26	11781.52	30044.52	2.46	2.55	-1.04	0	56461	0.012658
hsa-miR-18a	TAAGGTGCATCTAGTGCAGATAG	6729.64	7211.14	16350.32	2.43	2.27	1.07	0	31557	0.007075
hsa-miR-3150b/novel #95	TGAGGAGATCGTCGAGGTTGGC	59.08	116.60	142.86	2.39	1.22	1.96	2.076E-05	327	0.000073
Novel #116	AAAGGACCTTGTGAGACGGAG	53.61	76.68	128.75	2.38	1.67	1.42	2.4595E-05	268	0.000060
hsa-miR-19b-1*	AGTTTTGCAGGTTTGCATCCAGC	273.52	388.66	649.04	2.37	1.67	1.42	1.1598E-34	1356	0.000304
hsa-miR-146a	TGAGAACTGAATTCCATGGGTT	257981.11	310479.12	609439.89	2.36	1.96	1.20	0	1222470	0.274059
hsa-miR-188-5p	CATCCCTTGCATGGTGGAGGG	630.19	668.07	1486.79	2.36	2.22	1.06	1.941E-107	2898	0.000650
hsa-miR-376a*	GTAGATTCTCCTTCTATGAGTA	1596.25	1683.82	3748.73	2.35	2.23	1.05	5.951E-273	7313	0.001639
hsa-miR-665	ACCAGGAGGCTGAGGCCCCT	159.73	218.49	374.78	2.34	1.71	1.37	2.923E-19	779	0.000175
Novel #122	AGTTGCCTTTTTGTTCCCATGC	59.08	131.30	139.33	2.34	1.06	2.20	1.2814E-05	337	0.000076
hsa-miR-548f	AAAAACTGTAATTACTTTT	70.02	72.48	164.02	2.32	2.25	1.03	4.7266E-10	319	0.000072
hsa-miR-369-3p	AATAATACATGGTTGATCTTT	3427.73	2759.45	7933.98	2.31	2.87	-1.24	0	14757	0.003308
hsa-miR-449a	TGGCAGTGTATTGTTAGCTGGT	119.25	157.56	276.02	2.30	1.75	1.32	1.2638E-13	572	0.000128
hsa-miR-33a*	CAATGTTTCCACAGTGCATCAC	582.05	689.08	1319.24	2.26	1.91	1.18	1.1032E-77	2684	0.000602
hsa-miR-33b	GTGCATTGCTGTTGCATTGC	284.46	273.11	634.93	2.23	2.32	-1.04	4.4117E-44	1240	0.000278
hsa-miR-18a*	ACTGCCCTAAGTGCTCCTTCTGG	253.82	367.65	565.26	2.22	1.54	1.45	3.647E-25	1223	0.000274

hsa-miR-23a*	GGGGTTCCTGGGGATGGGATTT	217.72	348.74	485.02	2.22	1.39	1.60	4.8426E-20	1081	0.000242
hsa-miR-223*	CGTGTATTTGACAAGCTGAGTT	479.20	446.43	1050.28	2.19	2.35	-1.07	6.9441E-74	2054	0.000460
hsa-miR-187	TCGTGTCTTGTGTTGCAGCCGG	630.19	744.75	1371.27	2.17	1.84	1.18	2.1724E-73	2840	0.000637
hsa-miR-1276	TAAAGAGCCCTGTGGAGACA	107.22	91.39	230.16	2.14	2.50	-1.17	2.2078E-15	446	0.000100
hsa-miR-223	TGTCAGTTTGTCAAATACCCCA	18027.03	17264.71	38451.16	2.13	2.23	-1.04	0	76516	0.017154
hsa-miR-154*	AATCATACACGGTTGACCTATT	261.48	239.50	557.33	2.13	2.32	-1.09	1.209E-36	1099	0.000246
hsa-miR-487a	AATCATACAGGGACATCCAGTT	370.89	432.77	785.73	2.12	1.81	1.17	6.0323E-39	1642	0.000368
Novel #123	TTGGAGGGTGTGGAAGACATC	75.49	79.83	160.50	2.11	2.00	1.06	2.4622E-07	327	0.000073
hsa-miR-19b	TGTGCAAATCCATGCAAAACTGA	47813.14	45453.80	100637.24	2.10	2.21	-1.05	0	201095	0.045082
hsa-miR-212	TAACAGTCTCCAGTCACGGCC	251.64	226.89	525.58	2.08	2.31	-1.11	1.6155E-33	1042	0.000234
hsa-miR-92a-1*	AGGTTGGGATCGGTTGCAATGCT	354.48	436.97	731.05	2.06	1.67	1.23	1.9647E-31	1569	0.000352
hsa-miR-378*	CTCCTGACTCCAGGTCCTGTGT	1417.92	1373.95	2899.51	2.04	2.11	-1.03	1.682E-170	5892	0.001321
hsa-miR-205*	GATTTCAGTGGAGTGAAGTTC	549.22	597.69	1118.18	2.03	1.87	1.09	4.0103E-55	2339	0.000524
hsa-miR-1308	GCATGGGTGGTTCAGTGG	2130.16	2262.61	4330.75	2.03	1.91	1.06	2.437E-225	9012	0.002020
hsa-miR-1307	ACTCGGCGTGGCGTCGGTCGTG	7732.90	6553.57	15201.27	1.97	2.32	-1.18	0	30545	0.006848
hsa-miR-362-3p	AACACACCTATTCAAGGATTCA	405.90	391.81	793.66	1.95	2.02	-1.04	1.8114E-40	1644	0.000369
hsa-miR-590-3p	TAATTTTATGTATAAGCTAGT	1237.40	886.55	2400.39	1.94	2.71	-1.40	1.156E-178	4697	0.001053
hsa-miR-19a	TGTGCAAATCTATGCAAAACTGA	2609.36	2141.81	4938.34	1.89	2.31	-1.22	1.348E-299	10024	0.002247
hsa-miR-3065-3p	TCAGCACCAGGATATTGTTGGAG	562.35	480.04	1044.99	1.86	2.17	-1.17	5.033E-56	2156	0.000483
hsa-miR-377	ATCACACAAAGGCAACTTTTGT	912.46	768.91	1651.70	1.81	2.15	-1.19	1.3141E-85	3439	0.000771
hsa-miR-376b	ATCATAGAGGAAAATCCATGTT	716.62	582.98	1241.64	1.73	2.13	-1.23	4.79E-60	2618	0.000587
hsa-miR-509-5p	*TACTGCAGACAGTGGCAATCA*	352.29	720.59	567.91	*1.61*	*-1.27*	*2.04*	*4.1473E-25*	*1652*	*0.000370*
hsa-miR-542-3p	TGTGACAGATTGATAACTGAAA	5650.88	3641.81	7399.58	1.31	2.03	-1.55	6.645E-274	17023	0.003816
hsa-miR-2110	TTGGGGAAACGGCCGCTGAGTG	1932.13	2987.40	1227.53	-1.57	-2.43	1.55	3.596E-164	6002	0.001346
Novel #31	TTGGACAGAAAACACGCAGGA	1284.44	1554.62	746.92	-1.72	-2.08	1.21	2.4463E-59	3501	0.000785
hsa-miR-486-5p	TCCTGTACTGAGCTGCCCCGAG	134809.38	148860.36	74411.99	-1.81	-2.00	1.10	0	349315	0.078311
hsa-miR-628-3p	TCTAGTAAGAGTGGCAGTCGA	587.52	689.08	313.94	-1.87	-2.19	1.17	9.4618E-29	1549	0.000347
hsa-miR-1179	AAGCATTCTTTCATTGGTTGG	152.08	86.13	74.96	-2.02	-1.15	-1.76	3.9851E-05	306	0.000069
hsa-miR-99a	AACCCGTAGATCCGATCTTGTG	400593.41	260932.88	195318.48	-2.05	-1.34	-1.54	0	836045	0.187428
Novel #55	AAAGACATAGTTGCAAGATGGG	246.17	263.66	117.29	-2.09	-2.24	1.07	3.5043E-11	609	0.000137
Novel #59	TGGGCCATGCATTTCTAGAACT	135.66	114.50	64.37	-2.09	-1.77	-1.18	0.00180925	306	0.000069
Novel #333	TCTCTGCCGGCTTGATGGGCTAGC	164.11	131.30	77.60	-2.10	-1.68	-1.25	0.00014083	363	0.000081
has-miR-1468	CTCCGTTTGCCTGTTTCGCTG	133.48	105.04	59.97	-2.21	-1.74	-1.27	0.00065969	290	0.000065
Novel #337	ACACTTGTTGGGATGACCTGC	275.71	191.18	119.05	-2.30	-1.60	-1.44	1.432E-11	569	0.000128
hsa-miR-10a	TACCCTGTAGATCCGAATTTGTG	1435203.78	942025.60	621943.60	-2.31	-1.51	-1.52	0	2913882	0.653247
hsa-miR-100	AACCCGTAGATCCGAACTTGTG	838053.76	608920.42	362352.60	-2.31	-1.68	-1.38	0	1756589	0.393800
hsa-miR-137	TTATTGCTTAAGAATACGCGTAG	529.53	419.12	223.11	-2.37	-1.87	-1.26	1.1121E-24	1136	0.000255
hsa-miR-181a-2*	ACCACTGACCGTTGACTGTACC	20226.11	18849.80	8401.35	-2.41	-2.24	-1.07	0	45959	0.010303
hsa-miR-375	TTTGTTCGTTCGGCTCGCGTGA	16394.67	14909.67	6790.22	-2.41	-2.20	-1.10	0	36879	0.008268
Novel #120	AGGGGGATGGCAGAGCAAAATT	99.56	146.01	40.56	-2.42	-3.54	1.46	1.4895E-10	276	0.000062
hsa-miR-885-5p	TCCATTACACTACCCTGCCTCT	393.87	358.19	153.44	-2.56	-2.33	-1.10	4.1369E-22	875	0.000196
hsa-miR-486-3p	CGGGGCAGCTCAGTACAGGAT	933.24	861.34	363.32	-2.56	-2.37	-1.08	4.7199E-56	2085	0.000467
hsa-miR-129-5p	CTTTTTGCGGTCTGGGCTTGC	913.55	1569.33	347.45	-2.62	-4.51	1.72	6.515E-170	2723	0.000610
hsa-miR-483-3p	TCACTCCTCTCCTCCCGTCTT	159.73	87.18	53.79	-2.93	-1.61	-1.82	1.4868E-10	290	0.000065
Novel #342	CACCGACTCTGTCTCCTGCAG	3080.91	2169.12	1057.33	-2.94	-2.04	-1.43	5.083E-210	6080	0.001363
Novel #200	TGGGATTTCTGAGTAGCATCC	143.32	141.81	37.04	-3.79	-3.75	-1.01	7.6164E-13	308	0.000069
Novel #360	AAAAGTGATTGTGGTTTTTGCT	212.25	192.23	50.27	-4.16	-3.77	-1.10	3.6252E-20	434	0.000097
hsa-miR-675*	CTGTATGCCCTCACCGCTCA	387.30	173.32	86.42	-4.44	-1.99	-2.23	4.9873E-46	617	0.000138
hsa-miR-124	TAAGGCACGCGGTGAATGCC	2829.27	1455.88	481.49	-5.87	-3.02	-1.94	0	4518	0.001013
Novel #107	TCTGGTAAGAGATTTGGGCAT	184.90	138.66	22.05	-8.07	-6.06	-1.33	2.723E-24	326	0.000073

[a]+/- 2 fold change and Bonferroni adjusted p<0.05 in at least one comparison (PP/NN, PP/PN, PN/NN).

[b]Normal skin, NN; Uninvolved psoriatic skin, PN; Involved psoriatic skin, PP.

Table 3-2. Summary of differentially expressed intragenic miRNAs in psoriasis-related genes.

miRNA	FC (NN v. PP)	Host gene	Intragenic position	FC (NN v. PP)	Host gene function
miR-147b	2.79	NMES1	3'UTR	2.50	Unknown
miR-10a	-2.31	HOXB3	intron	-2.08	Homeobox transcription factor
miR-100	-2.31	LOC399959	intron	-2.22	Unknown
miR-125b	-1.99	LOC399959	intron	-2.22	Unknown
Novel #342	-2.94	KRT15	intron	-2.47	Keratin 15
miR-211	2.60	MLSN1	intron	ND	Suppressor of melanoma metastasis
miR-937	6.15	SCRIB	intron	1.34	Adherens junction subunit/regulator of cell polarity
miR-944	2.85	TP63	intron	1.72	Transcription factor involved in skin differentiation
miR-1908	-2.99	FADS1	intron	-5.73	Fatty acid desaturase
novel #23	8.80	IFI27	intron	8.00	alpha-interferon inducible protein
novel #47	3.78	IL18RAP	intron	ND	IL18 receptor subunit
novel #123	2.11	CALR	intron	ND	MHC class I peptide loading complex subunit
novel #116	2.38	TRAF3	3'UTR	ND	TNF receptor associated factor
novel #169	5.08	KRT72	intron	ND	High similarity to KRT6

[5]Normal skin, NN; Involved psoriatic skin, PP.

Table 3-3. Adalimumab study patient data.

			PASI			% improvement	
Patient ID	Sex	BMI	0 month	1 month	6 months	1 month	6 months
UCSF5	M	28.1	12.1	9.5	2.0	21.49	83.47
UCSF22	M	ND	12.9	7.0	2.4	45.74	81.40
UCSF1	M	27.9	15.8	8.4	2.0	46.84	87.34
UCSF30	M	28.4	15.2	6.9	0.9	54.61	94.08
UCSF26	M	28.7	13.3	5.2	0.9	60.90	93.23
UCSF4	M	ND	8.0	2.8	2.2	65.00	72.50
UCSF14	F	25.4	8.5	2.9	2.0	65.88	76.47

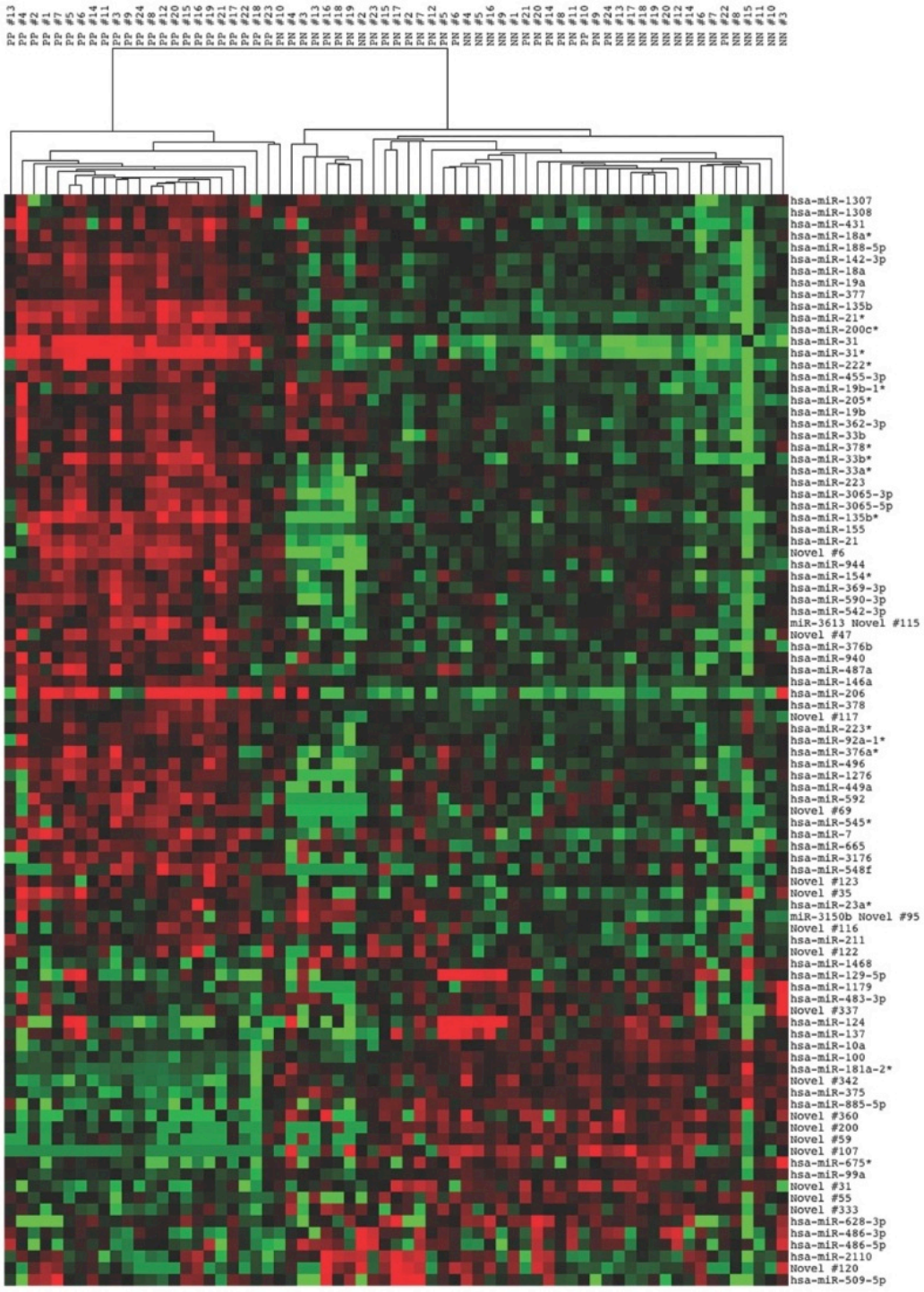

Figure 3-1. Heat map showing hierarchical clustering of skin samples on the basis of 98 differentially expressed miRNAs. Normal skin, NN; Uninvolved psoriatic skin, PN; Involved psoriatic skin, PP.

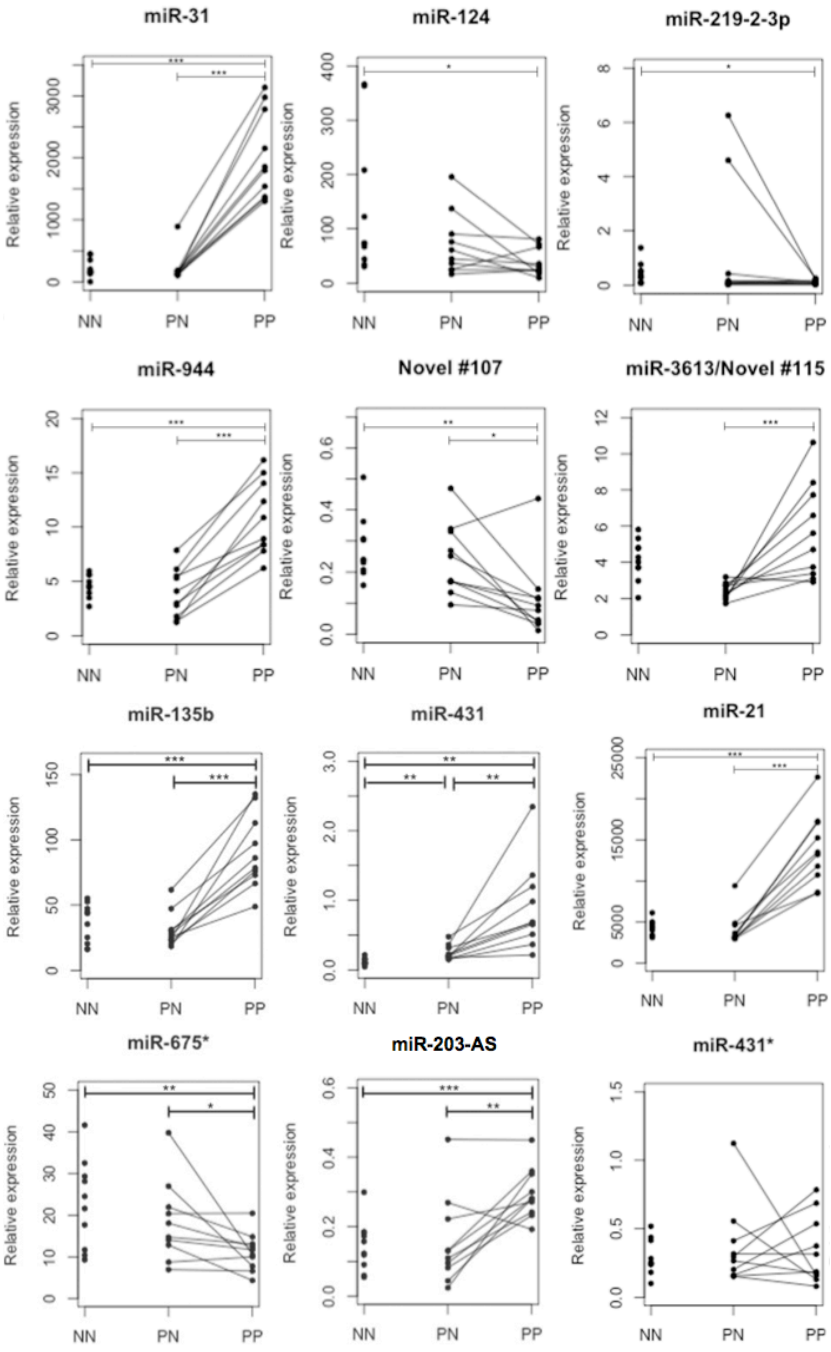

Figure 3-2. qRT-PCR validation of differentially expressed miRNAs. qRT-PCR levels of differentially expressed in ten normal controls and ten psoriasis patients. Lines indicate matched uninvolved and involved samples from the same patient (***p<0.001, **p<0.01,*p<0.05). Normal skin, NN; Uninvolved psoriatic skin, PN; Involved psoriatic skin, PP.

A

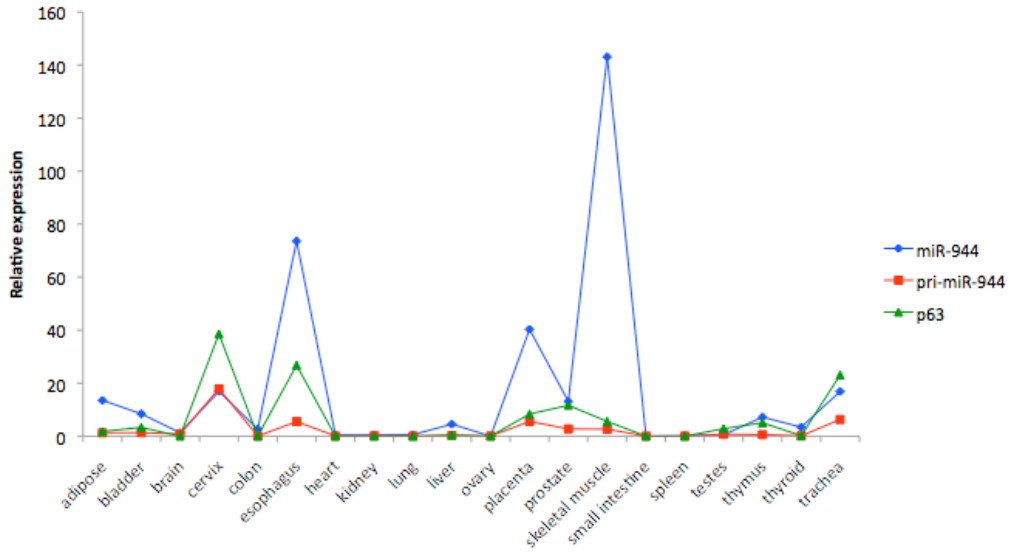
Relative expression
160
140
120
100
80
60
40
20
0
adipose
bladder
brain
cervix
colon
esophagus
heart
kidney
lung
liver
ovary
placenta
prostate
skeletal muscle
small intestine
spleen
testes
thymus
thyroid
trachea
miR-944
pri-miR-944
p63

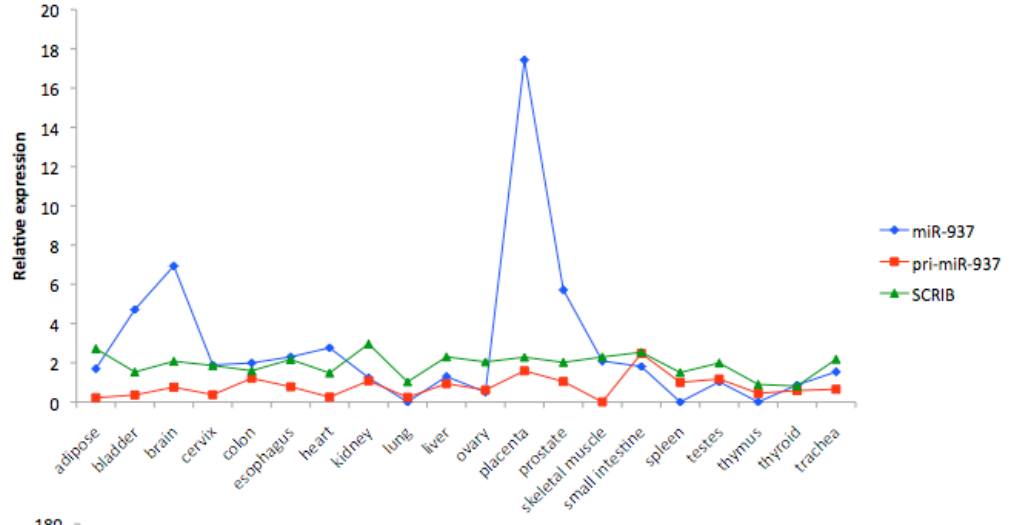
Relative expression
20
18
16
14
12
10
8
6
4
2
0
adipose
bladder
brain
cervix
colon
esophagus
heart
kidney
lung
liver
ovary
placenta
prostate
skeletal muscle
small intestine
spleen
testes
thymus
thyroid
trachea
miR-937
pri-miR-937
SCRIB

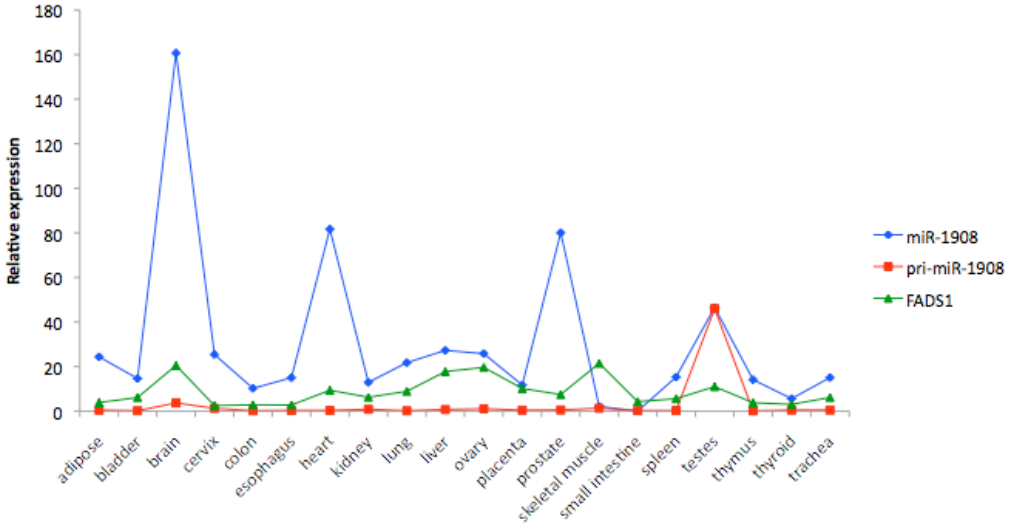
Relative expression
180
160
140
120
100
80
60
40
20
0
adipose
bladder
brain
cervix
colon
esophagus
heart
kidney
lung
liver
ovary
placenta
prostate
skeletal muscle
small intestine
spleen
testes
thymus
thyroid
trachea
miR-1908
pri-miR-1908
FADS1

B

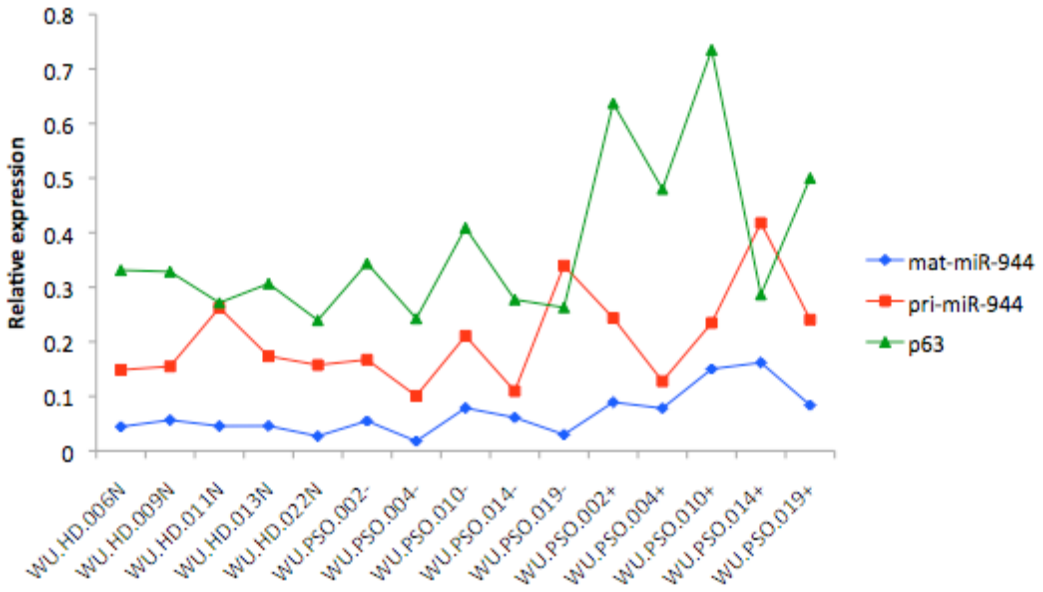

Figure 3-3. Analysis of intragenic miRNAs. (A) Relative expression of intragenic pri-miRNAs, mat-miRNAs, and host genes in a panel of human tissues. (B) Relative expression of pri-miR-944, mat-miR-944, and p63 in five normal, five uninvolved, and five involved skin samples. Normal skin, N; Uninvolved psoriatic skin, "-"; Involved psoriatic skin, "+".

A

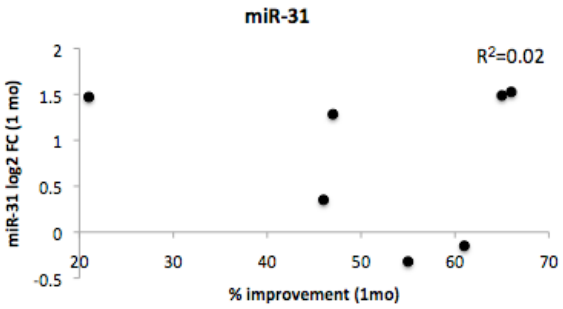
miR-31
R²=0.02
miR-31 log2 FC (1 mo)
% improvement (1mo)

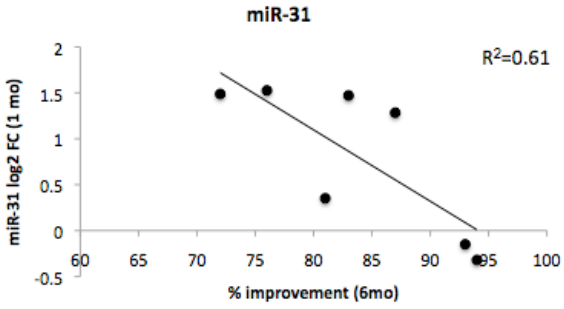
miR-31
R²=0.61
miR-31 log2 FC (1 mo)
% improvement (6mo)

B

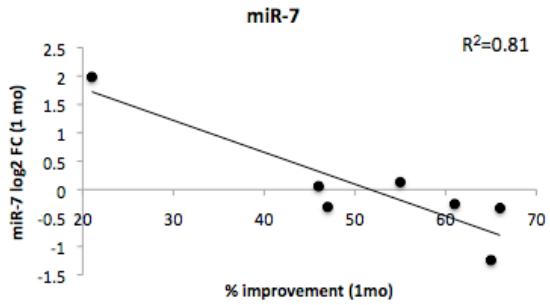
miR-7
R²=0.81
miR-7 log2 FC (1 mo)
% improvement (1mo)

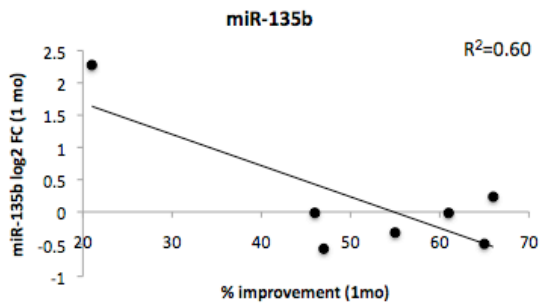
miR-135b
R²=0.60
miR-135b log2 FC (1 mo)
% improvement (1mo)

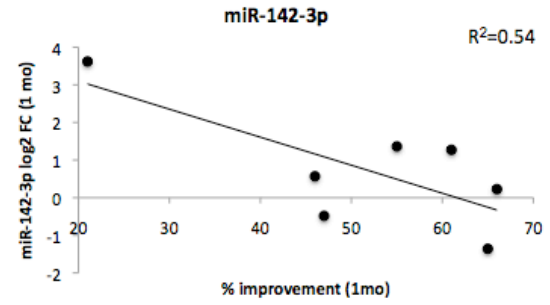
miR-142-3p
R²=0.54
miR-142-3p log2 FC (1 mo)
% improvement (1mo)

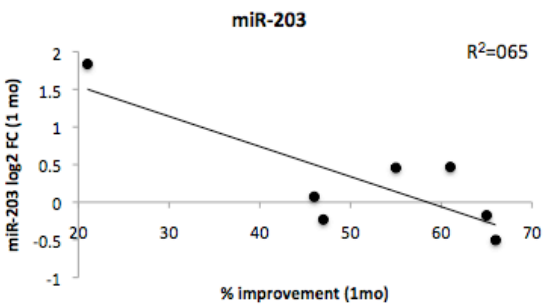
miR-203
R²=065
miR-203 log2 FC (1 mo)
% improvement (1mo)

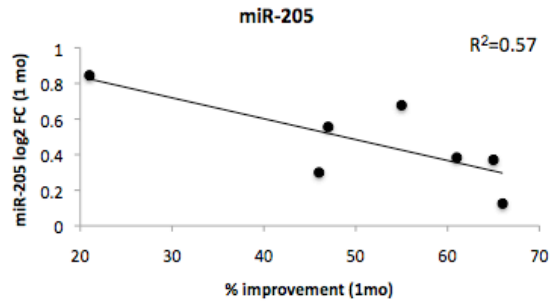
miR-205
R²=0.57
miR-205 log2 FC (1 mo)
% improvement (1mo)

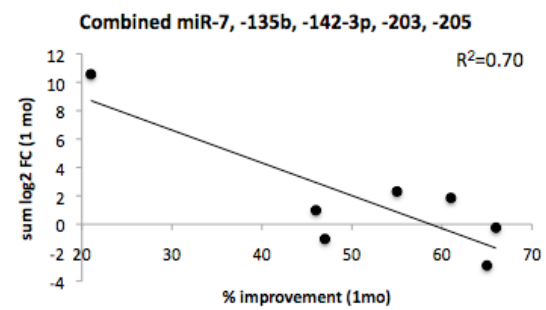
Combined miR-7, -135b, -142-3p, -203, -205
R²=0.70
sum log2 FC (1 mo)
% improvement (1mo)

Figure 3-4. miRNA expression changes in the skin are correlated with adalimumab treatment response. (A) Log2 fold change in miR-31 expression after one month of treatment plotted against % improvement in PASI score after one month or six months of treatment. (B) For miRNAs with R^2>0.5, log2 fold change in expression after one month of treatment plotted against plotted against % improvement in PASI score after one month of treatment. Lower right panel, sum of log2 fold changes for each of the five miRNAs plotted against % improvement in PASI score after one month of treatment.

Chapter 4.

Functional impact of miRNAs in psoriatic skin

ABSTRACT

Psoriasis is a chronic, inflammatory skin disease. Transcriptome analyses have revealed >1000 mRNA expression changes in psoriatic skin, and some of these gene expression changes may be driven by miRNAs. Indeed, involved psoriatic skin exhibits widespread misregulation of miRNAs: eighty known and 18 novel miRNAs are two- to 42-fold differentially expressed. Myriad others exhibit more modest fold changes. In order to understand the normal and pathogenic functions of differentially expressed miRNAs in the skin, I analyzed cell-type specific expression and potential miRNA targets in psoriatic skin. *In situ* hybridization revealed stratified epidermal expression of an upregulated, keratinocyte-derived miRNA, miR-135b. I found that the upregulation of miR-135b and a second microRNA, miR-7 in psoriasis is likely to reduce translation of the late cornified envelope-1B (LCE1B) transcript. The LCE family gene products are structural components of the epidermal barrier and a copy number variant in the LCE3 gene region is associated with psoriasis. I also found that the downregulation of miR-486 in psoriasis is likely to lead to increased translation of the LCE family member, LCE3E. These findings are consistent with previously described downregulation of LCE1 family members and upregulation of LCE3 family members in psoriatic skin. The miRNA binding sites in LCE1B and LCE3E are poorly conserved, even among primates. Thus, newly evolved miRNA regulation of the LCE gene family may influence human skin barrier formation, and misregulation of miR-135b, miR-7, and miR-486 may contribute to psoriasis by altering the skin barrier.

INTRODUCTION

microRNAs (miRNAs) are small noncoding RNAs that post-transcriptionally regulate gene expression (102). miRNAs function by directing the RNA silencing machinery to target mRNA transcripts. Target recognition is largely dependent on reverse complementarity between the 5' miRNA seed region, defined as nt 2-8, and the 3'UTR of the transcript (72). It was initially thought that miRNAs inhibited their targets mainly at the level of translational inhibition (41,169). However, combined proteomic and transcriptomic analyses in mammalian cells has indicated that up to 85% of miRNA inhibition could be due to mRNA destabilization (81,106,107). Another key finding of such studies is that manipulation of a single miRNA in a given cell type can have widespread effects. For example, deletion of miR-223 in mouse neutrophils leads to inhibition of hundreds of proteins, likely through direct targeting of 3'UTRs (106). Most targets are modestly inhibited, and some, but not all, show concomitant downregulation in mRNA levels as well (106). Based on the modest but widespread expression changes observed for most miRNA targets, it has been postulated that miRNAs may serve as fine tuners of gene expression (170). Such fine tuning may be particularly important in the epidermis, where gene expression is spatially and temporally regulated to allow continual renewal of the barrier and dynamic responses to environmental stimuli.

In chapter 3, I described the widespread misregulation of miRNAs in psoriatic skin. Some differentially expressed miRNAs have previously described roles in biological processes related to psoriasis pathogenesis, such as cell proliferation, differentiation, immunity, and inflammation, but many are of unknown function. Here, I

present evidence that a subset of differentially expressed miRNAs regulate components of the skin barrier.

RESULTS

RNA *in situ* hybridization reveals cell-type specific miRNA expression

I analyzed the expression of selected differentially expressed miRNAs in uninvolved (PN) and involved (PP) psoriatic skin with RNA *in situ* hybridization (RNA-*ish*). I selected five miRNAs with previously described roles in keratinocyte or immune cell biology (miR-31, miR-205, miR-142-3p, miR-338-5p, and miR-31), and several of unknown function (miR-944, miR-135b, miR-124, miR-937, miR-1908, and novel #115). In general, signal intensity did not correlate well with digital read count or qRT-PCR (Table 3-1; Figure 3-2; Figure 4-1), indicating that *RNA-ish* is not suitable for analysis of miRNA abundance. This is likely due to probe-specific differences in sensitivity and specificity, or variation in the quality of skin sections. Consistent with variability in sample quality, no *RNA-ish* signal was observed for any miRNA in one normal (NN) biopsy included in this experiment. Thus, spatial miRNA expression was only compared in PP versus PN skin.

miR-135b, miR-205 and miR-142-3p clearly labeled different cell types/skin layers. For example, miR-135b was upregulated in the suprabasal epidermis of PP skin, with highest expression just below the barrier, but was excluded from the basal layer (Figure 4-2). This pattern is consistent with the expression of miR-135b in cultured primary keratinocyte fractions where it is more highly expressed in transiently amplifying keratinocytes, compared to basal or terminally differentiated keratinocytes (87). In contrast, miR-205 was expressed primarily in the basal layer of PN skin, but in the basal and suprabasal layers of PP skin (Figure 4-2). This pattern is reminiscent of a number of

mRNAs such as integrins that are normally restricted to the basal layer of normal or uninvolved skin, but expressed in the suprabasal layer of involved skin (171). These staining patterns are strongly suggestive of roles for miR-135b and miR-205 in keratinocyte differentiation. miR-142-3p displayed evidence of immune cell staining, which is consistent with the previously described expression of miR-142-3p in hematopoietic tissues (Figure 4-2**;** 172). miR-142-3p exhibited dermal staining in PN skin, but was present in the dermis and epidermis of PP skin, suggesting it is expressed in immune cells that migrate to the epidermis in PP skin.

Predicted targets of differentially expressed miRNAs

In order to determine the potential functions of these and other differentially expressed miRNAs in psoriasis pathogenesis, I performed an *in silico* screen to identify their predicted targets. The pool of candidate targets was derived from a recent microarray-based transcriptome study, which reported differential expression of 1,089 transcripts in PP versus NN skin (19). I screened the 3'UTRs of candidate targets for binding sites for differentially expressed miRNAs, and returned only those binding sites that were predicted by two independent algorithms: TargetScan and miRanda (Appendix A). 37/98 differentially expressed miRNAs were excluded from this analysis because some of the poorly conserved miRNAs, miRNA*s, and novel miRNAs that I identified were not present in the target prediction databases. These excluded miRNAs included 11 of the top 20 differentially expressed miRNAs in PP versus NN skin. To identify their predicted targets I used TargetScan Custom to generate a global target profile. Their

predicted targets that are differentially expressed in psoriasis are also reported in Appendix A.

The output from these analyses included transcripts that were predicted to be targeted exclusively by either up- or downregulated miRNAs or by both up- and downregulated miRNAs. In the former case, where a transcript was predicted to be targeted by either up- or downregulated miRNAs, there were targets that were positively correlated with their predicted miRNAs and those that were negatively correlated with their predicted miRNAs. Because miRNAs are typically thought to inhibit their direct targets, I focused on predicted targets that were negatively correlated with differentially expressed miRNAs, of which there were 19 up- and 105 downregulated transcripts (Table 4-1). One notable observation was that the upregulated miRNA, miR-135b, which exhibited a suprabasally restricted expression gradient in PP epidermis, was predicted to target late cornified envelope-1B (LCE1B). This is a skin barrier constituent that is 2.1 fold downregulated in PP versus NN skin (19,173). Moreover, a second upregulated miRNA, miR-7, was also predicted to target LCE1B.

miRNA regulation of the LCE gene family

The LCE gene family is divided into three groups (LCE1-3) that are physically linked and coordinately transcribed in response to environmental stimuli and keratinocyte differentiation (174). However no other LCE family members were flagged as predicted targets of differentially expressed miRNAs in my initial screen. This was due to two factors. First, while qRT-PCR analysis of individual family members has shown clear differential expression of most LCE family members in PP versus PN and NN skin (173),

only two LCE genes (LCE1B and LCE3D) were reported as differentially expressed in the microarray study from which I generated my candidate target pool (19). Secondly, the screen required that miRNA binding sites be predicted by two target prediction algorithms. To further investigate miRNA regulation of the LCE gene family, I manually analyzed the 3'UTRs of all LCE family members, and also considered miRNA binding sites that were predicted by only one algorithm (Table 4-2). This revealed several other family members that were predicted to be targets of differentially expressed miRNAs. Most of these miRNA:target pairs exhibited inversely correlated expression changes in psoriatic skin (Table 4-2). Differentially expressed miRNAs that regulate barrier components may exert pathogenic functions by impairing barrier development or remodeling in response to environmental stimuli.

Some miRNAs that are abundant in the skin (top 20% of all expressed miRNAs), but are not differentially expressed in psoriasis, are also predicted to target LCE family members. Thus, it is likely that miRNAs also regulate barrier components in the context of the normal epidermis. A partial list of such miRNAs (limited to conserved miRNAs predicted by the miRanda algorithm) is provided in Table 4-3. However, since the current study pertains to the role of miRNAs in psoriasis, I have focused validation and follow up efforts on the differentially expressed miRNAs predicted to target LCE family members.

miR-135b and miR-7 regulate LCE1B through direct interactions with the 3'UTR

The upregulated miRNAs, miR-135b and miR-7, were predicted to target the downregulated transcript, LCE1B, by two independent algorithms. Predicted base pairing between the miRNAs and target sites within the LCE1B 3'UTR are shown in Figure 4-

3A. I used heterologous reporter assays to validate the predicted interactions between the upregulated miRNAs, miR-135b and miR-7, and the downregulated transcript, LCE1B. I generated a series of mammalian luciferase reporter constructs containing wild-type (WT) or mutant LCE1B 3'UTR inserts (Figure 4-3B) and transfected these constructs into WT HEK293 cells or HEK293 cells overexpressing miR-135b and/or miR-7. In the case of miR-135b, the presence of the WT 3'UTR led to a 14.2% (SEM±1.8) reduction in luciferase activity in response to miR-135b overexpression, and deletion of the miR-135b seed binding region rescued WT luciferase activity (Figure 4-3C). Likewise, for miR-7, the presence of the WT 3'UTR led to a 19.8% (SEM±1.4) reduction in luciferase activity in response to miR-7 overexpression. This was rescued by deletion of the miR-7 seed binding region (Figure 4-3C). Concomitant overexpression of both miR-7 and miR-135b did not enhance repression beyond 20%, but rescue of WT luciferase activity in this strain required deletion of both miRNA seed binding regions in the LCE1B 3'UTR (Figure 4-3C), suggesting that both miRNAs contribute to repression of the reporter transcript in this context. The reduction in luciferase activity in response to miR-135b and miR-7 was not associated with any decrease in mRNA level (Figure 4-4), suggesting that translational repression is the underlying mechanism for regulation of LCE1B by these microRNAs.

Recent origin of miR-135b and miR-7 binding sites

The mature miR-135b and miR-7 sequences are perfectly conserved in primates and mouse, but the 3'UTR of LCE1B is poorly conserved beyond primates. It is conserved in chimps (99% max identity) and rhesus macaque (92% max identity), but is

highly divergent in the mouse reference genome (Figure 4-5A). If we consider the individual miRNA binding sites in primates, the miR-135b binding site is perfectly conserved in chimp, but contains multiple substitutions and deletions in all other primate species and mouse (Figure 4-5B). For all but one primate species (marmoset), there is at least one substitution within the seed binding region, which would be predicted to strongly influence miR-135b binding. In marmoset, five nucleotides adjacent to the seed binding region are deleted, which could abrogate miR-135b binding by disrupting multiple non-seed base pairings (Figure 4-5B). Thus, miR-135b regulation of LCE1B is likely to have evolved 8-5.4 million years ago in an interval that separates chimps and humans from orangutan, Old World, and New World monkeys.

The miR-7 binding site initially appeared not to be conserved in chimps, as the first nucleotide in the 7-nt seed binding region, which is a G in the human reference sequence, is substituted to A in the chimp reference sequence (Figure 4-5C). I also identified one individual (unknown population) from the 1000 Genomes project carrying the A (chimp) allele of this variant (rs79341479, allele frequency in humans = 0.046%, 2/4376; 175). Sanger sequencing of this region in ten chimpanzee samples revealed that this site is actually polymorphic in chimps, as 4/10 individuals were homozygous for the G allele. Further analysis of this SNP with a luciferase reporter assay showed that the A allele does not abrogate miR-7 repression of LCE1B, indicating that this site is likely to be a neutral polymorphism in humans and primates (Figure 4-3C). This is probably because the variant lies in the first nucleotide of the 7-nt seed binding region, leaving a 6-nt seed binding region intact. This minimal 6-nt seed binding region is perfectly conserved in orangutan, rhesus, and baboon, while more distantly related primates such

as marmoset carry additional seed binding region substitutions that are likely to render the site non-functional. These results indicate that miR-7 regulation of LCE1B is likely to have evolved 30-40 million years ago, after separation from New World monkeys, in a common ancestor of Old World monkeys (rhesus and baboon), orangutan, chimps, and humans.

miR-486 regulates LCE3E by binding a recently evolved site within the 3'UTR

I next used heterologous reporter assays to validate the predicted interactions between additional differentially expressed miRNAs and LCE family members listed in Table 4-2. Among the predictions I was able to test, I validated a single interaction between the downregulated miRNA, miR-486, and the upregulated transcript, LCE3E (Table 4-2; Figure 4-6A,B). The presence of the WT 3'UTR led to a ~10.6% (SEM±1.4) reduction in luciferase activity in response to miR-486 overexpression, and deletion of the miR-486 seed site rescued WT luciferase activity (Figure 4-6B). The reduction in luciferase activity in response to miR-486 was not associated with any decrease in mRNA level (Figure 4-4C), suggesting that translational repression is the underlying mechanism for regulation of LCE1B by these microRNAs. The mature miR-486 sequence is perfectly conserved in primates and mouse. The LCE3E 3'UTR is present in chimps (98% max identity) and rhesus macaque (95% max identity), but is poorly conserved in mouse. The miR-486 binding site is perfectly conserved in chimp, but contains at least one internal seed binding region substitution in all other primate species (Figure 4-6D). The miR-486 seed region also exhibits variation in humans at position two of the 7-nt seed sequence (rs180816225); the ancestral G allele (allele frequency in humans = 99.863%) preserves the complementarity with miR-486, while the A allele

(allele frequency in humans = 0.137%, 6/4376) does not (Figure 4-6A,D; 175). Indeed, the presence of the A allele in the seed binding region abrogates miR-486 mediated repression of LCE3E (Figure 4-6B). This variant might lead to psoriasis susceptibility, but would not have been identified with GWAS, which cannot be used to analyze rare variants unless they are common in the one population being analyzed.

DISCUSSION

The misregulation of miRNAs has emerged as a common theme among most human diseases, such as cancer, autoimmune disease, and psoriasis(84). However, the functional contributions of miRNAs in normal and diseased human tissues have been more difficult to assess. This is due to the subtle effects exerted by singular miRNAs on target expression, issues of cell- and tissue-type specificity, and sensitivity of miRNA:mRNA interactions to stoichiometry. In this chapter, I described one approach to target identification which took into account cell-type specificity and relevance of candidate targets to psoriasis pathogenesis. I have shown that three differentially expressed miRNAs in psoriasis directly regulate members of the LCE family, and that miRNA regulation of the LCE family evolved after the separation of Old from New World monkeys.

miRNA regulation of LCE family members in the psoriatic epidermis

Members of the LCE gene family are encoded on chromosome 1 in the epidermal differentiation complex (EDC). This region contains many of the genes expressed during keratinocyte differentiation, such as filaggrin, loricrin, and the small proline rich proteins (SPRRs). The LCE group 1 and 2 gene products are normally expressed in the skin barrier, where they are constituents of the heavily crosslinked cornified envelope (176), and their expression is downregulated in the PP skin barrier (173). In contrast, the group 3 LCE genes are not normally expressed in the barrier, but are turned on in the PP epidermis (173). Despite this overall group-wise regulation, there is variability in the

overall abundance and in the magnitude of differential expression between group members. Taken together, these observations suggest that the incorporation of specific LCE gene products into the barrier may be favorable under different conditions.

miRNA-mediated regulation of LCE genes in the epidermis would be one way to achieve a fast and dynamic response to pathogenic or environmental stimuli. This is because small changes in miRNA expression can drastically influence their ability to regulate targets, due to their sensitivity to stoichiometry (177). Extending this model to psoriasis, the incorporation of LCE3 gene products into the barrier may be advantageous in the context of epidermal hyperproliferation and inflammation. Indeed, this is consistent with the finding that a deletion spanning the LCE3B/C genes is a psoriasis risk factor in European and Chinese populations (32,178). Thus, miRNAs that inhibit group 1 or 2 LCEs are upregulated (i.e.: miR-7 and miR-135b), while miRNAs that inhibit group 3 LCEs are downregulated (i.e.: miR-486) to promote barrier repair or remodeling.

Transcriptional regulation of miR-135b, miR-7, and miR-486

There are several conserved transcription factor binding sites within 2kb upstream of miR-135b (Chx10, SRF), miR-7 (miR-7-1: MEF2A, miR-7-2: ATF6, NKX25, POU3F2), and miR-486 (GATA). While none of these transcription factors have been reported as differentially expressed in psoriatic skin, transcription factors are not always detected on microarrays because of their overall low abundance. Interestingly, despite the fact that miR-135b and miR-7 regulate the same target, LCE1B, there were no conserved transcription factor binding sites present in both promoters. This may reflect the fact that the two miRNAs likely serve many non-redundant functions because their global target

profiles are largely distinct. An additional possibility, particularly in light of the recent evolution of the miRNA binding sites, is that the promoters contain non-conserved transcription factor binding sites or uncharacterized motifs that regulate their transcription in human skin. Also of note is the presence of a GATA site ~1kb upstream of the miR-486 gene. GATA-3 is required for establishment of the epidermal barrier in mice, and barrier-impaired skin from GATA-3 null mice exhibits increased levels of anti-microbial and innate immunity genes (179). It would be intriguing to determine whether a failure to transcriptionally activate miR-486 contributes to this psoriasoform phenotype.

Newly evolved miRNA regulation of LCE family members

Over the course of mammalian evolution, the epidermis has changed drastically. For example, the interfollicular epidermis in mice is much thinner and more resistant to scarring than in humans (112). Moreover, primates and humans have been exposed to the selective pressure of new environmental conditions, which could be particularly relevant to the skin. Thus, it is plausible that new mechanisms have arisen for the development and maintenance of the human/primate epidermis. Indeed, many genes involved in keratinization (including LCE1B and LCE3E) are under positive selection in primates and humans (180). Consistent with this, I have shown that recently evolved, functional miRNA binding sites exist in primates, and that these miRNA binding sites exhibit substantial variation between species and harbor rare variants in humans. This observation is particularly intriguing, considering that murine models typically fail to recapitulate all of the features of human psoriasis (112).

Significance of miRNA regulation in the normal epidermis

The majority of this chapter has focused on the pathogenic roles of three miRNAs that are differentially expressed in psoriatic skin. However, many barrier components (such as the LCEs) are predicted to be targeted by miRNAs that are abundant in the epidermis, but not differentially expressed in psoriasis. Thus, miRNAs are likely to play a role in establishment and maintenance of the skin barrier under normal conditions. One intriguing hypothesis is that the enucleated, terminally differentiated keratinocytes that populate the skin barrier have limited transcriptional capacity. Thus, barrier components must be transcribed prior to enucleation, and translationally repressed by miRNAs until keratinocytes reach the barrier.

Future directions and conclusions

Misregulation of miRNAs that target LCE family members may be one mechanism contributing to barrier dysfunction in PP skin. It remains to be seen whether the recent evolution of these regulatory interactions could underlie primate-specific features of the epidermis or influence differences in psoriasis susceptibility between species or individuals.

MATERIALS AND METHODS

MiRNA *in situ* hybridization. MiRNA *in situ* hybridizations were performed as previously described (181). Briefly, fresh skin biopsies were fixed in 10% formalin for 24-72h and paraffin embedded. 6um sections were mounted on glass slides, deparaffinized, and treated with 10ug/ml proteinase K for 20 min at 37°C. Slides were hybridized with 20-60nM double DIG-labeled LNA probes (Exiqon) overnight at 57°C (miR-135b, miR-205) or 50°C (miR-142). Slides were washed in 5X SSC, 1X SSC, and 0.2X SSC for 10 min at hybridization temperature. Staining was performed with NBT/BCIP (Roche) for 90 min at 32°C followed by nuclear fast red counterstain (Vector Laboratories). An LNA probe with scrambled sequence was used as a negative control (Exiqon).

Target prediction screen. Predicted miRNA targets were downloaded from the TargetScan (72,182) and miRanda (183,184) websites (http://www.targetscan.org/, http://www.microrna.org/microrna/home.do). The datasets were filtered against the differentially expressed transcripts (19) and miRNAs in psoriatic skin. Differentially expressed transcripts that were predicted to be targeted by one or more differentially expressed miRNAs with both target prediction algorithms were returned. Candidate targets were further sorted based on directionality of differential expression.

3' UTR reporter constructs. 3'UTR reporter constructs were generated from the si-CHECK2 vector (Promega). Briefly, 3' UTRs of candidate target genes were amplified from genomic DNA. PCR products were cloned into the XhoI and PmeI sites of the vector, thus fusing the Renilla luciferase gene to the candidate 3'UTR. Transformants

were selected on 1ug/ml ampicillin and validated by Sanger sequencing. miRNA binding site mutagenesis was performed by deleting the seven nucleotide miRNA seed region from the 3'UTR with the QuikChange lightning targeted mutagenesis kit (Agilent), according to manufacturer's protocol.

Transfections. HEK293 cells were cultured in DMEM supplemented with 2mM L-glutamine, 10mg/ml penicillin-streptomycin, and 10% fetal bovine serum at 37°C and 5% CO_2. Transfections were performed in triplicate. 24 hours prior to transfections, $1x10^5$ cells were plated in each well of a 24-well plate. Transfections were performed with TransIT-LT1 transfection reagent according to manufacturer's instructions (Mirus). Briefly, 250ng pEP-miR, 250ng psiCHECK2, and 250ng pUC18 (or pEP-miR for double overexpression treatments) were incubated in a solution of 46.25ul RPMI and 3.75ul LT-1 for 30 min at 22°C before treatment. Cells were collected 24 hours post-transfection.

Luciferase assays. Dual luciferase reporter assays were performed according to manufacturer's instructions (Promega). Briefly, transfected cells were lysed in passive lysis buffer for 15 minutes at room temperature. Lysates were diluted 10-fold and 20ul of diluted lysate was added to each assay. Renilla luciferase activity was normalized to firefly luciferase activity to control for transfection efficiency. Significance was determined with one way ANOVA and post-hoc two tailed t-tests.

mRNA qRT-PCR. mRNA qRT-PCR was performed as described in Chapter 3. Cells were collected 24 hours post-transfection. Primers sequences were targeted to the LCE1B and LCE3E 3'UTRs (173).

TABLES AND FIGURES

Table 4-1. Differentially expressed targeted by inversely correlated, differentially expressed miRNAs.

Downregulated transcripts targeted by upregulated miRNAs

Gene symbol	Transcript FC	miRNAs predicted to target transcript
THRSP	-9.40	hsa-miR-369-3p
CCL27	-7.72	hsa-miR-944
GAL	-6.38	hsa-miR-665
FABP7	-5.98	hsa-miR-548f
ACSBG1	-5.74	hsa-miR-223,hsa-miR-509-5p,hsa-miR-548f
HSD11B1	-4.95	hsa-miR-376b,hsa-miR-590-3p,hsa-miR-944
HS3ST6	-4.25	hsa-miR-18a
WDR72	-4.23	hsa-miR-1303,hsa-miR-155,hsa-miR-206,hsa-miR-21,hsa-miR-33b,hsa-miR-369-3p,hsa-miR-487a, hsa-miR-509-5p,hsa-miR-590-3p,hsa-miR-592,hsa-miR-7,hsa-miR-944
TPPP	-3.95	hsa-miR-188-5p,hsa-miR-211,hsa-miR-377
TMEM56	-3.93	hsa-miR-590-3p
TSPAN8	-3.84	hsa-miR-188-5p,hsa-miR-211
EMX2	-3.76	hsa-miR-206,hsa-miR-211,hsa-miR-944
MUC7	-3.74	hsa-miR-431,hsa-miR-542-3p,hsa-miR-590-3p,hsa-miR-7,hsa-miR-944
ZDHHC11	-3.71	hsa-miR-1308,hsa-miR-142-3p,hsa-miR-548f,hsa-miR-940
CLDN8	-3.51	hsa-miR-135b,hsa-miR-155,hsa-miR-21,hsa-miR-223,hsa-miR-548f,hsa-miR-940
FADS1	-3.44	hsa-miR-1276,hsa-miR-211,hsa-miR-431,hsa-miR-496,hsa-miR-590-3p
CLDN23	-3.27	hsa-miR-590-3p,hsa-miR-944
FAM70A	-2.92	hsa-miR-1308,hsa-miR-146a,hsa-miR-211,hsa-miR-223,hsa-miR-431,hsa-miR-496,hsa-miR-590-3p
CST6	-2.91	hsa-miR-542-3p
OSR2	-2.90	hsa-miR-142-3p
SNRPN	-2.85	hsa-miR-155
CA6	-2.71	hsa-miR-155
CILP	-2.69	hsa-miR-21,hsa-miR-33b,hsa-miR-542-3p,hsa-miR-665
SPRR4	-2.68	hsa-miR-455-3p
AGTR1	-2.67	hsa-miR-1303,hsa-miR-155,hsa-miR-206,hsa-miR-455-3p,hsa-miR-7,hsa-miR-944
ENPP5	-2.60	hsa-miR-1308,hsa-miR-188-5p,hsa-miR-542-3p,hsa-miR-590-3p,hsa-miR-940,hsa-miR-944
POSTN	-2.60	hsa-miR-135b,hsa-miR-18a,hsa-miR-33b,hsa-miR-592,hsa-miR-944
PPP4R2	-2.56	hsa-miR-509-5p,hsa-miR-548f
PLN	-2.56	hsa-miR-155,hsa-miR-21,hsa-miR-33b,hsa-miR-369-3p,hsa-miR-590-3p,hsa-miR-7
MTBP	-2.56	hsa-miR-1276,hsa-miR-590-3p
COBL	-2.53	hsa-miR-1303,hsa-miR-487a
HAO2	-2.53	hsa-miR-31
PCP4	-2.50	hsa-miR-33b
LONRF1	-2.49	hsa-miR-1276,hsa-miR-1303,hsa-miR-135b,hsa-miR-211,hsa-miR-548f,hsa-miR-590-3p
PLLP	-2.49	hsa-miR-18a,hsa-miR-496,hsa-miR-548f,hsa-miR-7
KRT15	-2.47	hsa-miR-940
GLDC	-2.46	hsa-miR-377,hsa-miR-455-3p,hsa-miR-548f
HOXA10	-2.45	hsa-miR-1303,hsa-miR-135b,hsa-miR-369-3p,hsa-miR-590-3p,hsa-miR-665
SYDE2	-2.44	hsa-miR-31,hsa-miR-33b,hsa-miR-496,hsa-miR-590-3p
PAPLN	-2.42	hsa-miR-1268,hsa-miR-1276,hsa-miR-155,hsa-miR-211,hsa-miR-31,hsa-miR-33b,hsa-miR-376b, hsa-miR-509-5p,hsa-miR-590-3p,hsa-miR-665
MAML2	-2.42	hsa-miR-211,hsa-miR-509-5p
PCYT1B	-2.39	hsa-miR-135b,hsa-miR-188-5p,hsa-miR-211,hsa-miR-496,hsa-miR-548f,hsa-miR-590-3p,hsa-miR-7
EEF2K	-2.39	hsa-miR-142-3p,hsa-miR-487a,hsa-miR-509-5p,hsa-miR-590-3p,hsa-miR-944
GSTM3	-2.39	hsa-miR-1276,hsa-miR-188-5p,hsa-miR-211,hsa-miR-31,hsa-miR-377,hsa-miR-431,hsa-miR-590-3p
TMEM47	-2.38	hsa-miR-155,hsa-miR-206,hsa-miR-211,hsa-miR-223,hsa-miR-369-3p,hsa-miR-496,hsa-miR-590-3p, hsa-miR-944
GSTA3	-2.36	hsa-miR-431
SSPN	-2.36	hsa-miR-21,hsa-miR-31,hsa-miR-378,hsa-miR-548f,hsa-miR-590-3p,hsa-miR-944
CORO2B	-2.35	hsa-miR-146a,hsa-miR-509-5p
CYP4B1	-2.35	hsa-miR-206,hsa-miR-944
CD34	-2.35	hsa-miR-1303,hsa-miR-431,hsa-miR-548f
ADRB2	-2.34	hsa-miR-548f,hsa-miR-590-3p
TCF7L2	-2.32	hsa-miR-548f
RTN4	-2.30	hsa-miR-1268,hsa-miR-21,hsa-miR-31,hsa-miR-455-3p,hsa-miR-542-3p,hsa-miR-944
LEP	-2.30	hsa-miR-1276,hsa-miR-146a,hsa-miR-211
TGFBR3	-2.28	hsa-miR-18a,hsa-miR-206,hsa-miR-21,hsa-miR-31,hsa-miR-548f
HMGCS2	-2.25	hsa-miR-21
SORCS2	-2.24	hsa-miR-1268,hsa-miR-33b,hsa-miR-509-5p
OMD	-2.22	hsa-miR-1276,hsa-miR-155,hsa-miR-590-3p
MEOX2	-2.21	hsa-miR-206,hsa-miR-33b,hsa-miR-369-3p,hsa-miR-377,hsa-miR-590-3p,hsa-miR-592
KLF9	-2.21	hsa-miR-1276,hsa-miR-142-3p,hsa-miR-21,hsa-miR-211,hsa-miR-376b,hsa-miR-548f
COL1A2	-2.20	hsa-miR-1308,hsa-miR-496,hsa-miR-590-3p,hsa-miR-7
DNM1	-2.17	hsa-miR-496,hsa-miR-940
FOS	-2.17	hsa-miR-155,hsa-miR-369-3p,hsa-miR-431,hsa-miR-548f

NCALD	-2.17	hsa-miR-1276,hsa-miR-212,hsa-miR-7,hsa-miR-940
PDLIM4	-2.17	hsa-miR-223,hsa-miR-542-3p
CES1	-2.17	hsa-miR-188-5p,hsa-miR-211
ACADL	-2.17	hsa-miR-1303,hsa-miR-135b,hsa-miR-211,hsa-miR-31,hsa-miR-548f,hsa-miR-590-3p,hsa-miR-944
ALS2CR4	-2.16	hsa-miR-135b,hsa-miR-146a,hsa-miR-155,hsa-miR-188-5p,hsa-miR-211,hsa-miR-376b,hsa-miR-377, hsa-miR-590-3p,hsa-miR-592,hsa-miR-7,hsa-miR-944
SNX1	-2.16	hsa-miR-1308,hsa-miR-135b,hsa-miR-146a,hsa-miR-155,hsa-miR-31,hsa-miR-369-3p,hsa-miR-377, hsa-miR-378,hsa-miR-590-3p,hsa-miR-944
WISP2	-2.16	hsa-miR-431,hsa-miR-590-3p,hsa-miR-940
MASP2	-2.16	hsa-miR-1276,hsa-miR-31,hsa-miR-509-5p
MAP1B	-2.15	hsa-miR-211,hsa-miR-223,hsa-miR-31,hsa-miR-369-3p,hsa-miR-376b,hsa-miR-487a,hsa-miR-496, hsa-miR-542-3p,hsa-miR-548f,hsa-miR-590-3p,hsa-miR-940
RORC	-2.14	hsa-miR-1276,hsa-miR-31,hsa-miR-592,hsa-miR-665
SCGB2A2	-2.13	hsa-miR-431
TM2D1	-2.12	hsa-miR-1276,hsa-miR-376b
ACTA1	-2.11	hsa-miR-155,hsa-miR-223
KLF8	-2.10	hsa-miR-147b,hsa-miR-206,hsa-miR-21
PNPLA3	-2.10	hsa-miR-146a,hsa-miR-212,hsa-miR-369-3p,hsa-miR-377,hsa-miR-590-3p
FKBP7	-2.10	hsa-miR-548f
PDZK1	-2.10	hsa-miR-377,hsa-miR-487a,hsa-miR-590-3p
ACOX2	-2.10	hsa-miR-590-3p
ALDH3A2	-2.10	hsa-miR-206,hsa-miR-211,hsa-miR-377,hsa-miR-378,hsa-miR-590-3p,hsa-miR-665,hsa-miR-944
FCGBP	-2.10	hsa-miR-21
PLA2R1	-2.09	hsa-miR-135b,hsa-miR-542-3p,hsa-miR-548f,hsa-miR-590-3p,hsa-miR-7
SUSD2	-2.09	hsa-miR-496,hsa-miR-940
SLC2A13	-2.08	hsa-miR-1303,hsa-miR-135b,hsa-miR-18a,hsa-miR-206,hsa-miR-21,hsa-miR-211,hsa-miR-223, hsa-miR-369-3p,hsa-miR-376b,hsa-miR-542-3p,hsa-miR-548f,hsa-miR-590-3p,hsa-miR-7,hsa-miR-944
CDON	-2.06	hsa-miR-1308,hsa-miR-146a,hsa-miR-206,hsa-miR-211,hsa-miR-223,hsa-miR-377,hsa-miR-455-3p, hsa-miR-509-5p,hsa-miR-548f,hsa-miR-590-3p,hsa-miR-944
LOR	-2.06	hsa-miR-135b
VAPA	-2.05	hsa-miR-1276,hsa-miR-146a,hsa-miR-155,hsa-miR-206,hsa-miR-211
CD1A	-2.05	hsa-miR-146a,hsa-miR-21,hsa-miR-31,hsa-miR-33b
C19orf2	-2.05	hsa-miR-548f,hsa-miR-590-3p
TNS1	-2.05	hsa-miR-31,hsa-miR-33b,hsa-miR-369-3p,hsa-miR-509-5p,hsa-miR-665
ALCAM	-2.04	hsa-miR-1276,hsa-miR-1303,hsa-miR-135b,hsa-miR-18a,hsa-miR-206,hsa-miR-211,hsa-miR-223, hsa-miR-377,hsa-miR-542-3p,hsa-miR-590-3p,hsa-miR-944
DPYSL3	-2.03	hsa-miR-211,hsa-miR-212,hsa-miR-31,hsa-miR-548f,hsa-miR-590-3p,hsa-miR-7
MYH14	-2.03	hsa-miR-31
BCAR3	-2.03	hsa-miR-18a,hsa-miR-487a,hsa-miR-496,hsa-miR-548f,hsa-miR-944
CCND1	-2.02	hsa-miR-1276,hsa-miR-155,hsa-miR-369-3p,hsa-miR-487a,hsa-miR-548f
AR	-2.01	hsa-miR-18a,hsa-miR-509-5p,hsa-miR-10a,hsa-miR-137
C1orf21	-2.01	hsa-miR-944
SERHL	-2.01	hsa-miR-665
LRFN5	-2.01	hsa-miR-212,hsa-miR-590-3p
TACC2	-2.01	hsa-miR-1303,hsa-miR-31,hsa-miR-509-5p,hsa-miR-590-3p
PPP1R1A	-2.01	hsa-miR-31,hsa-miR-509-5p,hsa-miR-940
GLDN	-2.00	hsa-miR-1276,hsa-miR-1303,hsa-miR-135b,hsa-miR-146a,hsa-miR-155,hsa-miR-18a,hsa-miR-21, hsa-miR-378,hsa-miR-496,hsa-miR-665
LCE1B	-2.00	hsa-miR-135b,hsa-miR-7

Upregulated transcripts targeted by downregulated miRNAs

Gene symbol	Transcript FC	miRNAs that target transcript
PANX1	2.01	hsa-miR-10a,hsa-miR-1179,hsa-miR-137,hsa-miR-885-5p
SLC27A4	2.02	hsa-miR-486-3p
TUBB6	2.05	hsa-miR-628-3p
SLC39A6	2.09	hsa-miR-1179,hsa-miR-137
CEBPD	2.12	hsa-miR-885-5p
LTB4R	2.27	hsa-miR-1179
EIF4EBP1	2.33	hsa-miR-486-3p
CALML3	2.41	hsa-miR-486-3p
EPHA2	2.55	hsa-miR-10a
CD2	2.58	hsa-miR-137
CCNE1	2.59	hsa-miR-1179
KRT17	2.59	hsa-miR-486-3p
BUB1B	2.62	hsa-miR-486-5p
TYMS	2.62	hsa-miR-129-5p
WDR4	2.63	hsa-miR-486-3p
CRABP2	3.16	hsa-miR-486-3p
SERPINB1	3.40	hsa-miR-137
ALOX12B	4.37	hsa-miR-129-5p
ZC3H12A	7.73	hsa-miR-486-3p

Table 4-2. Differentially expressed miRNAs predicted to target LCE transcripts.

	miRNAs predicted to target 3'UTR				
Downregulated LCE	**miRNA (FC PP/NN,PP/PN[a])**	**Algorithm**	**Position in 3'UTR**	**miRSVR[b]/Context+[c] score**	**Validated?[d]**
LCE1B	135b (5.65,5.32)	miRanda/TargetScan	150-156	-0.47/-0.14	Y
LCE1B	7 (3.05,2.31)	miRanda/TargetScan	70-76	-0.28/-0.15	Y
LCE1B	206 (12.80,4.84)	miRanda	301-306	-0.34/NA	N
LCE1C	378 (2.68,2.11)	miRanda	141-147	-0.41/NA	N
LCE1E	31 (42.93,14.03)	miRanda/TargetScan	71-77	-0.13/-0.17	N
LCE1E	miR-590-3p (1.94,2.71)	miRanda/TargetScan	699-705	-0.16/-0.15	N
LCE1E	miR-590-3p (1.94,2.71)	miRanda/TargetScan	739-745	-0.91-0.26	N
LCE1E	137 (-2.37,-1.87)	miRanda	735-740	-0.21/NA	N
LCE2B	19a (1.89,2.31)	miRanda/TargetScan	138-144	-0.28/-0.13	--
LCE2B	19b (2.10,2.21)	miRanda/TargetScan	138-144	-0.28/-0.13	--
Upregulated LCE	**miRNA (FC PP/NN,PP/PN[a])**	**Algorithm**	**Position in 3'UTR**	**miRSVR[b]/Context+[c] score**	**Validated?[d]**
LCE3E	486-5p	miRanda/TargetScan	178-185	-0.87/-0.35	Y

[a]Normal skin, NN; Uninvolved psoriatic skin, PN; Involved psoriatic skin, PP.

[b]The mirSVR score is given for miRanda predicted targets; more negative scores imply stronger probability of target inhibition

[c]The context+ score is given for TargetScan predicted targets; more negative scores imply stronger probability of target inhibition

[d]miR-19a/b interactions with LCE2B were not tested due to ineffective overexpression from the pEP-miR vector

Table 4-3. Abundant miRNAs predicted to target LCE transcripts by the miRanda algorithm.

LCE	miRNA predicted to bind[a]	miRSVR score[b]	miRNA rank (NN[c])	miRNA read counts (NN)
LCE1B	miR-24	-1.19	9	3375273
LCE1B	miR-1	-0.34	51	228174
LCE1B	miR-218	-0.21	121	25891
LCE1C	miR-24	-0.58	9	3375273
LCE1C	miR-182	-0.17	46	295736
LCE1E	miR-32/92ab/363 family[d]	-0.17	39	368268
LCE1E	miR-25	-0.17	80	77376
LCE1E	miR-425	-0.57	92	58762
LCE1E	miR-218	-0.18	121	25891
LCE1E	miR-144	-0.32	161	9282
LCE2A	let-7/miR-98 family	-0.12	1	48065414
LCE2B	let-7f/miR-98	-0.11	2	15566363
LCE2B	miR-130a/b	-0.35	94	54276
LCE2C	let-7/miR-98 family	-0.15	1	48065414
LCE2C	miR-335	-0.13	155	10394
LCE2D	let-7/miR-98 family	-0.14	1	48065414
LCE3D	miR-28-5p/708 family	-0.79	93	54506
LCE5A	miR-320a/b/c/d	-0.11	79	77548
LCE6A	miR-24	-0.33	9	3375273
LCE6A	miR-185	-0.12	98	47631

[a]Conserved miRNAs predicted to bind LCE 3'UTRs by miRanda algorithm

[b]More negative miRSVR scores imply stronger probability of target inhibition

[c]Normal skin, NN

[d]For miRNA families, rank and read count is reported for most abundant family member

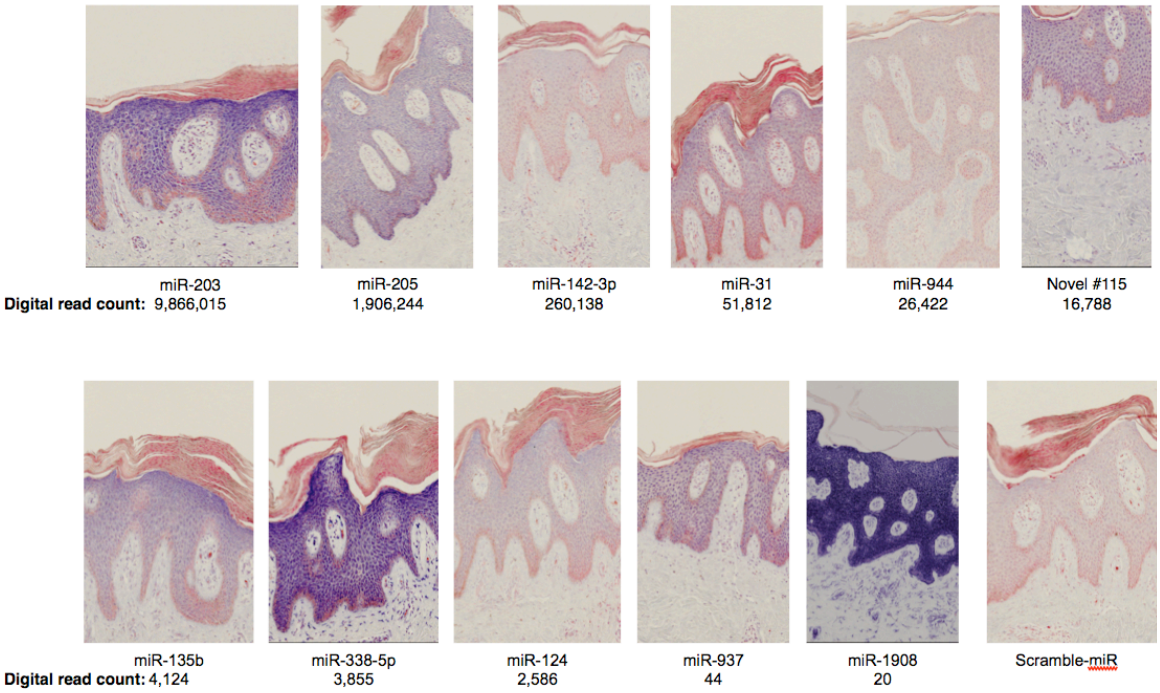

Figure 4-1. miRNA in situ hybridization for selected differentially expressed miRNAs in involved skin sections. Panels are arranged in descending according to digital read count, with the negative control scramble miR in the bottom right. Formalin fixed paraffin embedded skin sections were hybridized with DIG-labeled LNA probes and stained with NBT/BCIP (purple) and nuclear fast red. Signal intensity is poorly correlated with digital read count.

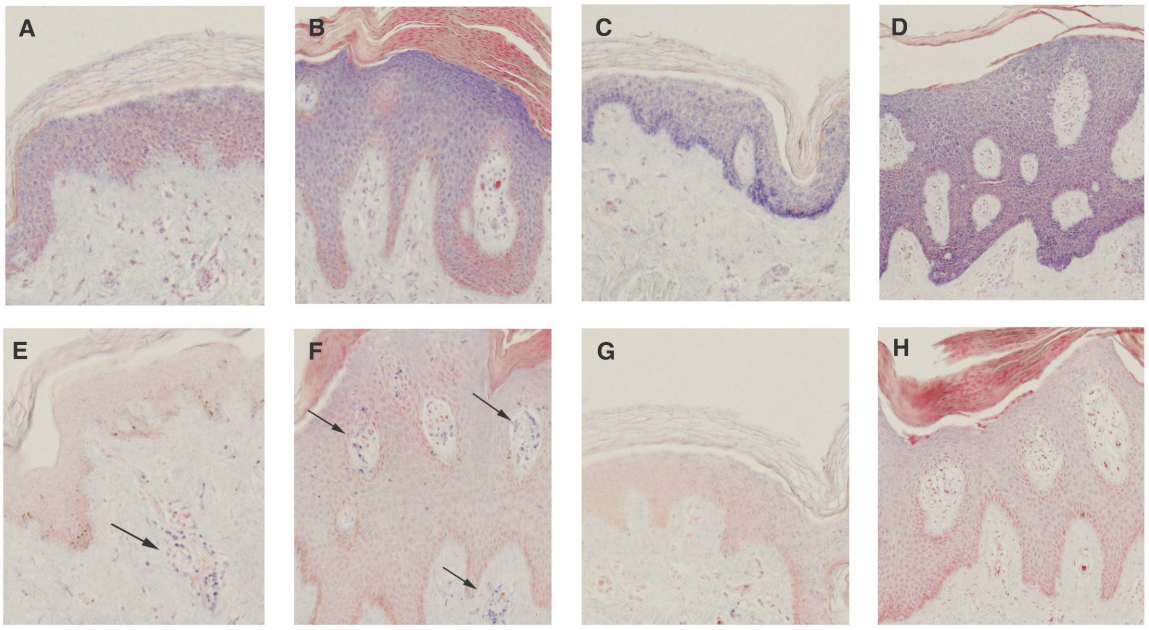

Figure 4-2. RNA *in situ* hybridization for skin expressed miRNAs in uninvolved psoriatic and involved psoriatic skin sections. Expression of miR-135b in the (A) PN and (B) PP epidermis. Expression of miR-205 in (C) PN and (D) PP epidermis. Expression of miR-142-3p in (E) dermal immune cells (arrowheads) in PN skin and (F) dermal/epidermal immune cells (arrowheads) in PP skin. Scramble-miR background signal in (G) PN and (H) PP skin. Uninvolved psoriatic skin, PN; Involved psoriatic skin, PP.

A

```
3' aguguauccUUACUUUUCGGUAu 5' hsa-miR-135b
           || |  |||||||
5' uucucccccAAAGCCAAGCCAUu 3' LCE1B

3' ugUUGUUUUAGUGA--UCAGAAGGu 5' hsa-miR-7
    ||  |  || ||   |||||||
5' ccAAAUAUUUCCCUUCCGUCUUCCu 3' LCE1B
```

B

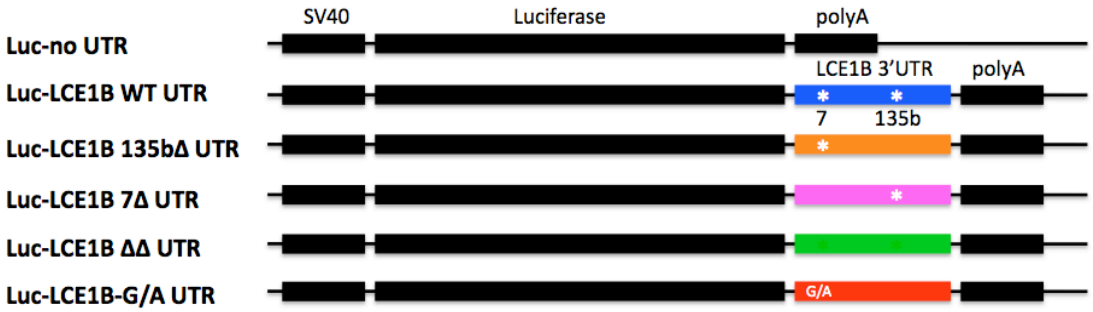

C

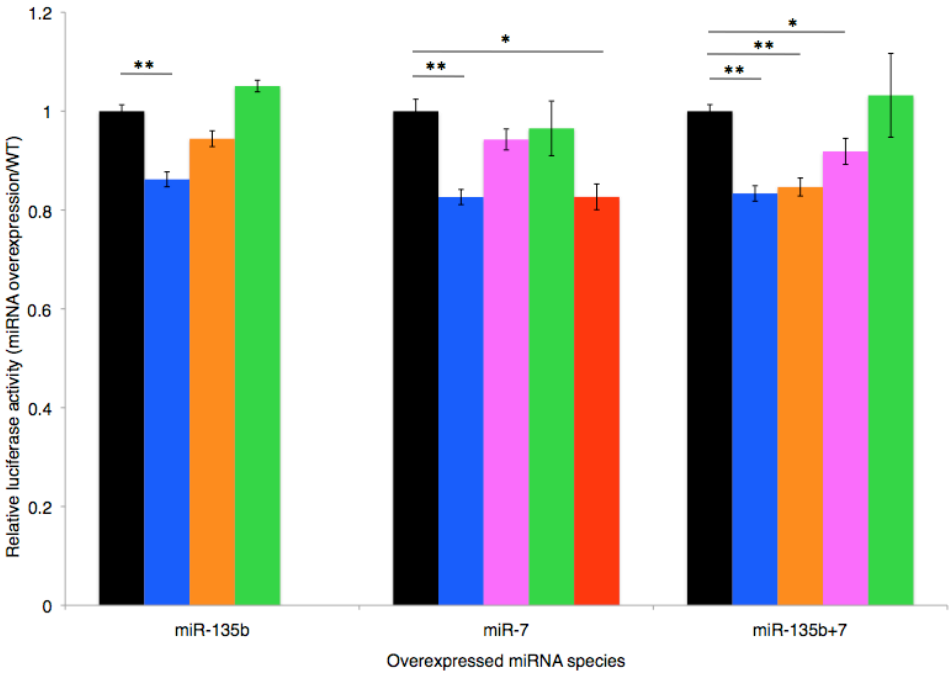

Figure 4-3. miR-135b and miR-7 inhibit LCE1B through direct interactions with the 3'UTR. (A) miRNA:mRNA duplex for miR-135b and miR-7 sites, as predicted by miRanda algorithm. Identical binding sites were also predicted by TargetScanS. **(**B) Schematic representation of luciferase-LCE1B 3'UTR reporter constructs. "*" indicate miRNA binding seed regions. The G/A construct encodes the LCE1B 3'UTR with the minor A allele for SNP rs79341479. (C) Relative luciferase activity in HEK293 cells overexpressing the indicated miRNAs compared to wild-type (WT) cells. Bar colors correspond with construct colors in part A. *$p<0.05$, **$p<0.01$.

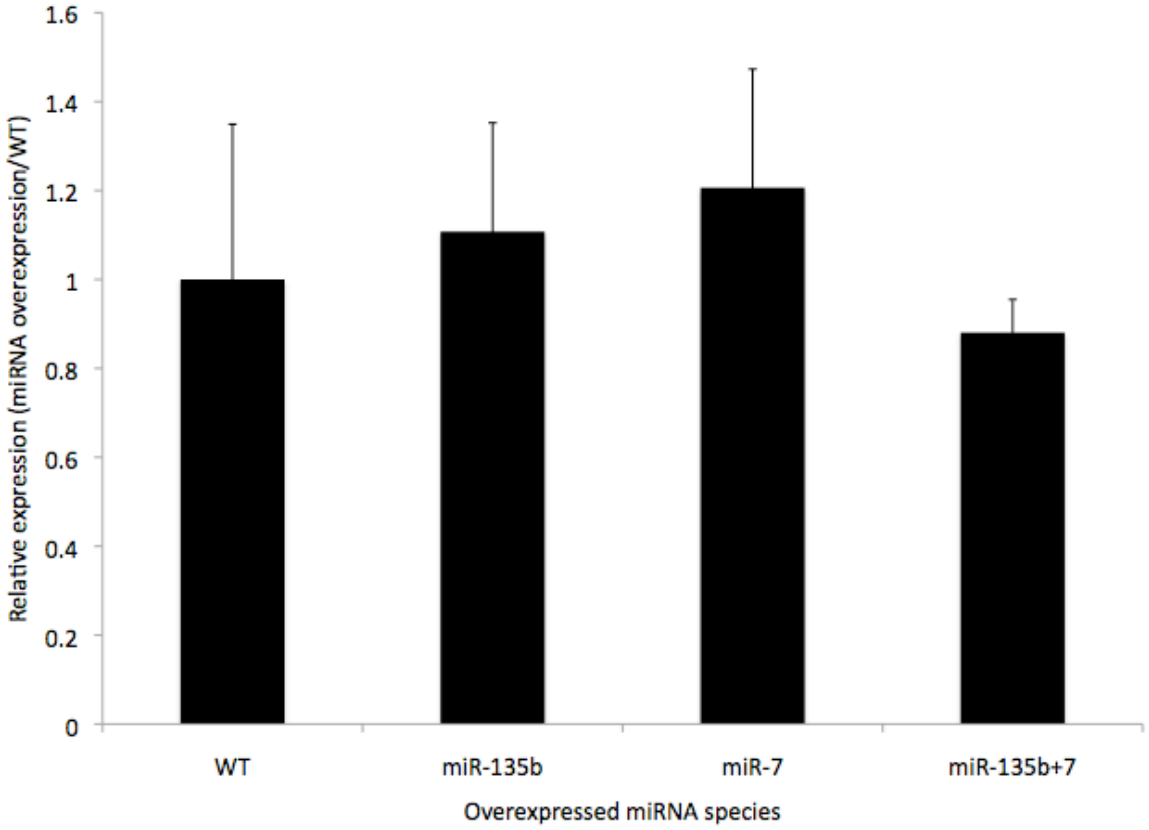

Figure 4-4. miR-135b and miR-7 have no effect on luciferase-LCE1B reporter transcript levels. Relative mRNA levels of the luciferase-LCE1B WT 3'UTR reporter in HEK293 cells overexpressing miR-135b and/or miR-7 compared to wild type (WT). Primers were targeted to the LCE1B 3'UTR (see methods).

A

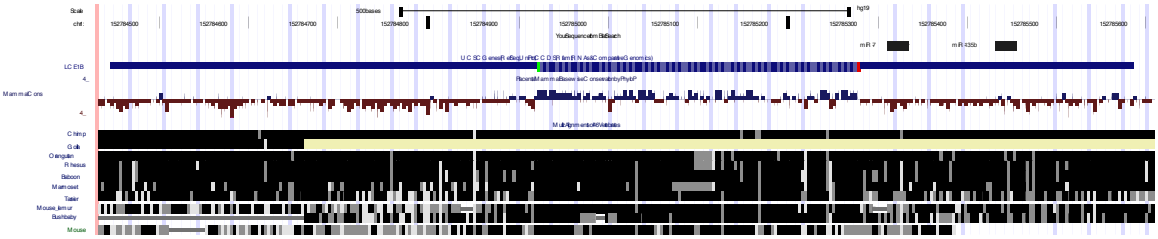

B

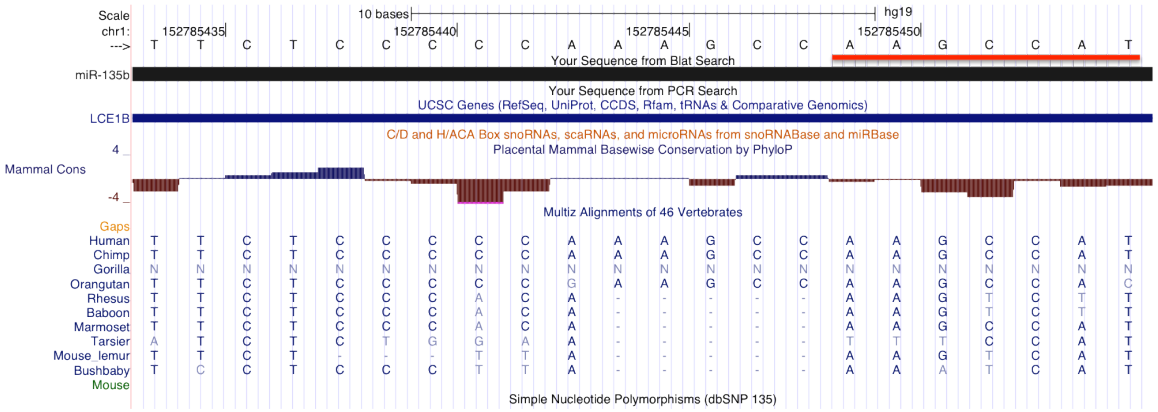
Scale
chr1:
10 bases
hg19
152785435
152785440
152785445
152785450
Your Sequence from Blat Search
miR-135b
Your Sequence from PCR Search
UCSC Genes (RefSeq, UniProt, CCDS, Rfam, tRNAs & Comparative Genomics)
LCE1B
C/D and H/ACA Box snoRNAs, scaRNAs, and microRNAs from snoRNABase and miRBase
Placental Mammal Basewise Conservation by PhyloP
Mammal Cons
Multiz Alignments of 46 Vertebrates
Gaps
Human
Chimp
Gorilla
Orangutan
Rhesus
Baboon
Marmoset
Tarsier
Mouse_lemur
Bushbaby
Mouse
Simple Nucleotide Polymorphisms (dbSNP 135)

C

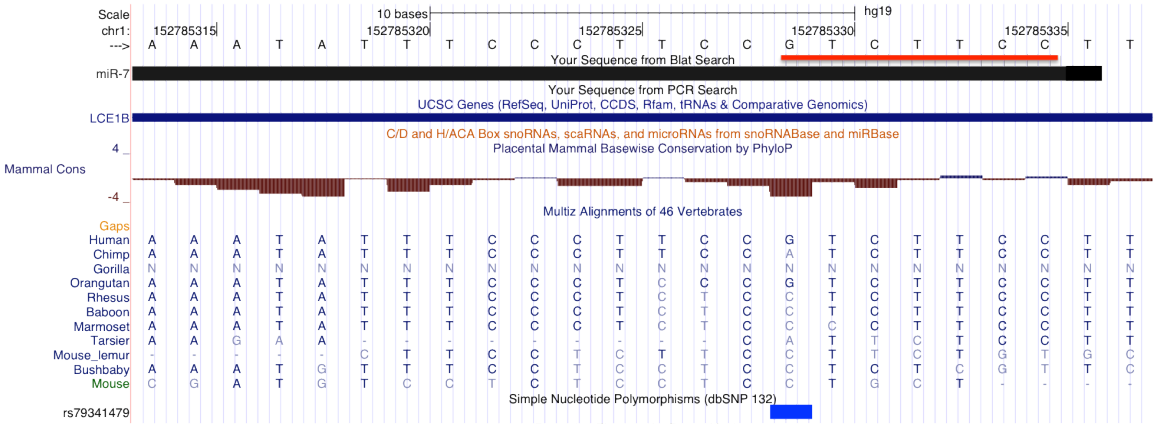
Scale
chr1:
10 bases
hg19
152785315
152785320
152785325
152785330
152785335
Your Sequence from Blat Search
miR-7
Your Sequence from PCR Search
UCSC Genes (RefSeq, UniProt, CCDS, Rfam, tRNAs & Comparative Genomics)
LCE1B
C/D and H/ACA Box snoRNAs, scaRNAs, and microRNAs from snoRNABase and miRBase
Placental Mammal Basewise Conservation by PhyloP
Mammal Cons
Multiz Alignments of 46 Vertebrates
Gaps
Human
Chimp
Gorilla
Orangutan
Rhesus
Baboon
Marmoset
Tarsier
Mouse_lemur
Bushbaby
Mouse
Simple Nucleotide Polymorphisms (dbSNP 132)
rs79341479

Figure 4-5. Multi-species alignments for the LCE1B 3'UTR and miRNA binding sites. (A) LCE1B locus on chromosome 1, with miR-135b and miR-7 binding sites (black bars under BLAT search heading) and conservation in chimp, rhesus macaque, and mouse indicated. (B) Sequence and conservation of miR-135b binding site in human, chimp, rhesus macaque, and mouse; red bar indicates seed region. (C) Sequence and conservation of miR-7 binding site in human, various primate species, and mouse; red bar indicates seed region.

A

```
3' gagccccgucGAGU-CAUGUCCu 5' hsa-miR-486-5p
             :|:| |||||||
5' cacuucuuguUUUAUGUACAGGa 3' LCE3E
```

B

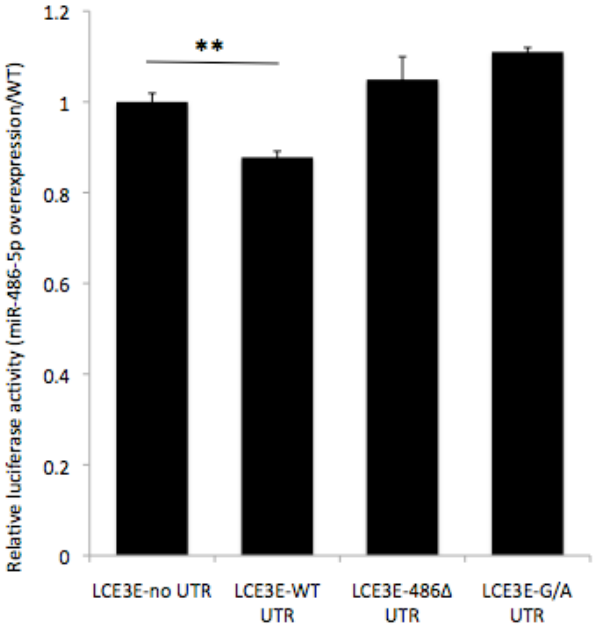

C

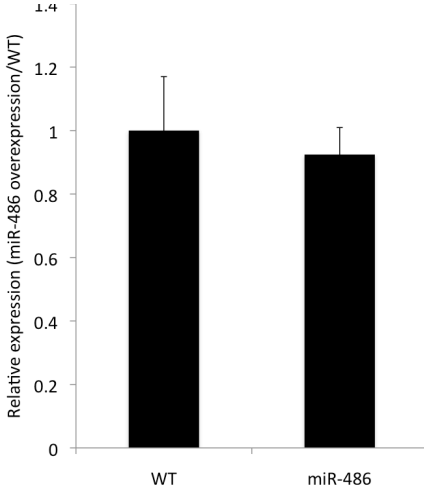

D

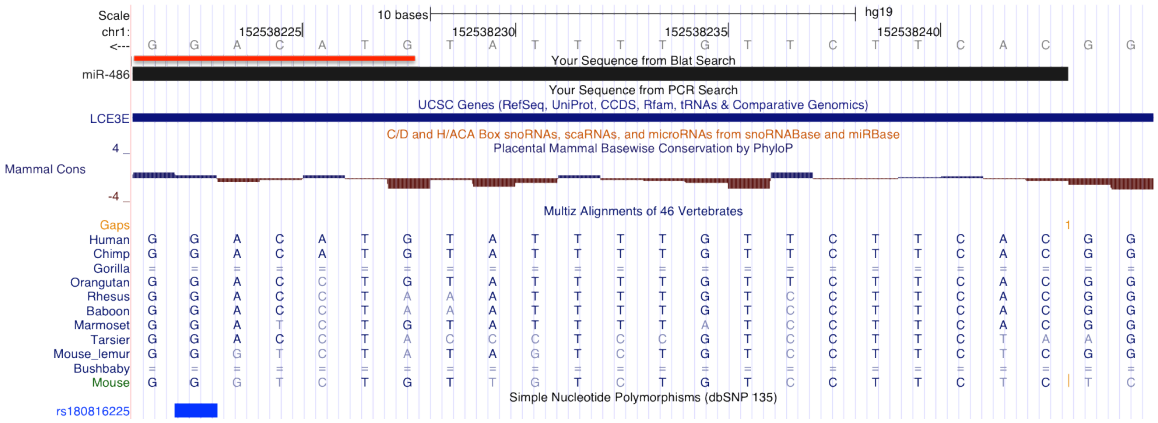

Figure 4-6. miR-486-5p inhibits LCE3E through a direct interaction with the 3'UTR. (A) miRNA:mRNA duplex for miR-486-5p binding site, as predicted by miRanda algorithm. (B) Relative luciferase activity in HEK293 cells overexpressing miR-486-5p compared to wild-type (WT) cells. **p<0.01. The G/A construct encodes the LCE3E 3'UTR with the minor A allele for SNP rs180816225. (C) Relative mRNA levels of the luciferase-LCE3E WT 3'UTR reporter in HEK293 cells overexpressing miR-486 compared to wild type (WT). Primers were targeted to the LCE3E 3'UTR (see methods). (D) Sequence and conservation of miR-486 binding site in human, various primate species, and mouse; red bar indicates seed region.

Chapter 5.

Expression of noncanonical miRNAs and endogenous siRNAs in normal and psoriatic skin

ABSTRACT

Noncanonical microRNAs (miRNAs), which bypass part of the canonical miRNA biogenesis pathway, and endogenous small interfering RNAs (endo-siRNAs) are key gene regulators in eukaryotes. Mounting evidence suggests that these small noncoding RNAs (sncRNAs) can originate from a variety of genomic loci. These include snoRNAs, tRNAs and introns for noncanonical miRNAs, and repetitive regions and mobile elements for endo-siRNAs. However, the roles of such sncRNAs in complex disease have yet to be characterized. To investigate their potential expression and function in psoriasis, we carried out a comprehensive, genome-wide search for noncanonical miRNAs and endo-siRNAs expressed in normal and psoriatic human skin with Next Generation sequencing of small RNAs. We identified 23 noncanonical miRNAs (3 snoRNA-derived and 2 tRNA-derived miRNAs and 18 miRtrons) and 39 endo-siRNAs that were expressed in skin. The expression of four sncRNAs was validated by qRT-PCR of total RNA and Argonaute immunoprecipitates isolated from human skin. Fifteen noncanonical miRNAs and endo-siRNAs were significantly differentially expressed in psoriatic involved versus normal skin, including an Alu-SINE-derived siRNA which was 17-fold upregulated in involved skin. These and other differentially expressed sncRNAs may function as regulators of gene expression in skin and play a role in psoriasis pathogenesis.

INTRODUCTION

MicroRNAs (miRNAs) and endogenous small interfering RNAs (endo-siRNAs) are classes of small noncoding regulatory RNAs (sncRNAs) that play critical roles in gene regulation for many biological processes in eukaryotic organisms (34). miRNAs in particular have been heavily studied in recent years and shown to be essential gene regulators that broadly contribute to disease pathogenesis.

miRNAs are produced from short hairpin-forming primary transcripts (pri-miRNAs) which are typically processed through a canonical pathway involving the RNase III enzymes Drosha, Dgcr8 and Dicer (103). Besides these canonical miRNAs, there exist noncanonical miRNAs whose biogenesis requires Dicer but neither Drosha nor Dgcr8 (185). The first example of noncanonical miRNA was the class of miRtrons, which arise from the splicing of 60-100nt introns, independent of Drosha. The debranched short introns may fold into stem-loop structures, which are then cleaved by Dicer to release miRNAs (104,105,186,187). Noncanonical miRNAs can also arise from local hairpin formation within larger noncoding RNA (ncRNA) species, such as small nucleolar RNAs (snoRNAs) and transfer RNAs (tRNAs; 118,188). While there have been several snoRNA-derived miRNAs described in eukaryotes, only one example of a tRNA-derived miRNA has been described. In this case, a murine tRNA, *IleTAT* can fold into an alternative secondary structure consisting of a stem-loop hairpin from which a miRNA is derived (189).

In contrast to miRNAs, endo-siRNAs are generated from long double-stranded RNAs (dsRNA) that can originate from the transcription of repetitive sequences,

transposable elements, or Piwi-interacting RNA (piRNA) loci. These long dsRNAs are processed by Dicer, but do not require Drosha or Dgcr8. Endo-siRNAs have been described in plants (34,190), *C. elegans* (191), *D. melanogaster* (192,193,194,195), and murine oocytes (196,197,198). There is also evidence suggesting that endo-siRNAs may be expressed in murine embryonic skin (86). Like miRNAs, siRNAs exert their regulatory functions through association with the RNA induced silencing complex (RISC), which contains an Argonaute (Ago) protein. However, unlike miRNAs, pairing between siRNAs and their targets requires fewer than three mismatches and elicits direct cleavage of target mRNAs (196).

In previous chapters, I have described the majority of known and novel miRNAs expressed in normal and psoriatic skin. In this chapter, I describe the identification of novel noncanonical miRNAs and endo-siRNAs expressed in skin, and their potential roles in psoriasis. This work has broadened current perspectives on the diversity of sncRNAs and their potential roles in gene regulation in human skin. This work was a collaborative effort between myself and Jing Xia, a graduate student in Weixiong Zhang's lab at Washington University.

RESULTS

Next Generation sequencing of small RNAs

A total of 67 small RNA libraries were prepared from human skin biopsies: 24 psoriatic involved skin (PP), 23 psoriatic uninvolved skin (PN), and 20 healthy controls (NN), as described in Chapter 2. Approximately 85% of the qualified reads from each category mapped perfectly to the human genome. Among these mappable reads, 55% originated from mature miRNAs or miRNA precursors; 39% originated from other noncoding RNAs and repeat regions; and 6% originated from other genomic loci such as coding sequence, untranslated regions, introns, and intergenic sequences (Table 5-1).

The presence of small RNA read clusters at various non-miRNA loci may reflect expression of unannotated, functional sncRNAs. Alternatively, genomic small RNA reads could arise from degradation products of mRNAs or unannotated transcripts. To address this question, we embarked on a systematic study of these small RNA reads with computational and experimental approaches. We first focused on noncanonical miRNAs that originated from snoRNAs, tRNAs and introns and then analyzed putative endo-siRNA loci. Reads derived from these loci are described in detail below and generally exhibited features of functional Dicer dependent sncRNAs, such as a 21-22-nt peak in length distribution, 5' homogeneity, and 5' nucleotide identity bias (Figure 5-1). Notably, ncRNA species that are not processed by Dicer, such as tRNAs and rRNAs, do not display these features.

Noncanonical miRNAs or miRNA-like RNAs expressed in human skin

miRNAs derived from snoRNAs and tRNAs

Some ncRNA species are substrates for Dicer-mediated miRNA production and eight human snoRNAs have been reported to produce miRNAs (118). Analysis of the small RNA reads from human skin revealed that 58 million reads (~8.8%) aligned to snoRNAs, including all eight of the previously described miRNA-producing snoRNAs (Table 5-2). The majority (86%) of these reads were 21 or 22-nt in length, and their 5' nucleotides were predominately A and G (89.7% of the total). We searched for novel snoRNA-derived miRNAs in this pool of reads, and identified three novel loci (Table 5-2). Remarkably, ~79% of snoRNA reads aligned to one C/D box snoRNA, U60, which has not been previously implicated as a miRNA locus. Of these reads, 98.9% were 21-22nt long. Folding structure analysis revealed that the U60 snoRNA could form an alternative RNA secondary structure that resembled a miRNA precursor hairpin (Figure 5-2A). Alignment of the most abundant small RNA reads to each arm of this hairpin resulted in a 22-nt RNA-RNA duplex with 3' overhangs (Figure 5-2A,B). Remarkably, the 22-nt miRNA-like small RNA was ranked as the second most highly expressed miRNA in human skin, based on sequencing read counts. However, the high abundance of U60 reads could result from established library preparation biases (113,114); indeed, qRT-PCR experiments were consistent with a more moderate expression level in the skin (see below).

We next examined small RNA reads that aligned to tRNAs (Table 5-2). First, we recognized that the mature mmu-miR-1983 sequence, derived from murine tRNA-IIeTAT (189), was conserved in humans and associated with 228 21-22nt small RNA

reads in our dataset (Figure 5-3A). A second tRNA candidate with short hairpin-forming potential, PseudoTTA, was associated with a cluster of 14 small RNA reads (Figure 5-3B). Both of these putative tRNA-originated miRNAs were expressed at very low levels in human skin. In the case of tRNA-IIeTAT, only ~2% of the reads aligning to the tRNA were consistent with the sequence of mmu-miR-1983, as compared to 92% in mouse embryonic stem cells (mESCs; GSM314552; 189). The higher expression level of miR-1983 in mESCs might indicate that the alternative hairpin structure is preferential to the original tRNA structure in this cell type or more generally, in the germ line. Alternatively, differences in sample preparation between the two studies may account for relative differences in abundance.

Intronic miRNAs and miRtrons

The miRNA subclass of miRtrons includes typical miRtrons that reside at the exon/intron boundaries of 60 to 100-nt introns, and tailed miRtrons that are generated from one end of longer introns (186,199). Fourteen typical miRtrons have been previously described in humans (104) and were also detected in the current study. Our analysis of small RNA reads from skin indicated that an additional 26 known human miRNAs were likely to have been processed by the miRtron biogenesis pathway (2 typical miRtrons and 24 tailed miRtrons). The currently annotated precursors for the majority of these known miRNAs, e.g. miR-636, miR-936 and miR-3064, extend beyond their respective host intron regions. However, 80% of the reads aligning to the intron/exon boundary terminated within 2-nt of the AG splice acceptor site, which strongly indicated that these pre-miRNAs were derived directly from debranched introns (Figure 5-4).

In Chapter 2, I described a number of novel miRtron candidates. Re-examination of these 67 miRtron candidates confirmed that 94% of reads aligning to the intron/exon boundary terminated within 2-nt of the AG splice acceptor site on average (Table 5-3). To identify additional novel miRtrons that are expressed in human skin, we carefully searched a 160bp window of intronic sequence at all intron/exon boundaries in the human genome for hairpin forming potential and small RNA read clusters. This analysis resulted in the identification of additional 18 candidates, which were not previously reported in Chapter 2 due to low abundance and/or atypical folding structures (Table 5-3). The lengths of the host introns varied from 70 to several thousand bases, suggesting that long introns can also give rise to miRtrons. In sum, this analysis increased the total number of miRtron candidates to 125 (19 typical miRtrons and 106 tailed miRtrons) in the human genome.

miRtrons are typically expressed at low levels (200), which is consistent with our observation in human skin. In the set of miRtrons we studied, the most highly expressed was the known miRtron, miR-877, with 4,827 reads. Interestingly, the recently described miRtrons, #80 and #103, and two newly annotated miRtrons, miR-1292 and miR-3605, were expressed at levels comparable to that of miR-877. Hairpin structures and read alignments for the two most abundant miRtrons, #80 and #103, are shown in Figure 5-5. The low abundance of miRtrons may be due to multiple factors: the presence of more bulges and unpaired bases in their hairpin structures than canonical miRNAs that lowers Dicer processing efficiency, susceptibility to endogenous lariat degradation pathways, and, in many cases, their recent evolution (see below).

Endogenous siRNAs expressed in human skin

The expression of endo-siRNAs in adult human tissues is not well understood. Our dataset of deeply sequenced small RNAs allowed us to perform a genome-wide search for putative endo-siRNAs that were associated with small RNA sequencing reads in human skin.

endo-siRNAs from repeats and transposable elements

A total of 27M reads (~4% of the total qualified reads) from our human skin dataset mapped to a variety of repeat elements in the human reference genome, such as SINEs, LINEs, LTRs and DNA transposons (Table 5-1). The locus with the most aligned reads was on chromosome 1 (Figure 5-6A). This was within an intron of the gon-4-like (GON4L) gene where three Alu SINEs appear in tandem. A total of 5,534 reads (53.4% of which were 21-23nt) aligned to this locus, with a cluster of 2,800 reads (83.7% of which were 21-23nt) uniquely mapped to the first Alu SINE (highlighted in green in Figure 5-6A). This putative endo-siRNA was the most differentially expressed siRNA between PP and NN skin (see below). In contrast, the expression level of the host gene GON4L shows little variation between PP and NN skin (data not shown), indicating that the SINEs and the host gene may be transcribed or processed independently.

To study the biogenesis of this putative endo-siRNA, we generated mammalian expression constructs with various combinations of the three Alu SINE elements (E1, E2, and E3) and transfected them into HEK293 cells. We found that transcription of the E1 segment, which does not form an intrinsic hairpin structure, is sufficient for siRNA production (Figure 5-6B). Thus, it is plausible that the E1 transcript may anneal to closely related Alu-SINE element transcripts in the genome to form a dsRNA for siRNA

production. Alternatively, transcription of E1 and E2 together may produce a long hairpin-structured dsRNA for siRNA production (Figure 5-6C). This possibility is consistent with slightly enhanced siRNA production from the E1+E2 fragment compared to the E1 fragment alone (Figure 5-6B).

We also identified two less abundant putative endo-siRNAs derived from other repetitive elements (Figure 5-7). In the first case, a cluster of 12 reads (83.3% were 21-23nt in length) uniquely mapped to inverted repeats of tandem L1 elements on chromosome 16. In the second case, a cluster of 72 reads (79.2% were 21-23nt in length) mapped to an LTR element on chromosome 4; however, 25% of the reads in this cluster did not map to this locus uniquely. Transcripts from these loci could form long hairpin structures of 98nt and 135nt, respectively. A clear 5' homogeneity of the clustered sequencing reads originating from these two loci was observed, suggesting that the small RNAs are authentic endo-siRNAs rather than random degradation products.

In addition, a striking ~11K reads uniquely mapped to Made1 elements, a human-specific subclass of miniature inverted repeat transposable element (MITE), which encodes the large hsa-miR-548 family. We confirmed that 34 Made1 elements, which were not previously associated with miRNA production, can give rise to hairpin structures (Table 5-4; Figure 5-8). Mapping of small RNA reads to both 5' and 3' arms of these hairpins generally revealed putative Dicer-cleavage products with 3' overhangs, which share sequence identity with individual members of the miR-548 family. Unlike most canonical miRNAs, the sncRNAs derived from Made1 elements have a large number of paralogs, including 58 annotated in miRBase (v.17) and 34 in this study. Thus,

based on its genomic origin within a common transposable element, we prefer to classify the miR-548 family members as siRNAs.

endo-siRNAs from piRNA loci

Analysis of reads aligned to piRNA-annotated loci uncovered two loci for which the length distributions of small RNAs had two dominant peaks at 21-23nt and at 27-30nt (Figure 5-9). This distribution would be indicative of expression of siRNAs and piRNAs, respectively. The two loci are within annotated Alu SINE elements and no hairpin structures could be detected by folding the corresponding flanking sequences. Hence, the origin of these siRNAs is unclear, but they could arise from annealing between closely related repetitive element-derived transcripts in the genome. Interestingly, the siRNAs from these two loci share sequences similar to miR-1285 and miR-1303 (Figure 5-9), two miRNA genes that overlap with Alu SINE elements. A search for paralogs of hsa-miR-1285 and hsa-miR-1303 mature miRNAs revealed more than 80 loci with exact sequence identity in the human genome, indicating miR-1285 and miR-1303 may be more accurately classified as siRNAs.

Conservation of noncanonical miRNAs and endo-siRNAs

We performed a comparative genomic analysis of all 130 noncanonical miRNAs (5 derived from tRNAs or snoRNAs and 125 miRtrons) and endo-siRNAs that were expressed in human skin (data not shown). To this end, we considered eight species: *Macaca mulatta* (rhesus), *Mus musculus* (mouse), *Canis lupus familiaris* (dog), *Loxodonta Africana* (elephant), *Monodelphis domestica* (opossum), *Gallus gallus*

(chicken), *Xenopus tropicalis* (frog) and *Danio rerio* (zebrafish). For 54/130 (41.5%) noncanonical miRNA loci we analyzed, the mature miRNA sequence was human specific. For 50/130 noncanonical miRNAs (38.5%), the mature sequence was present in *Macaca mulatta* but not in *Mus musculus*, suggesting that they might be primate specific. For the final 26/130 (20%) noncanonical miRNA loci (23 miRtrons, 1 snoRNA- and 2 tRNA-derived miRNAs) the mature miRNA sequence was conserved in one or more species beyond *Macaca mulatta*. The presence of snoRNA- and tRNA-derived miRNAs in non-primate mammals suggested potential roles for small RNAs derived from snoRNA and tRNA transcripts in human and other mammalian species. The 39 endo-siRNA loci described herein were present only in human and *Macaca mulatta*, largely due to the conservation of the hosting repeat elements (Alu SINEs) in primates (201). The majority of the noncanonical miRNAs and endo-siRNAs we studied were not conserved beyond primates, suggesting that these recently evolved sncRNAs could perhaps serve primate-specific functions.

qRT-PCR validation of noncanonical miRNAs and endo-siRNAs

We selected three noncanonical miRNAs and one endo-siRNA for validation with quantitative RT-PCR (qRT-PCR): the U60 snoRNA-derived miRNA, the pseudoTTA-derived miRNA, the recently described miRtron #103, and the Alu SINE-derived siRNA. We first set out to validate the endogenous expression of these sncRNAs in skin. While all four produced a consistent qRT-PCR signal that was both RNA and reverse transcriptase dependent (Figure 5-10A,B), we were not able to obtain a visible product for miRtron #103 (Figure 5-10B). This is likely due to its low abundance and the

established discrepancy between small RNA abundance as determined by Next Generation sequencing (NGS) versus qRT-PCR (113,114). Notably, the pseudoTTA miRNA was detected at higher levels with qRT-PCR in the human embryonic kidney cell line, HEK293, compared to skin (data not shown). This finding is consistent with the enrichment of the pseudoTTA miRNA in mESC sequencing data, and further suggests that this miRNA may be more abundant in embryonic tissues than in adult tissues.

We next determined whether the ectopic expression of genomic DNA encoding the putative sncRNA precursor was sufficient for the accumulation of sncRNAs. DNA fragments of ~200nt harboring these sncRNAs were cloned into a mammalian expression vector and transfected into HEK293 cells. For each of the four loci tested, there was a >5 fold enrichment in sncRNA production when the appropriate genomic segment was ectopically expressed, suggesting that these loci are indeed sufficient to generate sncRNAs (data not shown). Finally, we used these expression constructs to determine whether the ectopically expressed sncRNAs were present in Ago2 or Ago3 immunoprecipitates with RNA binding protein immunoprecipitation coupled with qRT-PCR (RIP-PCR; Figure 5-10C). Indeed, ectopically expressed miRtron #103 was significantly enriched in both Ago2 and Ago3 immunoprecipitates compared to IgG; the pseudoTTA-derived miRNA and the Alu-SINE derived siRNA were significantly enriched in Ago2 immunoprecipitates; and the U60-derived miRNA was modestly enriched in Ago2 and Ago3 immunoprecipitates, but these enrichments were not significant. This suggested that these novel sncRNAs may function through association with Ago effectors.

Differential expression of noncanonical miRNAs and endo-siRNAs in skin and predicted targets

In order to investigate the potential function of the newly identified noncanonical miRNAs and endo-siRNAs in skin, we performed digital gene expression (DGE) analysis on noncanonical miRNAs and endo-siRNAs in PP, PN and NN skin samples. A total of 15 out of 169 (8.9%) noncanonical miRNAs and endo-siRNAs exhibited significant differential expression with at least a 1.5-fold change in one or more comparisons (PP vs. NN; PP vs. PN; or PN vs. NN), with p-values less than 0.001. Ten sncRNAs were upregulated in PP vs. PN and NN skin (Alu-SINE-siRNA, Made1_#1, hsa-miR-937, tRNAIle-miRNA, miRtrons #14, #72, #144, #323 and #375, and U60 miRNA-5p), whereas five (miRtrons #80, #252, #145-5p and #145-3p and Made1_#47) were downregulated in PP vs. PN and NN skin (Table 5-5; Figure 5-11A). Notably, the expression of the most abundant Alu-SINE-derived siRNA was more than 17-fold increased in the PP vs. NN comparison. The differential expression of this siRNA and hsa-miR-937 (newly annotated as a canonical miRtron) was confirmed by qRT-PCR, while the more modest differential expression of the U60-derived miRNA did not validate (Figure 5-11B). The failure of U60 to validate could be a result of heterogeneity in PN and NN samples that is not related to disease. The clustering of samples based on the expression of the 15 differentially expressed small RNAs distinguished the majority of PP samples from PN and NN samples (Figure 5-11A).

We searched for potential mRNA targets of differentially expressed noncanonical miRNAs by TargetScan (72,79) and starBase (202) and that of endo-siRNAs with an in-house siRNA target finding method. We specifically focused on those targets that are

differentially expressed in psoriasis based on published microarray-based mRNA profiling data from PP, PN and NN skin and murine models of psoriasis (19,203) to help appreciate the potential roles of these sncRNAs in regulating the expression of their targets. Since miRNAs and siRNAs typically reduce the expression levels of targeted mRNAs, we focused on predicted targets for which the differential expression of the miRNA/siRNA was inversely correlated with the target expression. This analysis showed that 11 out of the 15 differentially expressed small RNAs were inversely correlated with a subset of their predicted target genes that were at least 1.5-fold differentially expressed in psoriasis (Table 5-6). These targeted genes included the p53 inhibitor, mouse double minute 4 homolog (MDM4; 204,205), and syndecan 4 (SDC4), which plays a role in wound repair (206). Such inverse expression patterns suggested that noncanonical miRNAs and endo-siRNAs might influence psoriasis pathogenesis by regulating the expression of target genes in the skin.

DISCUSSION

Most small RNA profiling studies have focused on canonical miRNAs. In order to examine other small RNA species expressed in skin, we searched for novel noncanonical miRNAs and endo-siRNAs from diverse origins in the human genome. We reported 23 novel noncanonical miRNAs derived from snoRNAs, tRNAs and intron lariats, and 39 putative endo-siRNA loci in repetitive sequences, transposable elements, and piRNA hosting regions. These included a snoRNA-derived miRNA that was moderately abundant in human skin, the first example of a tRNA-derived miRNA in an adult human tissue, and an siRNA derived from an Alu SINE element that was highly upregulated in psoriatic skin.

Common features of noncanonical miRNAs and endo-siRNAs from diverse genomic origins

The noncanonical miRNAs and endo-siRNAs that we identified have several distinctive characteristics that set them apart from RNA degradation products and other transcription products. First, these sncRNAs exhibited a size distribution centered around 21-22nt, which is distinct from other classes of small RNAs and degradation products. One exception to this is the Alu-SINE-derived siRNA we described in which potential bulges introduced by imperfect base pairings likely underlie the dominant read size of 23nt.

The second characteristic of noncanonical miRNAs and endo-siRNAs was the typical 5' homogeneity of read clusters. Dicer processing often produces small RNA isoforms that differ at the 3'-end, but 5'-end heterogeneity is much less common (110,111,207). In contrast, ncRNAs that are not generated by Dicer do not have this property. For example, reads that mapped to 3'-ends of tRNAs displayed dramatic 3'-end homogeneity, which is characteristic of cleavage activities of RNase Z, the endonuclease that releases tRNA sequences (207). One key exception to the typical 5' homogeneity we observed was the U60-derived miRNA, which exhibited three dominant isoforms with variable 5' ends. However, several of the previously described snoRNA-derived miRNAs also shared this feature (e.g. hsa-miR-1839/ACA45-derived miRNA), suggesting that the biogenesis of snoRNA-derived miRNAs is not fully characterized.

Lastly, the distribution of 5' nucleotide identities for noncanonical miRNAs and endo-siRNAs was non-random. For noncanonical miRNAs derived from snoRNAs and endo-siRNAs, the dominant 5' nucleotide was A (47.1% and 72.8%, respectively). Consistent with this, the presence of a U or A nucleotide facilitates RNA-protein interactions within the middle (MID) domain of the human Ago2 protein (208). Interestingly, canonical miRNAs have a stronger bias towards a 5' terminal U nucleotide (78.8%).

Association with protein components of the small RNA biogenesis and RNA silencing machinery

Noncanonical miRNAs and siRNAs both require Dicer but not Drosha nor Dgcr8 for their biogenesis. In agreement with this, the murine homologs of the ACA61- and

ACA25-derived miRNAs, the pseudoTTA-derived miRNA, and the newly annotated tailed miRtron, miR-3064, were present in deep sequencing datasets from Dgcr8-knockout mice but absent from Dicer-knockout mice (189,200). The additional noncanonical miRNAs that have murine homologs were not detected in these datasets, presumably due to lesser sequencing depth in the murine studies. It is likely that other novel sncRNAs from this study are Dgcr8-independent, but we have not been able to interrogate them with this analysis since they are not conserved in mouse.

miRNAs and siRNAs exert their functions through association with RISC complexes, which include an Ago protein. In humans, there are four Ago family members, but no direct evidence has been collected for the association of endo-siRNAs with particular Ago family members (209). Here we show that some noncanonical miRNAs and endo-siRNAs associate with Ago2 and Ago3 proteins, indicating that many of the noncanonical miRNAs and endo-siRNAs we have described potentially function through incorporation into Ago effector complexes. These findings are largely consistent with recently published deep sequencing data from human Ago1/2/3/4 immunoprecipitates (GSE21918) (210). Analysis of this dataset indicated that the pseudoTTA-derived miRNA, 50/125 miRtrons, 6/34 MADE1-derived siRNAs, the Alu-SINE-derived siRNA, and the piRNA-locus-derived siRNAs all associated with one or more Ago proteins. Interestingly, sequences derived from the U60 snoRNA were present in the Ago immunoprecipitates, but there were no exact matches to the abundant 22nt species we detected; these reads were consistent with the 5' terminus of the 22nt species but were typically 28nt in length. Also, the most abundant miRtron, #103, was not present in Ago1/2/3/4 immunoprecipitates. However, we found that this miRtron is not

endogenously expressed in the HEK293 cell line from which the Ago immunoprecipitation data was derived (data not shown). Thus, it is likely that cell-type specific expression underlies the absence of miRtron #103 and perhaps other sncRNA species from the Ago immunoprecipitation dataset as well.

Distinction between siRNAs and miRNAs

While miRNAs and siRNAs associate with many of the same cellular proteins for their biogenesis and function, they are thought to differ in their genomic origins. miRNAs tend to arise from non-repetitive regions of the genome encoding short, intramolecular hairpin sequences whereas siRNAs tend to originate from repetitive regions and transposable elements with long hairpin formation capability. Despite this, repetitive regions have been recently reported to give rise to both miRNAs and siRNAs in mouse, and now humans (189,211). This brings up the question: are there differences in the architecture of repetitive elements that encode siRNAs and miRNAs? One observation we made is that the L2 LINEs encoding canonical miRNAs, such as miR-28, are much shorter than typical L2 LINE consensus. Moreover, these short LINEs diverge from the L2 LINE consensus at a high rate, leading to the production of distinct small RNA species that map uniquely to the genome. Thus, we postulate that longer and less divergent transcripts, which have more paralogs, preferentially give rise to siRNAs, while shorter and divergent transcripts often produce miRNAs. This may be one reason that the number of annotated miRNAs greatly exceeds siRNAs; if, by definition, siRNAs originate from less divergent repetitive regions, many legitimate siRNA reads may be discarded during analysis due to promiscuous mapping.

Based on the distinct genomic origins of miRNAs and siRNAs, our findings suggested a small subset of annotated miRNAs should be annotated as siRNAs. One example is the miR-548 family, whose many members are derived from Made1 transposable elements. The characterization of the miR-548 family members as siRNAs would also be consistent with the finding that Tcl1 elements, of which Made1 elements are a human-specific subclass, are known to derive siRNAs in *C. elegans* (212). Interestingly, a model of evolution of miRNAs from tandem repeats in plants has been proposed (213). The model suggests an evolutionary pathway in which inverted repeats spawning siRNAs, under certain constraints, evolve to generate miRNAs. In mammals, it has been proposed that the insertion of transposable elements into new genomic sites could be one of the driving forces that create new miRNAs during mammalian evolution (211). Thus, we may have captured some evolutionarily transient sncRNA species with our NGS-based approach and systematic analysis.

miRNAs and siRNAs also differ in their mechanism of action. miRNAs typically bind imperfectly to target genes and induce translational repression or cause mRNA destabilization while siRNAs bind with near-perfect complementarity and lead to direct cleavage of target transcripts (196,214). We have begun the process of target prediction with computational methods, based on the proposed mechanisms of miRNA and siRNA function. However, it will be important in the future to validate the regulatory effects of the novel noncanonical miRNAs and endo-siRNAs on their targets. Such studies will improve our understanding of sncRNA regulation and also inform classification of sncRNAs as miRNAs or siRNAs.

Implications for psoriasis and other human diseases

For 11/15 differentially expressed noncanonical miRNAs and endo-siRNAs, we observed inversely correlated expression with a subset of their predicted targets that are differentially expressed in psoriasis. In several cases, these predicted targets were also predicted to be regulated by canonical miRNAs that are differentially expressed in psoriasis, as described in Chapter 3, suggesting that multiple sncRNAs may contribute to psoriasis pathogenesis through their interactions with a single target.

While all of these predicted targets have been implicated in psoriasis pathogenesis by their differential expression in PP skin, many are expressed at low levels in human skin, and their fold changes in PP versus NN skin are relatively low. Moreover, these targets have not yet been strongly implicated in psoriasis pathogenesis. Despite this, a few have particular functional relevance. First, the single predicted target for the highly upregulated Alu-SINE-derived siRNA was MDM4. This gene is an inhibitor of p53 that is frequently upregulated in cancers (204,205), but modestly downregulated in psoriasis (19,203). Thus, the down-regulation of MDM4 in psoriasis, which may be mediated by the novel Alu-SINE-derived siRNA we identified, might be one factor that distinguishes the benign hyperplasia in psoriatic involved skin from cancerous tumors. Another intriguing hypothesis about the function of the Alu-SINE siRNA is that it may bind and regulate transcription of genes that contain Alu elements. A second target with particular relevance to psoriasis pathogenesis was SDC4, which was predicted to be targeted by the tailed miRtron #72. SDC4 knockout mice display delayed wound healing and impaired angiogenesis (206). Thus, down-regulation of SDC4, which may be mediated by miRtron #72, might contribute to the chronic regenerative phenotype observed in psoriatic

involved skin. Both MDM4 and SDC4 are also predicted targets of canonical miRNAs that are upregulated in psoriasis.

We have shown that the sncRNAs described here may regulate genes that are differentially expressed in psoriatic lesions. However, some sncRNA species, such as piRNAs and endo-siRNAs, tend to exhibit developmentally-restricted expression patterns. Other sncRNAs described here may also exhibit this property, which would be consistent with their low expression in adult skin. Thus, it is important to consider the possibility that aberrant expression of certain sncRNAs during development may underlie innate skin barrier or immune defects that contribute to disease susceptibility.

Conclusions and future directions

In the future, the functionality of the small RNAs described in this chapter should be confirmed by RISC loading assays, and their predicted targets in psoriatic skin should be validated. Target identification for the Alu-SINE siRNA that is strongly upregulated in involved skin would be of particular interest. Overall, our discovery and analysis of noncanonical miRNAs and endo-siRNAs from a variety of genomic loci have substantially increased our appreciation for the diversity and prevalence of sncRNA expression in adult human tissues, provided insights into their biogenesis, and identified additional sncRNAs that are differentially expressed in psoriasis.

METHODS

Small RNA library preparation, sequencing, and read processing. These methods were described in Chapter 2.

Identification of noncanonical miRNA. Qualified reads that aligned to every locus of human snoRNAs, tRNAs and intro-exon boundaries were subjected to our novel miRNA prediction method, which was tailored for identifying noncanonical miRNAs. Any reads that mapped to previously specified miRNA loci were removed. For each snoRNA and tRNA, 50nt extensions on both sides were added for secondary structure analysis with RNAfold and mFold (131,132). Since the two programs can predict multiple secondary structures, many of which are different, we merged all the predictions from both programs for downstream analysis. Structures lacking stems of at least 18nt and lacking reads that mapped to any of their stems were excluded. To accommodate atypical stem structures that often appear in noncanonical miRNAs, more unpaired based, in some cases up to 9bp, were allowed. Candidate miRNAs were then prioritized based on 1) occurrence of sequencing reads on the stem of a predicted hairpin structure with minimum free energy less than -18kcal/mol; 2) possible presence of miRNA* reads on the opposite stem of the hairpin; 3) presence of ~2nt 3' overhangs on the highest likelihood miRNA/miRNA* duplex; and 4) reads length distribution peaks around ~22nt. To identify miRtrons, 160nt intronic sequence segments adjacent to exon/intron boundaries were extracted for introns analyzed. The same procedure as described above, without a sliding window, was then followed to identify miRtrons. In addition, we examined the presence of sequencing reads ending with AG dinucleotides as a

characteristic feature of miRtron. We also applied RNALfold (131) and manual analyses to find local secondary structures.

Identification of endogenous siRNAs from multiple genomic origins. We applied EINVERTED (215) on each 10kb segment of DNA sequences of whole human genome (hg 19 build) to search for inverted repeats and long hairpin structures they can fold into. We chose inverted repeats by setting a minimum score threshold of 70. Next, we filtered out those predicted inverted repeats that have no more than 10 mappable reads. We also analyzed the genomic annotation of the predicted inverted repeats, i.e. checking them if overlap with SINEs, LINEs or pseudogenes. We next blasted these mappable reads to the annotated human noncoding RNAs to rule out the possibility that such sequencing reads were byproducts of other types of noncoding RNAs. Finally, we examined genomic regions in which the mappable reads have lengths of dominantly 21~23nt, expected for the length of siRNAs. The amount of the normalized reads having unique genomic loci represented the expression levels of such inverted repeats in each skin category.

Conservation analysis of sncRNAs. We retrieved from the UCSC genome browser (216) the multiple alignments of nine species – *Homo sapiens* (human), *Macaca mulatta* (rhesus), *Mus musculus* (mouse), *Canis lupus familiaris* (dog), *Loxodonta Africana* (elephant), *Monodelphis domestica* (opossum), *Gallus gallus* (chicken), *Xenopus tropicalis* (frog) and *Danio rerio* (zebrafish) – for each novel miRNA and siRNA. We calculated the number of insertions, deletions and mismatches when each non-human sequence was compared with a human sncRNA based on the multiple alignments of the nine species. An sncRNA was considered conserved in one species if

the sequence in that species had no variation (insertions, deletions and mismatches) in the seed region for a miRNA or less than 2 variations in the whole region for a siRNA.

qRT-PCR. qRT-PCR of sncRNAs was performed with custom TaqMan small RNA assays (Life Technologies), as described in Chapter 2.

Cell culture. The cloning of sncRNAs into pEP-miR cloning and expression vectors (Cell Bio Labs) and transfections of HEK293 cells were performed as described in Chapter 2.

RIP-PCR. RIP-PCR was performed as described in Chapter 2 for Ago2. The same protocol was applied with a rabbit polyclonal antibody for Ago3 (Sigma-Aldrich). Significance was determined by one-way ANOVA and post-hoc two tailed t-tests.

Digital gene expression analysis. Digital gene expression analysis was performed as described in Chapter 2, except that no detection filter was applied, to allow for analysis of low abundance sncRNA species.

Putative targets of miRNAs and siRNAs. miRNA target genes were predicted by TargetScan (72,79) and starBase (202). We used the common target genes predicted by both programs. For predicting targets of siRNAs, human cDNA sequences were downloaded from UCSC genome browser (hg19 build) and the reverse complementary sequences of siRNAs were mapped to the cDNA sequences by BLAST (217). Hits with fewer than four mismatches were considered as putative targets of siRNAs.

mRNA gene expression analysis. Microarray data of mRNA genes of psoriatic and normal skin of human were downloaded from Gene Expression Omnibus (GEO) accession number GSE13355, which has a total of 122 samples containing 58 psoriatic

patients and 64 normal healthy controls. Differentially expressed genes were identified using Rank Product (218). We selected differentially expressed genes with a false discovery rate less than 0.05 for 1,000 permutations. Differentially expressed probe sets were aligned to corresponding genes according to the annotation of Affymetrix Human Genome U133 Plus 2.0 Array.

Table 5-1. Distribution of read alignments from normal, uninvolved psoriatic, and involved psoriatic skin.

	PP[a]		PN[a]		NN[a]	
	No. reads	**% reads**	**No. reads**	**% reads**	**No. reads**	**% reads**
Raw reads	412146550	NA	354772543	NA	314739262	100
Qualified reads	253203829	NA	212569115	NA	204087993	64.84
Known miRNAs	***123039749***	***48.59***	***87533132***	***41.18***	***94485131***	***46.3***
snoRNA	24780802	9.79	20345744	9.57	13687765	6.71
tRNA	6115824	2.42	3817151	1.8	3224792	1.58
rRNA	25372596	10.02	28449501	13.38	26312614	12.89
piRNA	5752317	2.27	4612138	2.17	4246907	2.08
other noncoding RNA (ncRNA)	6384477	2.52	7449126	3.5	7106395	3.48
ncRNA	***68406016***	***27.02***	***64673660***	***30.42***	***54578473***	***26.74***
SINE	4193072	1.66	4064101	1.91	4149100	2.03
LINE	3209985	1.27	2897377	1.36	2111062	1.03
LTR	985275	0.39	960934	0.45	733427	0.36
DNA transposon	263933	0.1	230930	0.11	205000	0.1
other repeats	1053451	0.42	1260037	0.59	826392	0.4
repeats	***9705716***	***3.84***	***9413379***	***4.42***	***8024981***	***3.92***
coding sequence (CDS)	540345	0.21	457173	0.22	391898	0.19
3'-Untranslated region (UTR)	391939	0.15	316873	0.15	276497	0.14
5'-UTR	300053	0.12	271589	0.13	233413	0.11
Intron	9204482	3.64	11082321	5.21	6492959	3.18
Intergenic	1241809	0.49	1057531	0.5	769015	0.38
genomic	***11138283***	***4.61***	***13185487***	***6.21***	***8163782***	***4***
Known miRNAs- up to 2 mismatch	34059885	13.45	29948970	14.09	32499128	15.92
Unaligned qualified reads	6313835	2.49	7814487	3.68	6336498	3.1
total	253203829	100	212569115	100	204087993	100

[a]Normal skin, NN; Uninvolved psoriatic skin, PN; Involved psoriatic skin, PP.

Table 5-2. Summary of noncanonical miRNAs derived from noncoding RNAs.

Previously described non-canonical miRNAs derived from larger ncRNA species

Type	Position	miRNA seq on 5' arm	No. reads	miRNA seq on 3' arm	No. reads	Annotation
snoRNA	1: 220373880-220373961 [-]	ACTGGCTAGGGAAAATGATTGG	4894	TATTCATTTATCCCCAGCCTACA	17584	ACA36B/ hsa-miR-664
scaRNA	15:83424639-83424888 [+]	AAGGTAGATAGAACAGGTCTTG	60082	AGACCTACTTATCTACCAACAG	2381	ACA45/ hsa-mir-1839
scaRNA	17:75085389-75085575 [+]	ATTTGCAGTAACAGGTGTGAGC	38	ATCATGTATGATACTGCAAACAG	121	ACA47
scaRNA	9:19063654-19063784 [-]	ACTGCCTTTTGATGACCGGGACG	62	TAACGGACAGATACGGGGCAGACA	119	U92
snoRNA	1:175937533-175937676 [-]	ATATGGAGGTCTCTGTCTGGC	1019	TCTGATCGTTCCCCTCCGTACA	21	HBI-100
snoRNA	X:154003273-154003401 [+]	AGTGGTGAGTTCTTCTGTCCAGC	29	TGGTGGCTTTAGACTTGCCAGA	17	ACA56
snoRNA	11:8705774-8705903 [+]	ATCGAGGCTAGAGTCACGCTTGG	279	AGTGTGCTAGAGTCCTCGAAG	5	ACA3
snoRNA	16:58593700-58593835 [-]	AAGCACTGCCTTTGAACCTGATG	194	ACGGGCCAAGCAACAGTGCTAGA	30	ACA50
tRNA	6:27599180-27599313 [+]	AAAGCATGCTCCAGTGGCGC	1	CTCACCTGGAGCATGTTTTCT	176	IleTAT/ hsa-miR-1983

Novel described non-canonical miRNAs derived from larger ncRNA species

Type	Position	miRNA seq on 5' arm	No. reads	miRNA seq on 3' arm	No. reads	Annotation
snoRNA	16:2205023-2205114 [-]	AGTCTGTGATGAATTGCTTTGA	23742894	TGATTATTTAGCAAGACTGAGG	422	U60
snoRNA	11:93463679-93463812 [-]	GTTCTCTATAGGAAGCCATAGC	1933	TATGTTTTCCTGAGGAGATATA	26	ACA25
snoRNA	1:28906276-28906405 [-]	TGTGGGCTAGTTTCAGACAGGT	3409	TAATAGTGAAGCTGGCCTAAATG	6	ACA61
tRNA	4:7325848-7325923 [-]	--		TTAGAGCCAGACTGCCTGGGT	8	pseudoTTA

Table 5-3. Summary of miRtrons expressed in human skin.

ID	Chr	Start	End	Strand	No. reads	Type	Host gene	Intron length	% terminating	AGO[a]
#8	chr1	161196984	161197047	+	875	tailed miRtron	TOMM40L	303	100	1,3,4
#14*	chr1	37945827	37945890	+	36	tailed miRtron	ZC3H12A	4351	83	
#20	chr12	48526580	48526650	+	341	tailed miRtron	PFKM	1475	94	1,4
#43	chr19	58846055	58846124	+	255	tailed miRtron	ZSCAN22	7638	100	
#64	chr1	201972254	201972364	+	42	tailed miRtron	RNPEP	1470	94	1,3
#67	chr12	48131469	48131537	-	42	tailed miRtron	RAPGEF3	337	65	1,3,4
#72	chr2	219144850	219144913	-	872	tailed miRtron	TMBIM1	1814	100	
#74*	chr11	62334483	62334540	-	32	tailed miRtron	EEF1G	389	91	
#75*	chr10	102798336	102798399	+	37	tailed miRtron	SFXN3	1212	85	
#77*	chr2	61008950	61009019	+	16	tailed miRtron	PAPOLG	1106	100	
#80	chr17	39673418	39673471	-	4729	tailed miRtron	KRT15	1165	99	
#91*	chr16	28735574	28735642	+	36	tailed miRtron	EIF3C	771	100	
#103	chr5	150901648	150901715	-	2606	tailed miRtron	FAT2	3682	100	
#114	chr11	62560174	62560243	-	440	tailed miRtron	NXF1	1557	100	3,4
#118	chr1	43830304	43830394	-	243	tailed miRtron	ELOVL1	91	87	
#119	chr15	75132983	75133046	-	317	tailed miRtron	ULK3	764	100	
#129	chr10	103870890	103870973	-	27	tailed miRtron	LDB1	112	100	1
#130	chr10	104139213	104139277	+	15	tailed miRtron	GBF1	87	92	
#141	chr1	1231489	1231547	-	47	tailed miRtron	ACAP3	102	100	1
#142	chr11	1857595	1857654	+	52	tailed miRtron	SYT8	141	100	
#144*	chr7	123329205	123329266	-	180	tailed miRtron	WASL	3197	100	
#145	chr17	40666218	40666306	+	388	tailed miRtron	ATP6V0A1	311	91	1,3,4
#150*	chr19	13063440	13063502	+	47	tailed miRtron	RAD23A	3281	97	3
#152	chr11	85989377	85989440	+	170	tailed miRtron	EED	408	100	3
#158	chr12	121442296	121442365	-	82	tailed miRtron	C12orf43	514	66	
#159	chr22	38363570	38363631	+	141	tailed miRtron	POLR2F	455	99	3
#168	chr1	25245836	25245902	-	72	tailed miRtron	RUNX3	8230	100	
#174	chr13	42142435	42142518	-	18	tailed miRtron	KIAA0564	2163	93	
#175*	chr22	30737875	30737948	-	31	tailed miRtron	SF3A1	315	80	3
#179	chr1	43914209	43914289	+	105	tailed miRtron	SZT2	128	77	1,3,4
#186	chr3	52557358	52557442	+	114	tailed miRtron	STAB1	86	96	
#203	chr17	74094090	74094160	-	64	tailed miRtron	EXOC7	3253	98	
#204	chr17	8048311	8048384	-	38	tailed miRtron	PER1	965	97	
#206	chr18	10759582	10759642	-	63	tailed miRtron	PIEZO2	122	97	
#210	chr19	3201454	3201531	+	26	tailed miRtron	NCLN	2626	100	
#211	chr7	143079629	143079685	+	40	tailed miRtron	ZYX	146	100	3
#212	chr19	35613605	35613671	+	101	tailed miRtron	FXYD3	1520	100	
#214	chr19	40486136	40486193	+	15	tailed miRtron	PSMC4	140	0**	
#215	chr19	41175925	41175995	-	17	tailed miRtron	NUMBL	3324	94	3
#217	chr19	48981457	48981542	+	23	tailed miRtron	CYTH2	130	95	
#218*	chr19	11333582	11333668	-	43	miRtron	DOCK6	88	100	3
#219	chr19	49513167	49513229	+	16	tailed miRtron	RUVBL2	91	100	
#220	chr19	55751279	55751340	-	173	tailed miRtron	PPP6R1	88	92	3
#221*	chr17	73775045	73775127	-	20	miRtron	H3F3B	84	100	1,3
#222	chr19	6389649	6389712	-	61	tailed miRtron	GTF2F1	2265	100	1,3
#228	chr20	60913663	60913725	-	21	tailed miRtron	LAMA5	7210	94	
#231	chr21	46898180	46898240	+	101	tailed miRtron	COL18A1	362	100	
#232	chr2	160043351	160043412	+	21	tailed miRtron	TANC1	1003	100	
#237	chr2	219206639	219206704	+	34	tailed miRtron	PNKD	355	100	
#239	chr22	30403042	30403102	+	76	tailed miRtron	MTMR3	4121	57	
#240	chr2	232658900	232658972	+	28	tailed miRtron	COPS7B	2455	100	
#246	chr2	69053052	69053118	+	27	tailed miRtron	ARHGAP25	3115	96	
#247*	chr11	118514732	118514789	+	298	tailed miRtron	PHLDB1	132	82	
#252*	chr6	32137816	32137887	-	170	tailed miRtron	AGPAT1	127	0**	3
#253	chr3	148601339	148601399	+	28	tailed miRtron	CPA3	1018	100	
#256	chr3	49843594	49843663	-	33	tailed miRtron	UBA7	1571	93	
#257	chr3	52437314	52437388	-	30	tailed miRtron	BAP1	118	100	
#258	chr6	32147595	32147653	+	41	tailed miRtron	RNF5P1	114	100	
#260	chr4	55956244	55956299	-	29	tailed miRtron	KDR	2539	100	
#271*	chr19	55756554	55756632	-	77	tailed miRtron	PPP6R1	80	97	3
#275	chr6	6152180	6152243	-	27	tailed miRtron	F13A1	15509	100	
#277	chr7	2297150	2297207	-	25	tailed miRtron	SNX8	221	100	
#279	chr7	44091368	44091428	+	52	tailed miRtron	DBNL	1550	75	
#281	chr7	64139446	64139555	+	319	tailed miRtron	ZNF107	9999	100	
#284*	chr19	55899552	55899610	+	29	tailed miRtron	RPL28	195	100	3
#285*	chr9	34709425	34709496	-	11	miRtron	CCL21	73	100	
#286	chr8	125579420	125579474	-	80	tailed miRtron	MTSS1	1201	100	
#304	chr9	33467863	33467931	-	47	tailed miRtron	NOL6	162	100	
#306	chr9	35732924	35732993	+	38	tailed miRtron	CREB3	95	100	
#309	chrX	153209603	153209674	-	22	tailed miRtron	RENBP	154	95	
#314	chr17	4872997	4873061	-	21	tailed miRtron	CAMTA2	201	0**	3
#318	chr8	62460768	62460813	-	26	tailed miRtron	ASPH	4823	0**	
#321	chr11	122928628	122928693	-	86	tailed miRtron	HSPA8	333	91	
#328	chr1	149937804	149937875	-	62	tailed miRtron	OTUD7B	1416	50	
#335	chr12	88193	88256	+	154	tailed miRtron	LOC1002887	240	87	1,3
#338	chr16	16418445	16418511	+	960	tailed miRtron	PKD1P1	128	96	1,3,4
#341	chr17	38318189	38318256	+	109	tailed miRtron	CASC3	91	100	
#344	chr17	40860101	40860165	-	72	tailed miRtron	EZH1	793	80	
#350*	chr3	127294109	127294173	-	30	tailed miRtron	TPRA1	138	0**	3
#354*	chr22	38165195	38165268	+	16	miRtron	TRIOBP	75	100	1,3,4
#359	chr6	42071617	42071692	-	72	tailed miRtron	C6orf132	585	100	3
#363	chr9	132631885	132631950	+	71	tailed miRtron	USP20	247	97	1,3,4
#371*	chr17	43011986	43012047	-	105	tailed miRtron	KIF18B	214	100	1,3,4
#375	chr19	13051296	13051354	+	328	tailed miRtron	CALR	89	100	1,3
#378	chr8	125520755	125520843	-	18	miRtron	TATDN1	89	100	2,4

[a]AGO immunoprecipitate data sets in which the mature miRtron sequence was present (Hafner et al., 2010).
* Low abundance or atypically folded miRtrons discovered by re-analysis
** No miRNA* reads terminating at splice sites were sequenced.

Table 5-4. Summary of MADE1 elements associated with small RNA reads.

ID	Chr	Start	End	Strand	Annotation	No. reads	AGO[a]
Made1_#1	chr1	82174864	82174941	-	DNA transposon	2025	
Made1_#2	chr1	183752471	183752547	-	DNA transposon	11	
Made1_#3	chr1	235107531	235107603	-	DNA transposon	11	
Made1_#4	chr10	24007027	24007109	-	DNA transposon	5	1
Made1_#5	chr10	68389161	68389229	-	DNA transposon	15	
Made1_#6	chr10	125670996	125671075	+	DNA transposon	19	3
Made1_#7	chr11	20033822	20033901	+	DNA transposon	15	
Made1_#8	chr12	72267908	72267986	+	DNA transposon	340	
Made1_#9	chr14	96672883	96672962	-	DNA transposon	24	
Made1_#10	chr14	102828042	102828118	+	DNA transposon	67	1
Made1_#11	chr15	94624333	94624411	-	DNA transposon	19	
Made1_#12	chr16	47708265	47708339	-	DNA transposon	26	
Made1_#13	chr16	79750312	79750392	+	DNA transposon	49	
Made1_#14	chr17	40646790	40646858	-	DNA transposon	29	3
Made1_#15	chr17	66383129	66383208	+	DNA transposon	14	
Made1_#16	chr2	49286730	49286810	-	DNA transposon	422	
Made1_#17	chr2	54806171	54806249	-	DNA transposon	20	
Made1_#18	chr2	72878633	72878708	-	DNA transposon	9	3
Made1_#19	chr2	96656055	96656137	+	DNA transposon	12	
Made1_#20	chr2	137402682	137402759	-	DNA transposon	25	
Made1_#21	chr21	36253203	36253279	+	DNA transposon	14	
Made1_#22	chr4	175636930	175637008	-	DNA transposon	22	
Made1_#23	chr5	31470534	31470597	-	DNA transposon	23	
Made1_#24	chr5	55858293	55858360	-	DNA transposon	24	
Made1_#25	chr5	150485436	150485514	+	DNA transposon	14	
Made1_#26	chr6	38630466	38630545	-	DNA transposon	10	2,3
Made1_#27	chr6	108097497	108097575	-	DNA transposon	40	
Made1_#28	chr6	119499447	119499519	+	DNA transposon	19	
Made1_#29	chr8	27082383	27082437	+	DNA transposon	13	
Made1_#30	chr8	41128575	41128654	+	DNA transposon	20	
Made1_#31	chr9	96357111	96357181	+	DNA transposon	30	
Made1_#32	chr2	60343031	60343108	+	DNA transposon	10	
Made1_#33	chr8	68965595	68965658	-	DNA transposon	8	
Made1_#47	chr9	135821094	135821159	-	DNA transposon	2198	

[a]AGO immunoprecipitate data sets in which the mature miRtron sequence was present (Hafner et al., 2010).

Table 5-5. ± 1.5 fold differentially expressed noncanonical miRNAs and endo-siRNAs.

ID	Normalized read count			Fold change			p-value
	NN[b]	PN[b]	PP[b]	PP/NN	PP/PN	PN/NN	
Alu-SINE-siRNA	91.81	220.54	1614.78	17.59	7.32	2.4	0.00E+00
miRtron #14	1	2.05	11.58	11.58	5.65	2.05	9.41E-04
hsa-mir-937	3.19	2.05	20.4	6.4	9.95	-1.56	4.25E-06
miRtron #323	17.41	11.5	32.75	1.88	2.85	-1.67	2.88E-03
tRNAIle-miRNA	23.98	25.16	117.4	4.9	4.67	1.05	3.33E-23
Made1_#1	293.12	354.99	1182.67	4.03	3.33	1.21	2.72E-176
miRtron #144	22.88	25.16	79.48	3.47	3.16	1.1	3.24E-11
miRtron #375	31.63	34.61	87.42	2.76	2.53	1.09	4.46E-09
U60 miRNA-5p	4671189.97	7638575.63	10759792.7	2.3	1.41	1.64	0.00E+00
miRtron #72	74.3	82.93	143.86	1.94	1.73	1.12	6.03E-07
miRtron #145-5p	42.57	64.03	10.7	-4	-5.88	1.5	1.01E-08
miRtron #252	34.92	20.96	10.7	-3.23	-1.96	-1.67	1.28E-03
miRtron #80	2179.3	1483.14	739.11	-2.94	-2	-1.47	2.84E-154
miRtron #145-3p	28.35	33.56	11.58	-2.43	-2.86	1.18	4.59E-03
Made1_#47	340.16	435.87	225.87	-1.52	-1.92	1.28	4.22E-15

[a]+/- 1.5 fold change and Bonferroni adjusted $p<0.05$ in at least one comparison (PP/NN, PP/PN, PN/NN).

[b]Normal skin, NN; Uninvolved psoriatic skin, PN; Involved psoriatic skin, PP.

Table 5-6. Differentially expressed transcripts that are putative targets of differentially expressed sncRNAs.

				Canonical miRNAs predicted to target transcript			
ID	sncRNA FC	Target symbol	Target FC[a]	Targetscan	FC miRNA	Starbase	FC miRNA
Alu-SINE-siRNA	17.59	MDM4	-1.54	miR-19	1.89	miR-7	3.05
miR-#14	11.58	ZNF207	-1.85	-		miR-21	3.95
miR-937	6.4	TSHZ1	-1.55	-		-	
mir#323	1.88	NFIB	-1.83	miR-19	1.89	miR-19b	2.1
tRNAIle-miRNA	4.9	BACH2	-1.93	miR-142-3p	2.52	-	
tRNAIle-miRNA	4.9	MBNL1	-1.91	miR-21	3.95	-	
made_#1	4.03	NRXN1	-1.75	-		-	
made_#1	4.03	ALG10B	-1.56	-		-	
made_#1	4.03	KATNAL1	-1.89	miR-19	1.89	miR-19b	2.1
mir#144	3.47	LZTFL1	-1.71	-		-	
u60	2.3	RGMB	-2.85	miR-449	2.3	-	
mirtron#72	1.94	MLL2	-1.56	miR-211	2.6	miR-146a	2.36
mirtron#72	1.94	SDC4	-1.86	miR-142-3p	2.52	miR-31	42.93
mirtron#72	1.94	TM9SF3	-1.75	miR-33b	2.23	-	
mirtron_252	-3.23	SSR1	1.54	-		-	
mirtron_#80	-2.94	AEN	1.66	-		-	

[a]Fold changes obtained from Gudjonsson *et al.*, 2010

A. microRNAs

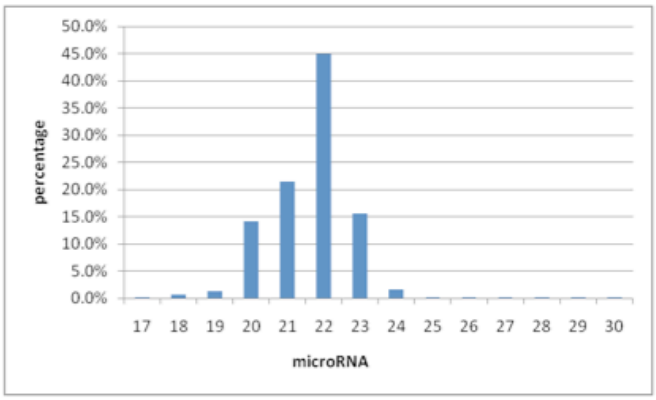

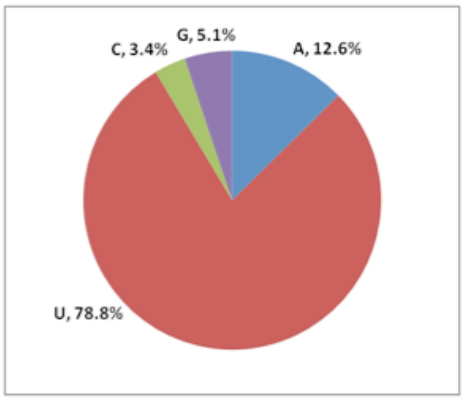

B. endo-siRNAs

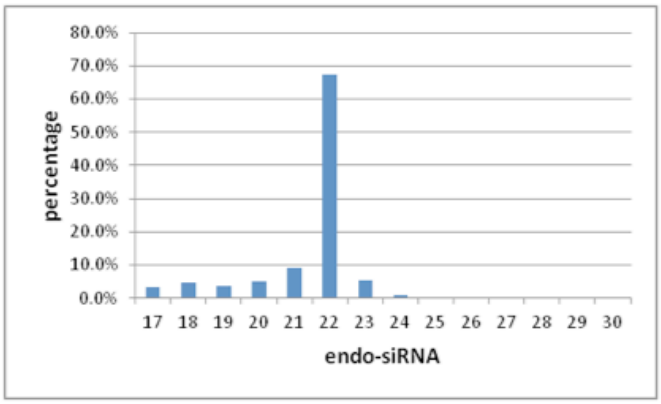

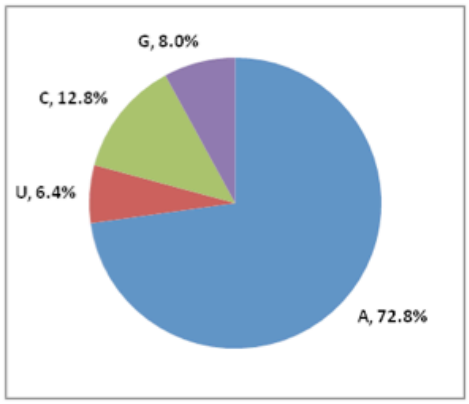

C. snoRNAs

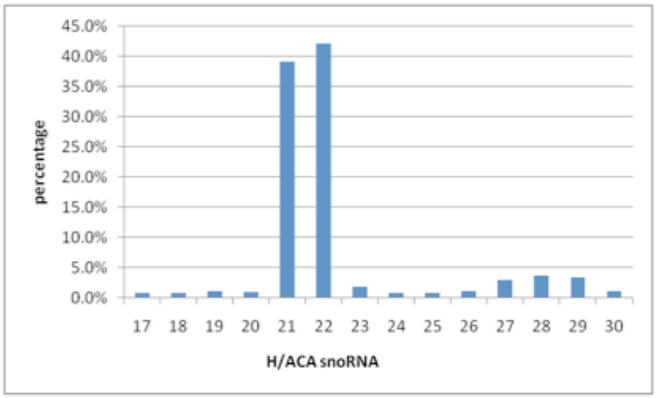

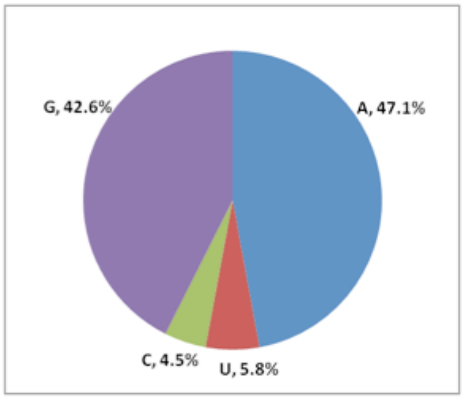

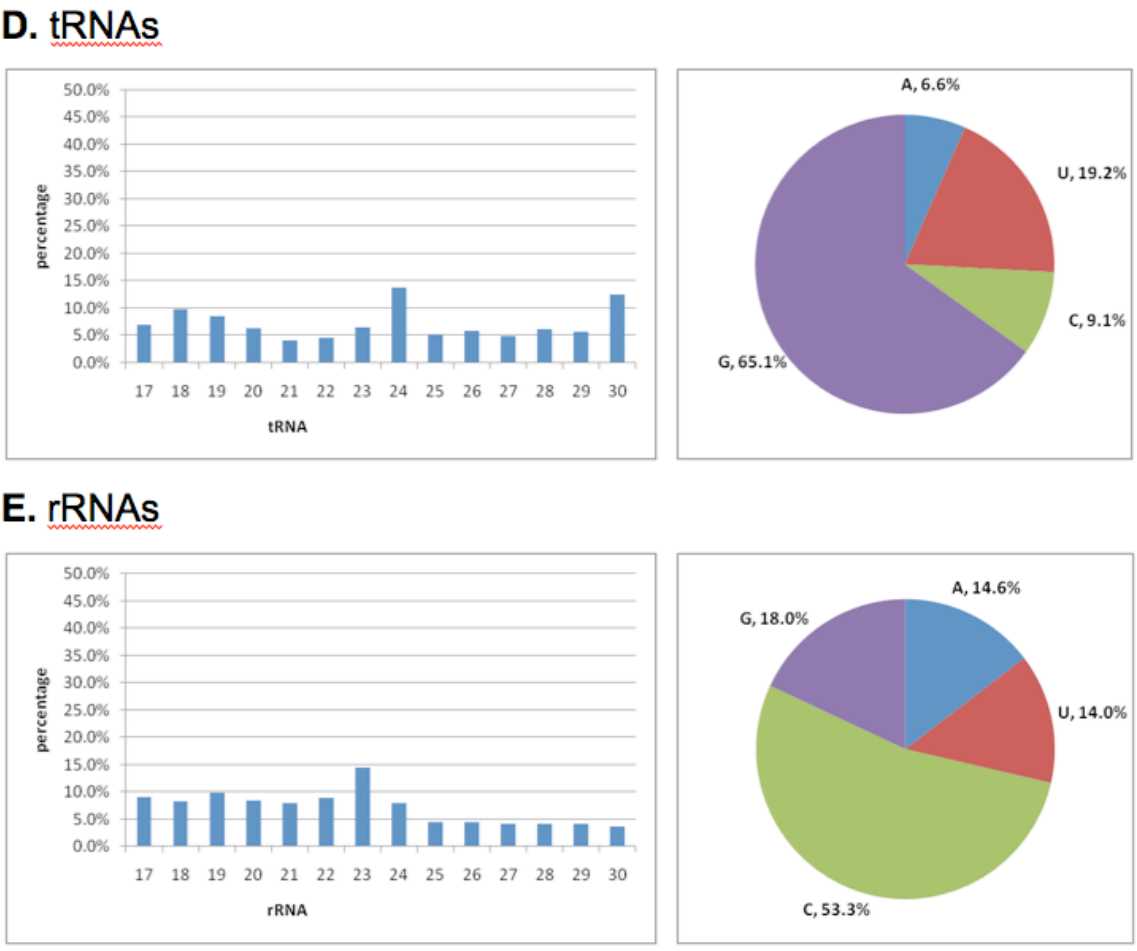

Figure 5-1. Length distribution and 5' nucleotide identity for all qualified reads aligned to (A) annotated miRNAs (miRbase version 17), (B) endo-siRNA loci identified in current study, (C) snoRNAs, (D) tRNAs and (E) rRNAs (Ensembl noncoding RNA version 61).

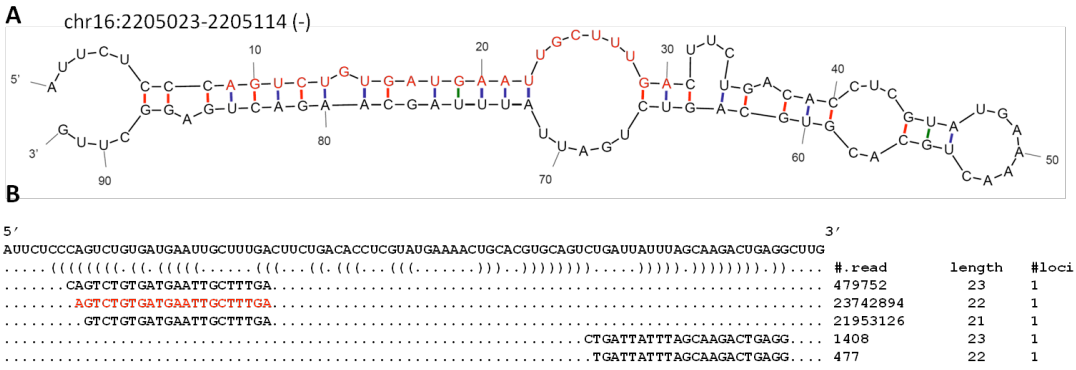

Figure 5-2. A miRNA derived from C/D box snoRNA U60. (A) The stem-loop hairpin structure of U60, with bases of the putative miRNA colored in red. (B) Read alignments with the number of sequencing reads, length of read and the number of genomic loci to which the read can be mapped with no mismatches.

A

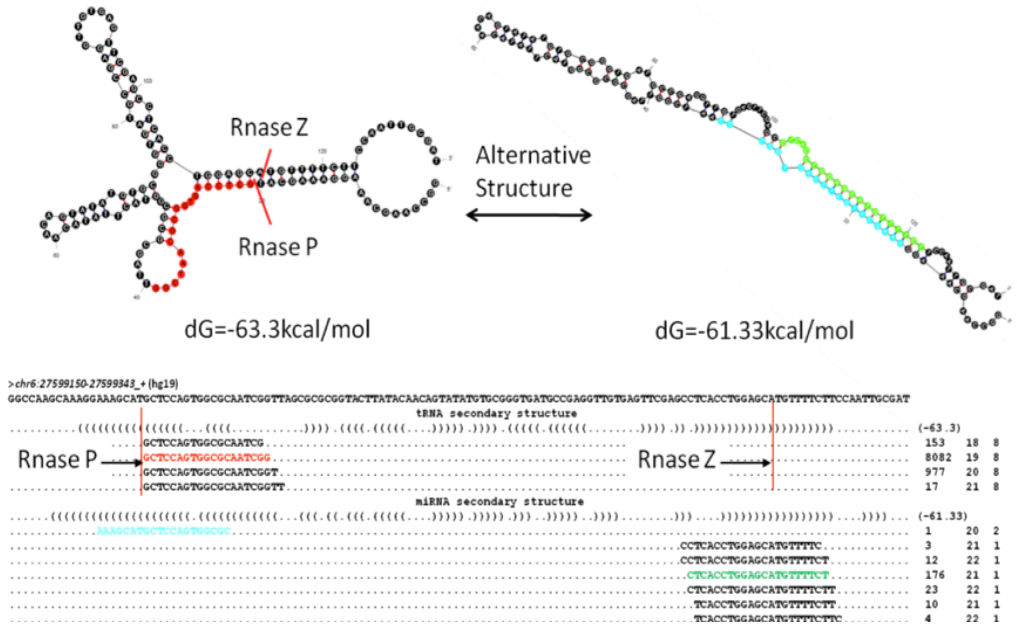
Rnase Z
Rnase P
Alternative
Structure
dG=-63.3kcal/mol
dG=-61.33kcal/mol
tRNA secondary structure
Rnase P
Rnase Z
miRNA secondary structure

B

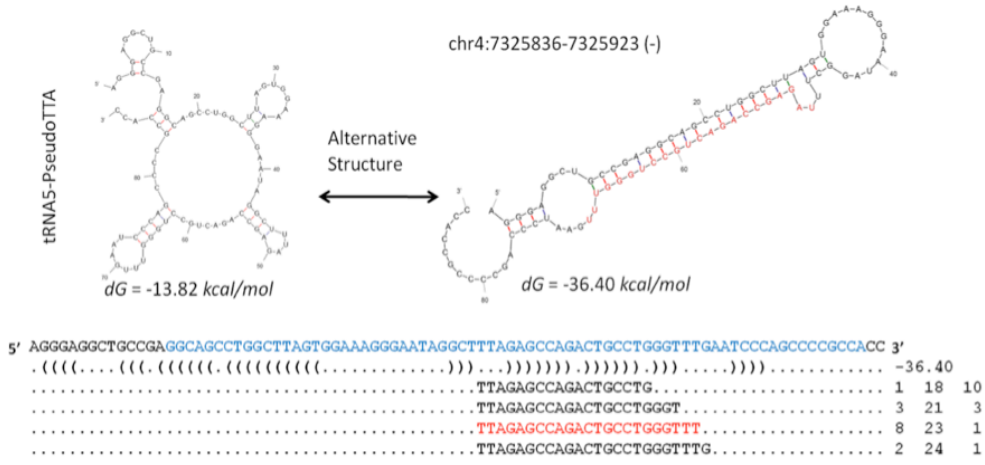
tRNA5-PseudoTTA
chr4:7325836-7325923 (-)
Alternative
Structure
dG = -13.82 kcal/mol
dG = -36.40 kcal/mol

Figure 5-3. Noncanonical miRNAs derived from tRNAs. (A) miRNA derived from tRNA candidate pseudoTTA. Top panel, tRNA folding structure with a presumed tRNA fragment highlighted in red, and the alternative miRNA hairpin structure with the miRNA and miRNA* highlighted in green and blue respectively. Bottom panel, read alignments, with the number of reads, length of read, and the number of genomic loci to which the read can be mapped with no mismatches. The red vertical lines represent the 5' and 3' ends of the tRNA. (B) miRNA derived from pseudo-TTA. Top panel, tRNA and predicted pre-miRNA hairpin structures. The putative mature miRNA sequence is indicated in red. Bottom panel, read alignments with the number of reads, length of read, and the number of genomic loci to which the read can be mapped with no mismatches. The pseudoTTA tRNA sequence is highlighted in blue.

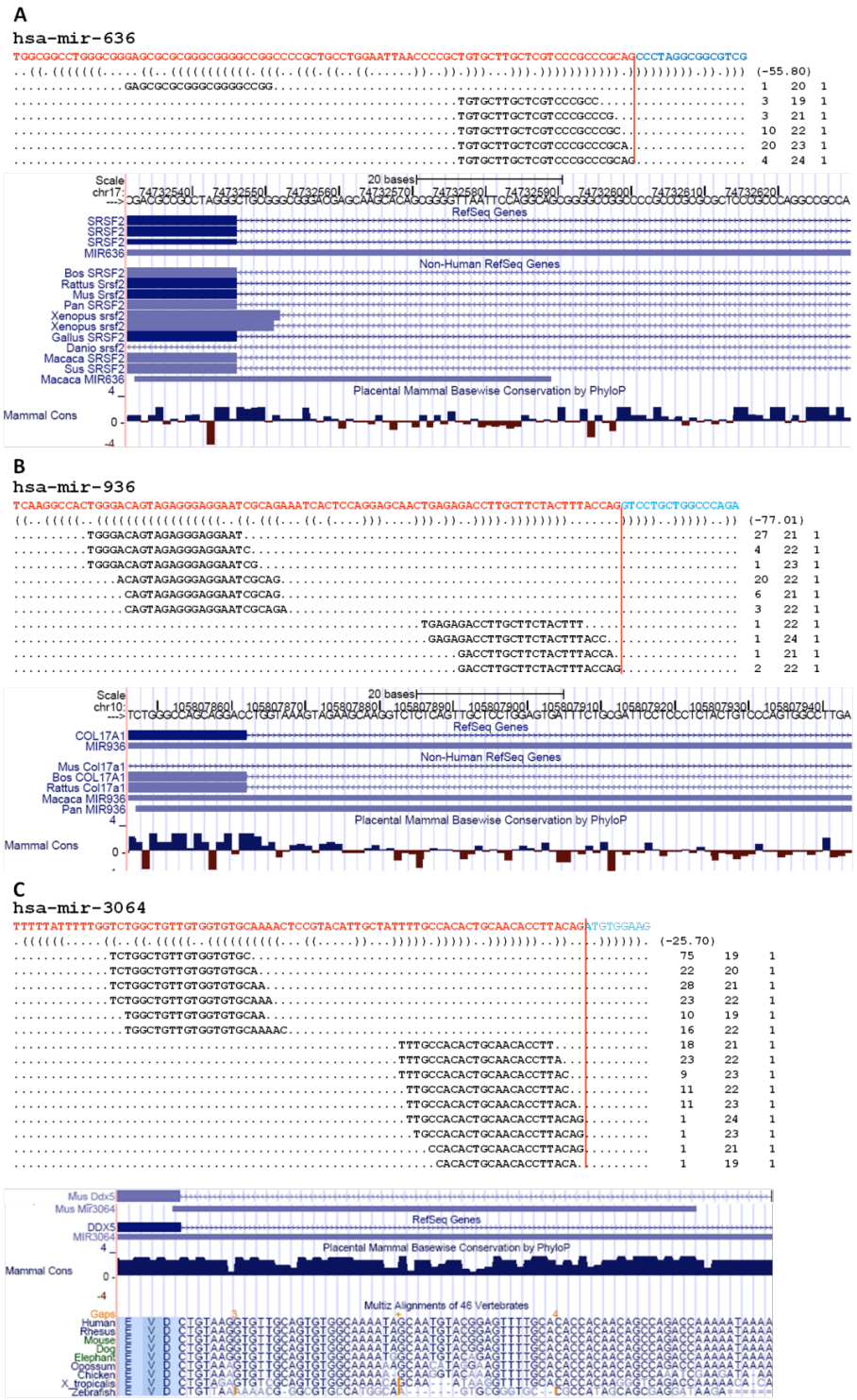

Figure 5-4. **Examples of newly annotated miRtrons**. (A) hsa-miR-636, (B) hsa-miR-936 and (C) hsa-miR-3064. The red vertical lines indicate exon/intron boundaries. Red bases represent intron sequences; blue bases represent exon sequences.

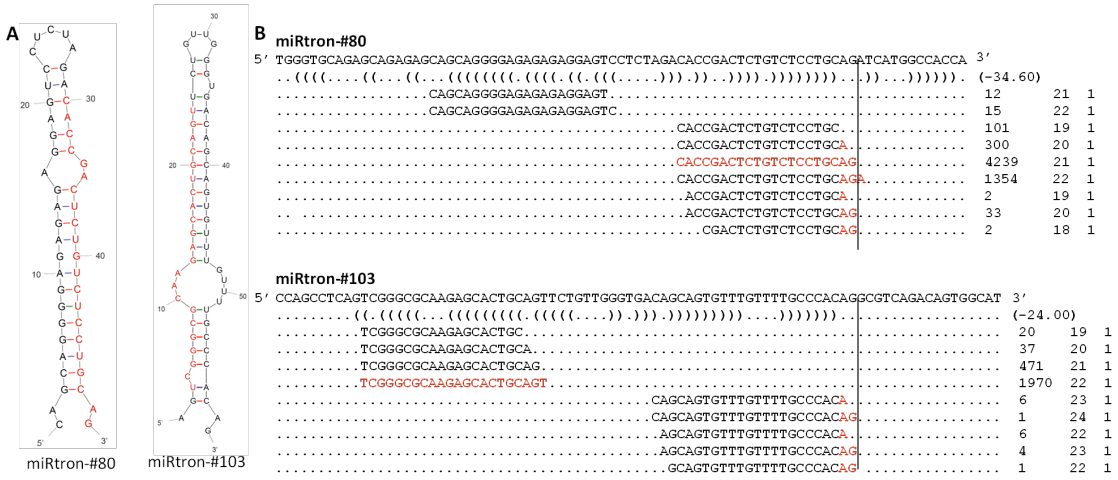

Figure 5-5. Features of novel tailed miRtrons, #80 and #103. (A) The hairpin structures with the putative mature miRNAs indicated in red. (B) Read alignments with the number of reads, length of read and the number of genomic loci to which the read can be mapped. The vertical lines indicate the intron/exon boundaries. Reads terminating within 1nt of intron 3' acceptor splice sites end with bases in red.

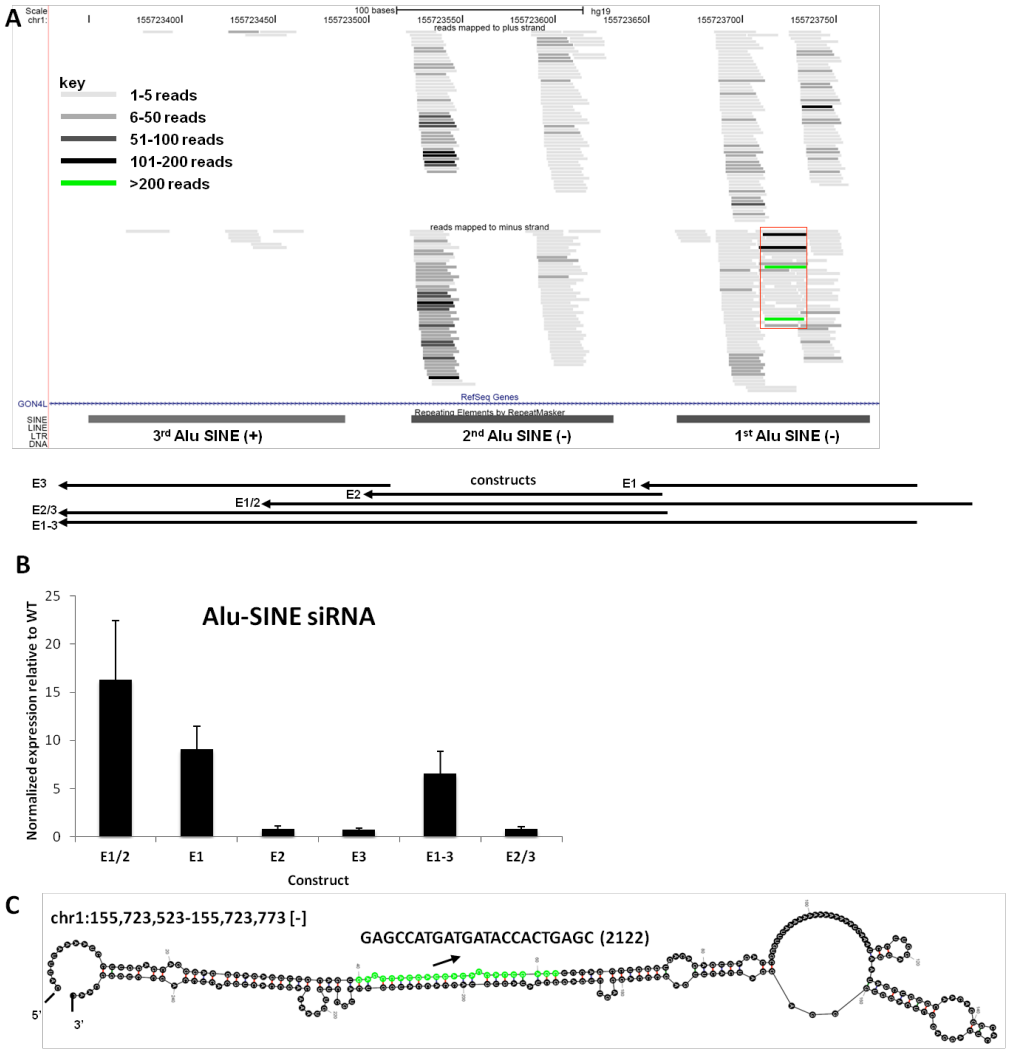

Figure 5-6. endo-siRNA derived from tandem Alu SINE transposable elements in an intron of the gon-4-like (GON4L) gene on chromosome 1. (A) Alignment of sequencing reads to the human genome (hg19). The three Alu SINEs are represented as thick grey lines with "+" or "-" indicating the plus or negative orientation. The red box indicates the reads uniquely mapped to this locus. (B) Abundance of siRNAs in six constructs that include six combinations of the three Alu SINEs. The y-axis indicates the normalized expression relative to the wide-type. (C) Predicted folding structure of the first two Alu SINEs. The most abundant RNA species is highlighted in green.

A

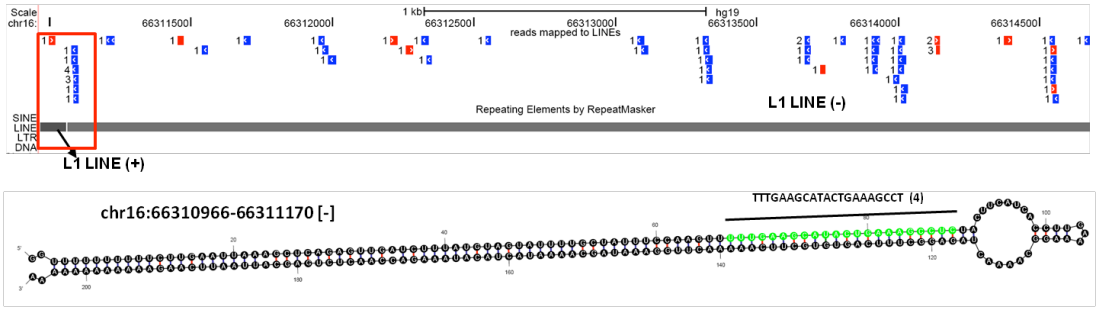

B

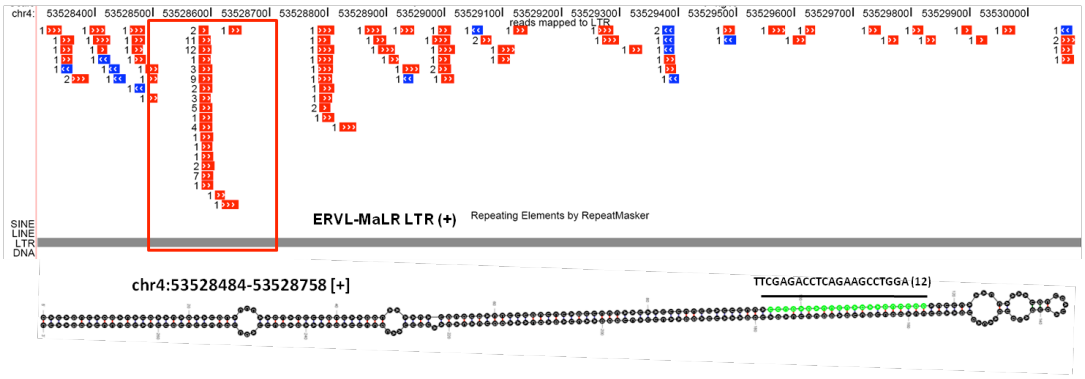

Figure 5-7. **Examples of endo-siRNAs derived from repetitive elements.** Small RNA reads aligned to (A) an L1 LINE (B) an LTR. The repeats are represented as thick grey lines. Filled red and blue rectangles indicate reads aligning to the + and – strands, respectively. Open red rectangles represent the dominant read clusters from each locus. The most abundant read from these clusters are highlighted in green along the hairpin structures.

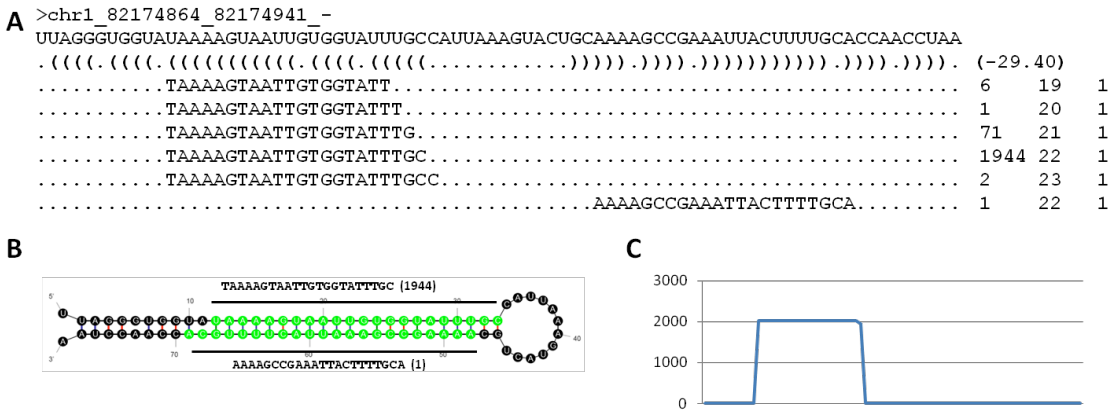

Figure 5-8. Example of endo-siRNAs derived from a MADE1 element. (A) Read alignments for a representative MADE1 locus on chromosome 1. (B) Predicted folding structure of the locus with a RNA/RNA duplex marked in green. (C) Distribution of reads within the locus.

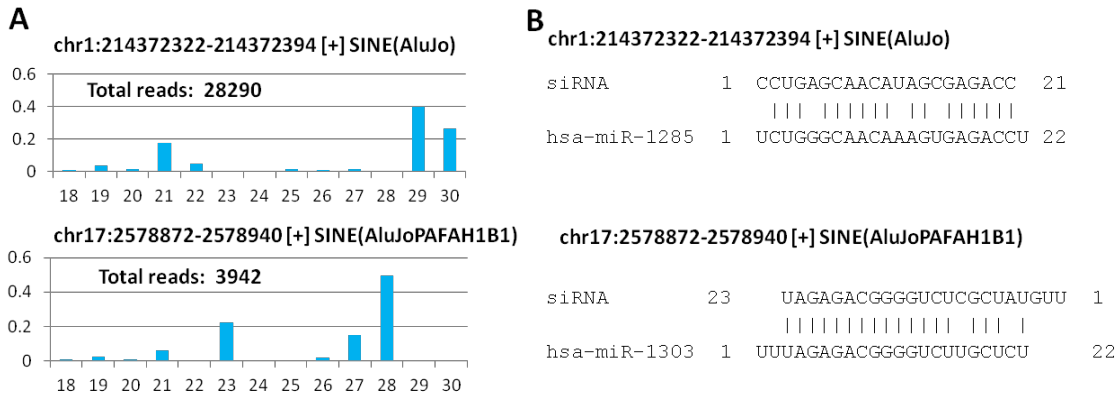

Figure 5-9. endo-siRNAs derived from two piRNA annotated loci. (A) Bimodal length distributions of reads mapped to the two piRNA loci. (B) Putative endo-siRNA sequences aligned to their respective paralagous known miRNAs.

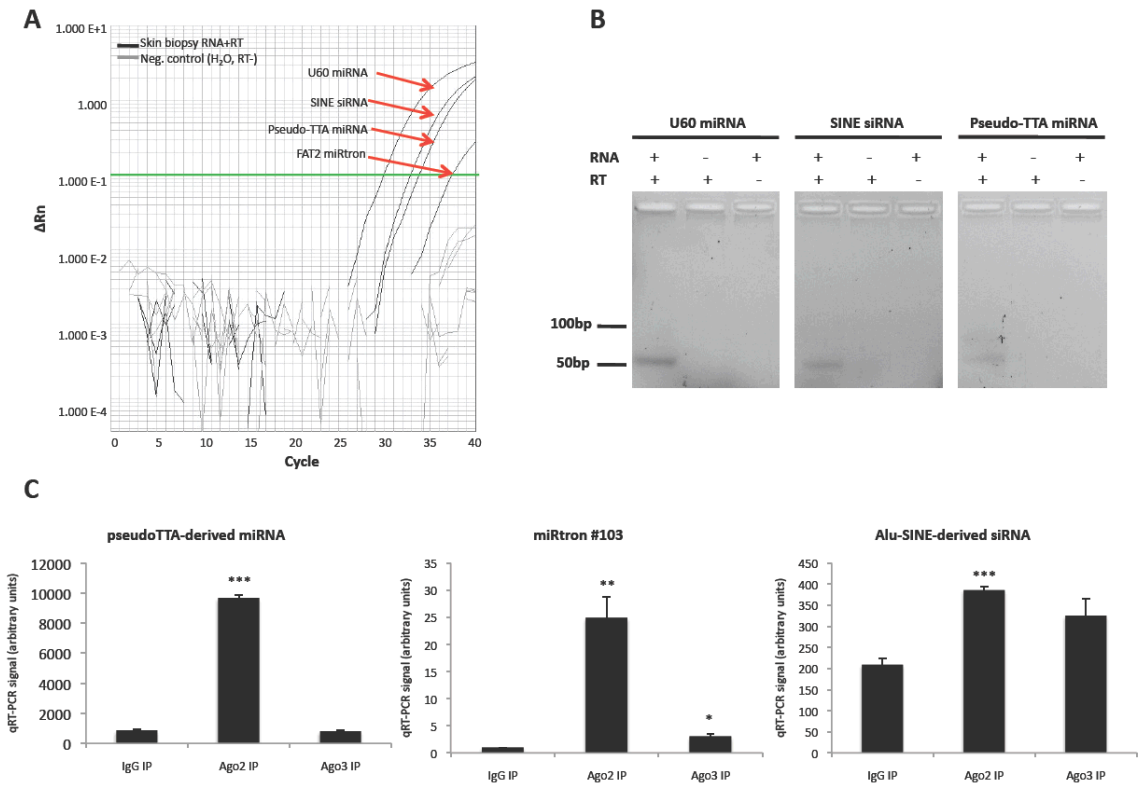

Figure 5-10. Endogenous expression of mature novel miRNAs in skin. (A**)** qRT-PCR amplification traces of sncRNAs from human skin biopsy RNA (black lines) and negative controls (grey lines). An arbitrary threshold used for relative quantitation of expression levels (not shown) is indicated in green. (B**)** qRT-PCR product bands from human skin biopsy RNA and negative controls. A band size of ~50bp corresponds to an ~21-nt RNA species due to the addition of arbitrary sequence during the reverse transcription step (see Methods). (C**)** Abundance of sncRNAs in Ago2 and Ago3 immunoprecipitates relative to IgG. (* $p<0.05$, ** $p<0.01$, *** $p<0.001$). RT = reverse transcriptase.

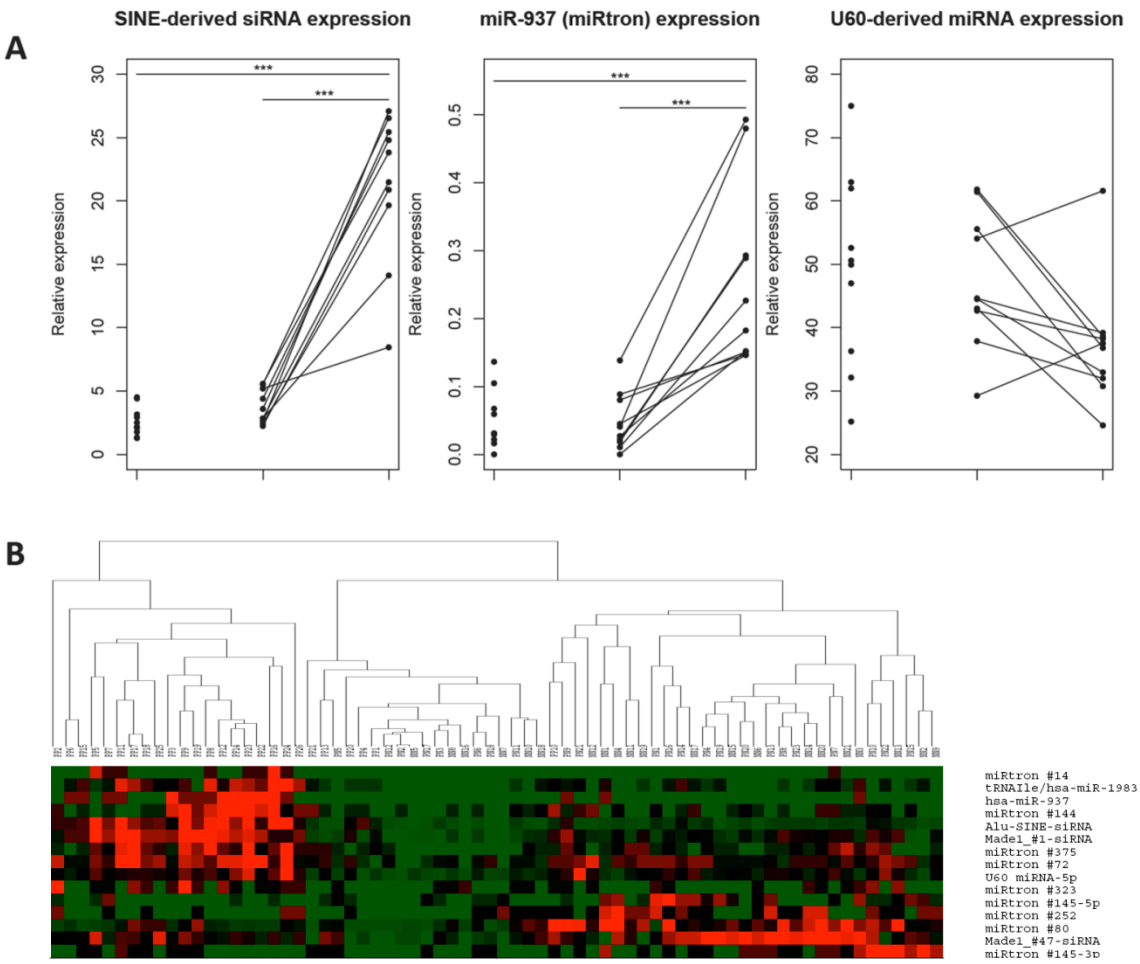

Figure 5-11. Differential expression of sncRNAs in involved psoriatic skin. (A) qRT-PCR levels of differentially expressed sncRNAs in ten normal (NN), ten uninvolved psoriatic (PN), and ten involved psoriatic (PP) skin samples. Lines indicate matched uninvolved and involved samples from the same patient. Relative expression was calculated with respect to the endogenous snoRNA Z30. (* $p<0.05$, **$p<0.01$, ***$p<0.001$). (B) Heat map of 15 differentially expressed sncRNAs across 67 skin samples.

Chapter 6.

Conclusions and future directions

SUMMARY

It has long been appreciated that gene expression is widely altered in psoriatic skin due to impaired keratinocyte differentiation, inflammation, and immune cell activation. I hypothesized that differential expression of small noncoding regulatory RNAs (sncRNAs) might underlie some of the gene expression changes in psoriatic skin. Thus, I sought to characterize the global landscape of sncRNA expression in human skin, and to investigate the functional roles of sncRNAs with respect to psoriasis pathogenesis.

In chapter two, I described the global microRNA (miRNA) landscape in human skin, as assessed by Next Generation sequencing (NGS). I detected nearly 900 known miRNAs and miRNA*s, a number of previously undescribed miRNA*s from known miRNA loci, variants of known miRNAs (isomiRs and putatively edited miRNAs), and nearly 300 novel miRNA loci expressed in skin. Chapters 3 and 4 focused on the contribution of miRNAs to psoriasis pathogenesis. I described the differential expression of 98 known and novel miRNAs in psoriatic skin, and showed that three differentially expressed miRNAs regulated components of the skin barrier. Lastly, in Chapter 6, I described the expression of noncanonical miRNAs and endogenous small interfering RNAs (endo-siRNAs) in normal and psoriatic skin, including the dramatic upregulation of a novel Alu SINE-derived siRNA in involved (PP) skin.

In summary, this thesis details the generation and analysis of the largest small RNA dataset produced from any human tissue to date and the use of molecular genetic approaches to validate and follow up on NGS-based findings. Future work should include functional analysis of the three miRNAs that regulate barrier components *in vivo*;

characterization of regulatory networks in skin involving both mRNAs and miRNAs; and profiling of poly(A)- RNA species, such as long noncoding RNAs, in normal and psoriatic skin.

FUTURE DIRECTIONS

Functional of miRNAs in the skin barrier

I have identified two members of the LCE gene family as direct targets of differentially expressed miRNAs in keratinocytes. This finding is significant because the LCE gene family has been strongly implicated in psoriasis, based on gene expression and GWAS studies. Moreover, LCE gene products are constituents of the skin barrier, which is dramatically impaired in psoriatic skin. It has also been suggested that innate barrier defects could predispose individuals to psoriasis later in life. Thus, it is important to characterize the phenotypic consequences of miRNA-mediated regulation of LCE family members.

Neither the miR-135b and miR-7 sites in LCE1B, nor the miR-486 binding site in LCE3E are conserved in mouse. Thus, primary human keratinocytes or epidermal equivalents provide the best system in which to study phenotypic effects of endogenous miRNA:LCE interactions. For primary keratinocytes, supplementation of medium with calcium induces differentiation over a period of seven days; for epidermal equivalents, the exposure of keratinocytes to an air-liquid interface induces stratification reminiscent of the native epidermis. In either case, it would possible to perturb miR-135b, miR-7, or miR-486 expression during the course of differentiation and screen for various phenotypes such as cell viability, proliferation, apoptosis, or gross morphology. Moreover, cells could be harvested at various time points and subjected to expression profiling or qRT-PCR for specific differentiation markers. These experiments would indicate whether perturbation of a single miRNA in keratinocytes is sufficient to induce a

differentiation defect in keratinocytes, and whether the misexpression of these miRNAs alters expression additional genes besides LCE that are related to keratinocyte differentiation.

An alternative means of studying the phenotypic effects of miR-135b, miR-7, and miR-486 in skin would be to generate transgenic mice expressing "humanized" LCE1B and LCE3E from their endogenous loci. This would render these genes susceptible to the miRNA regulation that I observed in humans. It would then be possible to assess whether the presence of human LCE1B or LCE3E affected characteristic features of the mouse epidermis (such as barrier thickness or hair follicle spacing), and whether such phenotypes were influenced by altered expression of miR-135b, miR-7, or miR-486. It might also be possible to perform these experiments in mouse models of psoriasis, to determine whether the presence of humanized LCE genes influences pathogenic features of the model. Such experiments could provide insight into innate differences between human and mouse epidermis and the functional impact of recently evolved miRNA:target interactions.

I hypothesize that miR-135b, miR-7, and miR-486 influence barrier composition in PP skin by regulating the translation of LCE1B and LCE3E in the spinous and granular layers of the skin, prior to terminal differentiation. This hypothesis was partially based on the suprabasally restricted expression pattern of miR-135b in the epidermis, as determined by RNA in situ hybridization However, the spatial expression patterns of miR-7, miR-486, and LCE mRNAs remain unknown. It would be extremely useful to visualize these species with RNA *in situ* hybridization in skin sections. In order for the

miRNAs to exert their proposed regulatory functions, I would expect that the miRNA and cognate LCE mRNA species would exhibit similar spatial expression patterns.

Characterization of regulatory networks in psoriatic skin

Small RNAs are differentially expressed in psoriatic skin, and are likely contribute to disease pathogenesis. Specifically, I have shown that the differentially expressed miRNAs miR-7, miR-135b, and miR-486 regulate the barrier constituents, LCE1B and LCE3E. However, miRNAs function pleiotropically, and can influence a large number of direct and indirect targets within a cell. Thus, regulation of singular targets likely accounts for a small fraction of a given miRNA's total activity, and it is important to characterize their regulatory impact on a larger scale. Indeed, I have shown that many of the differentially expressed transcripts in psoriatic skin are predicted to be targets of differentially expressed miRNAs. However, this approach relied on algorithms for target prediction that are not very accurate, and the transcript expression data was generated with array based techniques which are insensitive to low abundance species and exhibit a limited dynamic range.

In order to generate a more complete transcriptome profile from normal and psoriatic skin, our lab has generated poly(A)+ RNA libraries for deep sequencing from seven normal (NN), nine uninvolved (PN), and nine PP skin biopsy samples. Importantly, the set of skin biopsy samples we profiled overlap with small RNA sequencing samples, so that levels of small RNAs and mRNAs within a single biopsy can be directly compared. We are currently analyzing these data in order to characterize key gene expression networks that are perturbed in psoriatic skin. We will then perform sample-

matched comparisons of mRNA and miRNA expression in skin to elucidate concentration dependent relationships between mRNAs and miRNAs, independent of target prediction algorithms. This type of analysis has been successfully applied for the melanoma tumor suppressor miR-211 (95). In that case, strong anti-correlations were observed for known miR-211 targets. Additionally, it was found that miR-211 directly targets two of three central node genes in the melanoma metastasis network, which accounts for its strong influence on cell migration and invasiveness of melanoma cells.

Based on these findings in melanoma, we expect that a small number of differentially expressed miRNAs will regulate central nodes of gene expression networks in psoriasis. The misexpression of such miRNAs may exert strong pathogenic effects due to their indirect influence on large numbers of downstream targets. Many other miRNAs may directly regulate downstream factors, and would be expected to yield more subtle effects on disease pathogenesis. Such effects could be combinatorial, such that multiple miRNAs converge on a single target (as in the case of miR-7 and miR-135b on LCE1B), or a single miRNA regulates multiple targets. Overall, this approach has been shown to yield powerful insights into the role of miRNAs in melanoma pathogenesis, and should be similarly effective in psoriasis.

Despite the power of this analysis, it is important to note it does not assess the direct, physical association of miRNAs and their targets. Thus, the development and application of new techniques for the global identification of direct miRNA targets *in situ* or *in vivo* will be crucial in order to understand the full effect of miRNA regulation in the skin.

Non-polyadenylated noncoding RNAs

Polyadenylation of mRNAs is prevalent in eukaryotic cells, and associated with transcript stability. While the majority of expressed mRNAs are poly(A)+, poly(A)- transcripts account for the majority of expressed RNAs in the cell. These include classical examples, such as rRNA transcripts (which account for >90% of the RNA content in a cell) and histone transcripts, as well as some mRNAs and noncoding RNAs (219,220). Poly(A)- RNAs include those that are never adenylated, as well as those that are initially adenylated but later undergo regulated deadenylation (219,220).

Common RNA sequencing methods use poly(A)+ selection as a method for depleting highly abundant rRNA transcripts from the library, but such selection also excludes other poly(A)- species that may be of functional importance. Thus, new techniques are being developed for the analysis of poly(A)- species. One example is the RiboMinus method developed by Invitrogen, which depletes rRNA transcripts by hybridizing total RNA to biotinylated LNA probes designed against rRNA sequences, and then removing the hybridized RNAs with magnetic streptavidin-conjugated beads. Application of such poly(A)- profiling techniques has provided new insights into poly(A)- populations in human cells. For example, poly(A)- fractions in Hela and H9 cell lines included stable, excised introns; small noncoding RNAs such as snoRNAs, scaRNAs, and miRNA precursors; and intergenic, intragenic, and antisense long noncoding RNAs (220).

Based on the widespread expression changes in poly(A)+ and small noncoding RNAs in involved skin, we would expect that some species of poly(A)- RNA would also be misexpressed. Indeed, one long non-coding RNA, the psoriasis susceptibility-related

RNA gene induced by stress (PRINS), has been previously implicated in psoriasis susceptibility (221). PRINS is a ~7kb noncoding RNA that is transcribed by RNA polymerase II, and induced in keratinocytes under various stress conditions. PRINS is highly expressed in PN skin compared to NN and PP (221). While PRINS is polyadenylated, its connection to psoriasis highlights the potential contribution of long noncoding RNAs to disease susceptibility, thus motivating a more complete understanding of long noncoding RNA expression in psoriasis via deep sequencing of poly(A)- RNAs. Overall, deep sequencing of the poly(A)- fraction would complete the psoriasis transcriptome, and allow a full integrated analysis of regulatory networks comprised of mRNAs, sncRNAs, and long noncoding RNAs.

CONCLUDING REMARKS

Psoriasis is a complex disease, with many genes contributing to disease susceptibility and pathogenesis. Psoriatic skin exhibits myriad mRNA expression changes and, based on the work described in this thesis, misexpression of sncRNAs such as miRNAs. Some differentially expressed miRNAs have previously described functions and are likely to regulate targets involved in keratinocyte differentiation, inflammation and immunity, or angiogenesis; many others, including several novel miRNAs, are of unknown function. I have characterized three miRNAs of unknown function as negative regulators of skin barrier components. This finding adds to the increasing body of evidence that, despite the large number of immune-related psoriasis susceptibility genes, barrier defects also contribute to psoriasis pathogenesis. Overall, the work described in this thesis has advanced our understanding of sncRNA expression in skin, and implicated many new sncRNAs in psoriasis pathogenesis. Integrated analysis of global miRNA and mRNA expression in normal and psoriatic skin will likely refine our understanding of regulatory networks affected by the disease, and inform the development of new therapies for psoriasis.

REFERENCES

1. Fuchs E. (2007) Scratching the surface of skin development. *Nature,* **445**, 834-842.

2. Fuchs E. and Raghavan S. (2002) Getting under the skin of epidermal morphogenesis. *Nat. Rev. Genet.,* **3**, 199-209.

3. Halprin K.M. (1972) Epidermal "turnover time"--a re-examination. *Br. J. Dermatol.,* **86**, 14-19.

4. Liu Y., Krueger J.G. and Bowcock A.M. (2007) Psoriasis: Genetic associations and immune system changes. *Genes Immun.,* **8**, 1-12.

5. Roberson E.D. and Bowcock A.M. (2010) Psoriasis genetics: Breaking the barrier. *Trends Genet.,* **26**, 415-423.

6. Bowcock A.M. (2005) The genetics of psoriasis and autoimmunity. *Annu. Rev. Genomics Hum. Genet.,* **6**, 93-122.

7. Bhalerao J. and Bowcock A.M. (1998) The genetics of psoriasis: A complex disorder of the skin and immune system. *Hum. Mol. Genet.,* **7**, 1537-1545.

8. Griffiths C.E. and Barker J.N. (2007) Pathogenesis and clinical features of psoriasis. *Lancet,* **370**, 263-271.

9. Gelfand J.M., Dommasch E.D., Shin D.B., Azfar R.S., Kurd S.K., Wang X. and Troxel A.B. (2009) The risk of stroke in patients with psoriasis. *J. Invest. Dermatol.,* **129**, 2411-2418.

10. Gelfand J.M., Neimann A.L., Shin D.B., Wang X., Margolis D.J. and Troxel A.B. (2006) Risk of myocardial infarction in patients with psoriasis. *JAMA,* **296**, 1735-1741.

11. de Arruda L.H. and De Moraes A.P. (2001) The impact of psoriasis on quality of life. *Br. J. Dermatol.,* **144 Suppl 58**, 33-36.

12. Sommer D.M., Jenisch S., Suchan M., Christophers E. and Weichenthal M. (2006) Increased prevalence of the metabolic syndrome in patients with moderate to severe psoriasis. *Arch. Dermatol. Res.,* **298**, 321-328.

13. Nograles K.E., Brasington R.D. and Bowcock A.M. (2009) New insights into the pathogenesis and genetics of psoriatic arthritis. *Nat. Clin. Pract. Rheumatol.,* **5**, 83-91.

14. Herrier R.N. (2011) Advances in the treatment of moderate-to-severe plaque psoriasis. *Am. J. Health. Syst. Pharm.,* **68**, 795-806.

15. de Jongh G.J., Zeeuwen P.L., Kucharekova M., Pfundt R., van der Valk P.G., Blokx W., Dogan A., Hiemstra P.S., van de Kerkhof P.C. and Schalkwijk J. (2005) High expression levels of keratinocyte antimicrobial proteins in psoriasis compared with atopic dermatitis. *J. Invest. Dermatol.,* **125**, 1163-1173.

16. Lowes M.A., Lew W. and Krueger J.G. (2004) Current concepts in the immunopathogenesis of psoriasis. *Dermatol. Clin.,* **22**, 349-69, vii.

17. Mee J.B., Johnson C.M., Morar N., Burslem F. and Groves R.W. (2007) The psoriatic transcriptome closely resembles that induced by interleukin-1 in cultured keratinocytes: Dominance of innate immune responses in psoriasis. *Am. J. Pathol.,* **171**, 32-42.

18. Zhou X., Krueger J.G., Kao M.C., Lee E., Du F., Menter A., Wong W.H. and Bowcock A.M. (2003) Novel mechanisms of T-cell and dendritic cell activation revealed by profiling of psoriasis on the 63,100-element oligonucleotide array. *Physiol. Genomics,* **13**, 69-78.

19. Gudjonsson J.E., Ding J., Johnston A., Tejasvi T., Guzman A.M., Nair R.P., Voorhees J.J., Abecasis G.R. and Elder J.T. (2010) Assessment of the psoriatic transcriptome in a large sample: Additional regulated genes and comparisons with in vitro models. *J. Invest. Dermatol.,* **130**, 1829-1840.

20. Eyre R.W. and Krueger G.G. (1982) Response to injury of skin involved and uninvolved with psoriasis, and its relation to disease activity: Koebner and 'reverse' koebner reactions. *Br. J. Dermatol.,* **106**, 153-159.

21. Arnett F.C., Reveille J.D. and Duvic M. (1991) Psoriasis and psoriatic arthritis associated with human immunodeficiency virus infection. *Rheum. Dis. Clin. North Am.,* **17**, 59-78.

22. Rongioletti F., Fiorucci C. and Parodi A. (2009) Psoriasis induced or aggravated by drugs. *J. Rheumatol. Suppl.,* **83**, 59-61.

23. Hwu W.L., Yang C.F., Fann C.S., Chen C.L., Tsai T.F., Chien Y.H., Chiang S.C., Chen C.H., Hung S.I., Wu J.Y. *et al.* (2005) Mapping of psoriasis to 17q terminus. *J. Med. Genet.,* **42**, 152-158.

24. Tomfohrde J., Silverman A., Barnes R., Fernandez-Vina M.A., Young M., Lory D., Morris L., Wuepper K.D., Stastny P. and Menter A. (1994) Gene for familial psoriasis susceptibility mapped to the distal end of human chromosome 17q. *Science,* **264**, 1141-1145.

25. Jordan C.T., Cao L., Roberson E.D., Pierson K.C., Yang C.F., Joyce C.E., Ryan C., Duan S., Helms C.A., Liu Y. *et al.* (2012) PSORS2 is due to mutations in CARD14. *Am. J. Hum. Genet.,* **In press**.

26. Bertin J., Wang L., Guo Y., Jacobson M.D., Poyet J.L., Srinivasula S.M., Merriam S., DiStefano P.S. and Alnemri E.S. (2001) CARD11 and CARD14 are novel caspase recruitment domain (CARD)/membrane-associated guanylate kinase (MAGUK) family members that interact with BCL10 and activate NF-kappa B. *J. Biol. Chem.,* **276**, 11877-11882.

27. Tiilikainen A., Lassus A., Karvonen J., Vartiainen P. and Julin M. (1980) Psoriasis and HLA-Cw6. *Br. J. Dermatol.,* **102**, 179-184.

28. Cargill M., Schrodi S.J., Chang M., Garcia V.E., Brandon R., Callis K.P., Matsunami N., Ardlie K.G., Civello D., Catanese J.J. *et al.* (2007) A large-scale genetic association study confirms IL12B and leads to the identification of IL23R as psoriasis-risk genes. *Am. J. Hum. Genet.,* **80**, 273-290.

29. Nair R.P., Duffin K.C., Helms C., Ding J., Stuart P.E., Goldgar D., Gudjonsson J.E., Li Y., Tejasvi T., Feng B.J. *et al.* (2009) Genome-wide scan reveals association of psoriasis with IL-23 and NF-kappaB pathways. *Nat. Genet.,* **41**, 199-204.

30. Zhang X.J., Huang W., Yang S., Sun L.D., Zhang F.Y., Zhu Q.X., Zhang F.R., Zhang C., Du W.H., Pu X.M. *et al.* (2009) Psoriasis genome-wide association study identifies susceptibility variants within LCE gene cluster at 1q21. *Nat. Genet.,* **41**, 205-210.

31. Hollox E.J., Huffmeier U., Zeeuwen P.L., Palla R., Lascorz J., Rodijk-Olthuis D., van de Kerkhof P.C., Traupe H., de Jongh G., den Heijer M. *et al.* (2008) Psoriasis is associated with increased beta-defensin genomic copy number. *Nat. Genet.,* **40**, 23-25.

32. de Cid R., Riveira-Munoz E., Zeeuwen P.L., Robarge J., Liao W., Dannhauser E.N., Giardina E., Stuart P.E., Nair R., Helms C. *et al.* (2009) Deletion of the late cornified envelope LCE3B and LCE3C genes as a susceptibility factor for psoriasis. *Nat. Genet.,* **41**, 211-215.

33. Chen H., Poon A., Yeung C., Helms C., Pons J., Bowcock A.M., Kwok P.Y. and Liao W. (2011) A genetic risk score combining ten psoriasis risk loci improves disease prediction. *PLoS One,* **6**, e19454.

34. Carthew R.W. and Sontheimer E.J. (2009) Origins and mechanisms of miRNAs and siRNAs. *Cell,* **136**, 642-655.

35. Ambros V. (1989) A hierarchy of regulatory genes controls a larva-to-adult developmental switch in C. elegans. *Cell,* **57**, 49-57.

36. Chalfie M., Horvitz H.R. and Sulston J.E. (1981) Mutations that lead to reiterations in the cell lineages of C. elegans. *Cell,* **24**, 59-69.

37. Ambros V. and Horvitz H.R. (1984) Heterochronic mutants of the nematode caenorhabditis elegans. *Science,* **226**, 409-416.

38. Lee R.C., Feinbaum R.L. and Ambros V. (1993) The C. elegans heterochronic gene lin-4 encodes small RNAs with antisense complementarity to lin-14. *Cell,* **75**, 843-854.

39. Ha I., Wightman B. and Ruvkun G. (1996) A bulged lin-4/lin-14 RNA duplex is sufficient for caenorhabditis elegans lin-14 temporal gradient formation. *Genes Dev.,* **10**, 3041-3050.

40. Olsen P.H. and Ambros V. (1999) The lin-4 regulatory RNA controls developmental timing in caenorhabditis elegans by blocking LIN-14 protein synthesis after the initiation of translation. *Dev. Biol.,* **216**, 671-680.

41. Wightman B., Ha I. and Ruvkun G. (1993) Posttranscriptional regulation of the heterochronic gene lin-14 by lin-4 mediates temporal pattern formation in C. elegans. *Cell,* **75**, 855-862.

42. Moss E.G., Lee R.C. and Ambros V. (1997) The cold shock domain protein LIN-28 controls developmental timing in C. elegans and is regulated by the lin-4 RNA. *Cell,* **88**, 637-646.

43. Griffiths-Jones S. (2004) The microRNA registry. *Nucleic Acids Res.,* **32**, D109-11.

44. Griffiths-Jones S., Grocock R.J., van Dongen S., Bateman A. and Enright A.J. (2006) miRBase: MicroRNA sequences, targets and gene nomenclature. *Nucleic Acids Res.,* **34**, D140-4.

45. Griffiths-Jones S., Saini H.K., van Dongen S. and Enright A.J. (2008) miRBase: Tools for microRNA genomics. *Nucleic Acids Res.,* **36**, D154-8.

46. Lau N.C., Lim L.P., Weinstein E.G. and Bartel D.P. (2001) An abundant class of tiny RNAs with probable regulatory roles in caenorhabditis elegans. *Science,* **294**, 858-862.

47. Lagos-Quintana M., Rauhut R., Lendeckel W. and Tuschl T. (2001) Identification of novel genes coding for small expressed RNAs. *Science,* **294**, 853-858.

48. Lee Y., Kim M., Han J., Yeom K.H., Lee S., Baek S.H. and Kim V.N. (2004) MicroRNA genes are transcribed by RNA polymerase II. *EMBO J.,* **23**, 4051-4060.

49. Cai X., Hagedorn C.H. and Cullen B.R. (2004) Human microRNAs are processed from capped, polyadenylated transcripts that can also function as mRNAs. *RNA,* **10**, 1957-1966.

50. Lee Y., Ahn C., Han J., Choi H., Kim J., Yim J., Lee J., Provost P., Radmark O., Kim S. *et al.* (2003) The nuclear RNase III drosha initiates microRNA processing. *Nature,* **425**, 415-419.

51. Lund E., Guttinger S., Calado A., Dahlberg J.E. and Kutay U. (2004) Nuclear export of microRNA precursors. *Science,* **303**, 95-98.

52. Yi R., Qin Y., Macara I.G. and Cullen B.R. (2003) Exportin-5 mediates the nuclear export of pre-microRNAs and short hairpin RNAs. *Genes Dev.,* **17**, 3011-3016.

53. Bohnsack M.T., Czaplinski K. and Gorlich D. (2004) Exportin 5 is a RanGTP-dependent dsRNA-binding protein that mediates nuclear export of pre-miRNAs. *RNA,* **10**, 185-191.

54. Bernstein E., Caudy A.A., Hammond S.M. and Hannon G.J. (2001) Role for a bidentate ribonuclease in the initiation step of RNA interference. *Nature,* **409**, 363-366.

55. Grishok A., Pasquinelli A.E., Conte D., Li N., Parrish S., Ha I., Baillie D.L., Fire A., Ruvkun G. and Mello C.C. (2001) Genes and mechanisms related to RNA interference regulate expression of the small temporal RNAs that control C. elegans developmental timing. *Cell,* **106**, 23-34.

56. Hutvagner G., McLachlan J., Pasquinelli A.E., Balint E., Tuschl T. and Zamore P.D. (2001) A cellular function for the RNA-interference enzyme dicer in the maturation of the let-7 small temporal RNA. *Science,* **293**, 834-838.

57. Ketting R.F., Fischer S.E., Bernstein E., Sijen T., Hannon G.J. and Plasterk R.H. (2001) Dicer functions in RNA interference and in synthesis of small RNA involved in developmental timing in C. elegans. *Genes Dev.,* **15**, 2654-2659.

58. Knight S.W. and Bass B.L. (2001) A role for the RNase III enzyme DCR-1 in RNA interference and germ line development in caenorhabditis elegans. *Science,* **293**, 2269-2271.

59. Khvorova A., Reynolds A. and Jayasena S.D. (2003) Functional siRNAs and miRNAs exhibit strand bias. *Cell,* **115**, 209-216.

60. Schwarz D.S., Hutvagner G., Du T., Xu Z., Aronin N. and Zamore P.D. (2003) Asymmetry in the assembly of the RNAi enzyme complex. *Cell,* **115**, 199-208.

61. Ro S., Park C., Young D., Sanders K.M. and Yan W. (2007) Tissue-dependent paired expression of miRNAs. *Nucleic Acids Res.,* **35**, 5944-5953.

62. Sontheimer E.J. (2005) Assembly and function of RNA silencing complexes. *Nat. Rev. Mol. Cell Biol.,* **6**, 127-138.

63. Fabian M.R., Sonenberg N. and Filipowicz W. (2010) Regulation of mRNA translation and stability by microRNAs. *Annu. Rev. Biochem.,* **79**, 351-379.

64. Jinek M. and Doudna J.A. (2009) A three-dimensional view of the molecular machinery of RNA interference. *Nature,* **457**, 405-412.

65. Peters L. and Meister G. (2007) Argonaute proteins: Mediators of RNA silencing. *Mol. Cell,* **26**, 611-623.

66. Till S., Lejeune E., Thermann R., Bortfeld M., Hothorn M., Enderle D., Heinrich C., Hentze M.W. and Ladurner A.G. (2007) A conserved motif in argonaute-interacting proteins mediates functional interactions through the argonaute PIWI domain. *Nat. Struct. Mol. Biol.,* **14**, 897-903.

67. Landthaler M., Gaidatzis D., Rothballer A., Chen P.Y., Soll S.J., Dinic L., Ojo T., Hafner M., Zavolan M. and Tuschl T. (2008) Molecular characterization of human argonaute-containing ribonucleoprotein complexes and their bound target mRNAs. *RNA,* **14**, 2580-2596.

68. Azuma-Mukai A., Oguri H., Mituyama T., Qian Z.R., Asai K., Siomi H. and Siomi M.C. (2008) Characterization of endogenous human argonautes and their miRNA partners in RNA silencing. *Proc. Natl. Acad. Sci. U. S. A.,* **105**, 7964-7969.

69. Behm-Ansmant I., Rehwinkel J., Doerks T., Stark A., Bork P. and Izaurralde E. (2006) mRNA degradation by miRNAs and GW182 requires both CCR4:NOT deadenylase and DCP1:DCP2 decapping complexes. *Genes Dev.,* **20**, 1885-1898.

70. Baillat D. and Shiekhattar R. (2009) Functional dissection of the human TNRC6 (GW182-related) family of proteins. *Mol. Cell. Biol.,* **29**, 4144-4155.

71. Zipprich J.T., Bhattacharyya S., Mathys H. and Filipowicz W. (2009) Importance of the C-terminal domain of the human GW182 protein TNRC6C for translational repression. *RNA,* **15**, 781-793.

72. Lewis B.P., Burge C.B. and Bartel D.P. (2005) Conserved seed pairing, often flanked by adenosines, indicates that thousands of human genes are microRNA targets. *Cell,* **120**, 15-20.

73. Hutvagner G. and Zamore P.D. (2002) A microRNA in a multiple-turnover RNAi enzyme complex. *Science,* **297**, 2056-2060.

74. Zeng Y., Yi R. and Cullen B.R. (2003) MicroRNAs and small interfering RNAs can inhibit mRNA expression by similar mechanisms. *Proc. Natl. Acad. Sci. U. S. A.,* **100**, 9779-9784.

75. Doench J.G., Petersen C.P. and Sharp P.A. (2003) siRNAs can function as miRNAs. *Genes Dev.,* **17**, 438-442.

76. Song J.J., Smith S.K., Hannon G.J. and Joshua-Tor L. (2004) Crystal structure of argonaute and its implications for RISC slicer activity. *Science,* **305**, 1434-1437.

77. Brennecke J., Stark A., Russell R.B. and Cohen S.M. (2005) Principles of microRNA-target recognition. *PLoS Biol.,* **3**, e85.

78. Yue D., Liu H. and Huang Y. (2009) Survey of computational algorithms for MicroRNA target prediction. *Curr. Genomics,* **10**, 478-492.

79. Friedman R.C., Farh K.K., Burge C.B. and Bartel D.P. (2009) Most mammalian mRNAs are conserved targets of microRNAs. *Genome Res.,* **19**, 92-105.

80. Bagga S., Bracht J., Hunter S., Massirer K., Holtz J., Eachus R. and Pasquinelli A.E. (2005) Regulation by let-7 and lin-4 miRNAs results in target mRNA degradation. *Cell,* **122**, 553-563.

81. Guo H., Ingolia N.T., Weissman J.S. and Bartel D.P. (2010) Mammalian microRNAs predominantly act to decrease target mRNA levels. *Nature,* **466**, 835-840.

82. Bernstein E., Kim S.Y., Carmell M.A., Murchison E.P., Alcorn H., Li M.Z., Mills A.A., Elledge S.J., Anderson K.V. and Hannon G.J. (2003) Dicer is essential for mouse development. *Nat. Genet.,* **35**, 215-217.

83. Wienholds E., Koudijs M.J., van Eeden F.J., Cuppen E. and Plasterk R.H. (2003) The microRNA-producing enzyme Dicer1 is essential for zebrafish development. *Nat. Genet.,* **35**, 217-218.

84. Kloosterman W.P. and Plasterk R.H. (2006) The diverse functions of microRNAs in animal development and disease. *Dev. Cell.,* **11**, 441-450.

85. Yi R., O'Carroll D., Pasolli H.A., Zhang Z., Dietrich F.S., Tarakhovsky A. and Fuchs E. (2006) Morphogenesis in skin is governed by discrete sets of differentially expressed microRNAs. *Nat. Genet.,* **38**, 356-362.

86. Yi R., Pasolli H.A., Landthaler M., Hafner M., Ojo T., Sheridan R., Sander C., O'Carroll D., Stoffel M., Tuschl T. *et al.* (2009) DGCR8-dependent microRNA biogenesis is essential for skin development. *Proc. Natl. Acad. Sci. U. S. A.,* **106**, 498-502.

87. Hildebrand J., Rutze M., Walz N., Gallinat S., Wenck H., Deppert W., Grundhoff A. and Knott A. (2011) A comprehensive analysis of microRNA expression during human keratinocyte differentiation in vitro and in vivo. *J. Invest. Dermatol.,* **131**, 20-29.

88. Mazar J., Sinha S., Dinger M.E., Mattick J.S. and Perera R.J. (2010) Protein-coding and non-coding gene expression analysis in differentiating human keratinocytes using a three-dimensional epidermal equivalent. *Mol. Genet. Genomics,* **284**, 1-9.

89. Gracias D.T. and Katsikis P.D. (2011) MicroRNAs: Key components of immune regulation. *Adv. Exp. Med. Biol.,* **780**, 15-26.

90. Bak R.O. and Mikkelsen J.G. (2010) Regulation of cytokines by small RNAs during skin inflammation. *J. Biomed. Sci.,* **17**, 53.

91. Mueller D.W., Rehli M. and Bosserhoff A.K. (2009) miRNA expression profiling in melanocytes and melanoma cell lines reveals miRNAs associated with formation and progression of malignant melanoma. *J. Invest. Dermatol.,* **129**, 1740-1751.

92. Stark M.S., Tyagi S., Nancarrow D.J., Boyle G.M., Cook A.L., Whiteman D.C., Parsons P.G., Schmidt C., Sturm R.A. and Hayward N.K. (2010) Characterization of the melanoma miRNAome by deep sequencing. *PLoS One,* **5**, e9685.

93. Ryu S., Joshi N., McDonnell K., Woo J., Choi H., Gao D., McCombie W.R. and Mittal V. (2011) Discovery of novel human breast cancer microRNAs from deep sequencing data by analysis of pri-microRNA secondary structures. *PLoS One,* **6**, e16403.

94. Marti E., Pantano L., Banez-Coronel M., Llorens F., Minones-Moyano E., Porta S., Sumoy L., Ferrer I. and Estivill X. (2010) A myriad of miRNA variants in control and huntington's disease brain regions detected by massively parallel sequencing. *Nucleic Acids Res.,* **38**, 7219-7235.

95. Levy C., Khaled M., Iliopoulos D., Janas M.M., Schubert S., Pinner S., Chen P.H., Li S., Fletcher A.L., Yokoyama S. *et al.* (2010) Intronic miR-211 assumes the tumor suppressive function of its host gene in melanoma. *Mol. Cell,* **40**, 841-849.

96. Sonkoly E., Wei T., Janson P.C., Saaf A., Lundeberg L., Tengvall-Linder M., Norstedt G., Alenius H., Homey B., Scheynius A. *et al.* (2007) MicroRNAs: Novel regulators involved in the pathogenesis of psoriasis? *PLoS One,* **2**, e610.

97. Zibert J.R., Lovendorf M.B., Litman T., Olsen J., Kaczkowski B. and Skov L. (2010) MicroRNAs and potential target interactions in psoriasis. *J. Dermatol. Sci.,* **58**, 177-185.

98. Lena A.M., Shalom-Feuerstein R., Rivetti di Val Cervo P., Aberdam D., Knight R.A., Melino G. and Candi E. (2008) miR-203 represses 'stemness' by repressing DeltaNp63. *Cell Death Differ.,* **15**, 1187-1195.

99. Yi R., Poy M.N., Stoffel M. and Fuchs E. (2008) A skin microRNA promotes differentiation by repressing 'stemness'. *Nature,* **452**, 225-229.

100. Lerman G., Avivi C., Mardoukh C., Barzilai A., Tessone A., Gradus B., Pavlotsky F., Barshack I., Polak-Charcon S., Orenstein A. *et al.* (2011) MiRNA expression in psoriatic skin: Reciprocal regulation of hsa-miR-99a and IGF-1R. *PLoS One,* **6**, e20916.

101. Chen C.Z. (2005) MicroRNAs as oncogenes and tumor suppressors. *N. Engl. J. Med.,* **353**, 1768-1771.

102. Bartel D.P. (2004) MicroRNAs: Genomics, biogenesis, mechanism, and function. *Cell,* **116**, 281-297.

103. Kim V.N., Han J. and Siomi M.C. (2009) Biogenesis of small RNAs in animals. *Nat. Rev. Mol. Cell Biol.,* **10**, 126-139.

104. Berezikov E., Chung W.J., Willis J., Cuppen E. and Lai E.C. (2007) Mammalian mirtron genes. *Mol. Cell,* **28**, 328-336.

105. Ruby J.G., Jan C.H. and Bartel D.P. (2007) Intronic microRNA precursors that bypass drosha processing. *Nature,* **448**, 83-86.

106. Baek D., Villen J., Shin C., Camargo F.D., Gygi S.P. and Bartel D.P. (2008) The impact of microRNAs on protein output. *Nature,* **455**, 64-71.

107. Selbach M., Schwanhausser B., Thierfelder N., Fang Z., Khanin R. and Rajewsky N. (2008) Widespread changes in protein synthesis induced by microRNAs. *Nature,* **455**, 58-63.

108. Yang A., Schweitzer R., Sun D., Kaghad M., Walker N., Bronson R.T., Tabin C., Sharpe A., Caput D., Crum C. *et al.* (1999) P63 is essential for regenerative proliferation in limb, craniofacial and epithelial development. *Nature,* **398**, 714-718.

109. Rossi M., Aqeilan R.I., Neale M., Candi E., Salomoni P., Knight R.A., Croce C.M. and Melino G. (2006) The E3 ubiquitin ligase itch controls the protein stability of p63. *Proc. Natl. Acad. Sci. U. S. A.,* **103**, 12753-12758.

110. Morin R.D., O'Connor M.D., Griffith M., Kuchenbauer F., Delaney A., Prabhu A.L., Zhao Y., McDonald H., Zeng T., Hirst M. *et al.* (2008) Application of massively parallel sequencing to microRNA profiling and discovery in human embryonic stem cells. *Genome Res.,* **18**, 610-621.

111. Landgraf P., Rusu M., Sheridan R., Sewer A., Iovino N., Aravin A., Pfeffer S., Rice A., Kamphorst A.O., Landthaler M. *et al.* (2007) A mammalian microRNA expression atlas based on small RNA library sequencing. *Cell,* **129**, 1401-1414.

112. Gudjonsson J.E., Johnston A., Dyson M., Valdimarsson H. and Elder J.T. (2007) Mouse models of psoriasis. *J. Invest. Dermatol.,* **127**, 1292-1308.

113. Baker M. (2010) MicroRNA profiling: Separating signal from noise. *Nat. Methods,* **7**, 687-692.

114. Zhang W., Gao S., Zhou X., Chellappan P., Chen Z., Zhou X., Zhang X., Fromuth N., Coutino G., Coffey M. *et al.* (2011) Bacteria-responsive microRNAs regulate plant innate immunity by modulating plant hormone networks. *Plant Mol. Biol.,* **75**, 93-105.

115. Powell L.M., Wallis S.C., Pease R.J., Edwards Y.H., Knott T.J. and Scott J. (1987) A novel form of tissue-specific RNA processing produces apolipoprotein-B48 in intestine. *Cell,* **50**, 831-840.

116. Bass B.L. (1997) RNA editing and hypermutation by adenosine deamination. *Trends Biochem. Sci.,* **22**, 157-162.

117. Creighton C.J., Benham A.L., Zhu H., Khan M.F., Reid J.G., Nagaraja A.K., Fountain M.D., Dziadek O., Han D., Ma L. *et al.* (2010) Discovery of novel microRNAs in female reproductive tract using next generation sequencing. *PLoS One,* **5**, e9637.

118. Ender C., Krek A., Friedlander M.R., Beitzinger M., Weinmann L., Chen W., Pfeffer S., Rajewsky N. and Meister G. (2008) A human snoRNA with microRNA-like functions. *Mol. Cell,* **32**, 519-528.

119. Witten D., Tibshirani R., Gu S.G., Fire A. and Lui W.O. (2010) Ultra-high throughput sequencing-based small RNA discovery and discrete statistical biomarker analysis in a collection of cervical tumours and matched controls. *BMC Biol.,* **8**, 58.

120. Wyman S.K., Knouf E.C., Parkin R.K., Fritz B.R., Lin D.W., Dennis L.M., Krouse M.A., Webster P.J. and Tewari M. (2011) Post-transcriptional generation of miRNA variants by multiple nucleotidyl transferases contributes to miRNA transcriptome complexity. *Genome Res.,* **21**, 1450-1461.

121. Yang W., Chendrimada T.P., Wang Q., Higuchi M., Seeburg P.H., Shiekhattar R. and Nishikura K. (2006) Modulation of microRNA processing and expression through RNA editing by ADAR deaminases. *Nat. Struct. Mol. Biol.,* **13**, 13-21.

122. Kawahara Y., Zinshteyn B., Sethupathy P., Iizasa H., Hatzigeorgiou A.G. and Nishikura K. (2007) Redirection of silencing targets by adenosine-to-inosine editing of miRNAs. *Science,* **315**, 1137-1140.

123. Ebhardt H.A., Tsang H.H., Dai D.C., Liu Y., Bostan B. and Fahlman R.P. (2009) Meta-analysis of small RNA-sequencing errors reveals ubiquitous post-transcriptional RNA modifications. *Nucleic Acids Res.,* **37**, 2461-2470.

124. Stark A., Bushati N., Jan C.H., Kheradpour P., Hodges E., Brennecke J., Bartel D.P., Cohen S.M. and Kellis M. (2008) A single hox locus in drosophila produces functional microRNAs from opposite DNA strands. *Genes Dev.,* **22**, 8-13.

125. Cifuentes D., Xue H., Taylor D.W., Patnode H., Mishima Y., Cheloufi S., Ma E., Mane S., Hannon G.J., Lawson N.D. *et al.* (2010) A novel miRNA processing pathway independent of dicer requires Argonaute2 catalytic activity. *Science,* **328**, 1694-1698.

126. Kuhn R.M., Karolchik D., Zweig A.S., Wang T., Smith K.E., Rosenbloom K.R., Rhead B., Raney B.J., Pohl A., Pheasant M. *et al.* (2009) The UCSC genome browser database: Update 2009. *Nucleic Acids Res.,* **37**, D755-61.

127. Langmead B., Trapnell C., Pop M. and Salzberg S.L. (2009) Ultrafast and memory-efficient alignment of short DNA sequences to the human genome. *Genome Biol.,* **10**, R25.

128. Mituyama T., Yamada K., Hattori E., Okida H., Ono Y., Terai G., Yoshizawa A., Komori T. and Asai K. (2009) The functional RNA database 3.0: Databases to support mining and annotation of functional RNAs. *Nucleic Acids Res.,* **37**, D89-92.

129. Kozomara A. and Griffiths-Jones S. (2011) miRBase: Integrating microRNA annotation and deep-sequencing data. *Nucleic Acids Res.,* **39**, D152-7.

130. McCaskill J.S. (1990) The equilibrium partition function and base pair binding probabilities for RNA secondary structure. *Biopolymers,* **29**, 1105-1119.

131. Hofacker I.L., Fontana W., Stadler P.F., Bonhoeffer S., Tacker M. and Schuster P. (1994) Fast folding and comparison of RNA secondary structure. *Monatshefte f. Chemie,* **125**, 167-188.

132. Zuker M. and Stiegler P. (1981) Optimal computer folding of large RNA sequences using thermodynamics and auxiliary information. *Nucleic Acids Res.,* **9**, 133-148.

133. Livak K.J. and Schmittgen T.D. (2001) Analysis of relative gene expression data using real-time quantitative PCR and the 2(-delta delta C(T)) method. *Methods,* **25**, 402-408.

134. Lowes M.A., Bowcock A.M. and Krueger J.G. (2007) Pathogenesis and therapy of psoriasis. *Nature,* **445**, 866-873.

135. Chew A.L., Bennett A., Smith C.H., Barker J. and Kirkham B. (2004) Successful treatment of severe psoriasis and psoriatic arthritis with adalimumab. *Br. J. Dermatol.,* **151**, 492-496.

136. Patel T. and Gordon K.B. (2004) Adalimumab: Efficacy and safety in psoriasis and rheumatoid arthritis. *Dermatol. Ther.,* **17**, 427-431.

137. Gordon K.B., Langley R.G., Leonardi C., Toth D., Menter M.A., Kang S., Heffernan M., Miller B., Hamlin R., Lim L. *et al.* (2006) Clinical response to adalimumab treatment in patients with moderate to severe psoriasis: Double-blind,

randomized controlled trial and open-label extension study. *J. Am. Acad. Dermatol.,* **55**, 598-606.

138. Ohlsson R., Nystrom A., Pfeifer-Ohlsson S., Tohonen V., Hedborg F., Schofield P., Flam F. and Ekstrom T.J. (1993) IGF2 is parentally imprinted during human embryogenesis and in the beckwith-wiedemann syndrome. *Nat. Genet.,* **4**, 94-97.

139. Roberson E.D., Liu Y., Ryan C., Joyce C.E., Duan S., Cao L., Martin A., Liao W., Menter A. and Bowcock A.M. (2011) A subset of methylated CpG sites differentiate psoriatic from normal skin. *J. Invest. Dermatol.,* .

140. Furuta M., Kozaki K.I., Tanaka S., Arii S., Imoto I. and Inazawa J. (2010) miR-124 and miR-203 are epigenetically silenced tumor-suppressive microRNAs in hepatocellular carcinoma. *Carcinogenesis,* **31**, 766-776.

141. Wilting S.M., van Boerdonk R.A., Henken F.E., Meijer C.J., Diosdado B., Meijer G.A., le Sage C., Agami R., Snijders P.J. and Steenbergen R.D. (2010) Methylation-mediated silencing and tumour suppressive function of hsa-miR-124 in cervical cancer. *Mol. Cancer.,* **9**, 167.

142. Bertero T., Gastaldi C., Bourget-Ponzio I., Imbert V., Loubat A., Selva E., Busca R., Mari B., Hofman P., Barbry P. *et al.* (2011) miR-483-3p controls proliferation in wounded epithelial cells. *FASEB J.,* **25**, 3092-3105.

143. Liu Y., Helms C., Liao W., Zaba L.C., Duan S., Gardner J., Wise C., Miner A., Malloy M.J., Pullinger C.R. *et al.* (2008) A genome-wide association study of psoriasis and psoriatic arthritis identifies new disease loci. *PLoS Genet.,* **4**, e1000041.
144. Koster M.I., Kim S., Mills A.A., DeMayo F.J. and Roop D.R. (2004) P63 is the molecular switch for initiation of an epithelial stratification program. *Genes Dev.,* **18**, 126-131.

145. Shen C.S., Tsuda T., Fushiki S., Mizutani H. and Yamanishi K. (2005) The expression of p63 during epidermal remodeling in psoriasis. *J. Dermatol.,* **32**, 236-242.
146. Gu X., Lundqvist E.N., Coates P.J., Thurfjell N., Wettersand E. and Nylander K. (2006) Dysregulation of TAp63 mRNA and protein levels in psoriasis. *J. Invest. Dermatol.,* **126**, 137-141.

147. Qin Y., Capaldo C., Gumbiner B.M. and Macara I.G. (2005) The mammalian scribble polarity protein regulates epithelial cell adhesion and migration through E-cadherin. *J. Cell Biol.,* **171**, 1061-1071.

148. Marquardt A., Stohr H., White K. and Weber B.H. (2000) cDNA cloning, genomic structure, and chromosomal localization of three members of the human fatty acid desaturase family. *Genomics,* **66**, 175-183.

149. Suarez Y., Wang C., Manes T.D. and Pober J.S. (2010) Cutting edge: TNF-induced microRNAs regulate TNF-induced expression of E-selectin and intercellular adhesion molecule-1 on human endothelial cells: Feedback control of inflammation. *J. Immunol.,* **184**, 21-25.

150. Zarjou A., Yang S., Abraham E., Agarwal A. and Liu G. (2011) Identification of a microRNA signature in renal fibrosis: Role of miR-21. *Am. J. Physiol. Renal Physiol.,* **301**, F793-801.

151. Li N., Xu X., Xiao B., Zhu E.D., Li B.S., Liu Z., Tang B., Zou Q.M., Liang H.P. and Mao X.H. (2011) H. pylori related proinflammatory cytokines contribute to the induction of miR-146a in human gastric epithelial cells. *Mol. Biol. Rep.,* .

152. Fehniger T.A., Wylie T., Germino E., Leong J.W., Magrini V.J., Koul S., Keppel C.R., Schneider S.E., Koboldt D.C., Sullivan R.P. *et al.* (2010) Next-generation sequencing identifies the natural killer cell microRNA transcriptome. *Genome Res.,* **20**, 1590-1604.

153. Haider A.S., Lowes M.A., Suarez-Farinas M., Zaba L.C., Cardinale I., Blumenberg M. and Krueger J.G. (2008) Cellular genomic maps help dissect pathology in human skin disease. *J. Invest. Dermatol.,* **128**, 606-615.

154. Lin S., Cheung W.K., Chen S., Lu G., Wang Z., Xie D., Li K., Lin M.C. and Kung H.F. (2010) Computational identification and characterization of primate-specific microRNAs in human genome. *Comput. Biol. Chem.,* **34**, 232-241.

155. Najafi-Shoushtari S.H., Kristo F., Li Y., Shioda T., Cohen D.E., Gerszten R.E. and Naar A.M. (2010) MicroRNA-33 and the SREBP host genes cooperate to control cholesterol homeostasis. *Science,* **328**, 1566-1569.

156. Wang S. and Olson E.N. (2009) AngiomiRs--key regulators of angiogenesis. *Curr. Opin. Genet. Dev.,* **19**, 205-211.

157. Viac J., Palacio S., Schmitt D. and Claudy A. (1997) Expression of vascular endothelial growth factor in normal epidermis, epithelial tumors and cultured keratinocytes. *Arch. Dermatol. Res.,* **289**, 158-163.

158. Xia Y.P., Li B., Hylton D., Detmar M., Yancopoulos G.D. and Rudge J.S. (2003) Transgenic delivery of VEGF to mouse skin leads to an inflammatory condition resembling human psoriasis. *Blood,* **102**, 161-168.

159. Ansel J.C., Tiesman J.P., Olerud J.E., Krueger J.G., Krane J.F., Tara D.C., Shipley G.D., Gilbertson D., Usui M.L. and Hart C.E. (1993) Human keratinocytes are a major source of cutaneous platelet-derived growth factor. *J. Clin. Invest.,* **92**, 671-678.

160. Brown L.F., Harrist T.J., Yeo K.T., Stahle-Backdahl M., Jackman R.W., Berse B., Tognazzi K., Dvorak H.F. and Detmar M. (1995) Increased expression of vascular permeability factor (vascular endothelial growth factor) in bullous pemphigoid, dermatitis herpetiformis, and erythema multiforme. *J. Invest. Dermatol.,* **104**, 744-749.

161. Hua Z., Lv Q., Ye W., Wong C.K., Cai G., Gu D., Ji Y., Zhao C., Wang J., Yang B.B. *et al.* (2006) MiRNA-directed regulation of VEGF and other angiogenic factors under hypoxia. *PLoS One,* **1**, e116.

162. Bhushan M., McLaughlin B., Weiss J.B. and Griffiths C.E. (1999) Levels of endothelial cell stimulating angiogenesis factor and vascular endothelial growth factor are elevated in psoriasis. *Br. J. Dermatol.,* **141**, 1054-1060.

163. Suarez Y., Fernandez-Hernando C., Yu J., Gerber S.A., Harrison K.D., Pober J.S., Iruela-Arispe M.L., Merkenschlager M. and Sessa W.C. (2008) Dicer-dependent endothelial microRNAs are necessary for postnatal angiogenesis. *Proc. Natl. Acad. Sci. U. S. A.,* **105**, 14082-14087.

164. Grundmann S., Hans F.P., Kinniry S., Heinke J., Helbing T., Bluhm F., Sluijter J.P., Hoefer I., Pasterkamp G., Bode C. *et al.* (2011) MicroRNA-100 regulates neovascularization by suppression of mammalian target of rapamycin in endothelial and vascular smooth muscle cells. *Circulation,* **123**, 999-1009.

165. Farazi T.A., Spitzer J.I., Morozov P. and Tuschl T. (2011) miRNAs in human cancer. *J. Pathol.,* **223**, 102-115.

166. Dai R., Zhang Y., Khan D., Heid B., Caudell D., Crasta O. and Ahmed S.A. (2010) Identification of a common lupus disease-associated microRNA expression pattern in three different murine models of lupus. *PLoS One,* **5**, e14302.

167. Thum T., Gross C., Fiedler J., Fischer T., Kissler S., Bussen M., Galuppo P., Just S., Rottbauer W., Frantz S. *et al.* (2008) MicroRNA-21 contributes to myocardial disease by stimulating MAP kinase signalling in fibroblasts. *Nature,* **456**, 980-984.

168. Greco S., De Simone M., Colussi C., Zaccagnini G., Fasanaro P., Pescatori M., Cardani R., Perbellini R., Isaia E., Sale P. *et al.* (2009) Common micro-RNA signature in skeletal muscle damage and regeneration induced by duchenne muscular dystrophy and acute ischemia. *FASEB J.,* **23**, 3335-3346.

169. Lim L.P., Lau N.C., Garrett-Engele P., Grimson A., Schelter J.M., Castle J., Bartel D.P., Linsley P.S. and Johnson J.M. (2005) Microarray analysis shows that some microRNAs downregulate large numbers of target mRNAs. *Nature,* **433**, 769-773.

170. Herranz H. and Cohen S.M. (2010) MicroRNAs and gene regulatory networks: Managing the impact of noise in biological systems. *Genes Dev.,* **24**, 1339-1344.

171. Pellegrini G., De Luca M., Orecchia G., Balzac F., Cremona O., Savoia P., Cancedda R. and Marchisio P.C. (1992) Expression, topography, and function of integrin receptors are severely altered in keratinocytes from involved and uninvolved psoriatic skin. *J. Clin. Invest.,* **89**, 1783-1795.

172. Chen C.Z., Li L., Lodish H.F. and Bartel D.P. (2004) MicroRNAs modulate hematopoietic lineage differentiation. *Science,* **303**, 83-86.

173. Bergboer J.G., Tjabringa G.S., Kamsteeg M., van Vlijmen-Willems I.M., Rodijk-Olthuis D., Jansen P.A., Thuret J.Y., Narita M., Ishida-Yamamoto A., Zeeuwen P.L. *et al.* (2011) Psoriasis risk genes of the late cornified envelope-3 group are distinctly expressed compared with genes of other LCE groups. *Am. J. Pathol.,* **178**, 1470-1477.

174. Jackson B., Tilli C.M., Hardman M.J., Avilion A.A., MacLeod M.C., Ashcroft G.S. and Byrne C. (2005) Late cornified envelope family in differentiating epithelia--response to calcium and ultraviolet irradiation. *J. Invest. Dermatol.,* **124**, 1062-1070.

175. 1000 Genomes Project Consortium (2010) A map of human genome variation from population-scale sequencing. *Nature,* **467**, 1061-1073.

176. Marshall D., Hardman M.J., Nield K.M. and Byrne C. (2001) Differentially expressed late constituents of the epidermal cornified envelope. *Proc. Natl. Acad. Sci. U. S. A.,* **98**, 13031-13036.

177. Mukherji S., Ebert M.S., Zheng G.X., Tsang J.S., Sharp P.A. and van Oudenaarden A. (2011) MicroRNAs can generate thresholds in target gene expression. *Nat. Genet.,* **43**, 854-859.

178. Li M., Wu Y., Chen G., Yang Y., Zhou D., Zhang Z., Zhang D., Chen Y., Lu Z., He L. *et al.* (2011) Deletion of the late cornified envelope genes LCE3C and LCE3B is associated with psoriasis in a chinese population. *J. Invest. Dermatol.,* **131**, 1639-1643.

179. de Guzman Strong C., Wertz P.W., Wang C., Yang F., Meltzer P.S., Andl T., Millar S.E., Ho I.C., Pai S.Y. and Segre J.A. (2006) Lipid defect underlies selective skin barrier impairment of an epidermal-specific deletion of gata-3. *J. Cell Biol.,* **175**, 661-670.

180. George R.D., McVicker G., Diederich R., Ng S.B., MacKenzie A.P., Swanson W.J., Shendure J. and Thomas J.H. (2011) Trans genomic capture and sequencing of primate exomes reveals new targets of positive selection. *Genome Res.,* **21**, 1686-1694.

181. Nielsen B.S., Jorgensen S., Fog J.U., Sokilde R., Christensen I.J., Hansen U., Brunner N., Baker A., Moller S. and Nielsen H.J. (2011) High levels of microRNA-21 in the stroma of colorectal cancers predict short disease-free survival in stage II colon cancer patients. *Clin. Exp. Metastasis,* **28**, 27-38.

182. Garcia D.M., Baek D., Shin C., Bell G.W., Grimson A. and Bartel D.P. (2011) Weak seed-pairing stability and high target-site abundance decrease the proficiency of lsy-6 and other microRNAs. *Nat. Struct. Mol. Biol.,* **18**, 1139-1146.

183. Betel D., Koppal A., Agius P., Sander C. and Leslie C. (2010) Comprehensive modeling of microRNA targets predicts functional non-conserved and non-canonical sites. *Genome Biol.,* **11**, R90.

184. Betel D., Wilson M., Gabow A., Marks D.S. and Sander C. (2008) The microRNA.org resource: Targets and expression. *Nucleic Acids Res.,* **36**, D149-53.
185. Babiarz J.E. and Blelloch R. (2008) Small RNAs - their Biogenesis, Regulation and Function in Embryonic Stem Cells. In *StemBook.* Cambridge (MA), .

186. Chiang H.R., Schoenfeld L.W., Ruby J.G., Auyeung V.C., Spies N., Baek D., Johnston W.K., Russ C., Luo S., Babiarz J.E. *et al.* (2010) Mammalian microRNAs: Experimental evaluation of novel and previously annotated genes. *Genes Dev.,* **24**, 992-1009.

187. Okamura K., Hagen J.W., Duan H., Tyler D.M. and Lai E.C. (2007) The mirtron pathway generates microRNA-class regulatory RNAs in drosophila. *Cell,* **130**, 89-100.

188. Brameier M., Herwig A., Reinhardt R., Walter L. and Gruber J. (2011) Human box C/D snoRNAs with miRNA like functions: Expanding the range of regulatory RNAs. *Nucleic Acids Res.,* **39**, 675-686.

189. Babiarz J.E., Ruby J.G., Wang Y., Bartel D.P. and Blelloch R. (2008) Mouse ES cells express endogenous shRNAs, siRNAs, and other microprocessor-independent, dicer-dependent small RNAs. *Genes Dev.,* **22**, 2773-2785.

190. Chapman E.J. and Carrington J.C. (2007) Specialization and evolution of endogenous small RNA pathways. *Nat. Rev. Genet.,* **8**, 884-896.

191. Ruby J.G., Jan C., Player C., Axtell M.J., Lee W., Nusbaum C., Ge H. and Bartel D.P. (2006) Large-scale sequencing reveals 21U-RNAs and additional microRNAs and endogenous siRNAs in C. elegans. *Cell,* **127**, 1193-1207.

192. Czech B., Malone C.D., Zhou R., Stark A., Schlingeheyde C., Dus M., Perrimon N., Kellis M., Wohlschlegel J.A., Sachidanandam R. *et al.* (2008) An endogenous small interfering RNA pathway in drosophila. *Nature,* **453**, 798-802.

193. Ghildiyal M., Seitz H., Horwich M.D., Li C., Du T., Lee S., Xu J., Kittler E.L., Zapp M.L., Weng Z. *et al.* (2008) Endogenous siRNAs derived from transposons and mRNAs in drosophila somatic cells. *Science,* **320**, 1077-1081.

194. Okamura K., Balla S., Martin R., Liu N. and Lai E.C. (2008) Two distinct mechanisms generate endogenous siRNAs from bidirectional transcription in drosophila melanogaster. *Nat. Struct. Mol. Biol.,* **15**, 581-590.

195. Okamura K., Chung W.J., Ruby J.G., Guo H., Bartel D.P. and Lai E.C. (2008) The drosophila hairpin RNA pathway generates endogenous short interfering RNAs. *Nature,* **453**, 803-806.

196. Tam O.H., Aravin A.A., Stein P., Girard A., Murchison E.P., Cheloufi S., Hodges E., Anger M., Sachidanandam R., Schultz R.M. *et al.* (2008) Pseudogene-derived small interfering RNAs regulate gene expression in mouse oocytes. *Nature,* **453**, 534-538.

197. Watanabe T., Takeda A., Tsukiyama T., Mise K., Okuno T., Sasaki H., Minami N. and Imai H. (2006) Identification and characterization of two novel classes of small RNAs in the mouse germline: Retrotransposon-derived siRNAs in oocytes and germline small RNAs in testes. *Genes Dev.,* **20**, 1732-1743.

198. Watanabe T., Totoki Y., Toyoda A., Kaneda M., Kuramochi-Miyagawa S., Obata Y., Chiba H., Kohara Y., Kono T., Nakano T. *et al.* (2008) Endogenous siRNAs from naturally formed dsRNAs regulate transcripts in mouse oocytes. *Nature,* **453**, 539-543.

199. Flynt A.S., Greimann J.C., Chung W.J., Lima C.D. and Lai E.C. (2010) MicroRNA biogenesis via splicing and exosome-mediated trimming in drosophila. *Mol. Cell,* **38**, 900-907.

200. Babiarz J.E., Hsu R., Melton C., Thomas M., Ullian E.M. and Blelloch R. (2011) A role for noncanonical microRNAs in the mammalian brain revealed by phenotypic differences in Dgcr8 versus Dicer1 knockouts and small RNA sequencing. *RNA,* **17**, 1489-1501.

201. Jurka J. and Smith T. (1988) A fundamental division in the alu family of repeated sequences. *Proc. Natl. Acad. Sci. U. S. A.,* **85**, 4775-4778.

202. Yang J.H., Li J.H., Shao P., Zhou H., Chen Y.Q. and Qu L.H. (2011) starBase: A database for exploring microRNA-mRNA interaction maps from argonaute CLIP-seq and degradome-seq data. *Nucleic Acids Res.,* **39**, D202-9.

203. Swindell W.R., Johnston A., Carbajal S., Han G., Wohn C., Lu J., Xing X., Nair R.P., Voorhees J.J., Elder J.T. *et al.* (2011) Genome-wide expression profiling of five mouse models identifies similarities and differences with human psoriasis. *PLoS One,* **6**, e18266.

204. Terzian T., Torchia E.C., Dai D., Robinson S.E., Murao K., Stiegmann R.A., Gonzalez V., Boyle G.M., Powell M.B., Pollock P.M. *et al.* (2010) P53 prevents progression of nevi to melanoma predominantly through cell cycle regulation. *Pigment Cell. Melanoma Res.,* **23**, 781-794.

205. Danovi D., Meulmeester E., Pasini D., Migliorini D., Capra M., Frenk R., de Graaf P., Francoz S., Gasparini P., Gobbi A. *et al.* (2004) Amplification of mdmx (or Mdm4) directly contributes to tumor formation by inhibiting p53 tumor suppressor activity. *Mol. Cell. Biol.,* **24**, 5835-5843.

206. Echtermeyer F., Streit M., Wilcox-Adelman S., Saoncella S., Denhez F., Detmar M. and Goetinck P. (2001) Delayed wound repair and impaired angiogenesis in mice lacking syndecan-4. *J. Clin. Invest.,* **107**, R9-R14.

207. Berezikov E., Robine N., Samsonova A., Westholm J.O., Naqvi A., Hung J.H., Okamura K., Dai Q., Bortolamiol-Becet D., Martin R. *et al.* (2011) Deep annotation of drosophila melanogaster microRNAs yields insights into their processing, modification, and emergence. *Genome Res.,* **21**, 203-215.

208. Frank F., Sonenberg N. and Nagar B. (2010) Structural basis for 5'-nucleotide base-specific recognition of guide RNA by human AGO2. *Nature,* **465**, 818-822.
209. Czech B. and Hannon G.J. (2011) Small RNA sorting: Matchmaking for argonautes. *Nat. Rev. Genet.,* **12**, 19-31.

210. Hafner M., Landthaler M., Burger L., Khorshid M., Hausser J., Berninger P., Rothballer A., Ascano M.,Jr, Jungkamp A.C., Munschauer M. *et al.* (2010) Transcriptome-wide identification of RNA-binding protein and microRNA target sites by PAR-CLIP. *Cell,* **141**, 129-141.

211. Smalheiser N.R. and Torvik V.I. (2005) Mammalian microRNAs derived from genomic repeats. *Trends Genet.,* **21**, 322-326.

212. Okamura K. and Lai E.C. (2008) Endogenous small interfering RNAs in animals. *Nat. Rev. Mol. Cell Biol.,* **9**, 673-678.

213. Allen E., Xie Z., Gustafson A.M., Sung G.H., Spatafora J.W. and Carrington J.C. (2004) Evolution of microRNA genes by inverted duplication of target gene sequences in arabidopsis thaliana. *Nat. Genet.,* **36**, 1282-1290.

214. Huntzinger E. and Izaurralde E. (2011) Gene silencing by microRNAs: Contributions of translational repression and mRNA decay. *Nat. Rev. Genet.,* **12**, 99-110.

215. Rice P., Longden I. and Bleasby A. (2000) EMBOSS: The european molecular biology open software suite. *Trends Genet.,* **16**, 276-277.

216. Blanchette M., Kent W.J., Riemer C., Elnitski L., Smit A.F., Roskin K.M., Baertsch R., Rosenbloom K., Clawson H., Green E.D. *et al.* (2004) Aligning multiple genomic sequences with the threaded blockset aligner. *Genome Res.,* **14**, 708-715.

217. Altschul S.F., Gish W., Miller W., Myers E.W. and Lipman D.J. (1990) Basic local alignment search tool. *J. Mol. Biol.,* **215**, 403-410.

218. Breitling R., Armengaud P., Amtmann A. and Herzyk P. (2004) Rank products: A simple, yet powerful, new method to detect differentially regulated genes in replicated microarray experiments. *FEBS Lett.,* **573**, 83-92.

219. Wu Q., Kim Y.C., Lu J., Xuan Z., Chen J., Zheng Y., Zhou T., Zhang M.Q., Wu C.I. and Wang S.M. (2008) Poly A- transcripts expressed in HeLa cells. *PLoS One,* **3**, e2803.

220. Yang L., Duff M.O., Graveley B.R., Carmichael G.G. and Chen L.L. (2011) Genomewide characterization of non-polyadenylated RNAs. *Genome Biol.,* **12**, R16.

221. Sonkoly E., Bata-Csorgo Z., Pivarcsi A., Polyanka H., Kenderessy-Szabo A., Molnar G., Szentpali K., Bari L., Megyeri K., Mandi Y. *et al.* (2005) Identification and characterization of a novel, psoriasis susceptibility-related noncoding RNA gene, PRINS. *J. Biol. Chem.,* **280**, 24159-24167.

222. Joyce C.E., Zhou X., Xia J., Ryan C., Thrash B., Menter A., Zhang W., Bowcock, A.M. (2011) Deep sequencing of small RNAs from human skin reveals major alterations to the psoriasis miRNAome. *Hum. Mol. Genet.*, **20**, 4025-40.

Appendix A.

Differentially expressed miRNAs predicted to target differentially expressed transcripts in psoriatic skin

Table A-1. Differentially expressed miRNAs targeting differentially expressed transcripts in psoriasis

DOWNREGULATED TARGETS OF DE MIRNAs (up and downreg miRNAs listed):

Transcript	PP/NN	Targeting miRNA (PP/NN)
>AKR1B10	57.64	hsa-miR-375(-2.41),hsa-miR-665(2.34)
>SERPINB4	57.48	hsa-miR-542-3p(1.31)
>SERPINB3	40.89	hsa-miR-7(3.05),hsa-miR-542-3p(1.31)
>IL1F9	36.34	hsa-miR-155(2.7),hsa-miR-944(2.85)
>C10orf99	31.76	hsa-miR-431(3.91),hsa-miR-33b(2.23),hsa-miR-665(2.34)
>KYNU	25.46	hsa-miR-33b(2.23),hsa-miR-542-3p(1.31),hsa-miR-375(-2.41),hsa-miR-1307(1.97)
>IL8	17.47	hsa-miR-129-5p(-2.62),hsa-miR-944(2.85),hsa-miR-665(2.34),hsa-miR-369-3p(2.31)
>KRT16	16.98	hsa-miR-665(2.34)
>ADAMDEC1	15.86	hsa-miR-7(3.05),hsa-miR-378(2.68),hsa-miR-18a(2.43),hsa-miR-1276(2.14),hsa-miR-628-3p(-1.87)
>GDA	14.40	hsa-miR-211(2.6),hsa-miR-146a(2.36),hsa-miR-33b(2.23),hsa-miR-212(2.08),hsa-miR-590-3p(1.94),hsa-miR-10a(-2.31),hsa-miR-129-5p(-2.62),hsa-miR-944(2.85),hsa-miR-211(2.6),hsa-miR-146a(2.36),hsa-miR-665(2.34),hsa-miR-548f(2.32),hsa-miR-369-3p(2.31),hsa-miR-33b(2.23),hsa-miR-487a(2.12),hsa-miR-1308(2.03),hsa-miR-628-3p(-1.87),hsa-miR-1179(-2.02)
>TMPRSS11D	12.18	hsa-miR-135b(5.65),hsa-miR-431(3.91),hsa-miR-211(2.6),hsa-miR-142-3p(2.52),hsa-miR-590-3p(1.94),hsa-miR-944(2.85),hsa-miR-1308(2.03),hsa-miR-885-5p(-2.56)
>SLC6A14	10.59	hsa-miR-21(3.95),hsa-miR-377(1.81),hsa-miR-944(2.85),hsa-miR-1303(2.66)
>OASL	9.88	hsa-miR-944(2.85),hsa-miR-548f(2.32)
>KLK13	9.77	hsa-miR-206(12.8),hsa-miR-376b(1.73),hsa-miR-542-3p(1.31)
>RRM2	9.20	hsa-miR-31(42.93),hsa-miR-590-3p(1.94),hsa-miR-377(1.81),hsa-miR-548f(2.32),hsa-miR-486-3p(-2.56)
>OAS2	8.97	hsa-miR-206(12.8),hsa-miR-135b(5.65),hsa-miR-155(2.7),hsa-miR-378(2.68),hsa-miR-135b(5.65),hsa-miR-155(2.7),hsa-miR-885-5p(-2.56)
>CLEC7A	8.72	hsa-miR-135b(5.65),hsa-miR-10a(-2.31),hsa-miR-944(2.85),hsa-miR-940(2.79),hsa-miR-1303(2.66),hsa-miR-369-3p(2.31),hsa-miR-487a(2.12),hsa-miR-628-3p(-1.87)
>ATP12A	8.00	hsa-miR-1276(2.14),hsa-miR-885-5p(-2.56)
>STAT1	7.98	hsa-miR-155(2.7),hsa-miR-146a(2.36),hsa-miR-223(2.13),hsa-miR-590-3p(1.94),hsa-miR-592(2.92),hsa-miR-1303(2.66),hsa-miR-548f(2.32),hsa-miR-223(2.13)
>ZC3H12A	7.73	hsa-miR-486-3p(-2.56)
>GJB2	7.31	hsa-miR-592(2.92),hsa-miR-944(2.85),hsa-miR-1303(2.66),hsa-miR-665(2.34),hsa-miR-487a(2.12)
>HERC6	7.04	hsa-miR-10a(-2.31),hsa-miR-1303(2.66)
>RGS1	6.96	hsa-miR-21(3.95),hsa-miR-431(3.91),hsa-miR-211(2.6),hsa-miR-223(2.13),hsa-miR-376b(1.73),hsa-miR-21(3.95),hsa-miR-944(2.85),hsa-miR-211(2.6),hsa-miR-369-3p(2.31)
>IL1F5	6.62	hsa-miR-542-3p(1.31),hsa-miR-137(-2.37),hsa-miR-548f(2.32)
>SPRR3	6.61	hsa-miR-135b(5.65)
>SPRR1A	6.41	hsa-miR-7(3.05),hsa-miR-542-3p(1.31),hsa-miR-509-5p(1.61)
>CCL18	6.22	hsa-miR-33b(2.23)
>CXCL9	6.06	hsa-miR-31(42.93),hsa-miR-378(2.68),hsa-miR-211(2.6),hsa-miR-33b(2.23),hsa-miR-137(-2.37),hsa-miR-592(2.92),hsa-miR-944(2.85),hsa-miR-940(2.79),hsa-miR-211(2.6),hsa-miR-455-3p(2.46),hsa-miR-1308(2.03)
>CXCL13	6.01	hsa-miR-496(3.02),hsa-miR-590-3p(1.94),hsa-miR-376b(1.73),hsa-miR-486-5p(-1.81)
>CCNB1	5.97	hsa-miR-496(3.02),hsa-miR-590-3p(1.94),hsa-miR-548f(2.32)
>RGS20	5.93	hsa-miR-496(3.02),hsa-miR-211(2.6),hsa-miR-142-3p(2.52),hsa-miR-212(2.08),hsa-miR-188-5p(2.36)
>A2ML1	5.88	hsa-miR-431(3.91),hsa-miR-7(3.05),hsa-miR-944(2.85),hsa-miR-211(2.6)
>CXCL1	5.81	hsa-miR-944(2.85),hsa-miR-548f(2.32),hsa-miR-369-3p(2.31),hsa-miR-487a(2.12),hsa-miR-135b(5.65),hsa-miR-7(3.05),hsa-miR-212(2.08),hsa-miR-135b(5.65),hsa-miR-665(2.34),hsa-miR-369-3p(2.31),hsa-miR-1276(2.14),hsa-miR-1179(-2.02)
>GZMB	5.70	hsa-miR-378(2.68)
>TGM1	5.64	hsa-miR-142-3p(2.52)
>HAS3	5.62	hsa-miR-206(12.8),hsa-miR-155(2.7),hsa-miR-33b(2.23),hsa-miR-377(1.81),hsa-miR-486-5p(-1.81),hsa-miR-10a(-2.31),hsa-miR-375(-2.41),hsa-miR-21(3.95),hsa-miR-944(2.85),hsa-miR-155(2.7),hsa-miR-33b(2.23),hsa-miR-1308(2.03),hsa-miR-509-5p(1.61)
>SOD2	5.55	hsa-miR-211(2.6),hsa-miR-377(1.81),hsa-miR-129-5p(-2.62),hsa-miR-944(2.85),hsa-miR-211(2.6),hsa-miR-1276(2.14),hsa-miR-509-5p(1.61),hsa-miR-486-3p(-2.56)
>OAS1	5.52	hsa-miR-31(42.93),hsa-miR-378(2.68),hsa-miR-1303(2.66)
>EPSTI1	5.51	hsa-miR-944(2.85)
>MXD1	5.45	hsa-miR-31(42.93),hsa-miR-206(12.8),hsa-miR-137(-2.37),hsa-miR-1268(4.45),hsa-miR-21(3.95),hsa-miR-944(2.85),hsa-miR-211(2.6),hsa-miR-628-3p(-1.87),hsa-miR-885-5p(-2.56)
>CNFN	5.43	hsa-miR-7(3.05)
>RSAD2	5.26	hsa-miR-21(3.95),hsa-miR-431(3.91),hsa-miR-548f(2.32)
>WNT5A	5.02	hsa-miR-155(2.7),hsa-miR-142-3p(2.52),hsa-miR-590-3p(1.94),hsa-miR-129-5p(-2.62),hsa-miR-548f(2.32),hsa-miR-369-3p(2.31),hsa-miR-1276(2.14),hsa-miR-487a(2.12),hsa-miR-885-5p(-2.56)

>TGM3	5.00	hsa-miR-206(12.8),hsa-miR-1268(4.45),hsa-miR-486-3p(-2.56)
>SAMD9	4.98	hsa-miR-31(42.93),hsa-miR-21(3.95),hsa-miR-211(2.6),hsa-miR-590-3p(1.94),hsa-miR-137(-2.37),hsa-miR-129-5p(-2.62),hsa-miR-944(2.85),hsa-miR-211(2.6),hsa-miR-885-5p(-2.56)
>EHF	4.91	hsa-miR-206(12.8),hsa-miR-431(3.91),hsa-miR-7(3.05),hsa-miR-142-3p(2.52),hsa-miR-212(2.08),hsa-miR-590-3p(1.94),hsa-miR-377(1.81),hsa-miR-137(-2.37),hsa-miR-665(2.34),hsa-miR-548f(2.32),hsa-miR-1276(2.14),hsa-miR-377(1.81),hsa-miR-1179(-2.02)
>UPP1	4.90	hsa-miR-590-3p(1.94)
>ARSF	4.77	hsa-miR-206(12.8)
>KCNJ15	4.75	hsa-miR-206(12.8),hsa-miR-223(2.13),hsa-miR-129-5p(-2.62),hsa-miR-455-3p(2.46),hsa-miR-1276(2.14)
>HAL	4.72	hsa-miR-155(2.7),hsa-miR-137(-2.37),hsa-miR-369-3p(2.31),hsa-miR-885-5p(-2.56)
>LAMP3	4.65	hsa-miR-377(1.81),hsa-miR-375(-2.41),hsa-miR-944(2.85)
>VNN3	4.52	hsa-miR-31(42.93),hsa-miR-135b(5.65),hsa-miR-486-5p(-1.81),hsa-miR-455-3p(2.46)
>MX1	4.50	hsa-miR-211(2.6),hsa-miR-223(2.13),hsa-miR-188-5p(2.36)
>FCHSD1	4.40	hsa-miR-1268(4.45),hsa-miR-188-5p(2.36),hsa-miR-885-5p(-2.56)
>ALOX12B	4.37	hsa-miR-129-5p(-2.62)
>SLC5A1	4.34	hsa-miR-135b(5.65),hsa-miR-211(2.6)
>SPTLC2	4.34	hsa-miR-146a(2.36),hsa-miR-223(2.13),hsa-miR-212(2.08),hsa-miR-542-3p(1.31),hsa-miR-137(-2.37),hsa-miR-211(2.6),hsa-miR-146a(2.36),hsa-miR-1179(-2.02)
>WFDC12	4.33	hsa-miR-378(2.68),hsa-miR-377(1.81),hsa-miR-137(-2.37)
>SH3PXD2A	4.26	hsa-miR-590-3p(1.94),hsa-miR-944(2.85)
>KIAA0101	4.24	hsa-miR-378(2.68),hsa-miR-590-3p(1.94),hsa-miR-940(2.79),hsa-miR-378(2.68),hsa-miR-1303(2.66),hsa-miR-1276(2.14)
>TMEM45B	4.19	hsa-miR-431(3.91),hsa-miR-590-3p(1.94),hsa-miR-944(2.85),hsa-miR-548f(2.32),hsa-miR-10a(-2.31)
>OAS3	4.08	hsa-miR-378(2.68),hsa-miR-211(2.6),hsa-miR-146a(2.36),hsa-miR-542-3p(1.31),hsa-miR-944(2.85),hsa-miR-378(2.68),hsa-miR-188-5p(2.36),hsa-miR-665(2.34),hsa-miR-1276(2.14),hsa-miR-487a(2.12),hsa-miR-1179(-2.02),hsa-miR-486-3p(-2.56)
>CKS2	4.06	hsa-miR-7(3.05),hsa-miR-548f(2.32)
>CARHSP1	4.05	hsa-miR-31(42.93),hsa-miR-155(2.7),hsa-miR-665(2.34),hsa-miR-548f(2.32),hsa-miR-1276(2.14),hsa-miR-377(1.81)
>KLK10	4.04	hsa-miR-206(12.8),hsa-miR-21(3.95),hsa-miR-18a(2.43),hsa-miR-21(3.95),hsa-miR-486-3p(-2.56)
>CHRNA9	4.02	hsa-miR-590-3p(1.94),hsa-miR-129-5p(-2.62),hsa-miR-944(2.85)
>PLAT	3.97	hsa-miR-486-5p(-1.81),hsa-miR-455-3p(2.46),hsa-miR-548f(2.32)
>RAB27A	3.95	hsa-miR-31(42.93),hsa-miR-590-3p(1.94),hsa-miR-376b(1.73),hsa-miR-542-3p(1.31),hsa-miR-944(2.85),hsa-miR-940(2.79)
>CDKN3	3.95	hsa-miR-146a(2.36),hsa-miR-548f(2.32)
>LRG1	3.90	hsa-miR-431(3.91),hsa-miR-7(3.05),hsa-miR-590-3p(1.94),hsa-miR-940(2.79),hsa-miR-1308(2.03)
>KRT6B	3.87	hsa-miR-146a(2.36),hsa-miR-369-3p(2.31)
>XDH	3.84	hsa-miR-496(3.02),hsa-miR-542-3p(1.31),hsa-miR-940(2.79),hsa-miR-211(2.6),hsa-miR-455-3p(2.46)
>ERO1L	3.78	hsa-miR-590-3p(1.94),hsa-miR-542-3p(1.31),hsa-miR-944(2.85),hsa-miR-487a(2.12)
>PBK	3.70	hsa-miR-590-3p(1.94),hsa-miR-885-5p(-2.56)
>MELK	3.69	hsa-miR-944(2.85)
>FOXE1	3.66	hsa-miR-155(2.7),hsa-miR-590-3p(1.94),hsa-miR-129-5p(-2.62),hsa-miR-455-3p(2.46)
>C12orf5	3.66	hsa-miR-369-3p(2.31),hsa-miR-590-3p(1.94),hsa-miR-376b(1.73),hsa-miR-146a(2.36),hsa-miR-369-3p(2.31)
>PARP9	3.63	hsa-miR-455-3p(2.46),hsa-miR-369-3p(2.31),hsa-miR-509-5p(1.61),hsa-miR-628-3p(-1.87)
>RTP4	3.63	hsa-miR-31(42.93),hsa-miR-885-5p(-2.56)
>SLC26A9	3.62	hsa-miR-378(2.68),hsa-miR-590-3p(1.94)
>CCNB2	3.59	hsa-miR-548f(2.32)
>GBP1	3.58	hsa-miR-21(3.95),hsa-miR-377(1.81),hsa-miR-376b(1.73),hsa-miR-542-3p(1.31),hsa-miR-137(-2.37),hsa-miR-944(2.85)
>GJB6	3.57	hsa-miR-7(3.05)
>CDH3	3.54	hsa-miR-665(2.34),hsa-miR-628-3p(-1.87),hsa-miR-1179(-2.02)
>CEP55	3.49	hsa-miR-590-3p(1.94),hsa-miR-944(2.85),hsa-miR-940(2.79),hsa-miR-1308(2.03)
>HYAL4	3.49	hsa-miR-211(2.6),hsa-miR-590-3p(1.94),hsa-miR-211(2.6)
>CCNA2	3.49	hsa-miR-590-3p(1.94),hsa-miR-129-5p(-2.62),hsa-miR-1303(2.66),hsa-miR-146a(2.36),hsa-miR-548f(2.32)
>ABCA12	3.45	hsa-miR-206(12.8),hsa-miR-377(1.81),hsa-miR-1276(2.14)
>ZDHHC21	3.43	hsa-miR-206(12.8),hsa-miR-223(2.13),hsa-miR-590-3p(1.94),hsa-miR-129-5p(-2.62),hsa-miR-944(2.85),hsa-miR-548f(2.32),hsa-miR-487a(2.12),hsa-miR-628-3p(-1.87),hsa-miR-1179(-2.02),hsa-miR-486-3p(-2.56)
>DSC2	3.42	hsa-miR-21(3.95),hsa-miR-211(2.6),hsa-miR-590-3p(1.94),hsa-miR-137(-2.37),hsa-miR-129-5p(-2.62),hsa-miR-592(2.92),hsa-miR-188-5p(2.36),hsa-miR-548f(2.32),hsa-miR-369-3p(2.31),hsa-miR-33b(2.23),hsa-miR-628-3p(-1.87)

>ZIC1	3.42	hsa-miR-206(12.8),hsa-miR-146a(2.36),hsa-miR-542-3p(1.31),hsa-miR-375(-2.41),hsa-miR-944(2.85),hsa-miR-1303(2.66),hsa-miR-509-5p(1.61),hsa-miR-1179(-2.02)
>ACPP	3.41	hsa-miR-590-3p(1.94),hsa-miR-129-5p(-2.62),hsa-miR-31(42.93),hsa-miR-486-3p(-2.56)
>SERPINB1	3.40	hsa-miR-137(-2.37),hsa-miR-129-5p(-2.62),hsa-miR-1303(2.66),hsa-miR-548f(2.32)
>GGH	3.39	hsa-miR-944(2.85)
>PPIF	3.38	hsa-miR-7(3.05),hsa-miR-590-3p(1.94),hsa-miR-542-3p(1.31),hsa-miR-940(2.79),hsa-miR-665(2.34),hsa-miR-548f(2.32),hsa-miR-486-3p(-2.56)
>BIRC5	3.36	hsa-miR-135b(5.65),hsa-miR-377(1.81),hsa-miR-542-3p(1.31),hsa-miR-1303(2.66),hsa-miR-548f(2.32),hsa-miR-377(1.81)
>PRSS3	3.35	hsa-miR-509-5p(1.61)
>KIF20A	3.34	hsa-miR-496(3.02),hsa-miR-369-3p(2.31)
>VNN1	3.34	hsa-miR-223(2.13),hsa-miR-590-3p(1.94),hsa-miR-10a(-2.31),hsa-miR-369-3p(2.31),hsa-miR-1276(2.14),hsa-miR-223(2.13),hsa-miR-628-3p(-1.87)
>FUT2	3.33	hsa-miR-431(3.91),hsa-miR-944(2.85),hsa-miR-940(2.79),hsa-miR-1308(2.03)
>SLC7A5	3.32	hsa-miR-33b(2.23)
>AURKA	3.32	hsa-miR-377(1.81),hsa-miR-1179(-2.02)
>DDX58	3.30	hsa-miR-31(42.93),hsa-miR-135b(5.65),hsa-miR-146a(2.36),hsa-miR-377(1.81),hsa-miR-455-3p(2.46),hsa-miR-628-3p(-1.87),hsa-miR-885-5p(-2.56)
>IFI44	3.29	hsa-miR-211(2.6),hsa-miR-590-3p(1.94),hsa-miR-944(2.85),hsa-miR-188-5p(2.36),hsa-miR-31(42.93),hsa-miR-206(12.8),hsa-miR-590-3p(1.94),hsa-miR-129-5p(-2.62),hsa-miR-944(2.85),hsa-miR-1303(2.66),hsa-miR-548f(2.32),hsa-miR-1308(2.03),hsa-miR-509-5p(1.61)
>CCR7	3.28	hsa-miR-21(3.95),hsa-miR-378(2.68)
>MMP1	3.27	hsa-miR-188-5p(2.36),hsa-miR-590-3p(1.94),hsa-miR-455-3p(2.46)
>LASS3	3.27	hsa-miR-378(2.68),hsa-miR-590-3p(1.94),hsa-miR-592(2.92),hsa-miR-665(2.34),hsa-miR-548f(2.32),hsa-miR-369-3p(2.31),hsa-miR-509-5p(1.61)
>CHAC1	3.25	hsa-miR-940(2.79)
>SERPINA1	3.25	hsa-miR-212(2.08),hsa-miR-592(2.92),hsa-miR-940(2.79),hsa-miR-33b(2.23)
>SAMSN1	3.24	hsa-miR-206(12.8),hsa-miR-590-3p(1.94),hsa-miR-377(1.81),hsa-miR-375(-2.41),hsa-miR-129-5p(-2.62),hsa-miR-944(2.85),hsa-miR-1303(2.66),hsa-miR-548f(2.32),hsa-miR-1179(-2.02)
>MKI67	3.22	hsa-miR-206(12.8),hsa-miR-18a(2.43),hsa-miR-146a(2.36),hsa-miR-548f(2.32),hsa-miR-486-3p(-2.56)
>GBP6	3.20	hsa-miR-21(3.95),hsa-miR-146a(2.36),hsa-miR-129-5p(-2.62),hsa-miR-940(2.79),hsa-miR-146a(2.36),hsa-miR-628-3p(-1.87),hsa-miR-1179(-2.02)
>GM2A	3.19	hsa-miR-135b(5.65),hsa-miR-137(-2.37),hsa-miR-129-5p(-2.62),hsa-miR-940(2.79),hsa-miR-1303(2.66),hsa-miR-486-3p(-2.56)
>VSNL1	3.18	hsa-miR-21(3.95),hsa-miR-211(2.6),hsa-miR-590-3p(1.94),hsa-miR-376b(1.73),hsa-miR-137(-2.37),hsa-miR-455-3p(2.46),hsa-miR-369-3p(2.31),hsa-miR-509-5p(1.61),hsa-miR-1179(-2.02)
>CRABP2	3.16	hsa-miR-486-3p(-2.56)
>KLRC4	3.16	hsa-miR-223(2.13),hsa-miR-548f(2.32),hsa-miR-1308(2.03)
>OTUB2	3.14	hsa-miR-206(12.8),hsa-miR-155(2.7),hsa-miR-378(2.68),hsa-miR-590-3p(1.94),hsa-miR-377(1.81),hsa-miR-542-3p(1.31),hsa-miR-129-5p(-2.62),hsa-miR-592(2.92),hsa-miR-940(2.79),hsa-miR-455-3p(2.46),hsa-miR-188-5p(2.36),hsa-miR-487a(2.12)
>RNASE7	3.13	hsa-miR-7(3.05),hsa-miR-1303(2.66),hsa-miR-1276(2.14),hsa-miR-486-3p(-2.56)
>S100A2	3.11	hsa-miR-129-5p(-2.62),hsa-miR-665(2.34)
>DSG3	3.11	hsa-miR-135b(5.65),hsa-miR-21(3.95),hsa-miR-211(2.6),hsa-miR-223(2.13),hsa-miR-590-3p(1.94),hsa-miR-137(-2.37),hsa-miR-129-5p(-2.62),hsa-miR-21(3.95),hsa-miR-944(2.85),hsa-miR-188-5p(2.36),hsa-miR-369-3p(2.31)
>PI15	3.10	hsa-miR-206(12.8),hsa-miR-135b(5.65),hsa-miR-21(3.95),hsa-miR-378(2.68),hsa-miR-211(2.6),hsa-miR-146a(2.36),hsa-miR-590-3p(1.94),hsa-miR-377(1.81),hsa-miR-376b(1.73),hsa-miR-135b(5.65),hsa-miR-592(2.92),hsa-miR-944(2.85),hsa-miR-1303(2.66),hsa-miR-211(2.6),hsa-miR-369-3p(2.31),hsa-miR-1308(2.03)
>JMY	3.10	hsa-miR-155(2.7)
>TTK	3.08	hsa-miR-129-5p(-2.62),hsa-miR-455-3p(2.46)
>TMC5	3.08	hsa-miR-431(3.91),hsa-miR-496(3.02),hsa-miR-223(2.13),hsa-miR-590-3p(1.94),hsa-miR-486-3p(-2.56)
>CXCR4	3.08	hsa-miR-206(12.8),hsa-miR-211(2.6),hsa-miR-548f(2.32)
>ATP10B	3.07	hsa-miR-31(42.93),hsa-miR-135b(5.65),hsa-miR-211(2.6),hsa-miR-146a(2.36),hsa-miR-590-3p(1.94),hsa-miR-137(-2.37),hsa-miR-129-5p(-2.62),hsa-miR-592(2.92),hsa-miR-211(2.6),hsa-miR-455-3p(2.46),hsa-miR-188-5p(2.36),hsa-miR-1276(2.14),hsa-miR-487a(2.12),hsa-miR-509-5p(1.61),hsa-miR-1179(-2.02),hsa-miR-885-5p(-2.56)
>UHRF1	3.07	hsa-miR-7(3.05),hsa-miR-378(2.68),hsa-miR-146a(2.36),hsa-miR-590-3p(1.94),hsa-miR-378(2.68),hsa-miR-188-5p(2.36)
>ALDH1A3	3.04	hsa-miR-7(3.05),hsa-miR-590-3p(1.94),hsa-miR-1179(-2.02)
>LYZ	3.04	hsa-miR-206(12.8),hsa-miR-142-3p(2.52),hsa-miR-10a(-2.31),hsa-miR-944(2.85),hsa-miR-369-3p(2.31)
>SOCS3	3.03	hsa-miR-548f(2.32),hsa-miR-1276(2.14),hsa-miR-1179(-2.02)
>GRHL3	3.01	hsa-miR-7(3.05),hsa-miR-496(3.02),hsa-miR-129-5p(-2.62)
>TMPRSS4	3.00	hsa-miR-496(3.02),hsa-miR-142-3p(2.52),hsa-miR-137(-2.37),hsa-miR-188-5p(2.36),hsa-miR-369-3p(2.31),hsa-miR-1179(-2.02),hsa-miR-486-3p(-2.56)
>APOBEC3B	2.99	hsa-miR-7(3.05),hsa-miR-1303(2.66)
>TOP2A	2.97	hsa-miR-21(3.95),hsa-miR-590-3p(1.94),hsa-miR-377(1.81),hsa-miR-944(2.85),hsa-miR-548f(2.32)
>SLAMF7	2.96	hsa-miR-378(2.68),hsa-miR-33b(2.23),hsa-miR-378(2.68)

>NFKBIZ	2.96	hsa-miR-31(42.93),hsa-miR-187(2.17),hsa-miR-376b(1.73),hsa-miR-486-5p(-1.81),hsa-miR-10a(-2.31),hsa-miR-940(2.79),hsa-miR-1303(2.66),hsa-miR-548f(2.32),hsa-miR-369-3p(2.31)
>TRIM14	2.95	hsa-miR-142-3p(2.52),hsa-miR-223(2.13),hsa-miR-590-3p(1.94),hsa-miR-129-5p(-2.62),hsa-miR-18a(2.43)
>MMP9	2.95	hsa-miR-211(2.6),hsa-miR-1303(2.66)
>PTGER3	2.94	hsa-miR-211(2.6),hsa-miR-33b(2.23),hsa-miR-590-3p(1.94),hsa-miR-376b(1.73),hsa-miR-542-3p(1.31),hsa-miR-129-5p(-2.62),hsa-miR-944(2.85),hsa-miR-211(2.6),hsa-miR-369-3p(2.31),hsa-miR-33b(2.23),hsa-miR-223(2.13),hsa-miR-487a(2.12),hsa-miR-628-3p(-1.87)
>GK	2.93	hsa-miR-7(3.05),hsa-miR-590-3p(1.94),hsa-miR-542-3p(1.31),hsa-miR-137(-2.37),hsa-miR-129-5p(-2.62),hsa-miR-944(2.85),hsa-miR-369-3p(2.31),hsa-miR-1276(2.14),hsa-miR-1179(-2.02)
>MAD2L1	2.93	hsa-miR-376b(1.73),hsa-miR-548f(2.32)
>FAM43A	2.91	hsa-miR-146a(2.36),hsa-miR-542-3p(1.31),hsa-miR-146a(2.36)
>CD47	2.91	hsa-miR-206(12.8),hsa-miR-135b(5.65),hsa-miR-21(3.95),hsa-miR-431(3.91),hsa-miR-7(3.05),hsa-miR-155(2.7),hsa-miR-18a(2.43),hsa-miR-590-3p(1.94),hsa-miR-376b(1.73),hsa-miR-486-5p(-1.81),hsa-miR-129-5p(-2.62),hsa-miR-21(3.95),hsa-miR-944(2.85),hsa-miR-940(2.79),hsa-miR-1303(2.66),hsa-miR-665(2.34),hsa-miR-548f(2.32),hsa-miR-369-3p(2.31),hsa-miR-1276(2.14),hsa-miR-509-5p(1.61),hsa-miR-885-5p(-2.56)
>CDK5R1	2.90	hsa-miR-7(3.05),hsa-miR-142-3p(2.52),hsa-miR-33b(2.23),hsa-miR-129-5p(-2.62),hsa-miR-548f(2.32),hsa-miR-1308(2.03),hsa-miR-10a(-2.31)
>AMMECR1	2.90	hsa-miR-7(3.05),hsa-miR-542-3p(1.31),hsa-miR-137(-2.37),hsa-miR-129-5p(-2.62),hsa-miR-944(2.85),hsa-miR-940(2.79),hsa-miR-1303(2.66),hsa-miR-211(2.6),hsa-miR-188-5p(2.36),hsa-miR-885-5p(-2.56)
>SELE	2.86	hsa-miR-31(42.93),hsa-miR-7(3.05),hsa-miR-378(2.68),hsa-miR-211(2.6),hsa-miR-377(1.81),hsa-miR-944(2.85),hsa-miR-548f(2.32),hsa-miR-369-3p(2.31),hsa-miR-1179(-2.02)
>IVL	2.86	hsa-miR-665(2.34)
>CARD6	2.85	hsa-miR-590-3p(1.94),hsa-miR-944(2.85),hsa-miR-940(2.79),hsa-miR-1303(2.66),hsa-miR-369-3p(2.31)
>C14orf147	2.83	hsa-miR-31(42.93),hsa-miR-155(2.7),hsa-miR-590-3p(1.94),hsa-miR-129-5p(-2.62),hsa-miR-665(2.34),hsa-miR-548f(2.32),hsa-miR-885-5p(-2.56)
>GPX2	2.82	hsa-miR-18a(2.43)
>CLCA2	2.82	hsa-miR-7(3.05),hsa-miR-211(2.6),hsa-miR-590-3p(1.94),hsa-miR-377(1.81),hsa-miR-376b(1.73),hsa-miR-375(-2.41),hsa-miR-548f(2.32),hsa-miR-1276(2.14),hsa-miR-1308(2.03)
>SELL	2.81	hsa-miR-211(2.6),hsa-miR-548f(2.32),hsa-miR-1276(2.14),hsa-miR-1308(2.03),hsa-miR-885-5p(-2.56),hsa-miR-486-3p(-2.56)
>PLAC8	2.81	hsa-miR-369-3p(2.31)
>DNASE1L3	2.79	hsa-miR-31(42.93),hsa-miR-1303(2.66)
>NETO2	2.78	hsa-miR-206(12.8),hsa-miR-21(3.95),hsa-miR-155(2.7),hsa-miR-142-3p(2.52),hsa-miR-590-3p(1.94),hsa-miR-377(1.81),hsa-miR-944(2.85),hsa-miR-155(2.7),hsa-miR-1303(2.66),hsa-miR-1276(2.14)
>STEAP4	2.77	hsa-miR-135b(5.65),hsa-miR-211(2.6),hsa-miR-33b(2.23),hsa-miR-223(2.13),hsa-miR-590-3p(1.94),hsa-miR-137(-2.37),hsa-miR-944(2.85),hsa-miR-211(2.6),hsa-miR-188-5p(2.36),hsa-miR-369-3p(2.31),hsa-miR-33b(2.23),hsa-miR-1276(2.14)
>WWTR1	2.76	hsa-miR-590-3p(1.94),hsa-miR-486-3p(-2.56)
>FCGR3B	2.75	hsa-miR-7(3.05),hsa-miR-378(2.68),hsa-miR-944(2.85),hsa-miR-369-3p(2.31)
>PLA2G3	2.73	hsa-miR-10a(-2.31),hsa-miR-129-5p(-2.62),hsa-miR-592(2.92),hsa-miR-940(2.79),hsa-miR-1303(2.66)
>IRAK2	2.72	hsa-miR-10a(-2.31),hsa-miR-940(2.79)
>HSD17B1	2.70	hsa-miR-548f(2.32)
>FAM83D	2.70	hsa-miR-142-3p(2.52),hsa-miR-486-5p(-1.81),hsa-miR-665(2.34),hsa-miR-1276(2.14)
>IFIT3	2.69	hsa-miR-431(3.91)
>NUSAP1	2.69	hsa-miR-590-3p(1.94),hsa-miR-542-3p(1.31),hsa-miR-10a(-2.31),hsa-miR-509-5p(1.61)
>HK2	2.68	hsa-miR-590-3p(1.94)
>PRKCQ	2.67	hsa-miR-31(42.93),hsa-miR-665(2.34)
>HMMR	2.65	hsa-miR-590-3p(1.94),hsa-miR-944(2.85)
>SFT2D2	2.64	hsa-miR-548f(2.32),hsa-miR-1308(2.03)
>TK1	2.63	hsa-miR-18a(2.43),hsa-miR-1268(4.45),hsa-miR-486-3p(-2.56)
>GNA15	2.63	hsa-miR-211(2.6),hsa-miR-542-3p(1.31),hsa-miR-486-3p(-2.56)
>SLC16A6	2.63	hsa-miR-206(12.8),hsa-miR-7(3.05),hsa-miR-211(2.6),hsa-miR-590-3p(1.94),hsa-miR-137(-2.37)
>WDR4	2.63	hsa-miR-486-3p(-2.56)
>GPR68	2.63	hsa-miR-378(2.68),hsa-miR-885-5p(-2.56)
>MYO5A	2.62	hsa-miR-146a(2.36),hsa-miR-590-3p(1.94),hsa-miR-944(2.85),hsa-miR-146a(2.36),hsa-miR-548f(2.32),hsa-miR-369-3p(2.31),hsa-miR-33b(2.23)
>TYMS	2.62	hsa-miR-129-5p(-2.62)
>BUB1B	2.62	hsa-miR-486-5p(-1.81)
>LCK	2.62	hsa-miR-18a(2.43)
>TPX2	2.61	hsa-miR-548f(2.32)
>EPN3	2.61	hsa-miR-33b(2.23),hsa-miR-542-3p(1.31),hsa-miR-10a(-2.31),hsa-miR-486-3p(-2.56)
>TMEM86A	2.61	hsa-miR-496(3.02),hsa-miR-378(2.68),hsa-miR-211(2.6),hsa-miR-33b(2.23),hsa-miR-223(2.13),hsa-miR-496(3.02),hsa-miR-378(2.68),hsa-miR-211(2.6),hsa-miR-33b(2.23),hsa-miR-223(2.13),hsa-miR-211(2.6)
>FBXO45	2.60	hsa-miR-206(12.8),hsa-miR-135b(5.65),hsa-miR-211(2.6),hsa-miR-142-3p(2.52),hsa-miR-590-3p(1.94),hsa-miR-542-3p(1.31),hsa-miR-129-5p(-2.62),hsa-miR-944(2.85),hsa-miR-1303(2.66),hsa-miR-188-5p(2.36),hsa-miR-

		665(2.34),hsa-miR-548f(2.32),hsa-miR-369-3p(2.31),hsa-miR-487a(2.12)
>KRT17	2.59	hsa-miR-486-3p(-2.56)
>CCNE1	2.59	hsa-miR-1179(-2.02)
>CD2	2.58	hsa-miR-137(-2.37),hsa-miR-155(2.7),hsa-miR-377(1.81),hsa-miR-10a(-2.31),hsa-miR-137(-2.37),hsa-miR-129-5p(-2.62),hsa-miR-592(2.92),hsa-miR-940(2.79),hsa-miR-548f(2.32),hsa-miR-509-5p(1.61),hsa-miR-1179(-2.02)
>GPT2	2.57	hsa-miR-378(2.68),hsa-miR-211(2.6),hsa-miR-377(1.81),hsa-miR-548f(2.32),hsa-miR-1179(-2.02)
>EREG	2.57	hsa-miR-496(3.02),hsa-miR-142-3p(2.52),hsa-miR-590-3p(1.94),hsa-miR-376b(1.73),hsa-miR-129-5p(-2.62),hsa-miR-944(2.85),hsa-miR-548f(2.32),hsa-miR-369-3p(2.31),hsa-miR-1276(2.14),hsa-miR-628-3p(-1.87),hsa-miR-1179(-2.02)
>LIPG	2.56	hsa-miR-31(42.93),hsa-miR-155(2.7),hsa-miR-378(2.68),hsa-miR-18a(2.43),hsa-miR-146a(2.36),hsa-miR-590-3p(1.94),hsa-miR-1179(-2.02),hsa-miR-885-5p(-2.56)
>ARG2	2.55	hsa-miR-10a(-2.31),hsa-miR-137(-2.37)
>EPHA2	2.55	hsa-miR-10a(-2.31)
>ZWINT	2.54	hsa-miR-10a(-2.31),hsa-miR-455-3p(2.46),hsa-miR-369-3p(2.31),hsa-miR-1308(2.03)
>IDH3A	2.54	hsa-miR-206(12.8),hsa-miR-7(3.05),hsa-miR-592(2.92),hsa-miR-455-3p(2.46),hsa-miR-885-5p(-2.56),hsa-miR-486-3p(-2.56)
>HR	2.54	hsa-miR-369-3p(2.31),hsa-miR-486-3p(-2.56)
>PGM2	2.53	hsa-miR-206(12.8),hsa-miR-135b(5.65),hsa-miR-431(3.91),hsa-miR-378(2.68),hsa-miR-223(2.13),hsa-miR-137(-2.37),hsa-miR-1308(2.03)
>TPBG	2.52	hsa-miR-212(2.08),hsa-miR-129-5p(-2.62),hsa-miR-944(2.85),hsa-miR-548f(2.32)
>TMEM40	2.52	hsa-miR-590-3p(1.94),hsa-miR-1303(2.66)
>APOL6	2.52	hsa-miR-211(2.6),hsa-miR-377(1.81),hsa-miR-10a(-2.31),hsa-miR-944(2.85),hsa-miR-665(2.34),hsa-miR-548f(2.32)
>NT5C3	2.52	hsa-miR-33b(2.23),hsa-miR-590-3p(1.94),hsa-miR-548f(2.32)
>MPHOSPH6	2.51	hsa-miR-146a(2.36),hsa-miR-377(1.81),hsa-miR-146a(2.36),hsa-miR-369-3p(2.31)
>YKT6	2.50	hsa-miR-212(2.08)
>ZBED2	2.50	hsa-miR-377(1.81)
>APOL1	2.50	hsa-miR-940(2.79),hsa-miR-211(2.6),hsa-miR-33b(2.23)
>C15orf48	2.50	hsa-miR-590-3p(1.94),hsa-miR-376b(1.73),hsa-miR-137(-2.37)
>MOXD1	2.49	hsa-miR-21(3.95),hsa-miR-496(3.02),hsa-miR-211(2.6),hsa-miR-376b(1.73),hsa-miR-542-3p(1.31),hsa-miR-486-5p(-1.81),hsa-miR-21(3.95),hsa-miR-211(2.6),hsa-miR-548f(2.32)
>UBE2F	2.48	hsa-miR-940(2.79),hsa-miR-1303(2.66),hsa-miR-455-3p(2.46)
>AASS	2.48	hsa-miR-377(1.81),hsa-miR-944(2.85)
>LGALS3BP	2.48	hsa-miR-590-3p(1.94)
>OBFC2A	2.47	hsa-miR-496(3.02),hsa-miR-376b(1.73),hsa-miR-137(-2.37),hsa-miR-548f(2.32),hsa-miR-369-3p(2.31)
>APOBEC3A	2.46	hsa-miR-7(3.05),hsa-miR-590-3p(1.94),hsa-miR-944(2.85),hsa-miR-1303(2.66)
>FUT3	2.46	hsa-miR-206(12.8),hsa-miR-431(3.91),hsa-miR-1303(2.66)
>NEK2	2.45	hsa-miR-377(1.81),hsa-miR-486-5p(-1.81),hsa-miR-369-3p(2.31),hsa-miR-628-3p(-1.87)
>DHRS9	2.44	hsa-miR-211(2.6),hsa-miR-376b(1.73),hsa-miR-486-3p(-2.56)
>FAM83A	2.43	hsa-miR-206(12.8),hsa-miR-431(3.91),hsa-miR-7(3.05),hsa-miR-376b(1.73)
>PDSS1	2.42	hsa-miR-590-3p(1.94)
>IL7R	2.41	hsa-miR-211(2.6),hsa-miR-590-3p(1.94),hsa-miR-211(2.6)
>CALML3	2.41	hsa-miR-486-3p(-2.56)
>TMEM49	2.41	hsa-miR-206(12.8),hsa-miR-223(2.13),hsa-miR-542-3p(1.31),hsa-miR-592(2.92),hsa-miR-147b(2.79)
>CCNE2	2.40	hsa-miR-31(42.93),hsa-miR-590-3p(1.94),hsa-miR-31(42.93),hsa-miR-1303(2.66),hsa-miR-455-3p(2.46),hsa-miR-548f(2.32),hsa-miR-369-3p(2.31)
>C20orf24	2.40	hsa-miR-7(3.05)
>UGT1A6	2.39	hsa-miR-590-3p(1.94),hsa-miR-376b(1.73),hsa-miR-211(2.6),hsa-miR-548f(2.32),hsa-miR-486-3p(-2.56)
>CCL2	2.39	hsa-miR-206(12.8),hsa-miR-33b(2.23),hsa-miR-369-3p(2.31),hsa-miR-206(12.8),hsa-miR-21(3.95),hsa-miR-590-3p(1.94),hsa-miR-369-3p(2.31)
>LDLR	2.39	hsa-miR-135b(5.65),hsa-miR-592(2.92),hsa-miR-455-3p(2.46),hsa-miR-188-5p(2.36)
>SCO2	2.39	hsa-miR-509-5p(1.61)
>HSD17B2	2.38	hsa-miR-211(2.6)
>PCDH7	2.38	hsa-miR-496(3.02),hsa-miR-142-3p(2.52),hsa-miR-33b(2.23),hsa-miR-590-3p(1.94),hsa-miR-377(1.81),hsa-miR-129-5p(-2.62),hsa-miR-155(2.7),hsa-miR-1303(2.66),hsa-miR-548f(2.32),hsa-miR-369-3p(2.31),hsa-miR-1276(2.14),hsa-miR-1308(2.03)
>PRDM1	2.38	hsa-miR-206(12.8),hsa-miR-135b(5.65),hsa-miR-211(2.6),hsa-miR-223(2.13),hsa-miR-137(-2.37),hsa-miR-129-5p(-2.62),hsa-miR-944(2.85),hsa-miR-1303(2.66),hsa-miR-211(2.6),hsa-miR-369-3p(2.31),hsa-miR-885-5p(-2.56)
>GCH1	2.37	hsa-miR-33b(2.23),hsa-miR-223(2.13),hsa-miR-590-3p(1.94),hsa-miR-223(2.13)
>DUOXA1	2.36	hsa-miR-431(3.91)

>KIF4A	2.35	hsa-miR-223(2.13),hsa-miR-590-3p(1.94),hsa-miR-375(-2.41)
>SLC16A1	2.35	hsa-miR-33b(2.23),hsa-miR-590-3p(1.94),hsa-miR-377(1.81),hsa-miR-548f(2.32),hsa-miR-369-3p(2.31),hsa-miR-21(3.95),hsa-miR-33b(2.23),hsa-miR-944(2.85),hsa-miR-1276(2.14),hsa-miR-487a(2.12)
>ID1	2.35	hsa-miR-944(2.85)
>TNFRSF21	2.35	hsa-miR-135b(5.65),hsa-miR-33b(2.23),hsa-miR-1179(-2.02)
>TNIP3	2.34	hsa-miR-431(3.91),hsa-miR-590-3p(1.94),hsa-miR-376b(1.73),hsa-miR-509-5p(1.61)
>GINS3	2.34	hsa-miR-7(3.05),hsa-miR-211(2.6),hsa-miR-212(2.08),hsa-miR-10a(-2.31),hsa-miR-129-5p(-2.62),hsa-miR-147b(2.79),hsa-miR-1276(2.14),hsa-miR-1308(2.03),hsa-miR-628-3p(-1.87)
>UBE2L6	2.33	hsa-miR-206(12.8),hsa-miR-135b(5.65),hsa-miR-146a(2.36),hsa-miR-455-3p(2.46),hsa-miR-146a(2.36)
>INA	2.33	hsa-miR-142-3p(2.52),hsa-miR-212(2.08),hsa-miR-590-3p(1.94),hsa-miR-376b(1.73),hsa-miR-1303(2.66),hsa-miR-509-5p(1.61),hsa-miR-885-5p(-2.56)
>PRC1	2.33	hsa-miR-146a(2.36)
>SOX7	2.33	hsa-miR-21(3.95),hsa-miR-7(3.05),hsa-miR-378(2.68),hsa-miR-211(2.6),hsa-miR-376b(1.73),hsa-miR-211(2.6),hsa-miR-548f(2.32),hsa-miR-369-3p(2.31),hsa-miR-487a(2.12),hsa-miR-486-3p(-2.56)
>EIF4EBP1	2.33	hsa-miR-486-3p(-2.56)
>HBEGF	2.32	hsa-miR-31(42.93),hsa-miR-135b(5.65),hsa-miR-376b(1.73),hsa-miR-1303(2.66),hsa-miR-211(2.6)
>SMOX	2.32	hsa-miR-940(2.79),hsa-miR-486-3p(-2.56)
>KIF11	2.31	hsa-miR-431(3.91)
>ATP11B	2.31	hsa-miR-21(3.95),hsa-miR-431(3.91),hsa-miR-155(2.7),hsa-miR-33b(2.23),hsa-miR-590-3p(1.94),hsa-miR-137(-2.37),hsa-miR-135b(5.65),hsa-miR-21(3.95),hsa-miR-155(2.7),hsa-miR-211(2.6),hsa-miR-455-3p(2.46),hsa-miR-223(2.13),hsa-miR-487a(2.12),hsa-miR-509-5p(1.61),hsa-miR-1179(-2.02)
>TRIM22	2.30	hsa-miR-590-3p(1.94),hsa-miR-376b(1.73),hsa-miR-944(2.85),hsa-miR-486-3p(-2.56)
>HN1	2.28	hsa-miR-944(2.85),hsa-miR-940(2.79),hsa-miR-455-3p(2.46),hsa-miR-665(2.34)
>E2F8	2.28	hsa-miR-590-3p(1.94),hsa-miR-377(1.81)
>ECT2	2.28	hsa-miR-496(3.02),hsa-miR-223(2.13),hsa-miR-590-3p(1.94),hsa-miR-129-5p(-2.62),hsa-miR-944(2.85),hsa-miR-548f(2.32)
>LRP8	2.27	hsa-miR-206(12.8),hsa-miR-377(1.81),hsa-miR-944(2.85),hsa-miR-369-3p(2.31),hsa-miR-1276(2.14),hsa-miR-1308(2.03)
>SYNCRIP	2.27	hsa-miR-187(2.17),hsa-miR-590-3p(1.94),hsa-miR-375(-2.41),hsa-miR-187(2.17)
>ENSA	2.27	hsa-miR-31(42.93),hsa-miR-206(12.8),hsa-miR-7(3.05),hsa-miR-378(2.68),hsa-miR-18a(2.43),hsa-miR-377(1.81),hsa-miR-542-3p(1.31),hsa-miR-129-5p(-2.62),hsa-miR-18a(2.43),hsa-miR-369-3p(2.31),hsa-miR-1276(2.14),hsa-miR-1308(2.03)
>CDH26	2.27	hsa-miR-590-3p(1.94),hsa-miR-944(2.85)
>C12orf29	2.27	hsa-miR-135b(5.65),hsa-miR-155(2.7),hsa-miR-33b(2.23),hsa-miR-590-3p(1.94),hsa-miR-155(2.7)
>SMPD3	2.27	hsa-miR-18a(2.43),hsa-miR-212(2.08),hsa-miR-548f(2.32)
>USP6NL	2.27	hsa-miR-378(2.68),hsa-miR-142-3p(2.52),hsa-miR-223(2.13),hsa-miR-590-3p(1.94),hsa-miR-129-5p(-2.62),hsa-miR-548f(2.32),hsa-miR-223(2.13),hsa-miR-1179(-2.02)
>ANLN	2.27	hsa-miR-31(42.93),hsa-miR-590-3p(1.94),hsa-miR-377(1.81),hsa-miR-542-3p(1.31),hsa-miR-369-3p(2.31),hsa-miR-509-5p(1.61),hsa-miR-628-3p(-1.87)
>AIM2	2.27	hsa-miR-944(2.85),hsa-miR-509-5p(1.61)
>LTB4R	2.27	hsa-miR-1179(-2.02)
>FBXO6	2.27	hsa-miR-590-3p(1.94),hsa-miR-542-3p(1.31),hsa-miR-486-3p(-2.56)
>DEPDC1B	2.27	hsa-miR-33b(2.23),hsa-miR-590-3p(1.94),hsa-miR-944(2.85),hsa-miR-548f(2.32),hsa-miR-1179(-2.02)
>PLSCR1	2.26	hsa-miR-496(3.02),hsa-miR-375(-2.41),hsa-miR-129-5p(-2.62),hsa-miR-369-3p(2.31)
>TOP1	2.26	hsa-miR-590-3p(1.94),hsa-miR-137(-2.37),hsa-miR-375(-2.41),hsa-miR-129-5p(-2.62),hsa-miR-548f(2.32),hsa-miR-369-3p(2.31),hsa-miR-487a(2.12)
>DCUN1D3	2.26	hsa-miR-21(3.95),hsa-miR-211(2.6),hsa-miR-223(2.13),hsa-miR-212(2.08),hsa-miR-944(2.85),hsa-miR-211(2.6),hsa-miR-548f(2.32),hsa-miR-223(2.13),hsa-miR-1308(2.03)
>GINS2	2.25	hsa-miR-377(1.81)
>RIT1	2.25	hsa-miR-21(3.95),hsa-miR-378(2.68),hsa-miR-18a(2.43),hsa-miR-590-3p(1.94),hsa-miR-542-3p(1.31),hsa-miR-486-5p(-1.81),hsa-miR-129-5p(-2.62),hsa-miR-378(2.68),hsa-miR-665(2.34),hsa-miR-33b(2.23),hsa-miR-1276(2.14),hsa-miR-487a(2.12),hsa-miR-509-5p(1.61),hsa-miR-628-3p(-1.87)
>TNFSF10	2.25	hsa-miR-33b(2.23),hsa-miR-590-3p(1.94),hsa-miR-137(-2.37),hsa-miR-129-5p(-2.62),hsa-miR-548f(2.32)
>MX2	2.25	hsa-miR-542-3p(1.31),hsa-miR-188-5p(2.36)
>FOXM1	2.24	hsa-miR-211(2.6),hsa-miR-509-5p(1.61)
>CENPA	2.24	hsa-miR-211(2.6),hsa-miR-944(2.85),hsa-miR-940(2.79),hsa-miR-211(2.6),hsa-miR-455-3p(2.46),hsa-miR-146a(2.36),hsa-miR-1276(2.14)
>PLCXD1	2.24	hsa-miR-940(2.79),hsa-miR-665(2.34),hsa-miR-509-5p(1.61)
>CCL22	2.23	hsa-miR-21(3.95),hsa-miR-10a(-2.31),hsa-miR-1268(4.45),hsa-miR-940(2.79),hsa-miR-369-3p(2.31)
>AMPD3	2.23	hsa-miR-548f(2.32),hsa-miR-1276(2.14),hsa-miR-628-3p(-1.87)
>OSMR	2.23	hsa-miR-590-3p(1.94),hsa-miR-377(1.81),hsa-miR-486-5p(-1.81),hsa-miR-10a(-2.31),hsa-miR-548f(2.32),hsa-miR-369-3p(2.31)
>KIAA1199	2.23	hsa-miR-146a(2.36),hsa-miR-486-5p(-1.81),hsa-miR-211(2.6),hsa-miR-18a(2.43),hsa-miR-369-3p(2.31),hsa-miR-486-3p(-2.56)
>IL13RA1	2.23	hsa-miR-31(42.93),hsa-miR-135b(5.65),hsa-miR-431(3.91),hsa-miR-211(2.6),hsa-miR-590-3p(1.94),hsa-miR-129-5p(-2.62),hsa-miR-31(42.93),hsa-miR-944(2.85),hsa-miR-1303(2.66),hsa-miR-188-5p(2.36),hsa-miR-1308(2.03)

>SHCBP1	2.22	hsa-miR-431(3.91),hsa-miR-33b(2.23),hsa-miR-590-3p(1.94),hsa-miR-940(2.79),hsa-miR-211(2.6)
>SERPINA3	2.22	hsa-miR-137(-2.37),hsa-miR-944(2.85),hsa-miR-665(2.34)
>N4BP1	2.22	hsa-miR-431(3.91),hsa-miR-155(2.7),hsa-miR-509-5p(1.61)
>TLE3	2.21	hsa-miR-377(1.81),hsa-miR-10a(-2.31),hsa-miR-377(1.81),hsa-miR-10a(-2.31),hsa-miR-31(42.93)
>PTP4A1	2.21	hsa-miR-211(2.6),hsa-miR-590-3p(1.94),hsa-miR-129-5p(-2.62),hsa-miR-944(2.85),hsa-miR-211(2.6),hsa-miR-548f(2.32),hsa-miR-1276(2.14),hsa-miR-1179(-2.02)
>STS	2.21	hsa-miR-7(3.05),hsa-miR-155(2.7),hsa-miR-33b(2.23),hsa-miR-590-3p(1.94),hsa-miR-431(3.91),hsa-miR-944(2.85),hsa-miR-1303(2.66),hsa-miR-455-3p(2.46),hsa-miR-369-3p(2.31),hsa-miR-33b(2.23),hsa-miR-377(1.81),hsa-miR-509-5p(1.61),hsa-miR-628-3p(-1.87)
>KLHL18	2.21	hsa-miR-31(42.93),hsa-miR-590-3p(1.94),hsa-miR-944(2.85),hsa-miR-665(2.34),hsa-miR-548f(2.32),hsa-miR-369-3p(2.31),hsa-miR-509-5p(1.61)
>PRRG4	2.21	hsa-miR-431(3.91),hsa-miR-590-3p(1.94),hsa-miR-129-5p(-2.62)
>SOST	2.19	hsa-miR-378(2.68),hsa-miR-665(2.34)
>RAB38	2.19	hsa-miR-18a(2.43),hsa-miR-542-3p(1.31),hsa-miR-375(-2.41),hsa-miR-369-3p(2.31),hsa-miR-1276(2.14)
>MCM10	2.19	hsa-miR-590-3p(1.94),hsa-miR-10a(-2.31),hsa-miR-548f(2.32)
>TGFA	2.18	hsa-miR-7(3.05),hsa-miR-496(3.02),hsa-miR-590-3p(1.94),hsa-miR-376b(1.73),hsa-miR-137(-2.37),hsa-miR-129-5p(-2.62),hsa-miR-944(2.85),hsa-miR-455-3p(2.46),hsa-miR-1179(-2.02)
>SLC7A1	2.18	hsa-miR-212(2.08),hsa-miR-129-5p(-2.62),hsa-miR-21(3.95),hsa-miR-592(2.92),hsa-miR-211(2.6),hsa-miR-590-3p(1.94),hsa-miR-376b(1.73),hsa-miR-369-3p(2.31),hsa-miR-377(1.81)
>IL4R	2.18	hsa-miR-211(2.6),hsa-miR-665(2.34)
>LAD1	2.17	hsa-miR-431(3.91),hsa-miR-377(1.81),hsa-miR-376b(1.73),hsa-miR-431(3.91)
>HMOX1	2.17	hsa-miR-377(1.81)
>ELL2	2.17	hsa-miR-21(3.95),hsa-miR-431(3.91),hsa-miR-155(2.7),hsa-miR-211(2.6),hsa-miR-146a(2.36),hsa-miR-223(2.13),hsa-miR-590-3p(1.94),hsa-miR-542-3p(1.31),hsa-miR-129-5p(-2.62),hsa-miR-21(3.95),hsa-miR-944(2.85),hsa-miR-211(2.6),hsa-miR-548f(2.32),hsa-miR-1276(2.14),hsa-miR-885-5p(-2.56)
>C1QB	2.17	hsa-miR-33b(2.23),hsa-miR-1179(-2.02)
>ATP6V1C2	2.16	hsa-miR-135b(5.65),hsa-miR-146a(2.36),hsa-miR-944(2.85),hsa-miR-146a(2.36),hsa-miR-188-5p(2.36),hsa-miR-885-5p(-2.56)
>BDH1	2.16	hsa-miR-212(2.08),hsa-miR-10a(-2.31)
>H2AFX	2.16	hsa-miR-455-3p(2.46)
>CH25H	2.15	hsa-miR-376b(1.73),hsa-miR-1303(2.66)
>LGALS8	2.15	hsa-miR-223(2.13),hsa-miR-129-5p(-2.62),hsa-miR-592(2.92),hsa-miR-885-5p(-2.56)
>THBD	2.15	hsa-miR-18a(2.43),hsa-miR-542-3p(1.31),hsa-miR-21(3.95),hsa-miR-944(2.85),hsa-miR-455-3p(2.46),hsa-miR-1276(2.14)
>CYP2C18	2.15	hsa-miR-542-3p(1.31)
>RAB10	2.15	hsa-miR-7(3.05),hsa-miR-378(2.68),hsa-miR-211(2.6),hsa-miR-223(2.13),hsa-miR-486-5p(-1.81),hsa-miR-129-5p(-2.62),hsa-miR-944(2.85),hsa-miR-1303(2.66),hsa-miR-146a(2.36),hsa-miR-548f(2.32),hsa-miR-369-3p(2.31),hsa-miR-1276(2.14)
>TMEM79	2.14	hsa-miR-188-5p(2.36),hsa-miR-1276(2.14),hsa-miR-486-3p(-2.56)
>TSPAN4	2.14	hsa-miR-206(12.8),hsa-miR-665(2.34),hsa-miR-486-3p(-2.56)
>POLE2	2.14	hsa-miR-590-3p(1.94),hsa-miR-548f(2.32)
>STAT3	2.13	hsa-miR-21(3.95),hsa-miR-33b(2.23),hsa-miR-129-5p(-2.62),hsa-miR-21(3.95),hsa-miR-1303(2.66),hsa-miR-665(2.34),hsa-miR-1308(2.03),hsa-miR-885-5p(-2.56),hsa-miR-486-3p(-2.56)
>ELOVL7	2.13	hsa-miR-21(3.95),hsa-miR-7(3.05),hsa-miR-496(3.02),hsa-miR-142-3p(2.52),hsa-miR-590-3p(1.94),hsa-miR-376b(1.73),hsa-miR-137(-2.37),hsa-miR-129-5p(-2.62),hsa-miR-944(2.85),hsa-miR-548f(2.32),hsa-miR-369-3p(2.31),hsa-miR-1179(-2.02)
>IRF8	2.13	hsa-miR-206(12.8),hsa-miR-155(2.7),hsa-miR-1276(2.14)
>ZC3HAV1	2.12	hsa-miR-206(12.8),hsa-miR-590-3p(1.94),hsa-miR-486-5p(-1.81),hsa-miR-10a(-2.31),hsa-miR-944(2.85),hsa-miR-188-5p(2.36),hsa-miR-369-3p(2.31),hsa-miR-1276(2.14),hsa-miR-509-5p(1.61),hsa-miR-885-5p(-2.56)
>BIRC3	2.12	hsa-miR-155(2.7),hsa-miR-142-3p(2.52),hsa-miR-590-3p(1.94),hsa-miR-129-5p(-2.62),hsa-miR-940(2.79),hsa-miR-369-3p(2.31)
>CEBPD	2.12	hsa-miR-885-5p(-2.56)
>EZH2	2.12	hsa-miR-137(-2.37),hsa-miR-944(2.85),hsa-miR-509-5p(1.61)
>MCL1	2.12	hsa-miR-496(3.02),hsa-miR-944(2.85),hsa-miR-940(2.79),hsa-miR-1303(2.66),hsa-miR-455-3p(2.46),hsa-miR-885-5p(-2.56)
>CYP7B1	2.12	hsa-miR-378(2.68),hsa-miR-590-3p(1.94),hsa-miR-10a(-2.31),hsa-miR-1303(2.66),hsa-miR-628-3p(-1.87)
>LRRC8B	2.11	hsa-miR-590-3p(1.94)
>EIF5	2.11	hsa-miR-31(42.93),hsa-miR-206(12.8),hsa-miR-590-3p(1.94),hsa-miR-548f(2.32),hsa-miR-33b(2.23),hsa-miR-1276(2.14)
>HSPA4	2.11	hsa-miR-940(2.79),hsa-miR-548f(2.32),hsa-miR-369-3p(2.31),hsa-miR-431(3.91),hsa-miR-486-5p(-1.81),hsa-miR-548f(2.32)
>SUB1	2.11	hsa-miR-135b(5.65),hsa-miR-377(1.81),hsa-miR-548f(2.32)
>RALGPS2	2.11	hsa-miR-590-3p(1.94),hsa-miR-129-5p(-2.62),hsa-miR-369-3p(2.31),hsa-miR-1179(-2.02)
>TAP2	2.11	hsa-miR-31(42.93),hsa-miR-135b(5.65),hsa-miR-223(2.13),hsa-miR-590-3p(1.94),hsa-miR-486-5p(-1.81),hsa-miR-137(-2.37),hsa-miR-592(2.92),hsa-miR-944(2.85),hsa-miR-369-3p(2.31),hsa-miR-1308(2.03),hsa-miR-509-5p(1.61)
>SILV	2.10	hsa-miR-7(3.05),hsa-miR-496(3.02)

>CHEK1	2.10	hsa-miR-7(3.05)
>LYPD5	2.10	hsa-miR-129-5p(-2.62),hsa-miR-146a(2.36)
>RASGRP1	2.10	hsa-miR-21(3.95),hsa-miR-378(2.68),hsa-miR-146a(2.36),hsa-miR-223(2.13),hsa-miR-590-3p(1.94),hsa-miR-376b(1.73),hsa-miR-1303(2.66),hsa-miR-885-5p(-2.56)
>ST6GALNAC1	2.10	hsa-miR-21(3.95),hsa-miR-142-3p(2.52)
>MAP3K9	2.10	hsa-miR-7(3.05),hsa-miR-223(2.13),hsa-miR-377(1.81),hsa-miR-940(2.79),hsa-miR-1276(2.14),hsa-miR-1179(-2.02)
>CENPF	2.10	hsa-miR-33b(2.23),hsa-miR-487a(2.12)
>SERPINB9	2.10	hsa-miR-206(12.8),hsa-miR-590-3p(1.94),hsa-miR-376b(1.73),hsa-miR-455-3p(2.46),hsa-miR-665(2.34),hsa-miR-369-3p(2.31)
>PTAFR	2.10	hsa-miR-146a(2.36),hsa-miR-455-3p(2.46),hsa-miR-188-5p(2.36)
>CXCL11	2.10	hsa-miR-206(12.8),hsa-miR-496(3.02),hsa-miR-590-3p(1.94),hsa-miR-376b(1.73),hsa-miR-137(-2.37),hsa-miR-1303(2.66),hsa-miR-665(2.34),hsa-miR-487a(2.12)
>FOSL2	2.10	hsa-miR-135b(5.65),hsa-miR-486-3p(-2.56)
>MPZL1	2.10	hsa-miR-206(12.8),hsa-miR-211(2.6),hsa-miR-590-3p(1.94),hsa-miR-376b(1.73),hsa-miR-211(2.6),hsa-miR-18a(2.43),hsa-miR-665(2.34),hsa-miR-487a(2.12)
>AURKB	2.10	hsa-miR-188-5p(2.36)
>GART	2.09	hsa-miR-7(3.05),hsa-miR-496(3.02),hsa-miR-146a(2.36),hsa-miR-10a(-2.31),hsa-miR-137(-2.37)
>SLC39A6	2.09	hsa-miR-137(-2.37),hsa-miR-1179(-2.02)
>CD36	2.09	hsa-miR-155(2.7),hsa-miR-376b(1.73),hsa-miR-944(2.85),hsa-miR-1179(-2.02)
>CDCA5	2.08	hsa-miR-146a(2.36)
>CTPS	2.08	hsa-miR-135b(5.65),hsa-miR-137(-2.37),hsa-miR-31(42.93),hsa-miR-135b(5.65),hsa-miR-1303(2.66),hsa-miR-211(2.6),hsa-miR-509-5p(1.61)
>MFHAS1	2.08	hsa-miR-135b(5.65),hsa-miR-7(3.05),hsa-miR-223(2.13),hsa-miR-486-5p(-1.81),hsa-miR-940(2.79),hsa-miR-1276(2.14),hsa-miR-223(2.13)
>GINS1	2.08	hsa-miR-21(3.95),hsa-miR-7(3.05),hsa-miR-146a(2.36),hsa-miR-590-3p(1.94),hsa-miR-376b(1.73),hsa-miR-486-5p(-1.81),hsa-miR-137(-2.37),hsa-miR-21(3.95),hsa-miR-944(2.85),hsa-miR-548f(2.32),hsa-miR-1307(1.97)
>CCL19	2.08	hsa-miR-377(1.81)
>BID	2.08	hsa-miR-142-3p(2.52),hsa-miR-21(3.95)
>PON2	2.08	hsa-miR-376b(1.73),hsa-miR-129-5p(-2.62)
>ABCG1	2.07	hsa-miR-10a(-2.31),hsa-miR-129-5p(-2.62),hsa-miR-378(2.68),hsa-miR-10a(-2.31)
>PLA2G2F	2.07	hsa-miR-18a(2.43),hsa-miR-10a(-2.31)
>IFI30	2.07	hsa-miR-940(2.79),hsa-miR-1308(2.03)
>COTL1	2.07	hsa-miR-31(42.93),hsa-miR-590-3p(1.94),hsa-miR-940(2.79),hsa-miR-548f(2.32),hsa-miR-1276(2.14)
>IL1RN	2.07	hsa-miR-31(42.93),hsa-miR-223(2.13),hsa-miR-377(1.81),hsa-miR-129-5p(-2.62),hsa-miR-940(2.79),hsa-miR-509-5p(1.61),hsa-miR-1179(-2.02),hsa-miR-486-3p(-2.56)
>KCNK6	2.07	hsa-miR-211(2.6),hsa-miR-486-5p(-1.81),hsa-miR-378(2.68)
>RDH12	2.07	hsa-miR-940(2.79),hsa-miR-1303(2.66)
>GPR109B	2.06	hsa-miR-211(2.6),hsa-miR-665(2.34),hsa-miR-486-3p(-2.56)
>FCGR1A	2.06	hsa-miR-31(42.93),hsa-miR-378(2.68),hsa-miR-223(2.13),hsa-miR-378(2.68)
>DCTN5	2.06	hsa-miR-31(42.93),hsa-miR-146a(2.36),hsa-miR-376b(1.73),hsa-miR-18a(2.43),hsa-miR-146a(2.36),hsa-miR-665(2.34)
>NUP50	2.06	hsa-miR-206(12.8),hsa-miR-33b(2.23),hsa-miR-590-3p(1.94),hsa-miR-376b(1.73),hsa-miR-129-5p(-2.62),hsa-miR-592(2.92),hsa-miR-944(2.85),hsa-miR-455-3p(2.46),hsa-miR-548f(2.32),hsa-miR-1179(-2.02),hsa-miR-885-5p(-2.56)
>SAR1A	2.05	hsa-miR-31(42.93),hsa-miR-21(3.95),hsa-miR-378(2.68),hsa-miR-18a(2.43),hsa-miR-146a(2.36),hsa-miR-590-3p(1.94),hsa-miR-21(3.95),hsa-miR-455-3p(2.46),hsa-miR-18a(2.43),hsa-miR-1276(2.14),hsa-miR-487a(2.12),hsa-miR-1308(2.03),hsa-miR-486-3p(-2.56)
>NRBF2	2.05	hsa-miR-211(2.6),hsa-miR-33b(2.23),hsa-miR-212(2.08),hsa-miR-129-5p(-2.62),hsa-miR-944(2.85),hsa-miR-1179(-2.02)
>ZWILCH	2.05	hsa-miR-211(2.6)
>IL1B	2.05	hsa-miR-21(3.95),hsa-miR-211(2.6),hsa-miR-940(2.79),hsa-miR-211(2.6),hsa-miR-455-3p(2.46)
>LYN	2.05	hsa-miR-378(2.68),hsa-miR-212(2.08),hsa-miR-376b(1.73),hsa-miR-944(2.85),hsa-miR-31(42.93)
>TUBB6	2.05	hsa-miR-628-3p(-1.87)
>PTPRC	2.05	hsa-miR-33b(2.23),hsa-miR-590-3p(1.94),hsa-miR-377(1.81),hsa-miR-944(2.85),hsa-miR-487a(2.12)
>THAP2	2.05	hsa-miR-590-3p(1.94),hsa-miR-486-5p(-1.81),hsa-miR-944(2.85),hsa-miR-1303(2.66),hsa-miR-211(2.6)
>YOD1	2.05	hsa-miR-21(3.95),hsa-miR-7(3.05),hsa-miR-155(2.7),hsa-miR-211(2.6),hsa-miR-33b(2.23),hsa-miR-223(2.13),hsa-miR-590-3p(1.94),hsa-miR-542-3p(1.31),hsa-miR-10a(-2.31),hsa-miR-944(2.85),hsa-miR-211(2.6),hsa-miR-369-3p(2.31),hsa-miR-223(2.13)
>NFE2L3	2.04	hsa-miR-548f(2.32)
>SDCBP2	2.04	hsa-miR-1276(2.14)
>CTSC	2.04	hsa-miR-31(42.93),hsa-miR-135b(5.65),hsa-miR-21(3.95),hsa-miR-7(3.05),hsa-miR-590-3p(1.94),hsa-miR-377(1.81),hsa-miR-137(-2.37),hsa-miR-129-5p(-2.62),hsa-miR-155(2.7),hsa-miR-1303(2.66),hsa-miR-211(2.6),hsa-miR-455-3p(2.46),hsa-miR-548f(2.32),hsa-miR-1276(2.14),hsa-miR-885-5p(-2.56)
>RABIF	2.04	hsa-miR-431(3.91),hsa-miR-1303(2.66)

>FSCN1	2.04	hsa-miR-1268(4.45),hsa-miR-1303(2.66),hsa-miR-211(2.6),hsa-miR-1308(2.03)
>PGLYRP4	2.04	hsa-miR-378(2.68)
>SQLE	2.04	hsa-miR-548f(2.32)
>TMEM33	2.04	hsa-miR-155(2.7),hsa-miR-590-3p(1.94),hsa-miR-137(-2.37),hsa-miR-548f(2.32),hsa-miR-885-5p(-2.56)
>PPARD	2.04	hsa-miR-223(2.13),hsa-miR-18a(2.43),hsa-miR-369-3p(2.31),hsa-miR-223(2.13),hsa-miR-486-3p(-2.56)
>EPHB2	2.04	hsa-miR-211(2.6),hsa-miR-212(2.08),hsa-miR-10a(-2.31),hsa-miR-211(2.6),hsa-miR-509-5p(1.61),hsa-miR-486-3p(-2.56)
>SAR1B	2.04	hsa-miR-137(-2.37),hsa-miR-944(2.85),hsa-miR-548f(2.32)
>UGCG	2.03	hsa-miR-548f(2.32),hsa-miR-369-3p(2.31)
>PPP2R2C	2.03	hsa-miR-542-3p(1.31),hsa-miR-369-3p(2.31)
>SFN	2.03	hsa-miR-431(3.91),hsa-miR-486-3p(-2.56)
>TAP1	2.02	hsa-miR-590-3p(1.94),hsa-miR-211(2.6)
>PSPH	2.02	hsa-miR-940(2.79),hsa-miR-665(2.34),hsa-miR-369-3p(2.31)
>DIO2	2.02	hsa-miR-223(2.13),hsa-miR-590-3p(1.94),hsa-miR-376b(1.73),hsa-miR-944(2.85),hsa-miR-1303(2.66),hsa-miR-223(2.13),hsa-miR-487a(2.12)
>GLUL	2.02	hsa-miR-21(3.95),hsa-miR-590-3p(1.94),hsa-miR-129-5p(-2.62),hsa-miR-188-5p(2.36)
>MAP4K4	2.02	hsa-miR-33b(2.23),hsa-miR-590-3p(1.94),hsa-miR-10a(-2.31),hsa-miR-592(2.92),hsa-miR-211(2.6),hsa-miR-369-3p(2.31),hsa-miR-628-3p(-1.87),hsa-miR-1179(-2.02)
>HDHD1A	2.02	hsa-miR-431(3.91),hsa-miR-590-3p(1.94),hsa-miR-944(2.85)
>SLC27A4	2.02	hsa-miR-486-3p(-2.56)
>IRF1	2.02	hsa-miR-31(42.93),hsa-miR-590-3p(1.94),hsa-miR-377(1.81)
>CASP7	2.02	hsa-miR-18a(2.43),hsa-miR-146a(2.36),hsa-miR-212(2.08),hsa-miR-486-5p(-1.81),hsa-miR-129-5p(-2.62),hsa-miR-940(2.79),hsa-miR-18a(2.43),hsa-miR-146a(2.36),hsa-miR-1276(2.14)
>PGBD5	2.01	hsa-miR-18a(2.43)
>ALDH3B2	2.01	hsa-miR-187(2.17),hsa-miR-542-3p(1.31),hsa-miR-940(2.79),hsa-miR-486-3p(-2.56)
>WARS	2.01	hsa-miR-378(2.68),hsa-miR-542-3p(1.31),hsa-miR-592(2.92)
>CCL8	2.01	hsa-miR-33b(2.23),hsa-miR-944(2.85),hsa-miR-455-3p(2.46),hsa-miR-369-3p(2.31)
>MED8	2.01	hsa-miR-375(-2.41),hsa-miR-940(2.79),hsa-miR-211(2.6)
>PANX1	2.01	hsa-miR-10a(-2.31),hsa-miR-137(-2.37),hsa-miR-1179(-2.02),hsa-miR-885-5p(-2.56)
>PLEK	2.01	hsa-miR-31(42.93),hsa-miR-206(12.8),hsa-miR-378(2.68),hsa-miR-146a(2.36),hsa-miR-590-3p(1.94),hsa-miR-377(1.81),hsa-miR-1303(2.66),hsa-miR-486-3p(-2.56),hsa-miR-223(2.13),hsa-miR-590-3p(1.94),hsa-miR-375(-2.41),hsa-miR-129-5p(-2.62),hsa-miR-31(42.93),hsa-miR-944(2.85),hsa-miR-1303(2.66),hsa-miR-487a(2.12)
>PCSK6	2.01	hsa-miR-21(3.95),hsa-miR-7(3.05),hsa-miR-21(3.95)
>RAB27B	2.01	hsa-miR-21(3.95),hsa-miR-496(3.02),hsa-miR-211(2.6),hsa-miR-542-3p(1.31),hsa-miR-211(2.6),hsa-miR-548f(2.32),hsa-miR-628-3p(-1.87)
>CARD14	2.01	hsa-miR-18a(2.43),hsa-miR-509-5p(1.61)
>TRIP13	2.01	hsa-miR-155(2.7),hsa-miR-129-5p(-2.62),hsa-miR-885-5p(-2.56)
>SERPINB8	2.01	hsa-miR-31(42.93),hsa-miR-206(12.8),hsa-miR-33b(2.23),hsa-miR-212(2.08),hsa-miR-590-3p(1.94),hsa-miR-377(1.81),hsa-miR-542-3p(1.31),hsa-miR-592(2.92),hsa-miR-940(2.79),hsa-miR-455-3p(2.46),hsa-miR-33b(2.23)
>MAPKAPK3	2.01	hsa-miR-18a(2.43),hsa-miR-377(1.81),hsa-miR-18a(2.43),hsa-miR-1179(-2.02)
>HOMER1	2.01	hsa-miR-31(42.93),hsa-miR-21(3.95),hsa-miR-33b(2.23),hsa-miR-223(2.13),hsa-miR-590-3p(1.94),hsa-miR-129-5p(-2.62),hsa-miR-21(3.95),hsa-miR-944(2.85),hsa-miR-1303(2.66),hsa-miR-369-3p(2.31),hsa-miR-223(2.13),hsa-miR-487a(2.12),hsa-miR-628-3p(-1.87)
>MFN1	2.00	hsa-miR-590-3p(1.94),hsa-miR-548f(2.32),hsa-miR-369-3p(2.31)
>EXOSC3	2.00	hsa-miR-496(3.02),hsa-miR-377(1.81),hsa-miR-129-5p(-2.62),hsa-miR-944(2.85),hsa-miR-369-3p(2.31)
>PPIL1	2.00	hsa-miR-375(-2.41),hsa-miR-1268(4.45)
>CD83	2.00	hsa-miR-223(2.13),hsa-miR-590-3p(1.94),hsa-miR-377(1.81),hsa-miR-137(-2.37),hsa-miR-944(2.85),hsa-miR-665(2.34),hsa-miR-1308(2.03),hsa-miR-377(1.81),hsa-miR-628-3p(-1.87),hsa-miR-885-5p(-2.56)

DOWNREGULATED TARGETS OF DE MIRNAs (up and downreg miRNAs listed):

>DIXDC1	-2.00	hsa-miR-431(3.91),hsa-miR-155(2.7),hsa-miR-211(2.6),hsa-miR-146a(2.36),hsa-miR-590-3p(1.94),hsa-miR-376b(1.73),hsa-miR-129-5p(-2.62),hsa-miR-944(2.85),hsa-miR-1303(2.66),hsa-miR-211(2.6),hsa-miR-146a(2.36),hsa-miR-548f(2.32),hsa-miR-369-3p(2.31),hsa-miR-1276(2.14),hsa-miR-1179(-2.02),hsa-miR-885-5p(-2.56),hsa-miR-486-3p(-2.56)
>LCE1B	-2.00	hsa-miR-135b(5.65),hsa-miR-7(3.05)
>GLDN	-2.00	hsa-miR-135b(5.65),hsa-miR-21(3.95),hsa-miR-496(3.02),hsa-miR-155(2.7),hsa-miR-378(2.68),hsa-miR-146a(2.36),hsa-miR-1303(2.66),hsa-miR-18a(2.43),hsa-miR-146a(2.36),hsa-miR-665(2.34),hsa-miR-1276(2.14)
>NAP1L2	-2.00	hsa-miR-135b(5.65),hsa-miR-33b(2.23),hsa-miR-137(-2.37),hsa-miR-944(2.85),hsa-miR-548f(2.32),hsa-miR-509-5p(1.61)
>RBM25	-2.00	hsa-miR-496(3.02),hsa-miR-33b(2.23),hsa-miR-590-3p(1.94),hsa-miR-129-5p(-2.62),hsa-miR-944(2.85),hsa-miR-665(2.34),hsa-miR-1276(2.14)
>PPP1R1A	-2.01	hsa-miR-31(42.93),hsa-miR-940(2.79),hsa-miR-509-5p(1.61)
>TACC2	-2.01	hsa-miR-31(42.93),hsa-miR-590-3p(1.94),hsa-miR-31(42.93),hsa-miR-1303(2.66),hsa-miR-509-5p(1.61)

>DACH1	-2.01	hsa-miR-206(12.8),hsa-miR-7(3.05),hsa-miR-496(3.02),hsa-miR-155(2.7),hsa-miR-211(2.6),hsa-miR-33b(2.23),hsa-miR-590-3p(1.94),hsa-miR-376b(1.73),hsa-miR-129-5p(-2.62),hsa-miR-155(2.7),hsa-miR-1303(2.66),hsa-miR-211(2.6),hsa-miR-188-5p(2.36),hsa-miR-665(2.34),hsa-miR-548f(2.32),hsa-miR-369-3p(2.31),hsa-miR-487a(2.12),hsa-miR-1179(-2.02),hsa-miR-885-5p(-2.56)
>TFAP2B	-2.01	hsa-miR-206(12.8),hsa-miR-155(2.7),hsa-miR-211(2.6),hsa-miR-590-3p(1.94),hsa-miR-944(2.85),hsa-miR-369-3p(2.31),hsa-miR-885-5p(-2.56)
>LRFN5	-2.01	hsa-miR-212(2.08),hsa-miR-590-3p(1.94)
>SERHL	-2.01	hsa-miR-665(2.34)
>C1orf21	-2.01	hsa-miR-944(2.85)
>ARID1B	-2.01	hsa-miR-590-3p(1.94),hsa-miR-377(1.81),hsa-miR-129-5p(-2.62),hsa-miR-944(2.85),hsa-miR-940(2.79),hsa-miR-548f(2.32),hsa-miR-486-3p(-2.56)
>FAM117A	-2.01	hsa-miR-940(2.79),hsa-miR-486-3p(-2.56)
>AR	-2.01	hsa-miR-18a(2.43),hsa-miR-509-5p(1.61),hsa-miR-155(2.7),hsa-miR-590-3p(1.94),hsa-miR-129-5p(-2.62),hsa-miR-592(2.92),hsa-miR-1276(2.14)
>PECR	-2.02	hsa-miR-590-3p(1.94),hsa-miR-137(-2.37),hsa-miR-129-5p(-2.62),hsa-miR-944(2.85),hsa-miR-509-5p(1.61)
>CCND1	-2.02	hsa-miR-155(2.7),hsa-miR-548f(2.32),hsa-miR-369-3p(2.31),hsa-miR-1276(2.14),hsa-miR-487a(2.12)
>CREB5	-2.02	hsa-miR-206(12.8),hsa-miR-496(3.02),hsa-miR-155(2.7),hsa-miR-211(2.6),hsa-miR-212(2.08),hsa-miR-129-5p(-2.62),hsa-miR-592(2.92),hsa-miR-944(2.85),hsa-miR-211(2.6),hsa-miR-548f(2.32),hsa-miR-1276(2.14)
>DST	-2.02	hsa-miR-590-3p(1.94),hsa-miR-376b(1.73),hsa-miR-137(-2.37),hsa-miR-188-5p(2.36),hsa-miR-665(2.34),hsa-miR-369-3p(2.31),hsa-miR-487a(2.12),hsa-miR-509-5p(1.61)
>CYP2J2	-2.02	hsa-miR-944(2.85)
>LRP4	-2.02	hsa-miR-31(42.93),hsa-miR-940(2.79),hsa-miR-487a(2.12),hsa-miR-885-5p(-2.56),hsa-miR-486-3p(-2.56)
>SORBS1	-2.02	hsa-miR-431(3.91),hsa-miR-211(2.6),hsa-miR-33b(2.23),hsa-miR-223(2.13),hsa-miR-590-3p(1.94),hsa-miR-542-3p(1.31),hsa-miR-129-5p(-2.62),hsa-miR-944(2.85),hsa-miR-378(2.68),hsa-miR-1303(2.66),hsa-miR-455-3p(2.46),hsa-miR-146a(2.36),hsa-miR-548f(2.32),hsa-miR-33b(2.23),hsa-miR-1276(2.14),hsa-miR-509-5p(1.61)
>TMEM97	-2.03	hsa-miR-135b(5.65),hsa-miR-7(3.05),hsa-miR-377(1.81),hsa-miR-10a(-2.31),hsa-miR-592(2.92),hsa-miR-1303(2.66),hsa-miR-1276(2.14),hsa-miR-1179(-2.02)
>SOX5	-2.03	hsa-miR-206(12.8),hsa-miR-21(3.95),hsa-miR-142-3p(2.52),hsa-miR-33b(2.23),hsa-miR-212(2.08),hsa-miR-146a(2.36),hsa-miR-1276(2.14),hsa-miR-885-5p(-2.56)
>FRZB	-2.03	hsa-miR-155(2.7),hsa-miR-542-3p(1.31),hsa-miR-137(-2.37),hsa-miR-155(2.7),hsa-miR-542-3p(1.31),hsa-miR-137(-2.37),hsa-miR-155(2.7),hsa-miR-885-5p(-2.56),hsa-miR-155(2.7),hsa-miR-885-5p(-2.56)
>IL17RD	-2.03	hsa-miR-137(-2.37),hsa-miR-146a(2.36)
>DBN1	-2.03	hsa-miR-212(2.08),hsa-miR-137(-2.37)
>RNF128	-2.03	hsa-miR-33b(2.23),hsa-miR-590-3p(1.94),hsa-miR-129-5p(-2.62),hsa-miR-592(2.92),hsa-miR-1276(2.14),hsa-miR-487a(2.12)
>SGCG	-2.03	hsa-miR-211(2.6),hsa-miR-590-3p(1.94),hsa-miR-137(-2.37),hsa-miR-486-3p(-2.56)
>BCAR3	-2.03	hsa-miR-496(3.02),hsa-miR-18a(2.43),hsa-miR-944(2.85),hsa-miR-548f(2.32),hsa-miR-487a(2.12)
>NUAK1	-2.03	hsa-miR-135b(5.65),hsa-miR-211(2.6),hsa-miR-940(2.79),hsa-miR-211(2.6),hsa-miR-548f(2.32),hsa-miR-369-3p(2.31),hsa-miR-885-5p(-2.56)
>MYH14	-2.03	hsa-miR-31(42.93)
>NDFIP2	-2.03	hsa-miR-206(12.8),hsa-miR-135b(5.65),hsa-miR-7(3.05),hsa-miR-496(3.02),hsa-miR-378(2.68),hsa-miR-590-3p(1.94),hsa-miR-129-5p(-2.62),hsa-miR-944(2.85),hsa-miR-378(2.68),hsa-miR-548f(2.32),hsa-miR-369-3p(2.31),hsa-miR-509-5p(1.61)
>DPYSL3	-2.03	hsa-miR-7(3.05),hsa-miR-211(2.6),hsa-miR-212(2.08),hsa-miR-590-3p(1.94),hsa-miR-31(42.93),hsa-miR-548f(2.32)
>ZNF573	-2.03	hsa-miR-31(42.93),hsa-miR-885-5p(-2.56)
>MBNL2	-2.04	hsa-miR-431(3.91),hsa-miR-155(2.7),hsa-miR-378(2.68),hsa-miR-18a(2.43),hsa-miR-223(2.13),hsa-miR-590-3p(1.94),hsa-miR-137(-2.37),hsa-miR-135b(5.65),hsa-miR-944(2.85),hsa-miR-18a(2.43),hsa-miR-369-3p(2.31),hsa-miR-223(2.13),hsa-miR-487a(2.12)
>TCF7L1	-2.04	hsa-miR-211(2.6),hsa-miR-590-3p(1.94),hsa-miR-542-3p(1.31),hsa-miR-129-5p(-2.62),hsa-miR-455-3p(2.46)
>ZNF43	-2.04	hsa-miR-206(12.8),hsa-miR-135b(5.65),hsa-miR-155(2.7),hsa-miR-590-3p(1.94),hsa-miR-10a(-2.31),hsa-miR-135b(5.65),hsa-miR-592(2.92),hsa-miR-944(2.85),hsa-miR-548f(2.32),hsa-miR-1276(2.14),hsa-miR-487a(2.12)
>OLFML3	-2.04	hsa-miR-155(2.7),hsa-miR-369-3p(2.31),hsa-miR-486-3p(-2.56)
>SDC2	-2.04	hsa-miR-206(12.8),hsa-miR-223(2.13),hsa-miR-590-3p(1.94),hsa-miR-129-5p(-2.62),hsa-miR-548f(2.32),hsa-miR-369-3p(2.31),hsa-miR-509-5p(1.61),hsa-miR-486-3p(-2.56)
>C14orf28	-2.04	hsa-miR-211(2.6),hsa-miR-590-3p(1.94),hsa-miR-10a(-2.31),hsa-miR-137(-2.37),hsa-miR-129-5p(-2.62),hsa-miR-592(2.92),hsa-miR-944(2.85),hsa-miR-211(2.6),hsa-miR-548f(2.32),hsa-miR-369-3p(2.31),hsa-miR-628-3p(-1.87)
>PRELP	-2.04	hsa-miR-31(42.93),hsa-miR-211(2.6),hsa-miR-486-5p(-1.81),hsa-miR-1268(4.45)
>ALCAM	-2.04	hsa-miR-206(12.8),hsa-miR-135b(5.65),hsa-miR-211(2.6),hsa-miR-18a(2.43),hsa-miR-223(2.13),hsa-miR-590-3p(1.94),hsa-miR-377(1.81),hsa-miR-542-3p(1.31),hsa-miR-135b(5.65),hsa-miR-944(2.85),hsa-miR-1303(2.66),hsa-miR-211(2.6),hsa-miR-1276(2.14)
>EFEMP1	-2.04	hsa-miR-223(2.13),hsa-miR-590-3p(1.94),hsa-miR-628-3p(-1.87)
>NR3C1	-2.04	hsa-miR-206(12.8),hsa-miR-211(2.6),hsa-miR-18a(2.43),hsa-miR-590-3p(1.94),hsa-miR-377(1.81),hsa-miR-542-3p(1.31),hsa-miR-486-5p(-1.81),hsa-miR-129-5p(-2.62),hsa-miR-1303(2.66),hsa-miR-211(2.6),hsa-miR-1179(-2.02)
>GAN	-2.04	hsa-miR-211(2.6),hsa-miR-187(2.17),hsa-miR-223(2.13),hsa-miR-590-3p(1.94),hsa-miR-377(1.81),hsa-miR-129-5p(-2.62),hsa-miR-211(2.6),hsa-miR-455-3p(2.46),hsa-miR-1276(2.14),hsa-miR-509-5p(1.61)
>PCDHB16	-2.05	hsa-miR-135b(5.65),hsa-miR-590-3p(1.94),hsa-miR-10a(-2.31),hsa-miR-944(2.85),hsa-miR-369-3p(2.31)
>PIK3C2G	-2.05	hsa-miR-376b(1.73),hsa-miR-10a(-2.31)
>CRISPLD1	-2.05	hsa-miR-206(12.8),hsa-miR-7(3.05),hsa-miR-496(3.02),hsa-miR-33b(2.23),hsa-miR-590-3p(1.94),hsa-miR-377(1.81),hsa-miR-376b(1.73),hsa-miR-375(-2.41),hsa-miR-129-5p(-2.62),hsa-miR-944(2.85),hsa-miR-1303(2.66),hsa-miR-548f(2.32),hsa-miR-369-3p(2.31)
>TNS1	-2.05	hsa-miR-31(42.93),hsa-miR-33b(2.23),hsa-miR-665(2.34),hsa-miR-369-3p(2.31),hsa-miR-509-5p(1.61)

>C19orf2	-2.05	hsa-miR-590-3p(1.94),hsa-miR-548f(2.32)
>FASN	-2.05	hsa-miR-665(2.34),hsa-miR-486-3p(-2.56)
>CD1A	-2.05	hsa-miR-31(42.93),hsa-miR-21(3.95),hsa-miR-146a(2.36),hsa-miR-33b(2.23)
>TMEM99	-2.05	hsa-miR-542-3p(1.31),hsa-miR-129-5p(-2.62),hsa-miR-628-3p(-1.87)
>P4HA2	-2.05	hsa-miR-377(1.81),hsa-miR-129-5p(-2.62)
>PIK3R1	-2.05	hsa-miR-21(3.95),hsa-miR-431(3.91),hsa-miR-496(3.02),hsa-miR-155(2.7),hsa-miR-376b(1.73),hsa-miR-542-3p(1.31),hsa-miR-486-5p(-1.81),hsa-miR-129-5p(-2.62),hsa-miR-155(2.7),hsa-miR-1303(2.66),hsa-miR-455-3p(2.46),hsa-miR-188-5p(2.36),hsa-miR-548f(2.32),hsa-miR-369-3p(2.31)
>PDZD2	-2.05	hsa-miR-31(42.93),hsa-miR-135b(5.65),hsa-miR-21(3.95),hsa-miR-378(2.68),hsa-miR-211(2.6),hsa-miR-18a(2.43),hsa-miR-146a(2.36),hsa-miR-187(2.17),hsa-miR-486-5p(-1.81),hsa-miR-10a(-2.31),hsa-miR-592(2.92),hsa-miR-944(2.85),hsa-miR-211(2.6),hsa-miR-548f(2.32),hsa-miR-487a(2.12),hsa-miR-509-5p(1.61),hsa-miR-1179(-2.02)
>VAPA	-2.05	hsa-miR-206(12.8),hsa-miR-155(2.7),hsa-miR-211(2.6),hsa-miR-146a(2.36),hsa-miR-1276(2.14)
>LOR	-2.06	hsa-miR-135b(5.65)
>TNMD	-2.06	hsa-miR-940(2.79)
>BCL2	-2.06	hsa-miR-206(12.8),hsa-miR-135b(5.65),hsa-miR-211(2.6),hsa-miR-590-3p(1.94),hsa-miR-1303(2.66),hsa-miR-211(2.6),hsa-miR-548f(2.32),hsa-miR-369-3p(2.31),hsa-miR-1276(2.14),hsa-miR-1308(2.03),hsa-miR-486-3p(-2.56),hsa-miR-1303(2.66),hsa-miR-1308(2.03),hsa-miR-885-5p(-2.56)
>NCOR1	-2.06	hsa-miR-10a(-2.31)
>BAG2	-2.06	hsa-miR-223(2.13),hsa-miR-590-3p(1.94),hsa-miR-137(-2.37),hsa-miR-1303(2.66),hsa-miR-548f(2.32),hsa-miR-223(2.13),hsa-miR-628-3p(-1.87)
>CDON	-2.06	hsa-miR-206(12.8),hsa-miR-146a(2.36),hsa-miR-223(2.13),hsa-miR-590-3p(1.94),hsa-miR-377(1.81),hsa-miR-944(2.85),hsa-miR-211(2.6),hsa-miR-455-3p(2.46),hsa-miR-146a(2.36),hsa-miR-548f(2.32),hsa-miR-223(2.13),hsa-miR-1308(2.03),hsa-miR-509-5p(1.61)
>ACACB	-2.07	hsa-miR-665(2.34),hsa-miR-548f(2.32),hsa-miR-486-3p(-2.56)
>NSUN6	-2.07	hsa-miR-590-3p(1.94),hsa-miR-137(-2.37)
>CEP68	-2.07	hsa-miR-21(3.95),hsa-miR-496(3.02),hsa-miR-155(2.7),hsa-miR-211(2.6),hsa-miR-18a(2.43),hsa-miR-223(2.13),hsa-miR-590-3p(1.94),hsa-miR-376b(1.73),hsa-miR-129-5p(-2.62),hsa-miR-21(3.95),hsa-miR-592(2.92),hsa-miR-944(2.85),hsa-miR-1179(-2.02),hsa-miR-885-5p(-2.56)
>GALNTL2	-2.07	hsa-miR-206(12.8),hsa-miR-376b(1.73),hsa-miR-1303(2.66),hsa-miR-211(2.6),hsa-miR-665(2.34),hsa-miR-885-5p(-2.56)
>SLC29A1	-2.07	hsa-miR-223(2.13),hsa-miR-940(2.79),hsa-miR-486-3p(-2.56)
>EN1	-2.07	hsa-miR-211(2.6),hsa-miR-212(2.08),hsa-miR-944(2.85),hsa-miR-369-3p(2.31),hsa-miR-486-3p(-2.56)
>ELN	-2.07	hsa-miR-1303(2.66),hsa-miR-665(2.34),hsa-miR-486-3p(-2.56)
>HOXB3	-2.08	hsa-miR-7(3.05),hsa-miR-378(2.68),hsa-miR-10a(-2.31),hsa-miR-375(-2.41),hsa-miR-940(2.79),hsa-miR-548f(2.32),hsa-miR-369-3p(2.31),hsa-miR-10a(-2.31),hsa-miR-885-5p(-2.56)
>ZNF395	-2.08	hsa-miR-7(3.05),hsa-miR-211(2.6),hsa-miR-142-3p(2.52),hsa-miR-187(2.17),hsa-miR-223(2.13),hsa-miR-212(2.08),hsa-miR-129-5p(-2.62),hsa-miR-18a(2.43),hsa-miR-665(2.34),hsa-miR-369-3p(2.31)
>PPAP2B	-2.08	hsa-miR-129-5p(-2.62),hsa-miR-369-3p(2.31)
>ASPN	-2.08	hsa-miR-21(3.95),hsa-miR-129-5p(-2.62),hsa-miR-455-3p(2.46),hsa-miR-369-3p(2.31),hsa-miR-1276(2.14),hsa-miR-487a(2.12),hsa-miR-1179(-2.02)
>ITPR2	-2.08	hsa-miR-135b(5.65),hsa-miR-21(3.95),hsa-miR-496(3.02),hsa-miR-590-3p(1.94),hsa-miR-542-3p(1.31),hsa-miR-129-5p(-2.62),hsa-miR-21(3.95),hsa-miR-592(2.92),hsa-miR-944(2.85),hsa-miR-940(2.79),hsa-miR-548f(2.32),hsa-miR-33b(2.23),hsa-miR-509-5p(1.61)
>SLC2A13	-2.08	hsa-miR-206(12.8),hsa-miR-135b(5.65),hsa-miR-21(3.95),hsa-miR-7(3.05),hsa-miR-18a(2.43),hsa-miR-590-3p(1.94),hsa-miR-376b(1.73),hsa-miR-542-3p(1.31),hsa-miR-21(3.95),hsa-miR-944(2.85),hsa-miR-1303(2.66),hsa-miR-211(2.6),hsa-miR-18a(2.43),hsa-miR-548f(2.32),hsa-miR-369-3p(2.31),hsa-miR-223(2.13)
>PDGFC	-2.08	hsa-miR-31(42.93),hsa-miR-7(3.05),hsa-miR-18a(2.43),hsa-miR-590-3p(1.94),hsa-miR-376b(1.73),hsa-miR-486-5p(-1.81),hsa-miR-375(-2.41),hsa-miR-944(2.85),hsa-miR-1276(2.14)
>SPRY2	-2.08	hsa-miR-21(3.95),hsa-miR-590-3p(1.94),hsa-miR-548f(2.32),hsa-miR-369-3p(2.31),hsa-miR-1308(2.03),hsa-miR-885-5p(-2.56)
>SLC26A2	-2.08	hsa-miR-135b(5.65),hsa-miR-21(3.95),hsa-miR-155(2.7),hsa-miR-223(2.13),hsa-miR-129-5p(-2.62),hsa-miR-455-3p(2.46),hsa-miR-146a(2.36),hsa-miR-548f(2.32)
>LPL	-2.09	hsa-miR-590-3p(1.94),hsa-miR-377(1.81),hsa-miR-944(2.85),hsa-miR-155(2.7),hsa-miR-1303(2.66),hsa-miR-188-5p(2.36),hsa-miR-548f(2.32),hsa-miR-487a(2.12),hsa-miR-1179(-2.02)
>SUSD2	-2.09	hsa-miR-496(3.02),hsa-miR-940(2.79)
>ZNF559	-2.09	hsa-miR-377(1.81),hsa-miR-376b(1.73),hsa-miR-129-5p(-2.62),hsa-miR-377(1.81),hsa-miR-1179(-2.02)
>PLA2R1	-2.09	hsa-miR-135b(5.65),hsa-miR-7(3.05),hsa-miR-590-3p(1.94),hsa-miR-542-3p(1.31),hsa-miR-548f(2.32)
>NEGR1	-2.09	hsa-miR-135b(5.65),hsa-miR-21(3.95),hsa-miR-590-3p(1.94),hsa-miR-377(1.81),hsa-miR-376b(1.73),hsa-miR-10a(-2.31),hsa-miR-137(-2.37),hsa-miR-135b(5.65),hsa-miR-944(2.85),hsa-miR-1303(2.66),hsa-miR-455-3p(2.46),hsa-miR-548f(2.32),hsa-miR-628-3p(-1.87)
>FRMD3	-2.09	hsa-miR-21(3.95),hsa-miR-129-5p(-2.62),hsa-miR-455-3p(2.46),hsa-miR-369-3p(2.31),hsa-miR-1179(-2.02)
>FCGBP	-2.10	hsa-miR-21(3.95)
>ALDH3A2	-2.10	hsa-miR-206(12.8),hsa-miR-378(2.68),hsa-miR-590-3p(1.94),hsa-miR-944(2.85),hsa-miR-378(2.68),hsa-miR-211(2.6),hsa-miR-665(2.34),hsa-miR-377(1.81)
>ACOX2	-2.10	hsa-miR-590-3p(1.94)
>TPM1	-2.10	hsa-miR-33b(2.23),hsa-miR-542-3p(1.31),hsa-miR-375(-2.41),hsa-miR-548f(2.32)
>PCDH20	-2.10	hsa-miR-155(2.7),hsa-miR-211(2.6),hsa-miR-142-3p(2.52),hsa-miR-223(2.13),hsa-miR-590-3p(1.94),hsa-miR-377(1.81),hsa-miR-542-3p(1.31),hsa-miR-486-5p(-1.81),hsa-miR-375(-2.41),hsa-miR-211(2.6),hsa-miR-487a(2.12)
>CCRL1	-2.10	hsa-miR-206(12.8),hsa-miR-21(3.95),hsa-miR-590-3p(1.94),hsa-miR-376b(1.73),hsa-miR-137(-2.37),hsa-miR-21(3.95),hsa-miR-944(2.85),hsa-miR-548f(2.32)

>PDZK1	-2.10	hsa-miR-590-3p(1.94),hsa-miR-377(1.81),hsa-miR-487a(2.12)
>PDGFD	-2.10	hsa-miR-21(3.95),hsa-miR-496(3.02),hsa-miR-33b(2.23),hsa-miR-590-3p(1.94),hsa-miR-129-5p(-2.62),hsa-miR-21(3.95),hsa-miR-944(2.85),hsa-miR-1303(2.66),hsa-miR-188-5p(2.36),hsa-miR-548f(2.32)
>ZNF483	-2.10	hsa-miR-21(3.95),hsa-miR-590-3p(1.94),hsa-miR-129-5p(-2.62),hsa-miR-509-5p(1.61)
>FKBP7	-2.10	hsa-miR-548f(2.32)
>H3F3B	-2.10	hsa-miR-206(12.8),hsa-miR-21(3.95),hsa-miR-378(2.68),hsa-miR-18a(2.43),hsa-miR-590-3p(1.94),hsa-miR-486-5p(-1.81),hsa-miR-10a(-2.31),hsa-miR-137(-2.37),hsa-miR-21(3.95),hsa-miR-188-5p(2.36),hsa-miR-548f(2.32),hsa-miR-369-3p(2.31),hsa-miR-223(2.13)
>PNPLA3	-2.10	hsa-miR-146a(2.36),hsa-miR-212(2.08),hsa-miR-590-3p(1.94),hsa-miR-377(1.81),hsa-miR-146a(2.36),hsa-miR-369-3p(2.31)
>KLF8	-2.10	hsa-miR-206(12.8),hsa-miR-21(3.95),hsa-miR-147b(2.79)
>CTNNBIP1	-2.11	hsa-miR-211(2.6),hsa-miR-10a(-2.31),hsa-miR-188-5p(2.36),hsa-miR-486-3p(-2.56)
>TIMP3	-2.11	hsa-miR-206(12.8),hsa-miR-21(3.95),hsa-miR-590-3p(1.94),hsa-miR-377(1.81),hsa-miR-665(2.34),hsa-miR-548f(2.32),hsa-miR-509-5p(1.61),hsa-miR-486-3p(-2.56)
>ACTA1	-2.11	hsa-miR-155(2.7),hsa-miR-223(2.13)
>RHOB	-2.11	hsa-miR-21(3.95),hsa-miR-223(2.13),hsa-miR-590-3p(1.94),hsa-miR-21(3.95),hsa-miR-1303(2.66),hsa-miR-548f(2.32),hsa-miR-486-3p(-2.56),hsa-miR-211(2.6),hsa-miR-142-3p(2.52),hsa-miR-146a(2.36),hsa-miR-33b(2.23),hsa-miR-590-3p(1.94),hsa-miR-377(1.81),hsa-miR-129-5p(-2.62),hsa-miR-21(3.95),hsa-miR-944(2.85),hsa-miR-1303(2.66),hsa-miR-211(2.6),hsa-miR-455-3p(2.46),hsa-miR-548f(2.32),hsa-miR-369-3p(2.31),hsa-miR-33b(2.23),hsa-miR-223(2.13),hsa-miR-377(1.81)
>ADCY2	-2.11	hsa-miR-135b(5.65),hsa-miR-21(3.95),hsa-miR-155(2.7),hsa-miR-378(2.68),hsa-miR-211(2.6),hsa-miR-146a(2.36),hsa-miR-129-5p(-2.62),hsa-miR-944(2.85),hsa-miR-18a(2.43),hsa-miR-33b(2.23)
>TM2D1	-2.12	hsa-miR-376b(1.73),hsa-miR-1276(2.14)
>RHPN2	-2.12	hsa-miR-206(12.8),hsa-miR-496(3.02),hsa-miR-369-3p(2.31),hsa-miR-1179(-2.02)
>SCGB2A2	-2.13	hsa-miR-431(3.91)
>CNN1	-2.13	hsa-miR-10a(-2.31)
>ABCA9	-2.13	hsa-miR-135b(5.65),hsa-miR-155(2.7),hsa-miR-18a(2.43),hsa-miR-944(2.85),hsa-miR-18a(2.43),hsa-miR-146a(2.36),hsa-miR-188-5p(2.36),hsa-miR-369-3p(2.31),hsa-miR-1179(-2.02)
>COL3A1	-2.14	hsa-miR-33b(2.23),hsa-miR-590-3p(1.94),hsa-miR-376b(1.73),hsa-miR-129-5p(-2.62),hsa-miR-665(2.34),hsa-miR-1276(2.14),hsa-miR-487a(2.12)
>IGFBP5	-2.14	hsa-miR-146a(2.36),hsa-miR-33b(2.23),hsa-miR-137(-2.37),hsa-miR-129-5p(-2.62)
>PELI2	-2.14	hsa-miR-31(42.93),hsa-miR-135b(5.65),hsa-miR-21(3.95),hsa-miR-590-3p(1.94),hsa-miR-542-3p(1.31),hsa-miR-129-5p(-2.62),hsa-miR-944(2.85),hsa-miR-548f(2.32)
>RORC	-2.14	hsa-miR-31(42.93),hsa-miR-592(2.92),hsa-miR-665(2.34),hsa-miR-1276(2.14)
>TARDBP	-2.15	hsa-miR-211(2.6),hsa-miR-142-3p(2.52),hsa-miR-18a(2.43),hsa-miR-33b(2.23),hsa-miR-223(2.13),hsa-miR-590-3p(1.94),hsa-miR-137(-2.37),hsa-miR-592(2.92),hsa-miR-455-3p(2.46),hsa-miR-188-5p(2.36),hsa-miR-509-5p(1.61),hsa-miR-1179(-2.02)
>EDIL3	-2.15	hsa-miR-135b(5.65),hsa-miR-496(3.02),hsa-miR-377(1.81),hsa-miR-137(-2.37),hsa-miR-375(-2.41),hsa-miR-129-5p(-2.62),hsa-miR-944(2.85),hsa-miR-940(2.79),hsa-miR-548f(2.32),hsa-miR-1276(2.14),hsa-miR-509-5p(1.61)
>MAP1B	-2.15	hsa-miR-31(42.93),hsa-miR-496(3.02),hsa-miR-590-3p(1.94),hsa-miR-376b(1.73),hsa-miR-542-3p(1.31),hsa-miR-940(2.79),hsa-miR-211(2.6),hsa-miR-548f(2.32),hsa-miR-369-3p(2.31),hsa-miR-223(2.13),hsa-miR-487a(2.12)
>HOXC6	-2.15	hsa-miR-590-3p(1.94),hsa-miR-377(1.81),hsa-miR-129-5p(-2.62),hsa-miR-940(2.79),hsa-miR-147b(2.79),hsa-miR-665(2.34),hsa-miR-377(1.81),hsa-miR-486-3p(-2.56)
>CAMK2N1	-2.16	hsa-miR-18a(2.43),hsa-miR-33b(2.23),hsa-miR-590-3p(1.94),hsa-miR-377(1.81),hsa-miR-486-5p(-1.81),hsa-miR-129-5p(-2.62),hsa-miR-1303(2.66),hsa-miR-455-3p(2.46),hsa-miR-548f(2.32),hsa-miR-1276(2.14),hsa-miR-628-3p(-1.87),hsa-miR-1179(-2.02),hsa-miR-885-5p(-2.56)
>MASP2	-2.16	hsa-miR-31(42.93),hsa-miR-1276(2.14),hsa-miR-509-5p(1.61)
>TSPYL5	-2.16	hsa-miR-135b(5.65),hsa-miR-33b(2.23),hsa-miR-377(1.81),hsa-miR-944(2.85),hsa-miR-940(2.79),hsa-miR-1179(-2.02)
>EFNB2	-2.16	hsa-miR-206(12.8),hsa-miR-135b(5.65),hsa-miR-211(2.6),hsa-miR-33b(2.23),hsa-miR-590-3p(1.94),hsa-miR-377(1.81),hsa-miR-129-5p(-2.62),hsa-miR-188-5p(2.36),hsa-miR-369-3p(2.31),hsa-miR-487a(2.12),hsa-miR-377(1.81)
>ZC3H6	-2.16	hsa-miR-206(12.8),hsa-miR-155(2.7),hsa-miR-378(2.68),hsa-miR-146a(2.36),hsa-miR-223(2.13),hsa-miR-590-3p(1.94),hsa-miR-137(-2.37),hsa-miR-944(2.85),hsa-miR-1303(2.66),hsa-miR-211(2.6),hsa-miR-18a(2.43),hsa-miR-369-3p(2.31),hsa-miR-487a(2.12)
>WISP2	-2.16	hsa-miR-431(3.91),hsa-miR-590-3p(1.94),hsa-miR-940(2.79)
>SNX1	-2.16	hsa-miR-31(42.93),hsa-miR-135b(5.65),hsa-miR-155(2.7),hsa-miR-590-3p(1.94),hsa-miR-377(1.81),hsa-miR-944(2.85),hsa-miR-378(2.68),hsa-miR-146a(2.36),hsa-miR-369-3p(2.31),hsa-miR-1308(2.03)
>ALS2CR4	-2.16	hsa-miR-135b(5.65),hsa-miR-7(3.05),hsa-miR-155(2.7),hsa-miR-211(2.6),hsa-miR-590-3p(1.94),hsa-miR-377(1.81),hsa-miR-376b(1.73),hsa-miR-592(2.92),hsa-miR-944(2.85),hsa-miR-146a(2.36),hsa-miR-188-5p(2.36)
>ACADL	-2.17	hsa-miR-31(42.93),hsa-miR-135b(5.65),hsa-miR-211(2.6),hsa-miR-590-3p(1.94),hsa-miR-944(2.85),hsa-miR-1303(2.66),hsa-miR-548f(2.32)
>CES1	-2.17	hsa-miR-211(2.6),hsa-miR-188-5p(2.36)
>ZNF423	-2.17	hsa-miR-211(2.6),hsa-miR-369-3p(2.31),hsa-miR-509-5p(1.61)
>NFIB	-2.17	hsa-miR-21(3.95),hsa-miR-496(3.02),hsa-miR-223(2.13),hsa-miR-590-3p(1.94),hsa-miR-377(1.81),hsa-miR-137(-2.37),hsa-miR-129-5p(-2.62),hsa-miR-21(3.95),hsa-miR-944(2.85),hsa-miR-155(2.7),hsa-miR-211(2.6),hsa-miR-455-3p(2.46),hsa-miR-665(2.34),hsa-miR-369-3p(2.31),hsa-miR-509-5p(1.61)
>PDLIM4	-2.17	hsa-miR-223(2.13),hsa-miR-542-3p(1.31)
>NCALD	-2.17	hsa-miR-7(3.05),hsa-miR-212(2.08),hsa-miR-940(2.79),hsa-miR-1276(2.14)
>FOS	-2.17	hsa-miR-431(3.91),hsa-miR-155(2.7),hsa-miR-431(3.91),hsa-miR-548f(2.32),hsa-miR-369-3p(2.31),hsa-miR-147b(2.79)
>DNM1	-2.17	hsa-miR-496(3.02),hsa-miR-940(2.79)
>FAM19A5	-2.17	hsa-miR-548f(2.32),hsa-miR-369-3p(2.31),hsa-miR-187(2.17),hsa-miR-486-3p(-2.56)

>RPL37	-2.17	hsa-miR-10a(-2.31),hsa-miR-455-3p(2.46),hsa-miR-487a(2.12),hsa-miR-10a(-2.31)
>FNDC1	-2.18	hsa-miR-590-3p(1.94),hsa-miR-548f(2.32),hsa-miR-509-5p(1.61),hsa-miR-1179(-2.02)
>SRGAP2	-2.18	hsa-miR-31(42.93),hsa-miR-206(12.8),hsa-miR-7(3.05),hsa-miR-378(2.68),hsa-miR-211(2.6),hsa-miR-212(2.08),hsa-miR-590-3p(1.94),hsa-miR-377(1.81),hsa-miR-542-3p(1.31),hsa-miR-944(2.85),hsa-miR-940(2.79),hsa-miR-211(2.6),hsa-miR-548f(2.32),hsa-miR-1179(-2.02)
>FBLN1	-2.19	hsa-miR-31(42.93),hsa-miR-1276(2.14),hsa-miR-486-3p(-2.56)
>LIFR	-2.19	hsa-miR-206(12.8),hsa-miR-431(3.91),hsa-miR-155(2.7),hsa-miR-590-3p(1.94),hsa-miR-129-5p(-2.62),hsa-miR-944(2.85),hsa-miR-155(2.7),hsa-miR-369-3p(2.31)
>PKIB	-2.19	hsa-miR-33b(2.23),hsa-miR-590-3p(1.94),hsa-miR-129-5p(-2.62),hsa-miR-548f(2.32),hsa-miR-33b(2.23)
>ESR1	-2.20	hsa-miR-135b(5.65),hsa-miR-18a(2.43),hsa-miR-590-3p(1.94),hsa-miR-129-5p(-2.62),hsa-miR-211(2.6),hsa-miR-18a(2.43),hsa-miR-369-3p(2.31)
>COL1A2	-2.20	hsa-miR-7(3.05),hsa-miR-496(3.02),hsa-miR-590-3p(1.94),hsa-miR-1308(2.03)
>TNXB	-2.20	hsa-miR-486-5p(-1.81),hsa-miR-137(-2.37)
>KLF9	-2.21	hsa-miR-21(3.95),hsa-miR-142-3p(2.52),hsa-miR-376b(1.73),hsa-miR-211(2.6),hsa-miR-548f(2.32),hsa-miR-1276(2.14)
>CCDC73	-2.21	hsa-miR-590-3p(1.94),hsa-miR-375(-2.41),hsa-miR-628-3p(-1.87)
>MEOX2	-2.21	hsa-miR-206(12.8),hsa-miR-33b(2.23),hsa-miR-590-3p(1.94),hsa-miR-377(1.81),hsa-miR-592(2.92),hsa-miR-369-3p(2.31),hsa-miR-33b(2.23)
>MCOLN3	-2.22	hsa-miR-496(3.02),hsa-miR-211(2.6),hsa-miR-137(-2.37),hsa-miR-211(2.6)
>OMD	-2.22	hsa-miR-155(2.7),hsa-miR-590-3p(1.94),hsa-miR-1276(2.14)
>DMD	-2.22	hsa-miR-31(42.93),hsa-miR-211(2.6),hsa-miR-146a(2.36),hsa-miR-223(2.13),hsa-miR-212(2.08),hsa-miR-542-3p(1.31),hsa-miR-375(-2.41),hsa-miR-129-5p(-2.62),hsa-miR-944(2.85),hsa-miR-211(2.6),hsa-miR-146a(2.36),hsa-miR-548f(2.32),hsa-miR-369-3p(2.31),hsa-miR-223(2.13)
>PER1	-2.24	hsa-miR-486-3p(-2.56)
>DKK2	-2.24	hsa-miR-21(3.95),hsa-miR-496(3.02),hsa-miR-211(2.6),hsa-miR-142-3p(2.52),hsa-miR-146a(2.36),hsa-miR-590-3p(1.94),hsa-miR-486-5p(-1.81),hsa-miR-129-5p(-2.62),hsa-miR-944(2.85),hsa-miR-1303(2.66),hsa-miR-211(2.6),hsa-miR-369-3p(2.31),hsa-miR-509-5p(1.61),hsa-miR-1179(-2.02)
>SORCS2	-2.24	hsa-miR-33b(2.23),hsa-miR-1268(4.45),hsa-miR-509-5p(1.61)
>RNASE4	-2.25	hsa-miR-21(3.95),hsa-miR-155(2.7),hsa-miR-142-3p(2.52),hsa-miR-590-3p(1.94),hsa-miR-188-5p(2.36),hsa-miR-628-3p(-1.87)
>SCARA5	-2.25	hsa-miR-31(42.93),hsa-miR-378(2.68),hsa-miR-211(2.6),hsa-miR-665(2.34),hsa-miR-1179(-2.02)
>HMGCS2	-2.25	hsa-miR-21(3.95)
>SCIN	-2.26	hsa-miR-590-3p(1.94),hsa-miR-137(-2.37),hsa-miR-129-5p(-2.62)
>PPP1R1B	-2.26	hsa-miR-455-3p(2.46),hsa-miR-665(2.34),hsa-miR-486-3p(-2.56)
>TGFBR3	-2.28	hsa-miR-31(42.93),hsa-miR-206(12.8),hsa-miR-21(3.95),hsa-miR-18a(2.43),hsa-miR-21(3.95),hsa-miR-18a(2.43),hsa-miR-548f(2.32)
>NAP1L3	-2.28	hsa-miR-33b(2.23)
>MYH11	-2.29	hsa-miR-21(3.95),hsa-miR-187(2.17),hsa-miR-129-5p(-2.62),hsa-miR-665(2.34),hsa-miR-548f(2.32),hsa-miR-187(2.17),hsa-miR-487a(2.12),hsa-miR-1179(-2.02)
>LMOD1	-2.30	hsa-miR-665(2.34),hsa-miR-486-3p(-2.56)
>LEP	-2.30	hsa-miR-211(2.6),hsa-miR-146a(2.36),hsa-miR-211(2.6),hsa-miR-146a(2.36),hsa-miR-1276(2.14),hsa-miR-31(42.93),hsa-miR-21(3.95),hsa-miR-378(2.68),hsa-miR-211(2.6),hsa-miR-146a(2.36),hsa-miR-187(2.17),hsa-miR-223(2.13),hsa-miR-590-3p(1.94),hsa-miR-377(1.81),hsa-miR-129-5p(-2.62),hsa-miR-135b(5.65),hsa-miR-21(3.95),hsa-miR-1303(2.66),hsa-miR-211(2.6),hsa-miR-146a(2.36),hsa-miR-665(2.34),hsa-miR-548f(2.32),hsa-miR-369-3p(2.31),hsa-miR-187(2.17),hsa-miR-487a(2.12),hsa-miR-509-5p(1.61),hsa-miR-135b(5.65),hsa-miR-21(3.95),hsa-miR-7(3.05),hsa-miR-378(2.68),hsa-miR-590-3p(1.94),hsa-miR-377(1.81),hsa-miR-129-5p(-2.62),hsa-miR-944(2.85),hsa-miR-378(2.68),hsa-miR-1303(2.66),hsa-miR-146a(2.36),hsa-miR-548f(2.32),hsa-miR-369-3p(2.31)
>RTN4	-2.30	hsa-miR-31(42.93),hsa-miR-21(3.95),hsa-miR-542-3p(1.31),hsa-miR-1268(4.45),hsa-miR-944(2.85),hsa-miR-455-3p(2.46)
>HLF	-2.30	hsa-miR-31(42.93),hsa-miR-431(3.91),hsa-miR-18a(2.43),hsa-miR-223(2.13),hsa-miR-590-3p(1.94),hsa-miR-377(1.81),hsa-miR-486-5p(-1.81),hsa-miR-137(-2.37),hsa-miR-940(2.79),hsa-miR-548f(2.32),hsa-miR-223(2.13),hsa-miR-628-3p(-1.87)
>ADIPOQ	-2.31	hsa-miR-223(2.13),hsa-miR-590-3p(1.94),hsa-miR-10a(-2.31),hsa-miR-129-5p(-2.62),hsa-miR-378(2.68),hsa-miR-1303(2.66),hsa-miR-548f(2.32),hsa-miR-369-3p(2.31),hsa-miR-1308(2.03)
>LPHN3	-2.31	hsa-miR-155(2.7),hsa-miR-33b(2.23),hsa-miR-590-3p(1.94),hsa-miR-129-5p(-2.62),hsa-miR-592(2.92),hsa-miR-155(2.7),hsa-miR-1303(2.66),hsa-miR-1179(-2.02)
>PGM5	-2.32	hsa-miR-206(12.8),hsa-miR-223(2.13),hsa-miR-590-3p(1.94),hsa-miR-377(1.81),hsa-miR-129-5p(-2.62),hsa-miR-592(2.92),hsa-miR-369-3p(2.31),hsa-miR-1276(2.14),hsa-miR-377(1.81)
>TCF7L2	-2.32	hsa-miR-548f(2.32)
>NRN1	-2.33	hsa-miR-7(3.05),hsa-miR-129-5p(-2.62),hsa-miR-592(2.92),hsa-miR-944(2.85),hsa-miR-369-3p(2.31)
>GATA6	-2.34	hsa-miR-431(3.91),hsa-miR-7(3.05),hsa-miR-496(3.02),hsa-miR-211(2.6),hsa-miR-10a(-2.31),hsa-miR-375(-2.41),hsa-miR-944(2.85),hsa-miR-378(2.68),hsa-miR-211(2.6),hsa-miR-548f(2.32),hsa-miR-369-3p(2.31),hsa-miR-10a(-2.31)
>HOXC10	-2.34	hsa-miR-590-3p(1.94),hsa-miR-375(-2.41),hsa-miR-129-5p(-2.62)
>ADRB2	-2.34	hsa-miR-590-3p(1.94),hsa-miR-548f(2.32)
>CD34	-2.35	hsa-miR-431(3.91),hsa-miR-1303(2.66),hsa-miR-548f(2.32)
>CYP4B1	-2.35	hsa-miR-206(12.8),hsa-miR-944(2.85)
>CORO2B	-2.35	hsa-miR-146a(2.36),hsa-miR-509-5p(1.61)

>PDE4DIP	-2.36	hsa-miR-31(42.93),hsa-miR-206(12.8),hsa-miR-431(3.91),hsa-miR-455-3p(2.46),hsa-miR-665(2.34),hsa-miR-1179(-2.02)
>SSPN	-2.36	hsa-miR-31(42.93),hsa-miR-21(3.95),hsa-miR-378(2.68),hsa-miR-590-3p(1.94),hsa-miR-21(3.95),hsa-miR-944(2.85),hsa-miR-378(2.68),hsa-miR-548f(2.32)
>PLCB4	-2.36	hsa-miR-431(3.91),hsa-miR-590-3p(1.94),hsa-miR-129-5p(-2.62),hsa-miR-592(2.92),hsa-miR-944(2.85),hsa-miR-1303(2.66),hsa-miR-1276(2.14),hsa-miR-628-3p(-1.87)
>DDAH1	-2.36	hsa-miR-206(12.8),hsa-miR-21(3.95),hsa-miR-155(2.7),hsa-miR-378(2.68),hsa-miR-223(2.13),hsa-miR-377(1.81),hsa-miR-129-5p(-2.62),hsa-miR-21(3.95),hsa-miR-944(2.85),hsa-miR-1303(2.66),hsa-miR-146a(2.36),hsa-miR-509-5p(1.61)
>GSTA3	-2.36	hsa-miR-431(3.91)
>SH3D19	-2.36	hsa-miR-155(2.7),hsa-miR-10a(-2.31),hsa-miR-944(2.85),hsa-miR-211(2.6),hsa-miR-548f(2.32),hsa-miR-1308(2.03)
>RAI14	-2.37	hsa-miR-146a(2.36),hsa-miR-129-5p(-2.62),hsa-miR-147b(2.79),hsa-miR-155(2.7),hsa-miR-1276(2.14),hsa-miR-1179(-2.02),hsa-miR-486-3p(-2.56)
>FOXC1	-2.38	hsa-miR-31(42.93),hsa-miR-211(2.6),hsa-miR-590-3p(1.94),hsa-miR-137(-2.37),hsa-miR-188-5p(2.36),hsa-miR-548f(2.32),hsa-miR-369-3p(2.31)
>CHL1	-2.38	hsa-miR-21(3.95),hsa-miR-590-3p(1.94),hsa-miR-377(1.81),hsa-miR-376b(1.73),hsa-miR-10a(-2.31),hsa-miR-21(3.95),hsa-miR-369-3p(2.31),hsa-miR-487a(2.12),hsa-miR-628-3p(-1.87)
>NOVA1	-2.38	hsa-miR-496(3.02),hsa-miR-155(2.7),hsa-miR-211(2.6),hsa-miR-146a(2.36),hsa-miR-33b(2.23),hsa-miR-590-3p(1.94),hsa-miR-542-3p(1.31),hsa-miR-137(-2.37),hsa-miR-944(2.85),hsa-miR-155(2.7),hsa-miR-1303(2.66),hsa-miR-211(2.6),hsa-miR-455-3p(2.46),hsa-miR-146a(2.36),hsa-miR-188-5p(2.36),hsa-miR-548f(2.32),hsa-miR-369-3p(2.31),hsa-miR-1308(2.03)
>TMEM47	-2.38	hsa-miR-206(12.8),hsa-miR-496(3.02),hsa-miR-155(2.7),hsa-miR-211(2.6),hsa-miR-223(2.13),hsa-miR-590-3p(1.94),hsa-miR-944(2.85),hsa-miR-211(2.6),hsa-miR-369-3p(2.31)
>GSTM3	-2.39	hsa-miR-31(42.93),hsa-miR-431(3.91),hsa-miR-211(2.6),hsa-miR-590-3p(1.94),hsa-miR-377(1.81),hsa-miR-211(2.6),hsa-miR-188-5p(2.36),hsa-miR-1276(2.14)
>EEF2K	-2.39	hsa-miR-142-3p(2.52),hsa-miR-590-3p(1.94),hsa-miR-944(2.85),hsa-miR-487a(2.12),hsa-miR-509-5p(1.61)
>ADH1B	-2.39	hsa-miR-155(2.7),hsa-miR-590-3p(1.94),hsa-miR-377(1.81),hsa-miR-137(-2.37),hsa-miR-1303(2.66),hsa-miR-548f(2.32),hsa-miR-486-3p(-2.56)
>PCYT1B	-2.39	hsa-miR-135b(5.65),hsa-miR-7(3.05),hsa-miR-496(3.02),hsa-miR-211(2.6),hsa-miR-590-3p(1.94),hsa-miR-211(2.6),hsa-miR-188-5p(2.36),hsa-miR-548f(2.32)
>LAMB4	-2.40	hsa-miR-590-3p(1.94),hsa-miR-628-3p(-1.87)
>ZNF677	-2.41	hsa-miR-155(2.7),hsa-miR-369-3p(2.31),hsa-miR-628-3p(-1.87)
>CLDN1	-2.41	hsa-miR-31(42.93),hsa-miR-21(3.95),hsa-miR-496(3.02),hsa-miR-155(2.7),hsa-miR-211(2.6),hsa-miR-590-3p(1.94),hsa-miR-377(1.81),hsa-miR-21(3.95),hsa-miR-1303(2.66),hsa-miR-211(2.6),hsa-miR-548f(2.32),hsa-miR-1308(2.03),hsa-miR-509-5p(1.61),hsa-miR-1179(-2.02),hsa-miR-885-5p(-2.56)
>MYLK	-2.42	hsa-miR-206(12.8),hsa-miR-7(3.05),hsa-miR-155(2.7),hsa-miR-142-3p(2.52),hsa-miR-18a(2.43),hsa-miR-590-3p(1.94),hsa-miR-129-5p(-2.62),hsa-miR-1303(2.66),hsa-miR-369-3p(2.31),hsa-miR-1308(2.03)
>MAML2	-2.42	hsa-miR-211(2.6),hsa-miR-509-5p(1.61)
>PAPLN	-2.42	hsa-miR-31(42.93),hsa-miR-155(2.7),hsa-miR-211(2.6),hsa-miR-33b(2.23),hsa-miR-590-3p(1.94),hsa-miR-376b(1.73),hsa-miR-1268(4.45),hsa-miR-665(2.34),hsa-miR-1276(2.14),hsa-miR-509-5p(1.61)
>PEG3	-2.44	hsa-miR-135b(5.65),hsa-miR-129-5p(-2.62),hsa-miR-940(2.79),hsa-miR-1303(2.66)
>SYDE2	-2.44	hsa-miR-31(42.93),hsa-miR-496(3.02),hsa-miR-33b(2.23),hsa-miR-590-3p(1.94)
>PPFIBP1	-2.44	hsa-miR-542-3p(1.31),hsa-miR-10a(-2.31),hsa-miR-129-5p(-2.62),hsa-miR-135b(5.65),hsa-miR-1268(4.45),hsa-miR-944(2.85),hsa-miR-369-3p(2.31),hsa-miR-1308(2.03)
>PPARGC1A	-2.44	hsa-miR-211(2.6),hsa-miR-18a(2.43),hsa-miR-33b(2.23),hsa-miR-187(2.17),hsa-miR-590-3p(1.94),hsa-miR-377(1.81),hsa-miR-376b(1.73),hsa-miR-137(-2.37),hsa-miR-944(2.85),hsa-miR-147b(2.79),hsa-miR-211(2.6),hsa-miR-369-3p(2.31),hsa-miR-187(2.17),hsa-miR-487a(2.12),hsa-miR-1308(2.03),hsa-miR-1179(-2.02)
>HOXA10	-2.45	hsa-miR-135b(5.65),hsa-miR-590-3p(1.94),hsa-miR-1303(2.66),hsa-miR-665(2.34),hsa-miR-369-3p(2.31)
>SGEF	-2.46	hsa-miR-10a(-2.31),hsa-miR-1268(4.45),hsa-miR-940(2.79),hsa-miR-548f(2.32),hsa-miR-369-3p(2.31),hsa-miR-1276(2.14),hsa-miR-10a(-2.31)
>GLDC	-2.46	hsa-miR-377(1.81),hsa-miR-455-3p(2.46),hsa-miR-548f(2.32)
>KRT15	-2.47	hsa-miR-940(2.79)
>CGNL1	-2.47	hsa-miR-542-3p(1.31),hsa-miR-129-5p(-2.62),hsa-miR-1268(4.45),hsa-miR-378(2.68),hsa-miR-665(2.34),hsa-miR-369-3p(2.31)
>PLLP	-2.49	hsa-miR-7(3.05),hsa-miR-496(3.02),hsa-miR-18a(2.43),hsa-miR-548f(2.32)
>LONRF1	-2.49	hsa-miR-135b(5.65),hsa-miR-211(2.6),hsa-miR-590-3p(1.94),hsa-miR-1303(2.66),hsa-miR-548f(2.32),hsa-miR-1276(2.14)
>RAI2	-2.49	hsa-miR-590-3p(1.94),hsa-miR-487a(2.12),hsa-miR-885-5p(-2.56)
>GATA3	-2.50	hsa-miR-135b(5.65),hsa-miR-155(2.7),hsa-miR-10a(-2.31),hsa-miR-548f(2.32),hsa-miR-369-3p(2.31)
>PCP4	-2.50	hsa-miR-33b(2.23),hsa-miR-135b(5.65),hsa-miR-1308(2.03),hsa-miR-1179(-2.02)
>ZNF91	-2.51	hsa-miR-135b(5.65),hsa-miR-155(2.7),hsa-miR-542-3p(1.31),hsa-miR-486-5p(-1.81),hsa-miR-135b(5.65),hsa-miR-944(2.85),hsa-miR-455-3p(2.46),hsa-miR-548f(2.32),hsa-miR-223(2.13),hsa-miR-487a(2.12)
>HAO2	-2.53	hsa-miR-31(42.93)
>COBL	-2.53	hsa-miR-1303(2.66),hsa-miR-487a(2.12)
>AFF3	-2.54	hsa-miR-31(42.93),hsa-miR-33b(2.23),hsa-miR-223(2.13),hsa-miR-590-3p(1.94),hsa-miR-486-5p(-1.81),hsa-miR-944(2.85),hsa-miR-455-3p(2.46),hsa-miR-188-5p(2.36),hsa-miR-548f(2.32),hsa-miR-369-3p(2.31),hsa-miR-509-5p(1.61),hsa-miR-628-3p(-1.87)
>PTN	-2.55	hsa-miR-155(2.7),hsa-miR-590-3p(1.94),hsa-miR-137(-2.37),hsa-miR-129-5p(-2.62),hsa-miR-155(2.7)
>MTBP	-2.56	hsa-miR-590-3p(1.94),hsa-miR-1276(2.14)
>PLN	-2.56	hsa-miR-21(3.95),hsa-miR-7(3.05),hsa-miR-155(2.7),hsa-miR-33b(2.23),hsa-miR-590-3p(1.94),hsa-miR-369-3p(2.31),hsa-miR-33b(2.23)
>PPP4R2	-2.56	hsa-miR-548f(2.32),hsa-miR-509-5p(1.61)
>POSTN	-2.60	hsa-miR-135b(5.65),hsa-miR-18a(2.43),hsa-miR-33b(2.23),hsa-miR-592(2.92),hsa-miR-944(2.85)

>ENPP5	-2.60	hsa-miR-590-3p(1.94),hsa-miR-542-3p(1.31),hsa-miR-944(2.85),hsa-miR-940(2.79),hsa-miR-188-5p(2.36),hsa-miR-1308(2.03)
>SYNPO2	-2.60	hsa-miR-206(12.8),hsa-miR-155(2.7),hsa-miR-378(2.68),hsa-miR-142-3p(2.52),hsa-miR-146a(2.36),hsa-miR-33b(2.23),hsa-miR-590-3p(1.94),hsa-miR-377(1.81),hsa-miR-129-5p(-2.62),hsa-miR-21(3.95),hsa-miR-592(2.92),hsa-miR-155(2.7),hsa-miR-378(2.68),hsa-miR-146a(2.36),hsa-miR-369-3p(2.31),hsa-miR-1276(2.14),hsa-miR-885-5p(-2.56)
>CAB39L	-2.60	hsa-miR-31(42.93),hsa-miR-21(3.95),hsa-miR-590-3p(1.94),hsa-miR-377(1.81),hsa-miR-542-3p(1.31),hsa-miR-21(3.95),hsa-miR-455-3p(2.46),hsa-miR-146a(2.36),hsa-miR-548f(2.32),hsa-miR-1276(2.14),hsa-miR-1179(-2.02)
>MFAP5	-2.63	hsa-miR-135b(5.65),hsa-miR-7(3.05),hsa-miR-590-3p(1.94),hsa-miR-376b(1.73),hsa-miR-137(-2.37),hsa-miR-369-3p(2.31),hsa-miR-1179(-2.02)
>SCEL	-2.63	hsa-miR-590-3p(1.94),hsa-miR-137(-2.37),hsa-miR-548f(2.32)
>PRSS23	-2.63	hsa-miR-211(2.6),hsa-miR-18a(2.43),hsa-miR-590-3p(1.94),hsa-miR-542-3p(1.31),hsa-miR-129-5p(-2.62),hsa-miR-944(2.85),hsa-miR-211(2.6),hsa-miR-665(2.34),hsa-miR-33b(2.23),hsa-miR-1179(-2.02)
>SLITRK6	-2.63	hsa-miR-135b(5.65),hsa-miR-33b(2.23),hsa-miR-590-3p(1.94),hsa-miR-376b(1.73),hsa-miR-137(-2.37),hsa-miR-548f(2.32),hsa-miR-33b(2.23),hsa-miR-1179(-2.02)
>OGN	-2.64	hsa-miR-206(12.8),hsa-miR-155(2.7),hsa-miR-142-3p(2.52),hsa-miR-146a(2.36),hsa-miR-223(2.13),hsa-miR-590-3p(1.94),hsa-miR-129-5p(-2.62),hsa-miR-944(2.85),hsa-miR-548f(2.32),hsa-miR-628-3p(-1.87)
>PDK4	-2.65	hsa-miR-431(3.91),hsa-miR-496(3.02),hsa-miR-155(2.7),hsa-miR-378(2.68),hsa-miR-211(2.6),hsa-miR-590-3p(1.94),hsa-miR-377(1.81),hsa-miR-129-5p(-2.62),hsa-miR-1303(2.66),hsa-miR-211(2.6),hsa-miR-548f(2.32),hsa-miR-885-5p(-2.56)
>ITM2A	-2.66	hsa-miR-496(3.02),hsa-miR-590-3p(1.94),hsa-miR-1276(2.14),hsa-miR-1179(-2.02)
>AGTR1	-2.67	hsa-miR-206(12.8),hsa-miR-7(3.05),hsa-miR-155(2.7),hsa-miR-944(2.85),hsa-miR-1303(2.66),hsa-miR-455-3p(2.46)
>MAMDC2	-2.67	hsa-miR-590-3p(1.94),hsa-miR-376b(1.73),hsa-miR-129-5p(-2.62),hsa-miR-944(2.85),hsa-miR-1276(2.14),hsa-miR-628-3p(-1.87)
>SPRR4	-2.68	hsa-miR-455-3p(2.46)
>ID4	-2.69	hsa-miR-18a(2.43),hsa-miR-486-5p(-1.81),hsa-miR-10a(-2.31),hsa-miR-18a(2.43),hsa-miR-548f(2.32)
>ELMOD1	-2.69	hsa-miR-31(42.93),hsa-miR-431(3.91),hsa-miR-155(2.7),hsa-miR-211(2.6),hsa-miR-590-3p(1.94),hsa-miR-431(3.91),hsa-miR-940(2.79),hsa-miR-211(2.6),hsa-miR-146a(2.36),hsa-miR-369-3p(2.31),hsa-miR-487a(2.12),hsa-miR-1308(2.03),hsa-miR-10a(-2.31)
>CILP	-2.69	hsa-miR-21(3.95),hsa-miR-33b(2.23),hsa-miR-542-3p(1.31),hsa-miR-665(2.34)
>CA6	-2.71	hsa-miR-155(2.7)
>SORBS2	-2.72	hsa-miR-18a(2.43),hsa-miR-590-3p(1.94),hsa-miR-376b(1.73),hsa-miR-137(-2.37),hsa-miR-129-5p(-2.62),hsa-miR-944(2.85),hsa-miR-211(2.6),hsa-miR-548f(2.32),hsa-miR-1276(2.14)
>GPRASP1	-2.75	hsa-miR-129-5p(-2.62),hsa-miR-944(2.85),hsa-miR-487a(2.12)
>UST	-2.80	hsa-miR-206(12.8),hsa-miR-590-3p(1.94),hsa-miR-377(1.81),hsa-miR-376b(1.73),hsa-miR-129-5p(-2.62),hsa-miR-21(3.95),hsa-miR-944(2.85),hsa-miR-378(2.68),hsa-miR-211(2.6),hsa-miR-455-3p(2.46),hsa-miR-665(2.34),hsa-miR-1276(2.14),hsa-miR-486-3p(-2.56)
>FHL1	-2.80	hsa-miR-146a(2.36),hsa-miR-223(2.13),hsa-miR-590-3p(1.94),hsa-miR-129-5p(-2.62),hsa-miR-146a(2.36),hsa-miR-369-3p(2.31),hsa-miR-1276(2.14),hsa-miR-509-5p(1.61)
>CRAT	-2.81	hsa-miR-211(2.6),hsa-miR-1276(2.14),hsa-miR-487a(2.12),hsa-miR-486-3p(-2.56)
>PTPN21	-2.85	hsa-miR-155(2.7),hsa-miR-590-3p(1.94),hsa-miR-375(-2.41),hsa-miR-592(2.92),hsa-miR-944(2.85),hsa-miR-155(2.7),hsa-miR-548f(2.32),hsa-miR-369-3p(2.31),hsa-miR-885-5p(-2.56)
>SNRPN	-2.85	hsa-miR-155(2.7)
>RGMB	-2.85	hsa-miR-7(3.05),hsa-miR-146a(2.36),hsa-miR-137(-2.37),hsa-miR-944(2.85),hsa-miR-1303(2.66),hsa-miR-548f(2.32),hsa-miR-1276(2.14)
>SCD5	-2.86	hsa-miR-18a(2.43),hsa-miR-377(1.81),hsa-miR-542-3p(1.31),hsa-miR-10a(-2.31),hsa-miR-940(2.79)
>NR3C2	-2.88	hsa-miR-31(42.93),hsa-miR-135b(5.65),hsa-miR-431(3.91),hsa-miR-155(2.7),hsa-miR-211(2.6),hsa-miR-590-3p(1.94),hsa-miR-129-5p(-2.62),hsa-miR-944(2.85),hsa-miR-940(2.79),hsa-miR-211(2.6),hsa-miR-665(2.34),hsa-miR-548f(2.32),hsa-miR-1276(2.14)
>OSR2	-2.90	hsa-miR-142-3p(2.52)
>ZNF273	-2.90	hsa-miR-155(2.7),hsa-miR-590-3p(1.94),hsa-miR-377(1.81),hsa-miR-10a(-2.31),hsa-miR-137(-2.37),hsa-miR-375(-2.41),hsa-miR-592(2.92),hsa-miR-940(2.79),hsa-miR-548f(2.32),hsa-miR-369-3p(2.31),hsa-miR-377(1.81),hsa-miR-509-5p(1.61),hsa-miR-628-3p(-1.87)
>CST6	-2.91	hsa-miR-542-3p(1.31)
>GREM2	-2.92	hsa-miR-7(3.05),hsa-miR-377(1.81),hsa-miR-137(-2.37),hsa-miR-375(-2.41),hsa-miR-129-5p(-2.62),hsa-miR-944(2.85),hsa-miR-211(2.6),hsa-miR-369-3p(2.31),hsa-miR-377(1.81),hsa-miR-509-5p(1.61),hsa-miR-885-5p(-2.56)
>FAM70A	-2.92	hsa-miR-431(3.91),hsa-miR-496(3.02),hsa-miR-211(2.6),hsa-miR-146a(2.36),hsa-miR-223(2.13),hsa-miR-590-3p(1.94),hsa-miR-211(2.6),hsa-miR-146a(2.36),hsa-miR-223(2.13),hsa-miR-1308(2.03)
>SOAT1	-2.94	hsa-miR-590-3p(1.94),hsa-miR-129-5p(-2.62),hsa-miR-211(2.6),hsa-miR-548f(2.32),hsa-miR-487a(2.12),hsa-miR-885-5p(-2.56)
>SP8	-2.95	hsa-miR-496(3.02),hsa-miR-155(2.7),hsa-miR-142-3p(2.52),hsa-miR-146a(2.36),hsa-miR-377(1.81),hsa-miR-542-3p(1.31),hsa-miR-129-5p(-2.62),hsa-miR-944(2.85),hsa-miR-1308(2.03),hsa-miR-885-5p(-2.56),hsa-miR-486-3p(-2.56)
>CYP39A1	-2.98	hsa-miR-18a(2.43),hsa-miR-590-3p(1.94),hsa-miR-129-5p(-2.62),hsa-miR-944(2.85),hsa-miR-1179(-2.02)
>IGFL2	-3.00	hsa-miR-135b(5.65)
>FADS2	-3.01	hsa-miR-212(2.08),hsa-miR-486-3p(-2.56)
>FA2H	-3.05	hsa-miR-31(42.93),hsa-miR-940(2.79),hsa-miR-486-3p(-2.56)
>C1QTNF7	-3.05	hsa-miR-211(2.6),hsa-miR-18a(2.43),hsa-miR-33b(2.23),hsa-miR-223(2.13),hsa-miR-590-3p(1.94),hsa-miR-486-5p(-1.81),hsa-miR-137(-2.37),hsa-miR-129-5p(-2.62),hsa-miR-211(2.6)
>LRRC17	-3.18	hsa-miR-10a(-2.31),hsa-miR-369-3p(2.31),hsa-miR-1179(-2.02)
>GREM1	-3.23	hsa-miR-206(12.8),hsa-miR-7(3.05),hsa-miR-496(3.02),hsa-miR-211(2.6),hsa-miR-33b(2.23),hsa-miR-137(-2.37),hsa-miR-940(2.79),hsa-miR-155(2.7),hsa-miR-211(2.6),hsa-miR-188-5p(2.36),hsa-miR-369-3p(2.31),hsa-miR-33b(2.23)
>CLDN23	-3.27	hsa-miR-590-3p(1.94),hsa-miR-944(2.85)

>AQP9	-3.27	hsa-miR-18a(2.43),hsa-miR-146a(2.36),hsa-miR-590-3p(1.94),hsa-miR-1303(2.66),hsa-miR-146a(2.36),hsa-miR-885-5p(-2.56)
>FADS1	-3.44	hsa-miR-431(3.91),hsa-miR-496(3.02),hsa-miR-590-3p(1.94),hsa-miR-211(2.6),hsa-miR-1276(2.14)
>ST7L	-3.45	hsa-miR-135b(5.65),hsa-miR-7(3.05),hsa-miR-496(3.02),hsa-miR-211(2.6),hsa-miR-146a(2.36),hsa-miR-10a(-2.31),hsa-miR-1303(2.66),hsa-miR-211(2.6),hsa-miR-548f(2.32),hsa-miR-369-3p(2.31),hsa-miR-223(2.13)
>CLDN8	-3.51	hsa-miR-135b(5.65),hsa-miR-21(3.95),hsa-miR-155(2.7),hsa-miR-223(2.13),hsa-miR-940(2.79),hsa-miR-155(2.7),hsa-miR-548f(2.32)
>F3	-3.53	hsa-miR-155(2.7),hsa-miR-18a(2.43),hsa-miR-223(2.13),hsa-miR-129-5p(-2.62),hsa-miR-155(2.7),hsa-miR-548f(2.32),hsa-miR-369-3p(2.31)
>COCH	-3.60	hsa-miR-137(-2.37),hsa-miR-1303(2.66),hsa-miR-1276(2.14)
>ZDHHC11	-3.71	hsa-miR-142-3p(2.52),hsa-miR-940(2.79),hsa-miR-548f(2.32),hsa-miR-1308(2.03)
>MUC7	-3.74	hsa-miR-431(3.91),hsa-miR-7(3.05),hsa-miR-590-3p(1.94),hsa-miR-542-3p(1.31),hsa-miR-944(2.85)
>EMX2	-3.76	hsa-miR-206(12.8),hsa-miR-944(2.85),hsa-miR-211(2.6)
>TSPAN8	-3.84	hsa-miR-211(2.6),hsa-miR-188-5p(2.36)
>STXBP6	-3.88	hsa-miR-590-3p(1.94),hsa-miR-548f(2.32),hsa-miR-1179(-2.02)
>TMEM56	-3.93	hsa-miR-590-3p(1.94)
>TPPP	-3.95	hsa-miR-211(2.6),hsa-miR-377(1.81),hsa-miR-188-5p(2.36)
>HSD3B1	-4.04	hsa-miR-7(3.05)
>WDR72	-4.23	hsa-miR-206(12.8),hsa-miR-21(3.95),hsa-miR-7(3.05),hsa-miR-155(2.7),hsa-miR-33b(2.23),hsa-miR-590-3p(1.94),hsa-miR-21(3.95),hsa-miR-592(2.92),hsa-miR-944(2.85),hsa-miR-1303(2.66),hsa-miR-369-3p(2.31),hsa-miR-487a(2.12),hsa-miR-509-5p(1.61)
>HS3ST6	-4.25	hsa-miR-18a(2.43)
>IL1F7	-4.64	hsa-miR-486-3p(-2.56)
>HSD11B1	-4.95	hsa-miR-590-3p(1.94),hsa-miR-376b(1.73),hsa-miR-944(2.85)
>ACSBG1	-5.74	hsa-miR-223(2.13),hsa-miR-548f(2.32),hsa-miR-509-5p(1.61)
>FABP7	-5.98	hsa-miR-548f(2.32)
>GAL	-6.38	hsa-miR-665(2.34),hsa-miR-378(2.68),hsa-miR-212(2.08),hsa-miR-665(2.34)
>CCL27	-7.72	hsa-miR-944(2.85)
>THRSP	-9.40	hsa-miR-369-3p(2.31)
>BTC	-13.90	hsa-miR-211(2.6),hsa-miR-129-5p(-2.62),hsa-miR-369-3p(2.31),hsa-miR-628-3p(-1.87)
>WIF1	-14.03	hsa-miR-33b(2.23),hsa-miR-590-3p(1.94),hsa-miR-137(-2.37),hsa-miR-129-5p(-2.62)

Table A-2. TargetScan Custom predicted targets for Top 10 up- and downregulated miRNAs

Identifier	PP/NN[a]
miR31*	**34.51**
CD47	2.91
FOS	-2.17
KLF9	-2.21
PRDM1	2.38
RAI14	-2.37
STAT3	2.13
miR-21*	**8.80**
ALCAM	-2.04
CREB5	-2.02
CTPS	2.08
DCAMKL1	-2.25
HLF	-2.30
NFIB	-2.17
RNF128	-2.03
ST7L	-3.45
TAP1	2.02
UST	-2.80
miR-135b*	**8.00**
DMN	-2.17
GSPT1	2.27
TOP1	2.26
miR-33b*	**5.70**
C19orf2	-2.05
DCUN1D3	2.26
GAN	-2.04
LRP8	2.27
NR3C2	-2.88
miR-222*	**5.59**
BCAR3	-2.03
DIO2	2.02
EREG	2.57
MYO5A	2.62
NEGR1	-2.09
NOVA1	-2.38
NR3C1	-2.04
PIK3R1	-2.05
PON2	2.08
PTPN21	-2.85
RNF128	-2.03
SLC7A1	2.18

ZIC1	3.42
Novel #107	**-8.07**
DIXDC1	-2.00
EMX2	-3.76
FAM13A1	-2.05
NOVA1	-2.38
NRBF2	2.05
PIK3R1	-2.05
miR-124	**-5.87**
ALCAM	-2.04
ARG2	2.55
C20orf133	-3.66
CARHSP1	4.05
CCL2	2.39
CDON	-2.06
COTL1	2.07
CRAT	-2.81
DMD	-2.22
EFNB2	-2.16
ELL2	2.17
EZH2	2.12
FA2H	-3.05
FAM117A	-2.01
FLJ20152	-2.21
GATA6	-2.34
GPT2	2.57
HLF	-2.30
IRF1	2.02
LOC153222	-2.05
LONRF1	-2.49
MAP1B	-2.15
MGC13057	-2.03
MPZL1	2.10
MYO5A	2.62
NAP1L3	-2.28
NEGR1	-2.09
NFIB	-2.17
NOPE	-2.33
NR3C1	-2.04
NR3C2	-2.88
P4HA2	-2.05
PDZD2	-2.05
PEG3	-2.44

PLEKHH1	-2.27
PPIF	3.38
RAB10	2.15
RAB27A	3.95
RAB38	2.19
RAI14	-2.37
RNF128	-2.03
SFT2D2	2.64
SH3PXD2A	4.26
SLC16A1	2.35
SLC29A1	-2.07
SLC2A13	-2.08
SLC7A1	2.18
SLITRK6	-2.63
SMOX	2.32
SMPD3	2.27
SORCS2	-2.24
SPRY2	-2.08
SPTLC2	4.34
STAT3	2.13
TACC2	-2.01
THAP2	2.05
TMEM49	2.41
TUBB6	2.05
VSNL1	3.18
YOD1	2.05
miR-675*	**-4.44**
AFF3	-2.54
RABIF	2.04
Novel #360	**-4.16**
AMPD3	2.23
BHLHB3	-2.62
C14orf28	-2.04
C19orf2	-2.05
CCNE2	2.40
CORO2B	-2.35
CREB5	-2.02
DBN1	-2.03
DMD	-2.22
ENPP5	-2.60
F3	-3.53
FAM70A	-2.92
HLF	-2.30

HN1	2.28
LPHN3	-2.31
MCL1	2.12
RAB10	2.15
RNF128	-2.03
TIMP3	-2.11
ZIC1	3.42
Novel #200	**-3.79**
LPL	-2.09
VAPA	-2.05
miR-483-3p	**-2.93**
DIXDC1	-2.00
FHL1	-2.80
FOSL2	2.10
GAN	-2.04
HOMER1	2.01
ITPR2	-2.08
MFN1	2.00

[a]Normal skin, NN; Involved psoriatic skin, PP.